

Nagra

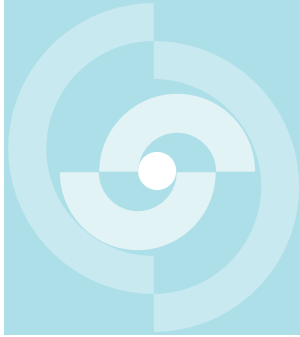
Nationale
Genossenschaft
für die Lagerung
radioaktiver Abfälle

Cédra

Société coopérative
nationale
pour l'entreposage
de déchets radioactifs

Cisra

Società cooperativa
nazionale
per l'immagazzinamento
di scorie radioattive



TECHNISCHER BERICHT 85-08

HYDROGEOLOGIC TESTING OF CRYSTALLINE ROCKS DURING THE NAGRA DEEP DRILLING PROGRAM

G. E. GRISAK
J. F. PICKENS
D. W. BELANGER
J. D. AVIS

JANUARY 1985

GTC GEOLOGIC TESTING CONSULTANTS,
OTTAWA, CANADA, AND
INTERA TECHNOLOGIES, HOUSTON, USA

Nagra

Nationale
Genossenschaft
für die Lagerung
radioaktiver Abfälle

Cédra

Société coopérative
nationale
pour l'entreposage
de déchets radioactifs

Cisra

Società cooperativa
nazionale
per l'immagazzinamento
di scorie radioattive

TECHNISCHER BERICHT 85-08

HYDROGEOLOGIC TESTING OF CRYSTALLINE ROCKS DURING THE NAGRA DEEP DRILLING PROGRAM

G. E. GRISAK
J. F. PICKENS
D. W. BELANGER
J. D. AVIS

JANUARY 1985

GTC GEOLOGIC TESTING CONSULTANTS,
OTTAWA, CANADA, AND
INTERA TECHNOLOGIES, HOUSTON, USA

Der vorliegende Bericht wurde im Auftrag der Nagra erstellt. Die Autoren haben ihre eigenen Ansichten und Schlussfolgerungen dargestellt. Diese müssen nicht unbedingt mit denjenigen der Nagra übereinstimmen.

Le présent rapport a été préparé sur demande de la Cédra. Les opinions et conclusions présentées sont celles des auteurs et ne correspondent pas nécessairement à celles de la Cédra.

This report was prepared as an account of work sponsored by Nagra. The viewpoints presented and conclusions reached are those of the author(s) and do not necessarily represent those of Nagra.

Zusammenfassung

Das Ziel dieses Berichtes ist es, für das hydrogeologische Testprogramm der Nagra sowohl die theoretischen Grundlagen darzustellen, als auch deren praktische Anwendung aufzuzeigen. Er behandelt die hydraulischen Testmethoden im Bohrloch nebst deren Auswertungsmethodik. Am Anfang stehen Erläuterungen zur mathematischen Beschreibung der Fliessvorgänge, gefolgt von deren Gebrauch bei verschiedenen Testverfahren. Dabei handelt es sich vornehmlich um Puls-Tests, Drill Stem Tests, Pumpversuchen und andere Untersuchungstechniken zur Bestimmung der hydraulischen Parameter.

Die theoretischen Betrachtungen beinhalten quantitative Abschätzungen der Bedeutung verschiedener Flüssigkeitseigenschaften, des Geräteverhaltens, der Druckvorgänge im Bohrloch, sowohl auch jener Druckveränderungen im Testabschnitt, die auf der Erwärmung des Bohrloches und der vorangegangenen Druckgeschichte basieren. Darunter fallen auch die sogenannten Skineffekte, die sich an der Bohrlochwand abspielen.

Bei der Analyse der Testdaten notwendige praktische Ueberlegungen sind Gegenstand ausführlicher Ueberlegungen. Sie erstrecken sich auf grundsätzliche Erläuterungen zum Fliessvorgang mit Erwähnung der beiden Konzepte der Strömung in Spalten einerseits oder im porösen Medium andererseits. Zur Diskussion stehen dann die Annahmen, welche den Rechenverfahren zugrunde gelegt werden müssen, ferner die Abschätzung vom hydraulischen Bezugsniveau. Hinzu kommen Diskussionen zur Frage des Speicherkoeffizienten, der Druck-Temperaturbedingungen vor Anfang des Testes und der Bedeutung des Bohrlochdurchmessers im Rahmen der Interpretation. Weitere Ausführungen betreffen die räumliche Orientierung von Spalten, sowie die Fragen der Messgenauigkeit respektive des Auflösungsvermögens in der Permeabilitätsbestimmung. Den genannten Betrachtungen sind zur Illustration Beispiele aus dem Nagra Testprogramm beigegeben.

Der Bericht schliesst mit detailliert ausgearbeiteten Richtlinien als Anleitung beim Messen des Wasserdruckes in der interessierenden Formation. Sie sind in der Weise ausgearbeitet, dass dem verantwortlichen Hydrogeologen im Felde eine logisch aufgebaute Entscheidungsgrundlage in die Hand gegeben werden kann.

ABSTRACT

The purpose of this report is to document the theoretical basis and practical application of the NAGRA hydrogeologic testing program. The report deals with borehole hydraulic testing methods and interpretations, commencing with the governing flow equations and their application to various test procedures, such as pulse tests, drill stem tests, pumping tests, etc. The theoretical considerations include quantitative assessment of the relative significance of various fluid properties, equipment compliance, borehole pressure history, thermally induced pressure responses and pressure/temperature skin effects. Practical considerations in the test analyses and interpretation are also quantitatively considered. These considerations include; the flow regime conceptualization (e.g., porous media or fractured media), assumptions inherent in the solutions, estimation of reference pressure, estimation of storage coefficient, pre-test pressure and thermal conditions, borehole diameter, measurement scale, radius of influence, fracture orientations, borehole/formation skin effects, fluid properties, equipment accuracy and resolution, equipment compliance, and test procedures. These considerations are illustrated with numerous examples based on the NAGRA program. The report concludes with detailed guidelines for the measurement of formation pressure. The guidelines are designed to provide a decision-making logic basis for the field hydrogeologists responsible for conducting hydraulic tests.

TABLE OF CONTENTS

	<u>Page</u>
ABSTRACT	
LIST OF FIGURES	
LIST OF TABLES	
1. INTRODUCTION	1
2. THEORETICAL ASPECTS OF BOREHOLE HYDRAULIC TESTING METHODS	3
2.1 Introduction	3
2.2 Governing Equations	3
2.3 Slug Injection or Withdrawal Test	6
2.4 Pulse Injection or Withdrawal Test	13
2.4.1 Pulse Test - Porous Media Approach	13
2.4.2 Pulse Test - Fractured Media Approach	16
2.5 Drill Stem Test	17
2.6 Pumping or Injection Test	22
2.7 Constant Drawdown Flow Test	25
2.8 Multiple Well Methods	28
2.9 Implementation of Data Analysis Methods	29
2.9.1 Type Curve Methods	29
2.9.2 Computer Implementation	30
3. ANALYSIS AND INTERPRETATION OF BOREHOLE HYDRAULIC TESTING IN DEEP BOREHOLES	31
3.1 Introduction	31
3.2 System Response	34
3.2.1 Fluid Properties/Response	34
3.2.2 Borehole/Formation Response	39

	<u>Page</u>	
3.3	Borehole Pressure History	40
3.4	Thermally-Induced Borehole Pressure Response	45
3.5	Borehole/Formation Skin Effects	53
3.6	Equipment Compliance Effects	54
3.7	Theory - Graph Theoretic Field Model (GTFM)	60
3.7.1	Data Analysis Requirements	60
3.7.2	Theoretical Development	62
3.7.3	Model Verification	79
3.8	Parameter Sensitivity Analyses	93
3.8.1	Borehole Pressure History	93
3.8.2	Thermally-Induced Borehole Pressure Response	103
3.8.3	Borehole/Formation Skin Effects	106
3.9	Applications to Field Tests	110
3.9.1	Boettstein Test 1326.2D	110
3.9.2	Boettstein Test 735.8S	118
3.9.3	Boettstein Test 1497.8S	123
4.	PRACTICAL CONSIDERATIONS IN EVALUATING BOREHOLE HYDRAULIC TESTING RESULTS	134
4.1	Introduction	134
4.2	Theoretical Aspects	135
4.2.1	Conceptualization and Assumptions Regarding the Flow Regime	135
4.2.2	Reference Pressure	139
4.2.3	Estimation of Storage Coefficient	140
4.3	Effects of Pre-Test Conditions	142
4.3.1	Borehole Pressure History	142
4.3.2	Thermally-Induced Borehole Pressure Response	143

	<u>Page</u>	
4.4	Borehole/Formation Considerations	145
4.4.1	Borehole Diameter	145
4.4.2	Measurement Scale	149
4.4.3	Radius of Influence	152
4.4.4	Porous Media Versus Fracture Flow Analyses	161
4.4.5	Orientation of Fractures or Higher Permeability Zones	163
4.4.6	Higher or Lower Permeability Skin Surrounding the Borehole	165
4.5	Fluid Considerations	166
4.6	Equipment Considerations	168
4.6.1	Accuracy of Equipment Readings and Depth Measurements	168
4.6.2	Equipment Compliance	169
4.6.3	Testing Procedures and Equipment Difficulties	171
4.7	Summary	172
5.	GUIDELINES FOR FORMATION PRESSURE MEASUREMENT AND BOREHOLE HYDRAULIC TESTING USING LYNES HYDROLOGIC TOOL	174
5.1	Introduction	174
5.2	Single Packer Testing For Estimation of Formation Pressure	176
5.2.1	Objectives	176
5.2.2	Procedures	176
5.2.3	Pressure Response Curves	185
5.3	Hydrogeologic Reconnaissance Logging for Hydraulic Conductivity Profiling	190
5.3.1	Objectives	190
5.3.2	Procedures	190
5.3.3	Pressure Response Curves	191
6.	REFERENCES	192

LIST OF FIGURES

	<u>Page</u>	
Figure 2.3-1	Schematic illustration of the interval pressure response during (a) a slug injection test and (b) a slug withdrawal test	9
Figure 2.3-2	Cooper et al. (1967) type curves to be used in the analysis of slug tests when h_0 and H_0 are known	10
Figure 2.3-3	Cooper et al. (1967) type curves to be used in the analysis of slug tests when h_0 is known and H_0 is unknown	11
Figure 2.3-4	Cooper et al. (1967) type curves to be used in the analysis of slug tests when H_0 is known and h_0 is unknown	12
Figure 2.4-1	Schematic illustration of the interval pressure response during (a) a pulse injection test and (b) a pulse withdrawal test	15
Figure 2.5-1	Schematic illustration of the interval pressure response during a drill stem test	18
Figure 2.5-2	Typical Horner plot for determination of formation pressure and permeability	21
Figure 2.6-1	Theis (1935) type curve for use in the analysis of pumping tests	24
Figure 2.6-2	Schematic illustration of the interval pressure response during a pumping test	26
Figure 3.1-1	Schematic illustration of (a) single packer and (b) double packer equipment configurations for borehole hydraulic testing	33
Figure 3.2-1a	Fluid density: variation with temperature and pressure	35

	<u>Page</u>	
Figure 3.2-1b	Fluid compressibility: variation with temperature and pressure	36
Figure 3.2-1c	Fluid coefficient of thermal expansion: variation with temperature and pressure	37
Figure 3.2-1d	Fluid viscosity: variation with temperature (Note: viscosity is relatively insensitive to changes in pressure)	38
Figure 3.3-1	Schematic pressure (P) and temperature (T) profiles in the formation on completion of drilling an interval	41
Figure 3.3-2	Schematic pressure responses for the test interval utilizing recommended test procedures to allow hydraulic conductivity determination (i.e., the pressure P_{SI} at the start of the test is substantially different from annulus pressure P_a or formation pressure P_f)	43
Figure 3.3-3	Schematic pressure responses for the test interval utilizing inadequate test procedures for hydraulic conductivity determination (i.e., the pressure P_{SI} at the start of the test is at or close to the annulus pressure P_a or formation pressure P_f)	44
Figure 3.3-4	Schematic illustration of the borehole pressure history that develops during a testing sequence	46
Figure 3.4-1	Schematic illustration of temperature profiles in the formation at the end of drilling and corresponding temperature variations in the borehole interval during testing for conditions of drill fluid temperature (a) greater than formation temperature and (b) less than formation temperature	48
Figure 3.4-2	Induced head change resulting from a temperature change in the test interval at initial temperatures of 20, 40, 60 and 80 °C (assuming no fluid loss to the formation)	49

	<u>Page</u>	
Figure 3.4-3	Schematic pressure responses during a pulse injection test in a low permeability formation for conditions corresponding to a temperature increase, a constant temperature and a temperature decrease	51
Figure 3.4-4	Schematic pressure responses during a pulse withdrawal test in a low permeability formation for conditions corresponding to a temperature increase, a constant temperature and a temperature decrease	52
Figure 3.6-1	Schematic illustration of applied forces in a single-packer test configuration. Packer deformation may occur in response to the forces acting on the tubing string, the head differential imposed on the test zone at the start of a test and the changing head differential between zones	57
Figure 3.6-2	Schematic illustration of double-packer test configuration showing pressures in various zones. Packer deformation may occur in response to the head differential imposed in the test zone at the start of a test and the changing head differentials between zones during the progress of the test	58
Figure 3.6-3	Induced head increase resulting from a reduction in test interval length for initial packed off intervals of 2, 10, and 50 m (assuming no fluid loss to the formation)	59
Figure 3.7-1	Schematic illustration of spatial discretization	65
Figure 3.7-2	Field graph fragments for three classes of nodes	68
Figure 3.7-3	Field graph for problem discretization	69
Figure 3.7-4	Field graph fragment illustrating geometric parameters and physical properties	71
Figure 3.7-5	Example graph segment for illustrating vertex postulate	76
Figure 3.7-6	Comparison between GTFM and Cooper et al., (1967) analytical solution results	82

	<u>Page</u>	
Figure 3.7-7	Comparison between GTFM and Bredehoeft and Papadopoulos (1980) analytical solution results	83
Figure 3.7-8	Comparison between GTFM and Lohman (1972) analytical solution results	84
Figure 3.7-9	Comparison between GTFM and Wang et al. (1978) analytical solution results for (a) infinite radius and (b) finite radius with zero flow boundary	85
Figure 3.7-9	Comparison between GTFM and Wang et al. (1978) analytical solution results for (c) finite radius with constant pressure boundary	86
Figure 3.7-10	Comparison between GTFM and SWIFT (from Faust and Mercer, 1984) results for a borehole/formation skin	87
Figure 3.7-11	Conditions for SWIFT simulation of nonisothermal case: (a) borehole temperature response and (b) borehole pressure response	90
Figure 3.7-12	SWIFT calculated temperature response and cubic-spline approximation utilized in GTFM	91
Figure 3.7-13	Comparison between GTFM and SWIFT calculated pressure responses	92
Figure 3.8-1	Illustration of the pretest conditions for the borehole pressure history simulation cases	94
Figure 3.8-2	GTFM calculated borehole pressure response for borehole pressure history cases for a pulse injection test with formation hydraulic conductivities of (a) 1×10^{-6} m/s and (b) 1×10^{-11} m/s	96
Figure 3.8-2	GTFM calculated borehole pressure response for borehole pressure history cases for a pulse injection test with formation hydraulic conductivities of (c) 1×10^{-12} m/s and (d) 1×10^{-13} m/s	97

	<u>Page</u>	
Figure 3.8-3	GTFM calculated borehole pressure response for borehole pressure history cases for a pulse withdrawal test with formation hydraulic conductivities of (a) 1×10^{-6} m/s and (b) 1×10^{-11} m/s	98
Figure 3.8-3	GTFM calculated borehole pressure response for borehole pressure history cases for a pulse withdrawal test with formation hydraulic conductivities of (c) 1×10^{-12} m/s and (d) 1×10^{-13} m/s	99
Figure 3.8-4	GTFM calculated radial pressure profiles in the formation at the start of the pulse withdrawal test of the borehole pressure history cases for borehole open periods of (a) 1 day and (b) 30 days	100
Figure 3.8-4	GTFM calculated radial pressure profiles in the formation at the start of the pulse withdrawal test of the borehole pressure history cases for borehole open periods of (c) 365 days	101
Figure 3.8-5	GTFM calculated borehole pressure response for borehole pressure history cases for a slug withdrawal test with formation hydraulic conductivities of (a) 1×10^{-6} m/s and (b) 1×10^{-8} m/s	102
Figure 3.8-6	Temperature response curves utilized in GTFM calculated borehole pressure responses for the pulse test cases involving thermal effects	104
Figure 3.8-7	GTFM calculated borehole pressure responses for various temperature response curves for (a) pulse injection test and (b) pulse withdrawal test	105
Figure 3.8-8	GTFM calculated borehole pressure responses for temperature response curve III and various hydraulic conductivities: (a) pulse injection test and (b) pulse withdrawal test	107

	<u>Page</u>	
Figure 3.8-9	GTFM calculated borehole pressure responses for a slug test for cases involving a borehole/formation skin	108
Figure 3.8-10	GTFM calculated borehole pressure responses for a pulse test for cases involving a borehole/formation skin	109
Figure 3.9-1	Assumed borehole pretest pressure history for Boettstein test 1326.2D	114
Figure 3.9-2	Measured (Δ) and best-fit simulated pressure response for Boettstein test 1326.2D using estimated formation pressures of 13650 kPa	115
Figure 3.9-3	Measured (Δ) and simulated pressure response for Boettstein test 1326.2D using estimated formation pressure of (A) 13600 kPa and (B) 13700 kPa	116
Figure 3.9-4	Schematic diagram showing equipment configuration and estimated formation pressure for Boettstein test 1326.2D	117
Figure 3.9-5	Measured (Δ) pressure data for test interval in Boettstein test 735.8S showing two pulse withdrawal tests, Psta and Pw02	120
Figure 3.9-6	Boettstein test 735.8S: (A) Assumed borehole pretest pressure history, and (B) Temperature history data and cubic spline temperature curve used in simulations	122
Figure 3.9-7	Measured (Δ) and simulated pressure response for Boettstein test 735.8S: (A) Test Psta showing best-fit hydraulic conductivity of 1×10^{-13} m/s, and (B) Test Pw02 showing best-fit hydraulic conductivity of 1×10^{-13} m/s	124
Figure 3.9-8	Measured interval pressure response for Boettstein test 1497.8S showing the initial pressure increase due to thermal effects, the 55 kPa pulse caused by packer "squeeze" and the subsequent pressure recovery	126

	<u>Page</u>	
Figure 3.9-9	Boettstein test 1497.8S: (A) Temperature history data during testing and cubic spline temperature curve used in GTFM simulations, and (B) Assumed borehole pretest pressure history	128
Figure 3.9-10	Boettstein test 1497.8S: (A) Sensitivity of simulated response to changes in hydraulic conductivity with best-fit hydraulic conductivity of 9.5×10^{-14} m/s, and (B) Sensitivity of simulated response to changes in formation pressure with best-fit formation pressure of 15179 kPa	131
Figure 3.9-11	Schematic diagram showing equipment configuration and estimated formation pressure for Boettstein test 1497.8S	132
Figure 4.2-1	Idealized conceptualization of hydraulic testing in a packer-isolated interval	136
Figure 4.4-1	Calculation of the effect of borehole diameter on calculated pressure response for a pulse test using the Bredehoeft and Papadopulos (1980) analytical solution	147
Figure 4.4-2	Calculation of the effect of borehole diameter on calculated pressure for a pulse test using the Cooper et al. (1967) analytical solution	148
Figure 4.4-3	Conceptualization of the importance of measurement scale illustrating a case with the packer-isolated interval being much larger than the formation thickness	151
Figure 4.4-4	Radial pressure profiles into the rock formation for various times during a pulse test for a formation hydraulic conductivity of 1×10^{-11} m/s	153
Figure 4.4-5	Radial pressure profiles into the rock formation for various times during a pulse test for a formation hydraulic conductivity of 1×10^{-12} m/s	154

	<u>Page</u>	
Figure 4.4-6	Radial pressure profiles into the rock formation for various times during a pulse test for a formation hydraulic conductivity of 1×10^{-13} m/s	155
Figure 4.4-7	Radial pressure profiles into the rock formation for various times during a slug test for a formation hydraulic conductivity of 1×10^{-6} m/s	158
Figure 4.4-8	Radial pressure profiles into the rock formation for various times during a slug test for a formation hydraulic conductivity of 1×10^{-8} m/s	159
Figure 4.4-9	Radial pressure profiles into the rock formation for various times during a slug test for a formation hydraulic conductivity of 1×10^{-10} m/s	160
Figure 4.4-10	Schematic illustration of three different types of flow models (a) porous media flow model (e.g., Bredehoeft and Papadopoulos, 1980) where flow occurs throughout the homogeneous media, (b) single fracture flow model (e.g., Wang et al., 1978) where flow occurs in the fractures only and (c) fracture/matrix flow model (e.g., Barker and Black, 1983) where flow occurs in fractures and between fractures in the rock matrix	162
Figure 4.4-11	Comparison between fracture flow simulation results (symbols) using Wang et al. (1978) solution and porous media simulation results (lines) using Bredehoeft and Papadopoulos (1980) for various hydraulic conductivities	164
Figure 4.5-1	Various field conditions under which formation pressures or water levels are measured	167
Figure 5.2-1	Flow chart for formation pressure measurement with LYNES hydrologic test tool	180

	<u>Page</u>
Figure 5.2-2 Procedures for in-situ pressure measurement	181
Figure 5.2-3 Pressure response curves: $P_{\text{formation est}} > P_{\text{annulus}}$	182
Figure 5.2-4 Pressure response curves: $P_{\text{formation est}} < P_{\text{annulus}}$	183

LIST OF TABLES

		<u>Page</u>
Table 3.7-1	Summary of Parameter Values Utilized in Verification Cases Comparing GTFM to Analytical Solution Results	81
Table 3.7-2	Summary of Parameter Values Utilized in SWIFT - GTFM Model Comparison Case	89
Table 3.9-1	Physical description of test conditions for Boettstein test 1326.2D	112
Table 3.9-2	Model parameters for test data analysis for Boettstein test 1326.2D	113
Table 3.9-3	Physical description of test conditions for Boettstein test 735.8S	119
Table 3.9-4	Model parameters for test data analysis for Boettstein test 735.8S	121
Table 3.9-5	Physical description of test conditions for Boettstein test 1497.8S	125
Table 3.9-6	Model parameters for test data analysis for Boettstein test 1497.8S	130

1. INTRODUCTION

Hydraulic testing refers to the tests required to obtain representative measurements of formation pressure and hydraulic conductivity. Hydraulic testing has, as its basis, the quantitative description of transient ground water movement through porous media based on an analogy with heat flow (Theis, 1935). Until recent years hydraulic testing was conducted for the most part in "aquifers" or relatively permeable formations. As the concept of deep geologic disposal of radioactive wastes matured, the need developed to conduct hydraulic tests at depth in relatively impermeable formations where the most significant permeability is that associated with fractures or fracture zones. As this need developed, it has become apparent that many of the assumptions normally applied in the field of hydrogeology are inappropriate for accurate test interpretation in deep low-permeability formations. Two of the most obvious assumptions which are immediately apparent as inappropriate are those of isothermal test conditions and constant fluid properties. The depths at which measurements are required (several thousand metres) clearly include a large range of temperature and fluid density conditions. A further assumption which has generated considerable quantitative evaluation in recent years is the suitability of porous media flow equations for fractured media analyses. The results of these evaluations (e.g., Barker and Black, 1983) has provided considerable insight into the conditions under which porous/fractured media conceptualizations differ.

Review of the published literature on hydraulic testing and interpretive methods conducted at the commencement of the NAGRA program in 1982 indicated a need for a comprehensive hydraulic testing interpretive capability. The identified capability was one which needed to allow for variability in test conditions beyond the normal initial and boundary conditions inherent in the classic hydrogeologic methods (e.g., Theis, 1935; Jacob 1940; Hvorslev, 1951; Cooper et al., 1967) and the more recent analytical solutions specific to fractured or low permeability formations (e.g., Wang et al., 1978; Bredehoeft and Papadopoulos, 1980). The interpretive requirements included the ability

- 2 -

to quantitatively account for thermally induced pressure responses, borehole pressure history (resulting in a variable pressure "skin" developing around the test interval) as well as equipment compliance. The hydrogeologic and reservoir engineering literature contain numerous papers dealing with many of the above, however, an interpretive capability combining all of the important aspects was not available. Consequently, a comprehensive hydraulic testing model was developed for microcomputer and field or office application using Graph Theoretic Field Model techniques. The model has extended interpretive capability, allowing numerous combinations of borehole history, thermal effects and equipment compliance, to be quantitatively incorporated in the analysis. The model (GTFM) is successfully benchmarked against the more restrictive analytical solutions and provides a considerably advanced borehole testing interpretive capability. The application and use of GTFM as well as other analytical and numerical interpretive techniques are provided throughout the report.

2. THEORETICAL ASPECTS OF BOREHOLE HYDRAULIC TESTING METHODS

2.1 Introduction

The purpose of this section is to provide an introduction to the theoretical basis for each of the more common hydraulic testing methods and a brief development of the appropriate analytical solution that may be used for analysis of the field measured pressure or water level response data. Examples of the application of each method are found in the original papers and the interested reader is directed to the appropriate references.

The following methods are included in this section:

- Slug injection or withdrawal tests;
- Pulse injection or withdrawal tests;
- Drill stem tests;
- Pumping or injection tests;
- Constant drawdown flow tests;
- Multiple well tests.

Sections 3 and 4 deal with the basic difficulties associated with many of the measurement and interpretation techniques and quantitatively address the uncertainty associated with hydraulic testing from both theoretical and practical points of view.

2.2 Governing Equations

The basis of ground water flow lies in the development of Darcy's Law which relates the rate of ground water flow to a hydraulic gradient. Darcy's Law is defined as:

$$v = - K \frac{dh}{dl} \quad (2.2-1)$$

where	v	specific discharge, $L^3L^{-2}t^{-1}$;
	K	hydraulic conductivity, Lt^{-1} ;
	h	hydraulic head, L;
	l	distance between head measurements, L;
	dh/dl	hydraulic gradient, L^{-1} .

In equation 2.2-1, K is a constant of proportionality and is a function of both the medium and the fluid. The hydraulic conductivity can be defined in terms of medium and fluid properties as:

$$K = \frac{k\rho g}{\mu} \quad (2.2-2)$$

where

k	intrinsic permeability, L^2
ρ	fluid density, ML^{-3} ;
μ	fluid viscosity, $ML^{-1}t^{-1}$;
g	gravitational constant, Lt^{-2} .

For the case of a porous medium, the intrinsic permeability is a property of the medium alone being a function of the grain size, sphericity and roundness of the grains, the nature of their packing and degree of cementation.

The concept of a hydraulic potential developed by Hubbert (1940) was derived on the basis of energy relationships for a homogeneous fluid. The fluid potential (ϕ) in a porous medium is simply defined as follows:

$$\phi = gh \quad (2.2-3)$$

For situations dealing with homogeneous fluids (i.e., constant properties spatially and temporally), the hydraulic head is related to pressure by the following equation:

$$h = z + \frac{p}{\rho g} \quad (2.2-4)$$

where

z	elevation head (distance from the measuring point to a reference datum) L ;
p	pressure, $ML^{-1}t^{-2}$.

When Darcy's Law and the concept of hydraulic potential are combined with an equation of continuity that describes the conservation of fluid mass during flow through porous media the equation for steady state flow results. This equation for a

homogeneous, isotropic and incompressible medium is given by (Hubbert, 1940):

$$\frac{\partial^2 h}{\partial x^2} + \frac{\partial^2 h}{\partial y^2} + \frac{\partial^2 h}{\partial z^2} = 0 \quad (2.2-5)$$

where x , y , z are the spatial coordinates.

Hydraulic testing methods are generally based on an assumption of radial flow into a confined, elastic formation. The equation of flow used in hydraulic testing that takes into account the compressibility and effective stress of the formation is the transient radial flow equation.

The mathematical formulation of the transient radial ground water flow equation for a homogeneous, isotropic medium is given by (Theis, 1935):

$$\frac{\partial^2 h}{\partial r^2} + \frac{1}{r} \frac{\partial h}{\partial r} = \frac{S}{T} \frac{\partial h}{\partial t} \quad (2.2-6)$$

where	r	radial distance from borehole axis, L;
	S	storage coefficient, dimensionless;
	T	transmissivity of tested interval, L^2t^{-1} .

The transmissivity and storage coefficient of the tested interval are defined by:

$$T = Kb \quad (2.2-7)$$

$$\text{and } S = S_s b \quad (2.2-8)$$

where	S_s	specific storage, L^{-1} ;
	b	length of tested interval, L.

The following methods have as their common starting point the transient radial flow equation.

2.3 Slug Injection or Withdrawal Test

The pressure recovery in a borehole after the injection or withdrawal of a known volume (slug) of water can be analyzed using the method of Cooper et al. (1967). The slug test method is derived from the transient radial flow equation (equation 2.2.6). The boundary conditions for a slug injection or slug withdrawal test are:

$$h(r_s, t) = H(t) \quad (2.3-1)$$

$$h(\infty, t) = h_o \quad (2.3-2)$$

$$h(r, 0) = h_o \quad (2.3-3)$$

$$H(0, 0) = H_o \quad (2.3-4)$$

$$\frac{2\pi r_s T \partial h(r_s, t)}{\partial r} = \frac{\pi r_c^2 \partial H(t)}{\partial t} \quad (2.3-5)$$

where

- h $h(r, t)$ is the hydraulic head in the borehole and formation, L;
- h_o the in-situ formation hydraulic head, L;
- H $H(t)$ is the hydraulic head in the borehole test interval during the recovery period, L;
- H_o the initial head in the borehole or well due to the injection or withdrawal slug, L;
- S the storage coefficient of the tested interval, dimensionless;
- T transmissivity of the tested interval, $L^2 t^{-1}$;
- r radial distance from the borehole axis, L;
- r_s radius of the borehole or well screen, L;
- r_c radius of the casing, L;
- t time since start of the injection or withdrawal, t.

Equation 2.3-1 states that at the start of the test the head in the formation at r_s is equal to the head in the borehole. Equation 2.3-2 states that at infinite distance the head in the formation remains unchanged. Equations 2.3-3 and 2.3-4 state that initially the head outside the well is equal to h_o and inside the well is equal to H_o . Equation 2.3-5 states that the rate of flow of water out of (or into) the formation is equal to the water volume decrease (or increase) in the borehole or well.

An appropriate solution to the problem can be obtained by applying the Laplace transform with respect to time to the governing equations. The solution of the problem presented in Cooper et al. (1967) is

$$H' = \frac{H-h_o}{H_o-h_o} = \frac{8\alpha}{\pi^2} \int_0^\alpha \frac{e^{-\beta u^2/\alpha}}{u[(uJ_0(u)-2\alpha J_1(u))^2 + (uY_0(u)-2\alpha Y_1(u))^2]} du \quad (2.3-6)$$

where

$J_0(u)$	zero order Bessel function of the first kind;
$J_1(u)$	first order Bessel function of the first kind;
$Y_0(u)$	zero order Bessel function of the second;
$Y_1(u)$	first order Bessel function of the second kind;

$$\alpha = r_s^2 S / r_c^2 \quad (2.3-7)$$

is the dimensionless storage coefficient and

$$\beta = Tt / r_c^2 \quad (2.3-8)$$

represents dimensionless time.

In this form the head change can be computed numerically by integration of equation 2.3-6.

Under actual test conditions a typical pressure response (or hydraulic head response) for a slug injection or withdrawal test is as shown in

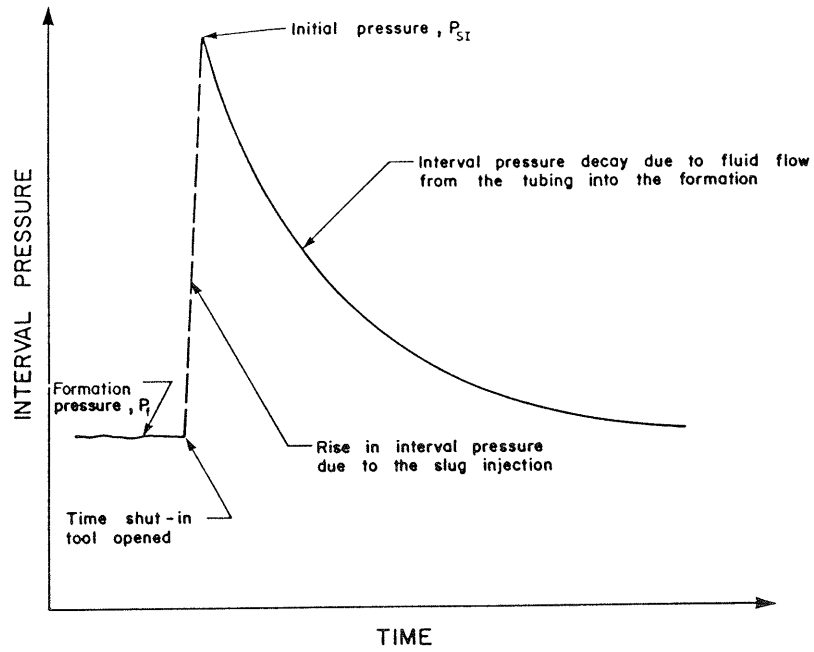
Figure 2.3-1. For illustrative purposes, the procedures utilizing a drill tubing and the Lynes downhole hydrologic tool and packer equipment will be discussed. The Lynes hydrologic tool measures the pressure in the packer-isolated interval, therefore the following discussion and the figures use the term pressure when referring to the transducer measured response. First the test interval is isolated from the drill tubing by closing the shut-in tool. The drill tubing is then bailed out for the initial condition for a slug withdrawal test or water is added to the drill tubing of a slug injection test. Once the water level in the casing string is substantially different from the initial water level corresponding to the head in the formation, the shut-in valve is opened and the test begins. The water level or pressure recovery occurs as water flows into or out of the formation and the water level returns to its initial position (i.e., h_0).

To aid in the interpretation of slug tests three sets of type curves can be produced from equation 2.3-6 depending on the method of plotting. The type curve sets are:

- (1) H' versus $\log_{10} \beta$ (Figure 2.3-2);
- (2) $\log_{10} H'$ versus $\log_{10} \beta$
(Figure 2.3-3);
- (3) $\log_{10} (1-H')$ versus $\log_{10} \beta$
(Figure 2.3-4);

where H' is the hydraulic head recovery from equation 2.3-6 and β is the dimensionless time (equation 2.3-8). Each of these set of curves can be used under different conditions. Set 1 can be used for analysing slug test data when both the initial hydraulic head in the borehole or well due to the slug injection or withdrawal (i.e., H_0) and the in-situ hydraulic head of the formation (i.e., h_0) are known. Set 2 is best used when the initial hydraulic head (H_0) is unknown but the in-situ formation head is known. Set 3 can be used when the in-situ formation head (h_0) is unknown and the initial hydraulic head (H_0) is known. The following table summarizes which type curve is best

a INTERVAL PRESSURE RESPONSE DURING A SLUG INJECTION TEST



b INTERVAL PRESSURE RESPONSE DURING A SLUG WITHDRAWAL TEST

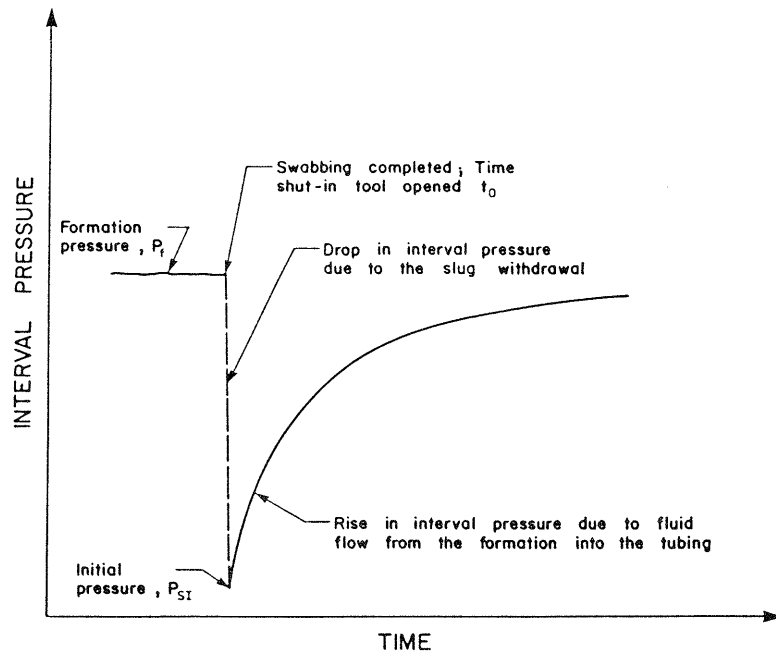


Figure 2.3-1

Schematic illustration of the interval pressure response during (a) a slug injection test and (b) a slug withdrawal test

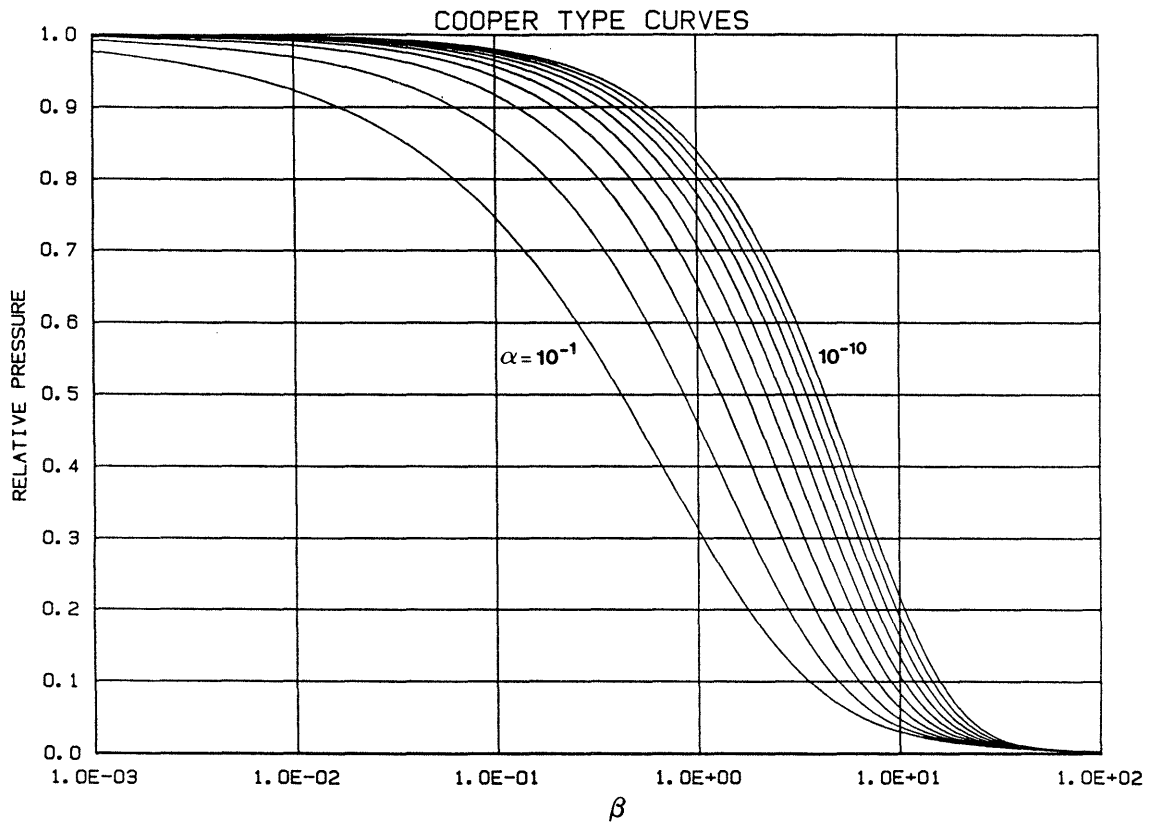


Figure 2.3-2 Cooper et al. (1967) type curves to be used in the analysis of slug tests when h_0 and H_0 are known

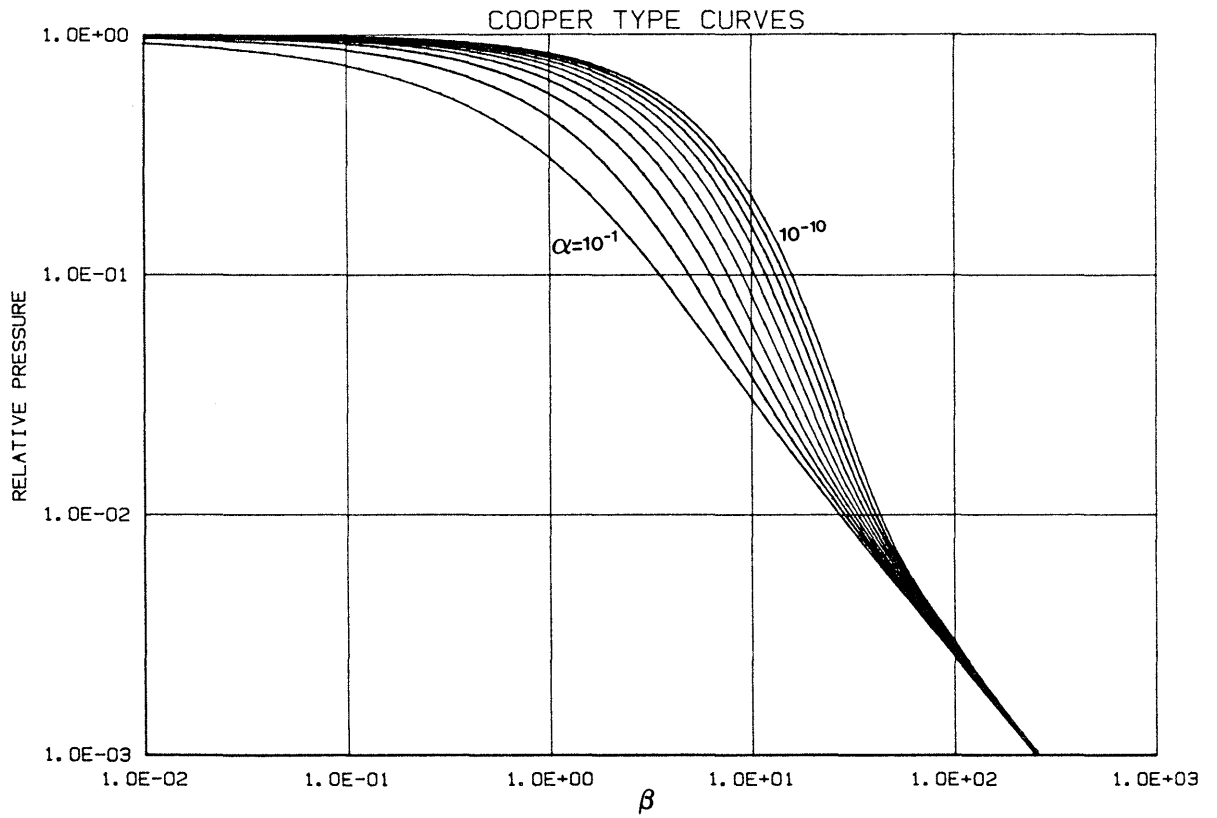


Figure 2.3-3 Cooper et al. (1967) type curves to be used in the analysis of slug tests when h_0 is known and H_0 is unknown

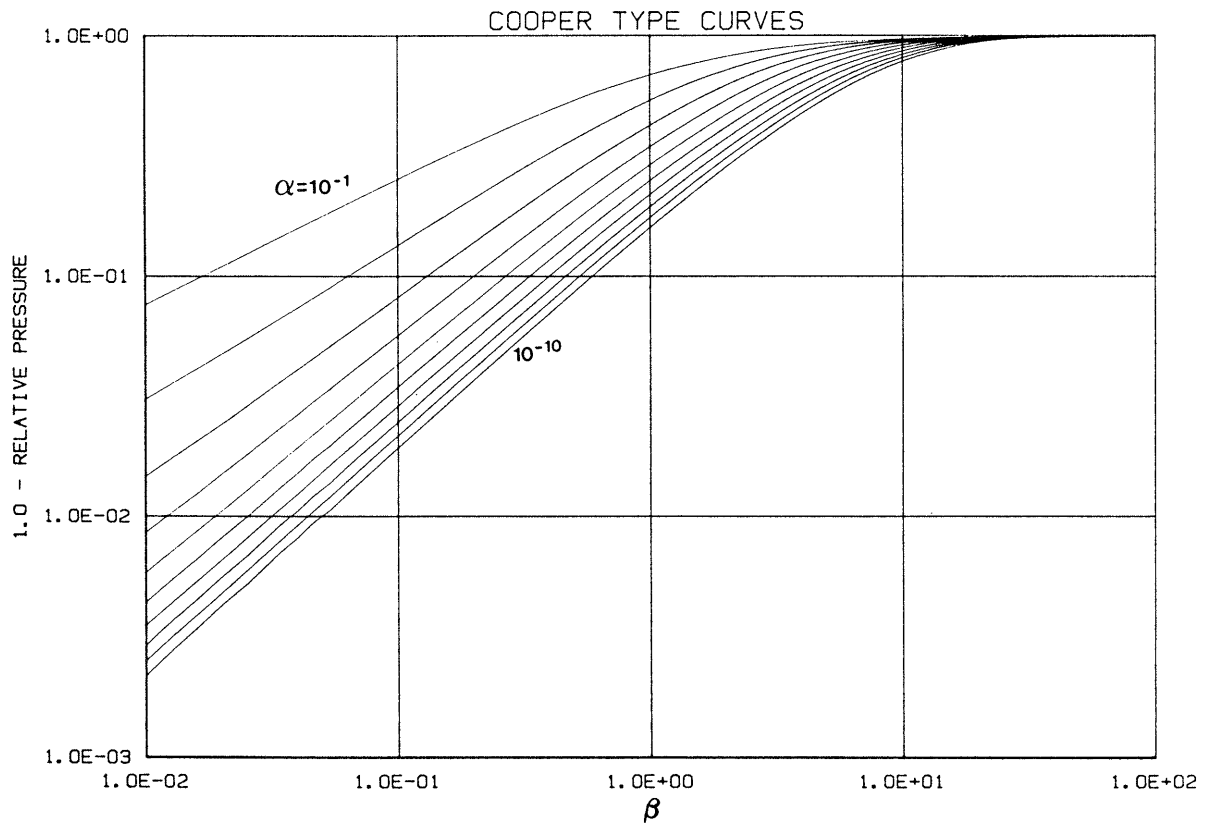


Figure 2.3-4 Cooper et al. (1967) type curves to be used in the analysis of slug tests when H_0 is known and h_0 is unknown

to use under a given condition:

Type Curve	Conditions	Figure
H' versus $\log_{10} \beta$	H_o known h_o known	2.3-2
$\log_{10} H'$ versus $\log_{10} \beta$	h_o known H_o unknown	2.3-3
$\log_{10} (1-h_o)$ versus $\log_{10} \beta$	H_o known h_o unknown	2.3-4

To determine the formation hydraulic parameters, the appropriate type curves (Figure 2.3-2, 2.3-3 or 2.3-4, depending on the known initial conditions) can be superimposed and compared to the formation response to determine which type curve best matches the formation response. A match point is chosen and values at the match point of real time t and dimensionless time β are used to solve for transmissivity in equation 2.3-8. The best-fit curve gives a value of α which in turn can be used to solve for storage coefficient, S , in equation 2.3-7.

2.4 Pulse Injection or Withdrawal Test

2.4.1 Pulse Test - Porous Media Approach

The pulse test method is essentially a modification of the conventional slug test described by Cooper et al. (1967). Instead of allowing water to flow to or from the borehole as in the slug test, in the pulse test the interval is suddenly over or under pressured with an addition or removal of a volume of water and then shut-in. The pressure decay or recovery with time is then observed. The hydraulic response in a test interval for a pulse injection and a pulse withdrawal test is shown schematically

in Figure 2.4-1. The theoretical development of the method is outlined in Bredehoeft and Papadopoulos (1980).

The pulse test mathematical formulation is similar to the slug test and uses equations 2.2-6 and 2.3-1 to 2.3-4. It differs only in the fact that equation 2.3-5 is written in terms of the rate at which the water flows from the well into the formation being equal to the rate at which the volume of water stored within the pressurized system expands as the head or pressure within the system declines. In the slug test the rate at which water flows from the well into the formation is equal to the rate at which the volume of water stored in the well changes as the water level declines in the well. The corresponding boundary condition for the pulse test (replacing equation 2.3-5 for the slug test) takes the form:

$$2\pi r_s T \frac{\partial h}{\partial r}(r_s, t) = V_w C_w \rho_w g \frac{\partial H}{\partial t}(t) \quad (2.4-1)$$

where

V_w	volume of water within the pressurized section of the system, L^3 ;
C_w	compressibility of water, $M^{-3}Lt^2$;
ρ_w	density of water, ML^{-3} ;
g	gravitational constant, Lt^{-2} .

and all other terms are as previously defined.

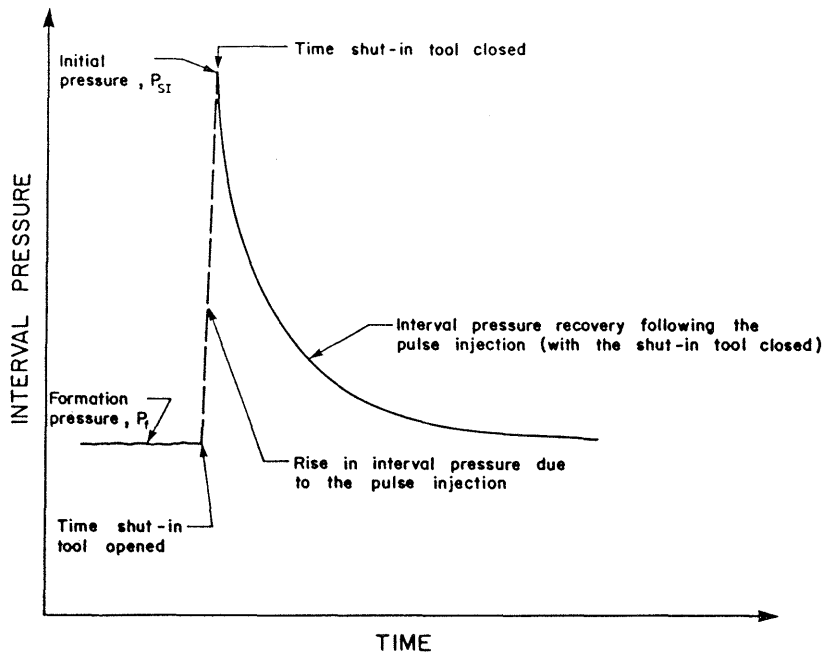
Note that if r_c^2 in equation 2.3-5 is replaced by $V_w C_w \rho_w g / \pi$ then equation 2.3-5 is equivalent to equation 2.4-1 and therefore the same solution, equation 2.3-6, can be used with the following changes:

$$\alpha = \frac{\pi r_s^2 S}{V_w C_w \rho_w g} \quad (2.4-2)$$

and

$$\beta = \frac{Tt}{V_w C_w \rho_w g} \quad (2.4-3)$$

a INTERVAL PRESSURE RESPONSE DURING A PULSE INJECTION TEST



b INTERVAL PRESSURE RESPONSE DURING PULSE WITHDRAWAL TEST

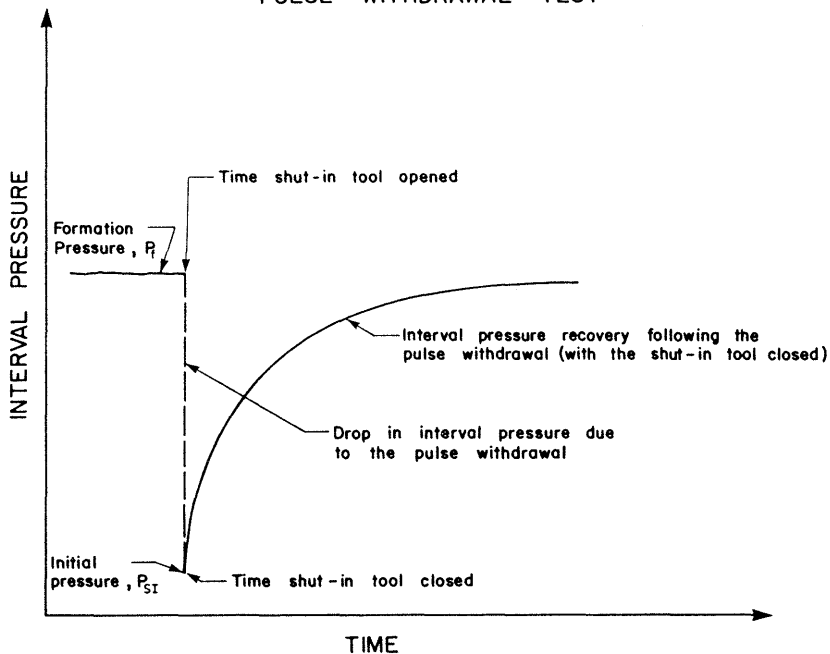


Figure 2.4-1 Schematic illustration of the interval pressure response during (a) a pulse injection test and (b) a pulse withdrawal test

Equation 2.3-6, 2.4-2 and 2.4-3 can then be used to generate, by computer, a series of type curves of hydraulic head recovery, $H' = (H_0 - h_0)$, versus dimensionless time, β , at various values of transmissivity (or hydraulic conductivity) as was done for the slug test. The type curves produced for the pulse test are identical to those produced for the slug test (Figures 2.3-2, 2.3-3 and 2.3-4). The only difference in the two are the terms used to describe α and β .

The use of the type curves is the same as the slug test. The field recovery data is plotted at the same scale as the type curves. The type curves are superimposed on the field data and a match point is chosen. Using the values of real time t and dimensionless time β at the match point, equation 2.4-3 can be solved to yield a value for T , the aquifer transmissivity. The value of α for the best-fit type curve can then be used in equation 2.4-2 to determine the storage coefficient, S .

2.4.2 Pulse Test - Fractured Media Approach

Wang et al. (1978) describe a method whereby the early pulse test data can be used to estimate an equivalent single fracture aperture width ($2b$).

The method is based on the flow between parallel plates relationship given by

$$K = \frac{\rho g (2b)^2}{12\mu} \quad (2.4-4)$$

where

K	hydraulic conductivity, Lt^{-1} ;
ρ	fluid density, ML^{-3} ;
μ	fluid viscosity, $ML^{-1}t^{-1}$;
$2b$	fracture aperture, L .

The boundary condition at the wellbore radius is the continuity of flow velocities in the fracture and at the wellbore fracture contact. Wang et al. (1978) give analytical solutions for calculating the pressure in the packer-isolated borehole interval for a variety of cases involving fracture(s) perpendicular to the wellbore:

- single infinite fracture;
- single finite fracture with no-flow fracture boundary;

- 17 -

- single finite fracture with constant pressure fracture boundary;
- finite fracture in series with infinite fracture;
- finite fracture in parallel with infinite fracture.

The interested reader is referred to the paper by Wang et al. (1978) for the appropriate analytical solutions available for computer implementation to assist in data interpretation of pulse tests in fractured media.

2.5 Drill Stem Test

Drill stem tests (DST) are a method of permeability testing whereby the formation is allowed to flow (i.e., similar to a slug test) and then is shut-in and the pressure allowed to build-up. The pressure response in an interval during a DST is shown schematically in Figure 2.5-1.

Graphical analysis or "Horner plot" methods are frequently used for evaluation of drill stem tests and are well documented in the petroleum engineering literature (eg., Matthews and Russell, 1967; Earlougher, 1977; Lee, 1982). The methods are based upon approximating the pressure behaviour of a formation with the analytic equation for a line source well in an infinite reservoir. The equation for the bottom-hole flowing pressure of a well that has produced at a rate q for a time t is:

$$P_f = P_i + \frac{q\mu}{4\pi kb} \operatorname{Ei}\left(\frac{-\theta\mu cr_w^2}{4kt}\right) \quad (2.5-1)$$

where	P_f bottom hole flowing pressure at time t , $ML^{-1}t^{-2}$; P_i initial static formation pressure, $ML^{-1}t^{-2}$; q flow rate, L^3t^{-1} ; μ viscosity of formation fluid, $ML^{-1}t^{-2}$;
-------	---

INTERVAL PRESSURE RESPONSE DURING
A DRILL STEM TEST

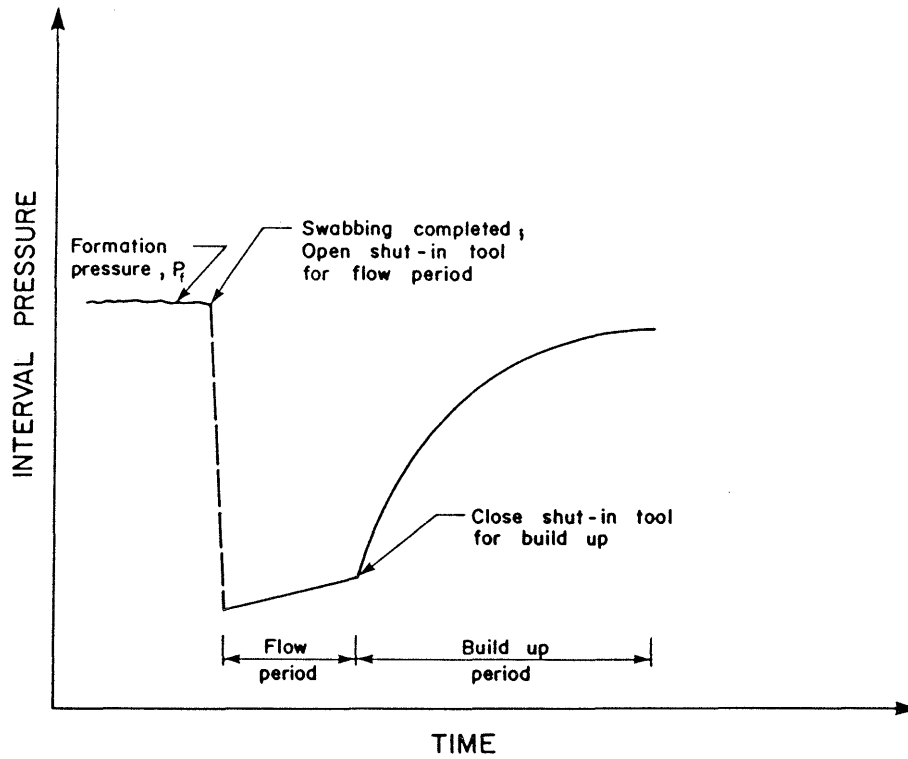


Figure 2.5-1 Schematic illustration of the interval pressure response during a drill stem test

- 19 -

- b formation or interval thickness,
 L;
 θ porosity of formation,
 dimensionless;
 c formation/fluid compressibility,
 $M^{-1}Lt^2$;
 r_w radius of well, L;
 t time since start of flow period,
 t;
 k intrinsic permeability, L^2 ;
 Ei exponential integral.

Equation 2.5-1 can be approximated by using the first two terms of the series expansion for Ei. This approximation is valid for large flow times. Therefore:

$$P_f = P_i + \frac{q\mu}{4\pi kb} \ln \left(\frac{\gamma\theta\mu cr_w^2}{4kt} \right) \quad (2.5-2)$$

where γ Eulers' constant.

If the formation is then shut-in (i.e., $q = 0$) for a time Δt after producing for a time t , the principle of superposition can be used to obtain the pressure change at time Δt .

$P_i - P_s =$ (pressure change caused by rate q
 for time $t + \Delta t$) + (pressure
 change caused by rate change $-q$ for
 time Δt)

$$P_i - P_s = \frac{-q\mu}{4\pi kb} \left[\ln \left(\frac{\gamma\theta\mu cr_w^2}{4k(t + \Delta t)} \right) - \ln \left(\frac{\gamma\theta\mu cr_w^2}{4k\Delta t} \right) \right] \quad (2.5-3)$$

where P_s pressure after shut-in,
 $ML^{-1}t^{-2}$;

Rearranging 2.5-3:

$$P_s = P_i - \frac{q\mu}{4\pi kb} \ln \left(\frac{t+\Delta t}{\Delta t} \right) \quad (2.5-4)$$

$$P_s = P_i - \frac{q\mu \ln(10)}{4\pi kb} \log \left(\frac{t+\Delta t}{\Delta t} \right)$$

Equation 2.5-4 is valid when q is constant over the duration of the flow period (t). In many cases the well production rate varies during the flow period. This may be compensated for by calculating a pseudo flow time t^* :

$$t^* = \frac{Q_T}{q_e} \quad (2.5-5)$$

where Q_T total volume of flow during the flow period, L^3 ;
 q_e flow rate immediately prior to shut-in, L^3t^{-1} .

The parameters t^* and q_e may be substituted into equation 2.5-4 yielding:

$$P_s = P_i - \frac{q_e \mu \ln(10)}{4\pi kb} \log \frac{t^* + \Delta t}{\Delta t} \quad (2.5-6)$$

If the observed pressure during the shut-in period is plotted against the logarithm of $\frac{t^* + \Delta t}{\Delta t}$, a straight line should result. This graphical plot is called a Horner plot, an example of which is given in Figure 2.5-2. When used in conjunction with equation 2.5-6, the Horner plot can be used as follows to determine the formation pressure P_i and the hydraulic conductivity of the test interval.

After a very long shut-in time: ($\Delta t \rightarrow \infty$) and

$$\frac{t^* + \Delta t}{\Delta t} \approx 1.$$

Under these conditions, equation 2.5-6 reduces to

$$P_s = P_i \quad (2.5-7)$$

P_i can therefore be determined by extrapolating the curve plotted through the data points to

$$\frac{t^* + \Delta t}{\Delta t} = 1.$$

Hydraulic conductivity can be determined from the slope of the plotted graph. From equation 2.5-6:

$$m = \frac{q_e \mu \ln(10)}{4\pi kb} \quad (2.5-8)$$

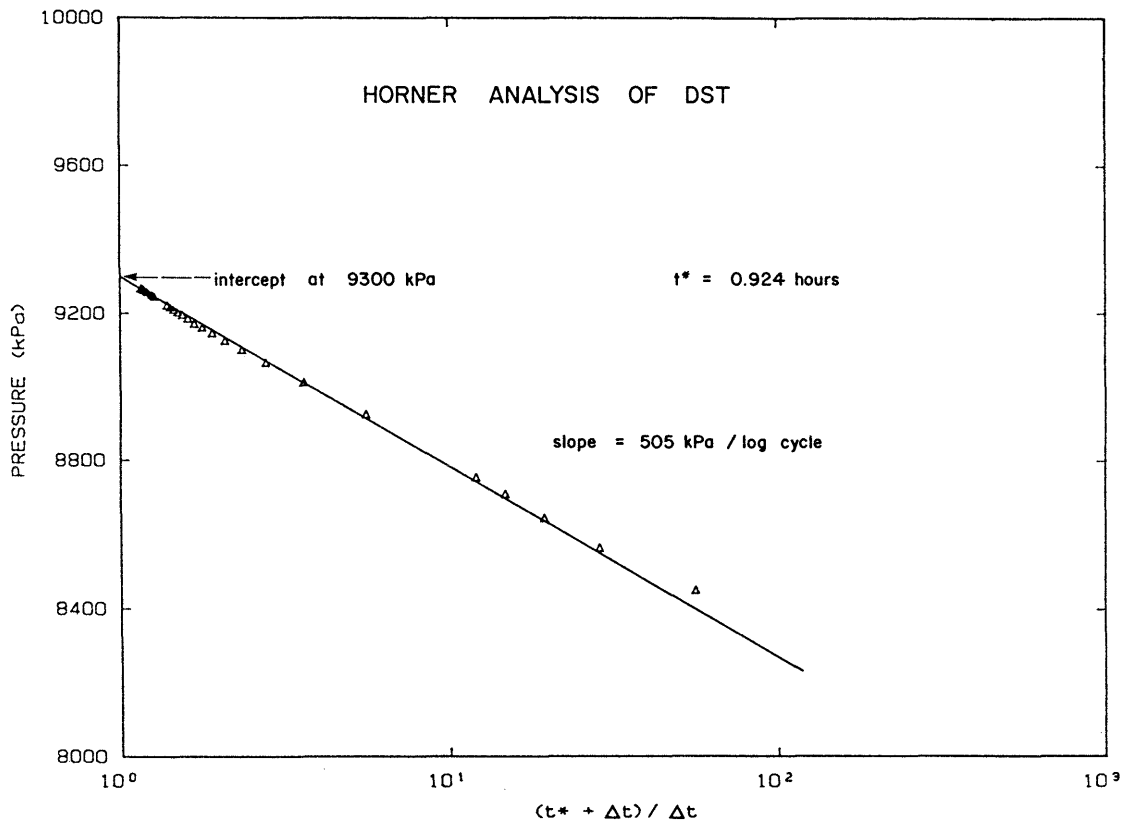


Figure 2.5-2 Typical Horner plot for determination of formation pressure and permeability

where m slope of graph (i.e., absolute change in pressure over one log cycle of $\frac{(t^* + \Delta t)}{\Delta t}$)

Also,

$$k = \frac{K\mu}{\rho g} \quad (2.5-9)$$

where K hydraulic conductivity, Lt^{-1} ;
 ρ density of formation fluid, ML^{-3} ;
 g gravitational constant, Lt^{-2} .

Substituting equation 2.5-9 into 2.5-8 and rearranging yields the following expression for calculating the hydraulic conductivity

$$K = \frac{q_e \rho g \ln(10)}{4\pi mb} \quad (2.5-10)$$

In summary, the pressure response data from a DST test when displayed graphically as a Horner plot can be used in conjunction with equation 2.5-10 to yield an estimate of the hydraulic conductivity of the formation.

2.6 Pumping or Injection Test

The analysis of pumping or injection tests is given in standard text books on hydrogeology. The following theory is based on the original publication by Theis (1935).

Using the transient radial flow equation, (equation 2.2-1, Theis (1935) utilized an analogous heat flow problem to develop the analytical solution corresponding to the following initial and boundary conditions

$$h(r, 0) = h_0, \quad r_w \leq r \leq \infty \quad (2.6-1)$$

$$h(\infty, t) = h_0, \quad t \geq 0 \quad (2.6-2)$$

$$\lim_{r=r_w \rightarrow 0} 2\pi rT \frac{\partial h}{\partial r} = Q \quad t \geq 0 \quad (2.6-3)$$

- 23 -

where	h	hydraulic head in the borehole and formation, L;
	h_0	in-situ formation hydraulic head, L;
	r	radial distance from the borehole axis, L;
	r_w	borehole or well radius, L;
	t	time, t;
	T	transmissivity, L^2t^{-1} ;
	Q	borehole pumping or injection rate, L^3t^{-1} .

This analytical solution written in terms of the drawdown in the aquifer is:

$$h_0 - h(r, t) = \frac{Q}{2\pi T} \int_u^\infty \frac{e^{-u} du}{u} \quad (2.6-4)$$

where:

$$u = \frac{r^2 S}{4Tt} \quad (2.6-5)$$

where S storage coefficient, LL^{-1} .

The integral given in equation 2.6-4 is called the well function $W(u)$ and is obtained from tables of the exponential integral or it can be calculated from the relationship:

$$W(u) = \left[-0.5772 - \ln(u) + u - \frac{u^2}{2 \cdot 2!} + \frac{u^3}{3 \cdot 3!} - \frac{u^4}{4 \cdot 4!} + \dots \right] \quad (2.6-6)$$

The integral can be written as the well function $W(u)$ and equation 2.6-4 rewritten as:

$$h_0 - h = \frac{Q}{4\pi T} W(u) \quad (2.6-7)$$

The graphical illustration of u versus $W(u)$, the well known Theis curve, is given in Figure 2.6-1.

In a pumping test using equations 2.6-5 and 2.6-7, the drawdown in the well or in any piezometer at a radius of r in the formation can be predicted given

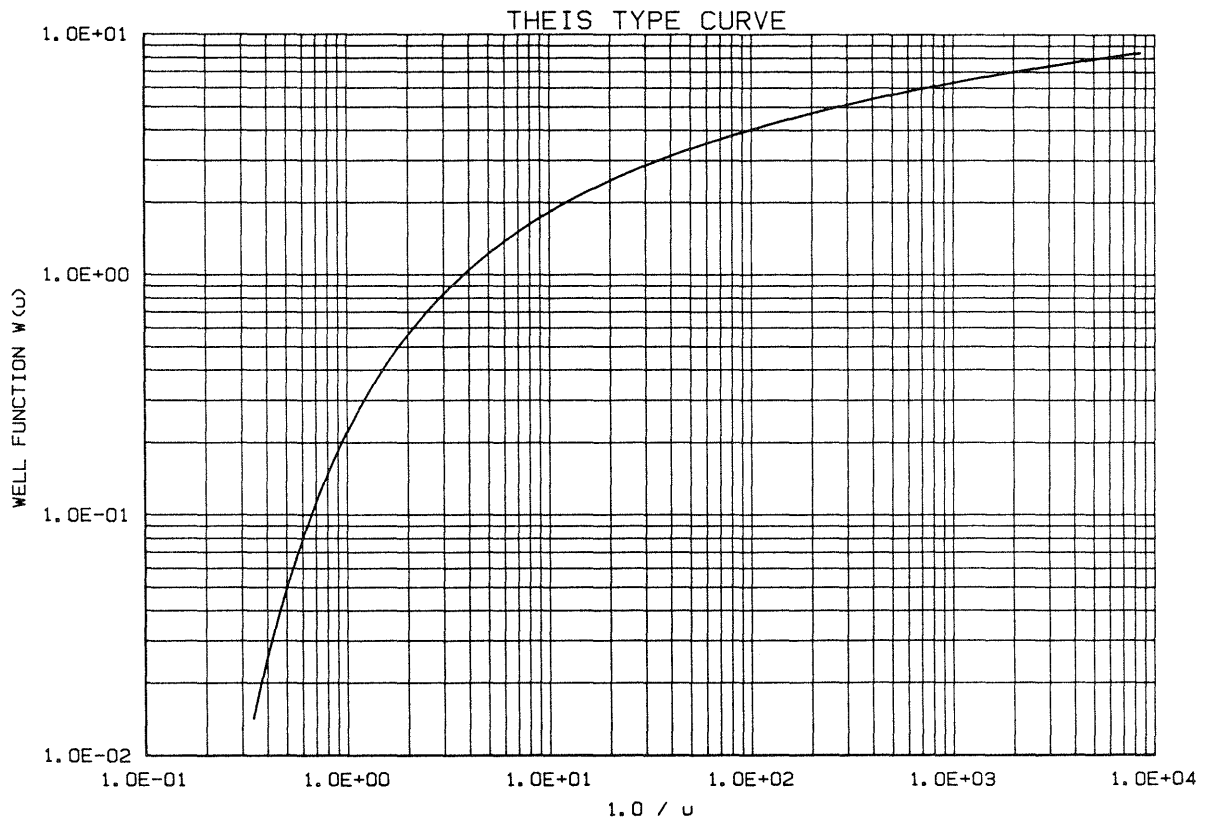


Figure 2.6-1 Theis (1935) type curve for use in the analysis of pumping tests

the rate at which the well is pumped (see Figure 2.6-2). The magnitude of the drawdown is dependent of the values of T and S. To determine T and S from a pump test, the drawdown with time in the well or an adjacent piezometer during pumping at a rate Q is compared to the Theis type curve. The values of u and W(u) are obtained for a specific match point. The values of u and W(u) are then applied against equations 2.6-5 and 2.6-7 to compute T and S for the formation. The same technique is applied to an injection test with the exception that the injection rate is different in sign from the pumping rate and the drawdown is a water level increase.

For variable-rate pumping or injection, the principle of superposition can be utilized to calculate the change in hydraulic head for various choices of parameter values. The drawdown at distance r and time t can be written:

$$h_0 - h(r, t) = \frac{1}{4\pi T} \sum_{i=1}^n (Q_i - Q_{i-1}) W\left(\frac{r^2 S}{4T(t-t_i)}\right)$$

where Q_i pumping or injection rate from time t_{i-1} to t_i , $L^3 t^{-1}$.

2.7 Constant Drawdown Flow Test

Constant drawdown flow tests can be conducted using variable-rate pumping while holding the drawdown at a constant level or with wells that have hydraulic heads above ground surface and therefore are free flowing wells. To conduct a flow test for the latter case, the flowing well is shut-in and allowed to fully recover. The well is then opened and allowed to flow during which period the declining flow rate is measured. The method of analysis for a flow test is given in Jacob and Lohman (1952). The appropriate initial and boundary conditions are:

$$h(r, 0) = h_0, \quad r_w \leq r \leq \infty \quad (2.7-1)$$

$$h(\infty, t) = h_0 \quad t \geq 0 \quad (2.7-2)$$

$$h(r_w, t) = \bar{h} \quad t > 0 \quad (2.7-3)$$

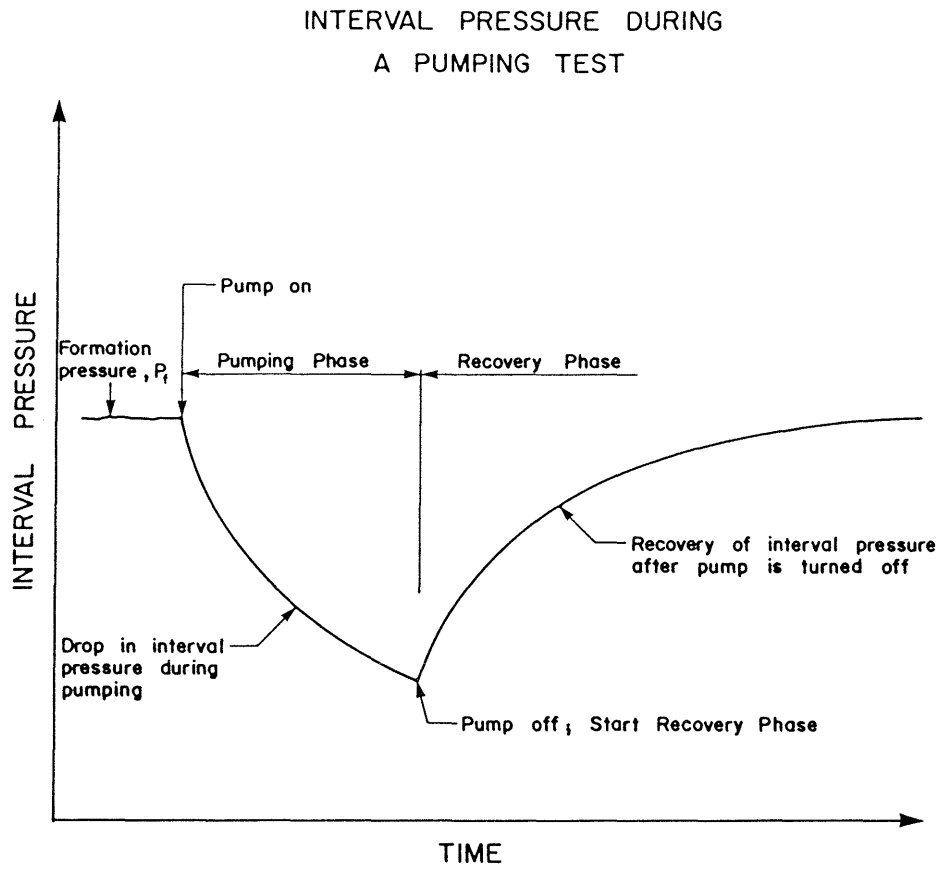


Figure 2.6-2 Schematic illustration of the interval pressure response during a pumping test

where

h	constant hydraulic head in the borehole or well, L;
r	radial distance from the borehole axis, L;
t	time, t;
h	hydraulic head in the formation, L;
h ₀	in-situ formation hydraulic head, L;
r _w	discharging well (or borehole) radius, L.

The corresponding analytical solution to the radial flow equation 2.6-6, can be written as:

$$T = \frac{Q}{2\pi G(\psi) s_w} \quad (2.7-4)$$

where

$$\psi = \frac{Tt}{Sr_w^2} \quad (2.7-5)$$

and s_w is the drawdown given by:

$$s_w = h_0 - \bar{h}$$

where

Q	borehole or well discharge rate as a function of time, L ³ t ⁻¹ ;
T	transmissivity, L ² t ⁻¹ ;
S	storage coefficient, dimensionless.

The G function is given by:

$$G(\psi) = \frac{4\psi}{\pi} \int_0^\infty x e^{-\psi x^2} \left[\frac{\pi}{2} + \tan^{-1} \frac{Y_0(x)}{J_0(x)} \right] dx \quad (2.7-6)$$

where

J ₀ (x)	Bessel function of zero order of the first kind;
Y ₀ (x)	Bessel function of zero order of the second kind.

Equation 2.7-6 can be solved using an equivalent summation to yield values of G(ψ) and ψ. G(ψ) and ψ can be plotted to obtain type curves from which field data can be analysed using type curve procedures.

Jacob and Lohman (1952) also provide a semi-logarithmic straight line solution by assuming at large values of t , $G(\psi)$ can be approximated by $2/W(u)$. Under these conditions, the straight line semi-logarithmic solution can be used to determine the formation parameter, T and S (transmissivity and storativity). The solution, which is similar to the straight line solution of Cooper and Jacob (1946), can be approximated as follows:

$$W(u) = 2.30 \log_{10} \left(2.25 Tt/r_w^2 S \right) \quad (2.7-7)$$

Using this equation and solving the partial differential equation for nonsteady radial flow, a solution can be written as:

$$T = \frac{2.30Q}{4\pi s_w} \log_{10} \left(\frac{2.25Tt}{r_w^2 S} \right) \quad (2.7-8)$$

Differentiating this equation and changing from infinitesimals to finite values yields the following solution as is given by Jacob and Lohman (1952):

$$T = \frac{2.30}{4\pi \Delta(s_w/Q) / \Delta \log_{10} t/r_w^2} \quad (2.7-9)$$

Thus by plotting s_w/Q versus $\log_{10} t/r_w^2$, the values of $\Delta(s_w/Q)$ and $\Delta \log_{10} t/r_w^2$ can be determined graphically and equation (2.7-9) solved to yield the transmissivity.

2.8 Multiple Well Methods

The theoretical aspects of hydraulic testing described in section 2.3 to 2.7 are those that are mostly suited to single borehole tests. Other testing methods exist that are designed to measure the hydraulic response in larger volumes of rock by monitoring the hydraulic response in more than one borehole or well. Examples of these types of methods include interference testing and pulse-wave testing.

An interference test is similar to a common pump test where one well is pumped at a specific rate and the hydraulic response in an adjacent well is monitored. The analytical techniques used for an

interference test are the same as those for a pump test as are described in Section 2.6. The result of the test however yields, in many situations, formation properties that are representative of a larger volume (i.e., the volume between the pump well and the monitor well) of the formation than those obtained from a single well test.

The pulse-wave test uses a series of short-rate pulses generated at one well to obtain a hydraulic response in an adjacent well. The pulses can be generated by alternating periods of pumping (at the same rate) and recovery. The analytical methods for pulse-wave tests are given in Johnson et al. (1966) and Black and Kipp (1981).

2.9 Implementation of Data Analysis Methods

The results of the various testing methods described above give a hydraulic head or pressure response that varies with time according to the hydraulic properties of the formation being tested. To determine the formation hydraulic parameters from a field data base consisting of measured head or pressure responses, it is necessary to apply an appropriate analysis technique. The methods that are commonly used for these purposes are (1) matching to type curves or (2) a computer implementation to solve the appropriate equations for a suite of parameter values and calibrating the calculated results to the field-measured response.

2.9.1 Type Curve Methods

Type curve methods are applicable to most of the methods described above to provide an estimate of the formation parameters.

The method consists of solving the governing equations using a representative range of parameters to obtain a series of curves. For example, the slug test type curves (Figure 2.3-2) were generated by solving equation 2.3-6 for various values of α and β . To determine the appropriate formation parameters the field data is plotted at the same scale and compared to the type curves. With the axes coincident, the data plot is translated horizontally into a position where the data best fit one of the type curves. A matchpoint is chosen and its type curve values are used to solve for the formation parameters. For example, in the slug test

a match point would yield values of t and β which in turn can be used in equation 2.3-8 to solve for the formation transmissivity. Similarly the value of α for the best-fit type curve can be used in equation 2.3-7 to compute a formation storage coefficient. A similar technique can be used in the other test methods.

Type curve methods are appropriate for determining an estimate of the formation parameters. However, because the field data rarely fits a type curve exactly it is often possible to match the field data to various parts of different type curves. If this is the case, then considerable error could be introduced into the results (i.e., nonuniqueness of estimated parameters). The use of type curves also requires extrapolation between curves if an accurate match can not be obtained with the available curves. A more accurate and flexible analysis method is by computer implementation.

2.9.2 Computer Implementation

Solving the appropriate analytical solution for each testing method by computer implementation allows a more accurate match to be obtained. In the computer implementation the analytical solution is solved directly using appropriate ranges of formation parameter values. Each computer simulation is compared to the field data until a best fit curve is found. The formation parameters for the field data are the same as those for the best-fit curve. The advantages of the computer implementation method are: (1) sensitivity analyses can be conducted to assess the effects of parameter value variation on the simulated pressure or head responses; (2) the formation parameters can be more easily varied to determine a more accurate best-fit curve; and (3) errors due to extrapolation and matching to the wrong curve are reduced.

3. ANALYSIS AND INTERPRETATION OF BOREHOLE HYDRAULIC TESTING IN DEEP BOREHOLES

3.1 Introduction

The determination of the three-dimensional permeability and in-situ pressure distribution of a hydrogeologic system forms the basis for developing a conceptual model and understanding of the flow system. With an adequate data base with respect to these parameters, the boundaries (either flux or pressure) of the hydrogeologic domain of interest can be ascertained. The utilization of proper borehole testing procedures and appropriate data analysis methods are critical for obtaining accurate estimates of the formation parameters.

Hydraulic testing is the term used to describe tests (primarily field tests) which yield the previously mentioned parameters for characterizing hydrogeologic systems. In the past few years, considerable hydraulic testing research has been directed towards low permeability media. This is due to the selection of potential radioactive disposal sites at depth in rock types such as layered basalts, tuffs, granites and salts. Due to the interest and relevance of such research, this section will consider in detail the principles and difficulties of hydraulic testing in low permeability media.

Most of these hydraulic testing programs are conducted during or immediately subsequent to drilling, with multilevel packer installations sometimes utilized for long term pressure monitoring. The borehole pressure measurements are usually conducted using single or double packer testing techniques. One of the most critical difficulties in hydraulic testing is to establish the fact that values for the formation parameters such as pressure and permeability are 'representative' of the formation. Since the hydraulic regime in the formation has been disrupted to some extent by the drilling process, these transient effects must be considered in the subsequent testing and data interpretation.

There are two principal instrumentation types utilized in hydraulic testing: (1) wells and piezometers screened over an isolated portion of the formation and (2) packer tests isolating a selected

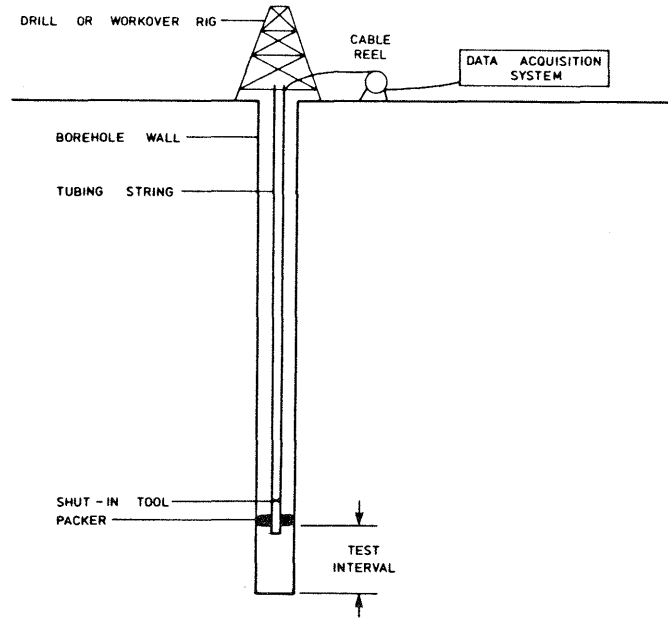
portion of the borehole. Hydraulic isolation of the screened portion of the formation from shallower depths (annular disturbed region surrounding the casing) is usually accomplished using cement or grout seals. Packer tests refer to testing in open boreholes where isolation of an interval is provided by means of expandable packers lowered in the borehole and expanded against the borehole wall. Packer tests are usually conducted in either a single or double packer configuration (see Figure 3.3-1).

Double packer systems are used by numerous borehole testing programs. The double packer systems are configured either: (1) with drill tubing as both the backbone of the system as well as the fluid carrier for the hydraulic tests, or (2) with wireline and using narrow diameter tubing as the fluid carrier between surface and the downhole packer system and test interval.

Other packer testing systems have also employed guard packers above and below the packers that are isolating the interval being tested (e.g., see the system described by Peterson et al., 1984). Packer systems with greater than two to four packers have also been utilized for long-term pressure monitoring and hydraulic conductivity testing. The equipment configuration and application of an eight-packer system developed by Lynes Inc. is presented by Belanger et al. (1985). One of the advantages of these systems is that they allow the long-term (i.e., weeks, months or even years) testing of low permeability zones without the high costs associated with a drill or work-over rig on site.

As noted in Section 2, the permeability and in-situ pressure are intrinsic properties of the formation. These parameters are related to the more widely-used parameters hydraulic conductivity and hydraulic head through their definition with respect to formation and/or fluid properties. As will be discussed later in this Section, it is not possible to define hydraulic head in a system where the fluid properties are nonhomogeneous (as is the case when dealing with deep boreholes) as a result of temperature, pressure and salinity variations. Hydraulic conductivity can be defined (and evaluated from the data from a hydraulic test), but it corresponds to the specific fluid properties at which the in-situ tests are being conducted. For discussion purposes throughout this Section, the terms formation pressure and hydraulic conductivity will be used with regards to the interpretation and

(a) SINGLE PACKER EQUIPMENT CONFIGURATION



(b) DOUBLE PACKER EQUIPMENT CONFIGURATION

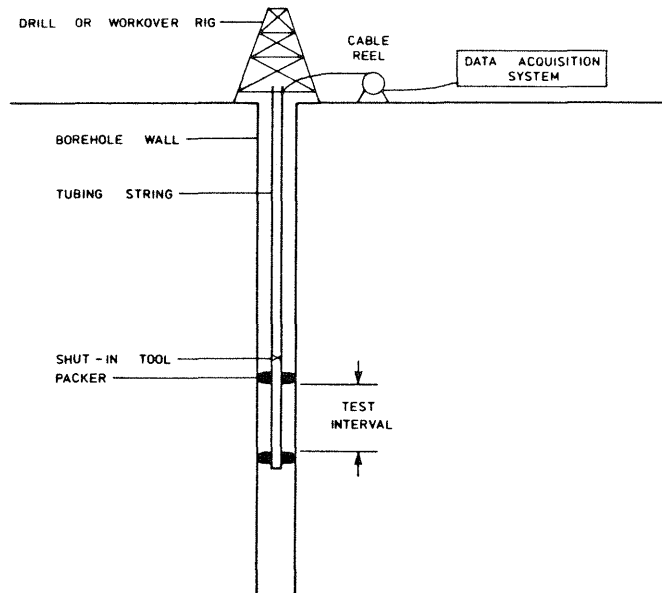


Figure 3.1-1

Schematic illustration of (a) single packer and (b) double packer equipment configurations for borehole hydraulic testing

evaluation of pressure response data from borehole hydraulic tests.

The main objectives of this Section are to identify and evaluate the processes and factors important in the analysis and interpretation of borehole hydraulic tests for formation hydraulic conductivities and pressures. The processes and factors which are of particular importance in evaluating low permeability formations include formation/fluid response, borehole pressure history, thermally-induced borehole pressure responses, borehole/formation skin effects and equipment compliance. These considerations were evaluated through the development and application of a numeric model for borehole test analysis based on an approach called the Graph Theoretic Field Model (denoted GTFM). Model applications include sensitivity analyses with variations in model input parameter values and testing conditions as well as field cases involving borehole tests conducted in the NAGRA deep borehole (1500 m depth) in crystalline rock at Boettstein in northern Switzerland.

3.2 System Response

3.2.1 Fluid Properties/Response

For borehole pressure measurements using single or double packer equipment, the monitored pressure response may be dependent on a number of fluid and formation parameters (and their spatial and temporal variation) including fluid compressibility, fluid density, fluid thermal expansion coefficient, fluid viscosity, fluid heat capacity, formation hydraulic conductivity, formation thermal conductivity, formation heat capacity and, in some cases, their dependence on pressure, temperature and salinity. The relative importance of the pressure and temperature dependence of the fluid parameters is summarized in Figures 3.2-1a to 3.2-1d.

The ground water fluid parameters generally vary spatially within any large-scale (deep) flow system. Nelson and Oberlander (1984) have discussed the theoretical and practical considerations of the flow of "nonhomogeneous" fluids when interpreting flow directions and velocities in deep ground water flow systems. They emphasize that field measurements should include: (1) accurate determination of fluid pressure, and (2) measurement of variables required to accurately characterize the variation

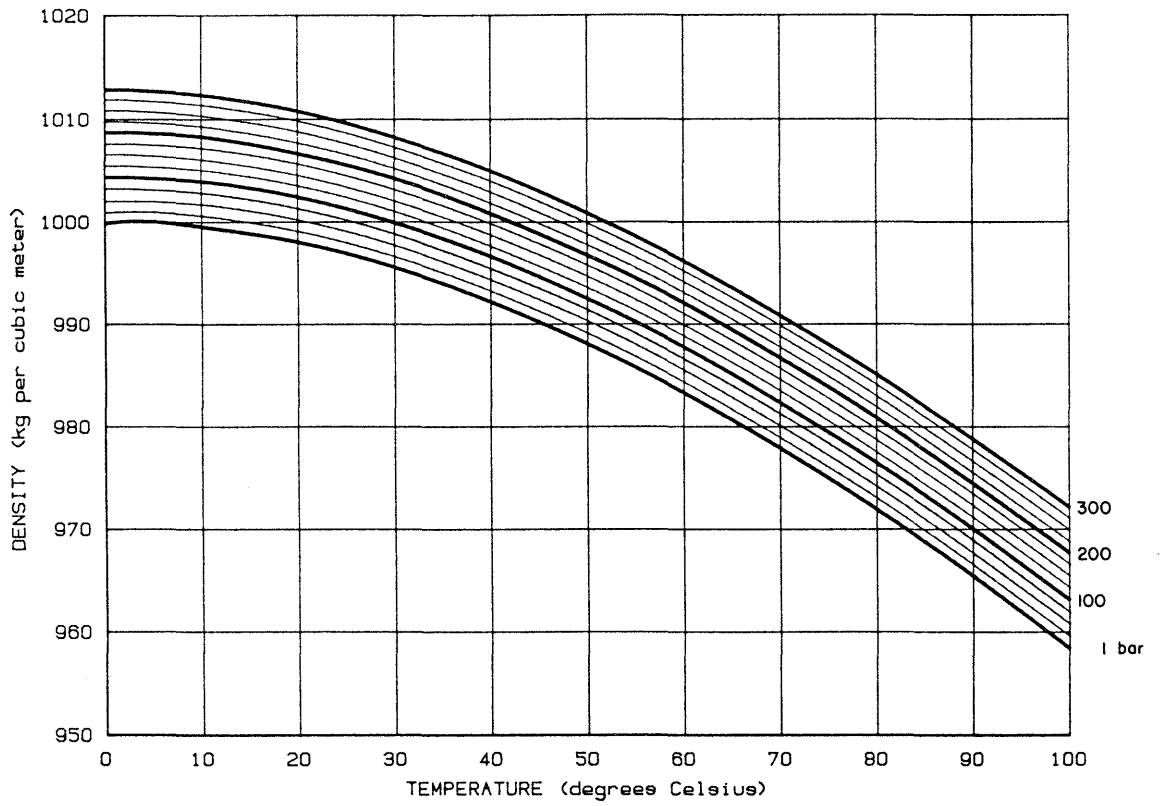


Figure 3.2-1a Fluid density: variation with temperature and pressure

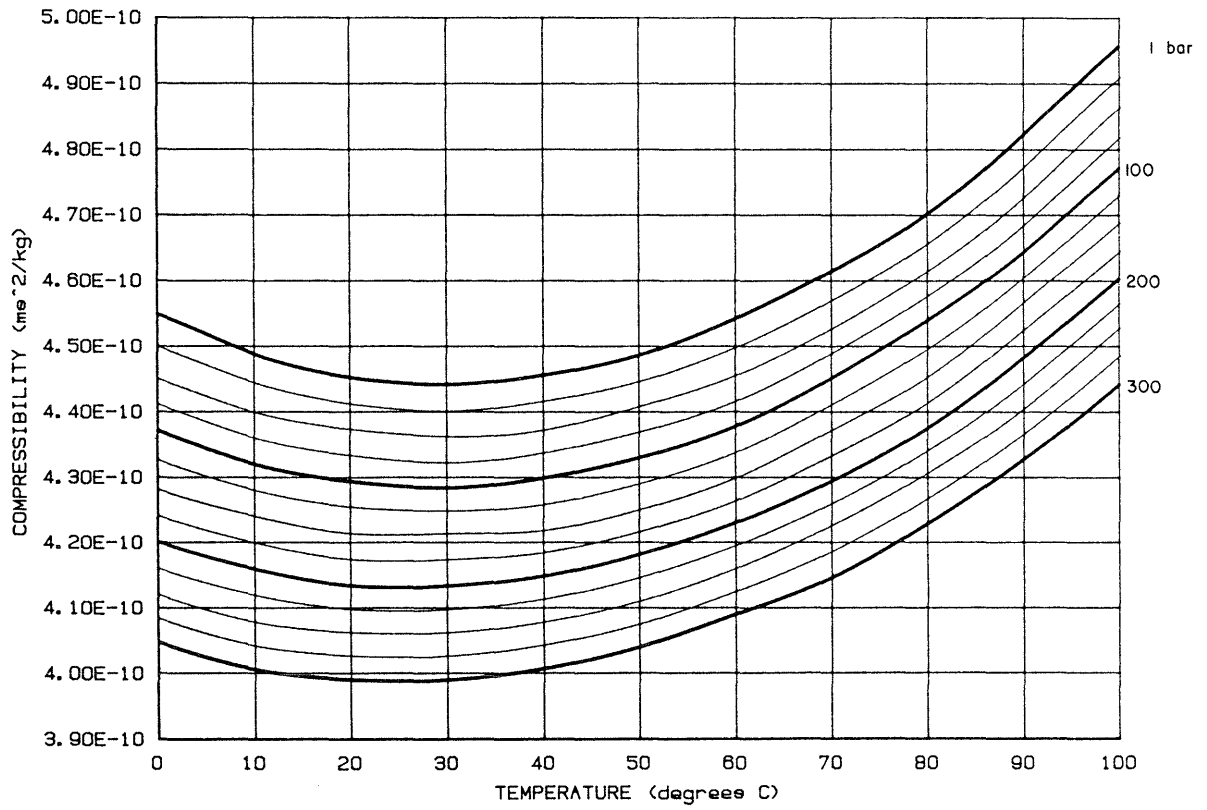


Figure 3.2-1b Fluid compressibility: variation with temperature and pressure

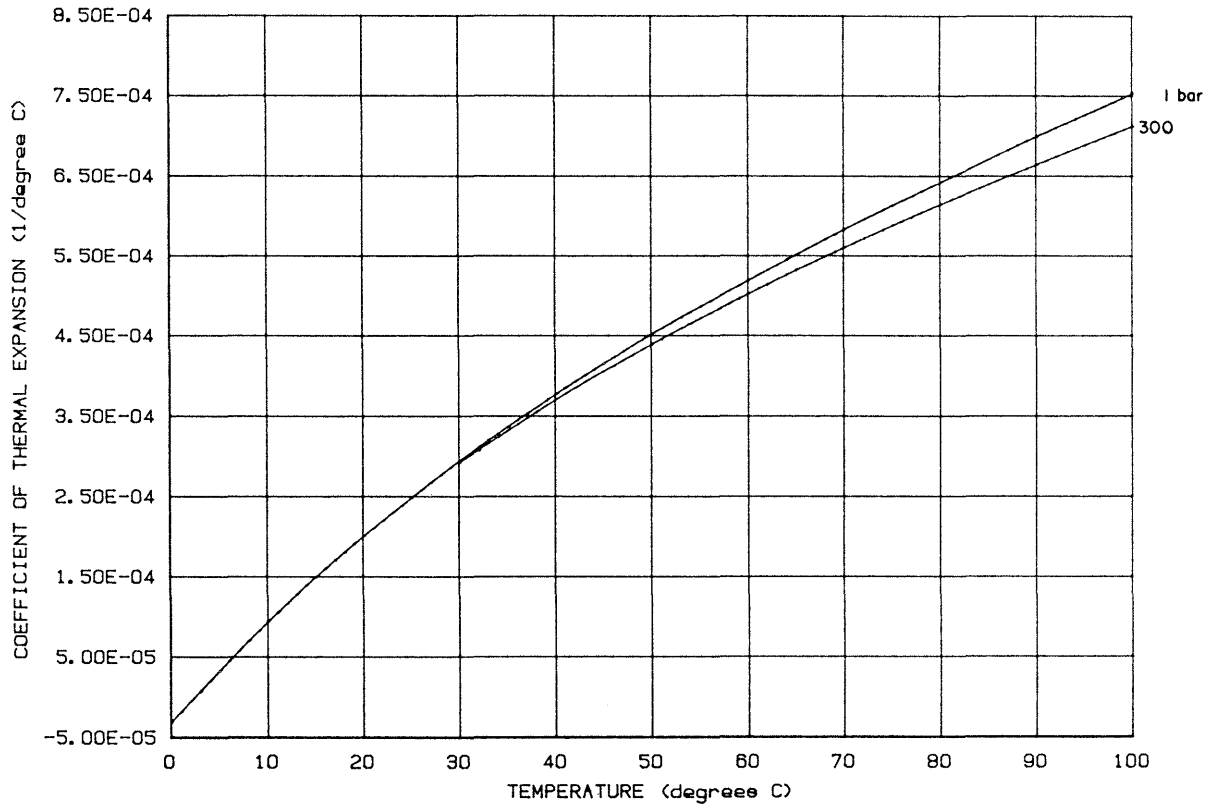


Figure 3.2-1c Fluid coefficient of thermal expansion: variation with temperature and pressure

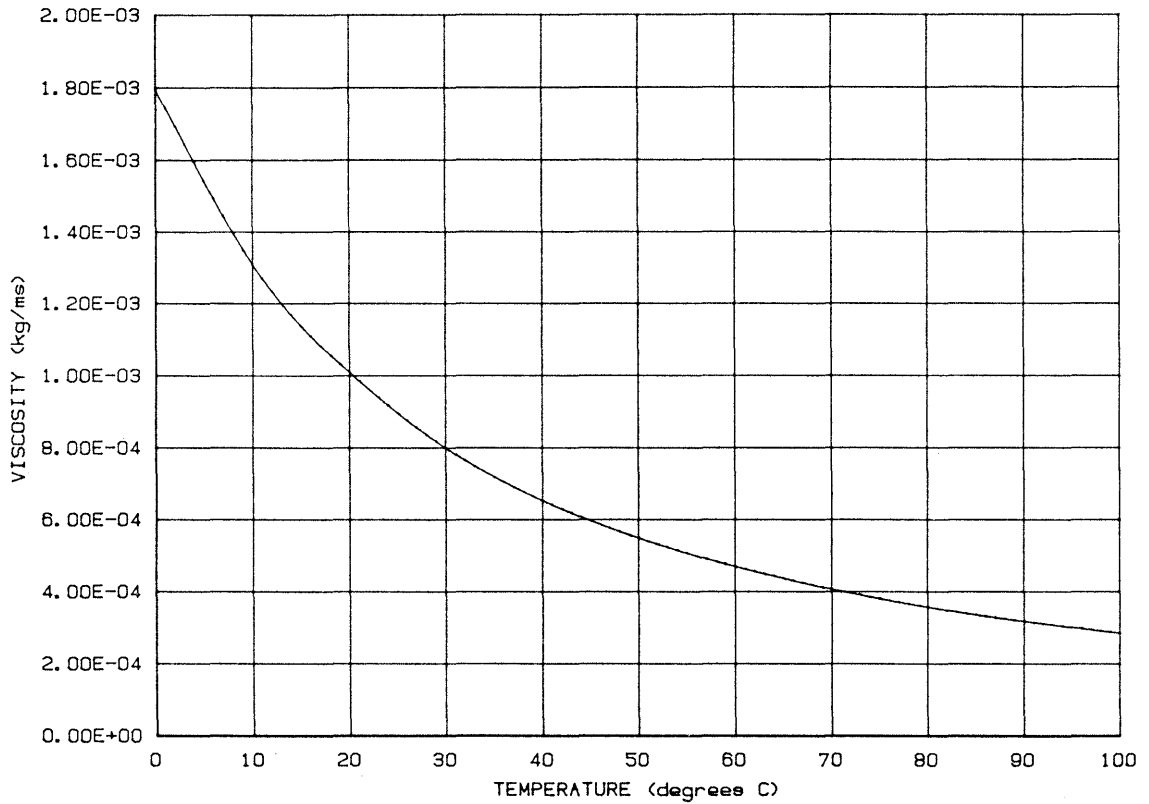


Figure 3.2-1d Fluid viscosity: variation with temperature
 (Note: viscosity is relatively insensitive to changes in pressure)

in fluid density throughout the system (i.e., variations in temperature, dissolved constituents and salinity). They note that the other fluid properties can be derived based on a knowledge of the fluid density spatial variation. Nelson and Oberlander also concluded that the use of a scalar energy potential (i.e., potential head) is not appropriate for use in the analysis of the flow of nonhomogeneous fluids in geologic systems.

For analysis of the hydraulic test data for the determination of hydraulic conductivity, the density, viscosity, compressibility and thermal expansion coefficient (for some cases) of the in-situ fluids are required. It is usually assumed that the borehole and formation fluids have the same properties. Measurement of the fluid specific gravity at surface conditions and temperature and pressure at in-situ conditions allow the estimation of relatively accurate estimates of density and viscosity for use in hydraulic conductivity analyses.

Contributions to a measured flow at the surface instrumentation may occur from fluid contraction and expansion due to temperature and pressure changes; for example, when the pressure that may exist on a packer-isolated zone is released flow may occur (during early time) that is due solely to the expansion of the fluid. Volume expansion also affects the fluid as it flows from the interval towards the surface. This type of flow occurs as a result of a pressure decrease as it rises and therefore a small contribution to the total flow could be attributed to this volume expansion. Due to the thermal gradient that occurs with depth in deep boreholes, fluid rising up the tubing will undergo a temperature decrease and result in a net decrease in flow measured at surface. These types of flow modification described above are generally minor in magnitude under typical borehole testing situations. However, representative calculations should routinely be conducted to quantify the significance of these fluid expansion and contraction effects on flow, especially for testing low permeability formations.

3.2.2 Borehole/Formation Response

Borehole response refers to the pressure and temperature responses within the borehole during drilling and testing activities. Hydraulic testing

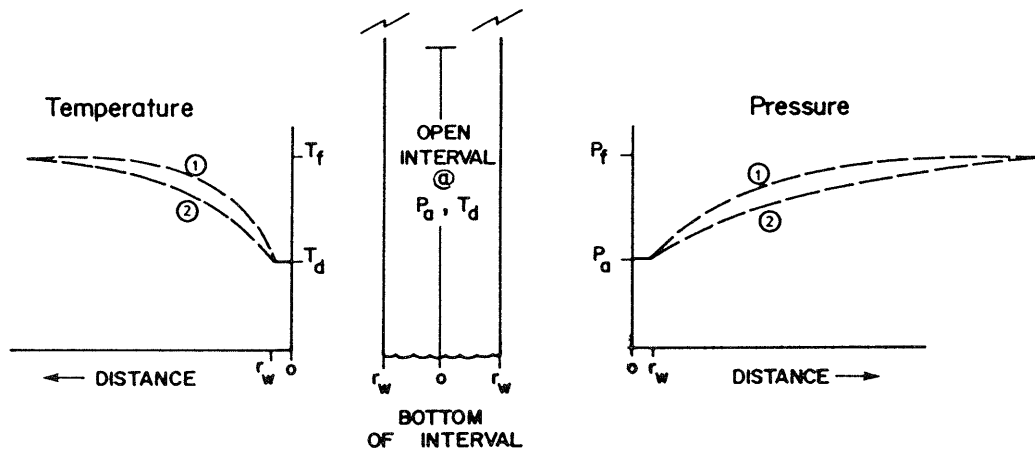
is conducted using a variety of techniques (see Section 2); however, most testing and analysis methods are concerned with a pressure or hydraulic head change in a test interval and the return of the pressure in the interval to the pretest pressure conditions. The hydraulic parameters of the formation are determined from the duration and shape of the pressure recovery curve. The monitored pressure in the interval is related to the formation, hydraulic properties as well as the pressure history to which the interval has been subjected prior to testing, pressure changes resulting from nonisothermal conditions, and equipment-related factors. The following subsections provide a discussion of the effects and significance of these factors on hydraulic testing results.

3.3 Borehole Pressure History

It is instructive to approach the problem of formation responses to drilling and testing by considering the sequential occurrence of events from the time a geologic interval is intersected during drilling until the completion of a packer test. For illustrative and discussion purposes, cases will be considered when the in-situ formation pressure is greater than the annulus fluid pressure. Annulus pressure refers to the downhole absolute pressure corresponding to overflow of the drilling fluid at the wellhead.

Prior to drilling into an interval the pressure of the interval is considered to be at in-situ or formation conditions (P_f). As the interval is drilled, the formation is subject to annulus pressure (P_a). A pressure profile is developed radially in response to the differential pressures between the borehole fluid and the formation. The pressure profile into the formation for the test interval is schematically illustrated in Figure 3.3-1. (In reality, the pressure profile will be different between the top and the bottom of the interval, since the upper portion has been open to drilling conditions for a longer period of time than the lower portion). The longer the interval is open the further into the formation the pressure profile develops.

The net effect of the "pressure skin" developed during the drilling and pretest period is the development of testing conditions that do not meet



- P_a annulus pressure
- P_f formation (in-situ) pressure
- T_f formation (in-situ) temperature
- T_d drill fluid temperature
- ① profile on completion of drilling
- ② profile after some period of continual drilling
- r_w radius of borehole

Figure 3.3-1 Schematic pressure (P) and temperature (T) profiles in the formation on completion of drilling an interval

the assumptions involved in analytical solution or type-curve analysis methods. For instance, the pressure recovery in the interval will not be simply related to the recovery to in-situ formation pressure from an initial pressure at the start of the test. The pressure skin developed during drilling and prior to testing will, in some cases, strongly affect the pressure recovery curve.

In conducting hydraulic tests for obtaining pressure response data for hydraulic conductivity determination, it is necessary to choose testing procedures that take into account the magnitude of the annulus and formation pressures. Schematic pressure response curves for pulse or slug tests are shown in Figure 3.3-2 for recommended test procedures. For the illustrated injection and withdrawal tests, a strong pressure pulse or head differential is required such that the difference between the pressure (P_{SI}) at the start of the test and both annulus pressure (P_a) and formation pressure (P_f) is much larger than the pressure difference between P_a and P_f .

Schematic pressure response curves for pulse or slug tests which would not provide suitable data for correct hydraulic conductivity determinations are illustrated in Figure 3.3-3. In these cases, a strong pressure pulse or head differential has not been utilized as the starting condition for the tests. The pressure at the start of the test is either equal to the annulus pressure or is not substantially different than the annulus or formation pressure. The net effect of these inadequate test procedures is a high degree of uncertainty in the interpreted hydraulic conductivity. For example, analytical solution or type-curve analysis methods of a test where the starting pressure (P_{SI}) equals the annulus pressure (P_a) could yield a hydraulic conductivity estimate that is several orders of magnitude too low.

A long period open to annulus pressure conditions causes a sufficiently large pressure skin to develop such that, for the purposes of hydraulic conductivity determination, the annulus pressure can be assumed as the "reference" or pretest pressure. With a long borehole open period and adequate testing procedures, the choice of annulus pressure as the reference pressure may be preferable. In this case the actual formation pressure may have a relatively small effect on the measured borehole pressure response during short-term hydraulic tests.

RECOMMENDED TEST PROCEDURES

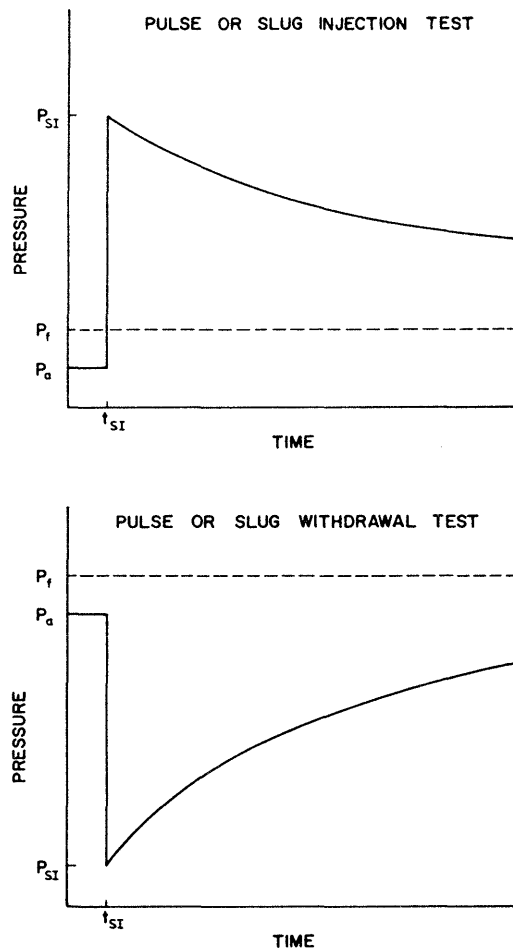


Figure 3.3-2

Schematic pressure responses for the test interval utilizing recommended test procedures to allow hydraulic conductivity determination (i.e., the pressure P_{SI} at the start of the test is substantially different from annulus pressure P_a or formation pressure P_f)

INADEQUATE TEST PROCEDURES

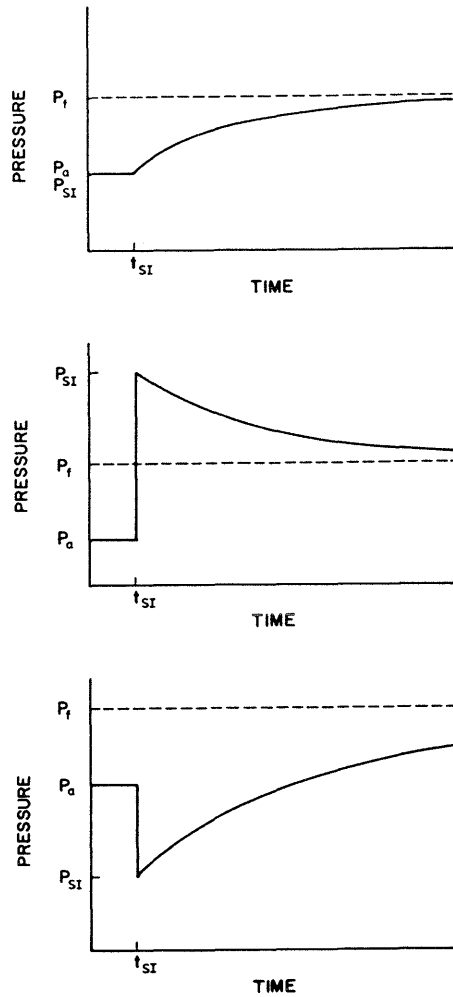


Figure 3.3-3

Schematic pressure responses for the test interval utilizing inadequate test procedures for hydraulic conductivity determination (i.e., the pressure P_{SI} at the start of the test is at or close to the annulus pressure P_a or formation pressure P_f)

The recovery from the pressure pulse responds as if the annulus pressure were the actual formation pressure.

Borehole pressure history can also be important during a testing sequence involving more than one test (e.g., a pulse withdrawal test followed by a pulse injection test). Each individual hydraulic test causes some modification of the pressure profile radially from the borehole. This pressure skin can have an important effect on the measured borehole pressure response during subsequent tests. The borehole pressure history that may be imposed on the test interval during a test sequence is shown schematically in Figure 3.3-4.

Hydraulic tests should be designed and conducted to minimize the effects of pretest borehole pressure history. When using type-curve analysis methods, the choice of the reference pressure should not be determined solely by type-curve extrapolation but rather should be chosen based on an evaluation of the annulus pressure and estimated formation pressure as well as the length of time that the interval has been exposed to annulus pressure conditions. In many cases, type curve or analytical solutions may not be adequate for data analysis; but rather computer implementation of numerical methods which include the borehole history effects may be required for accurate evaluations of the formation parameters. The effect of pretest borehole history is demonstrated quantitatively by examples in section 3.8.1.

3.4 Thermally-Induced Borehole Pressure Response

Pressure changes resulting from thermal expansion (or contraction) of the borehole fluid can exert a very important effect on the measured borehole pressure response during hydraulic testing. Prior to drilling into an interval the temperature of the interval is considered to be at in-situ or formation conditions (T_f). As the interval is drilled, the formation is subjected to drilling fluid temperatures (T_d). A temperature profile is developed in response to the differential temperatures between the borehole fluid and the formation. The temperature profile into the formation is illustrated schematically in Figure 3.3-1. The longer the interval is open the further into the formation the temperature profile develops.

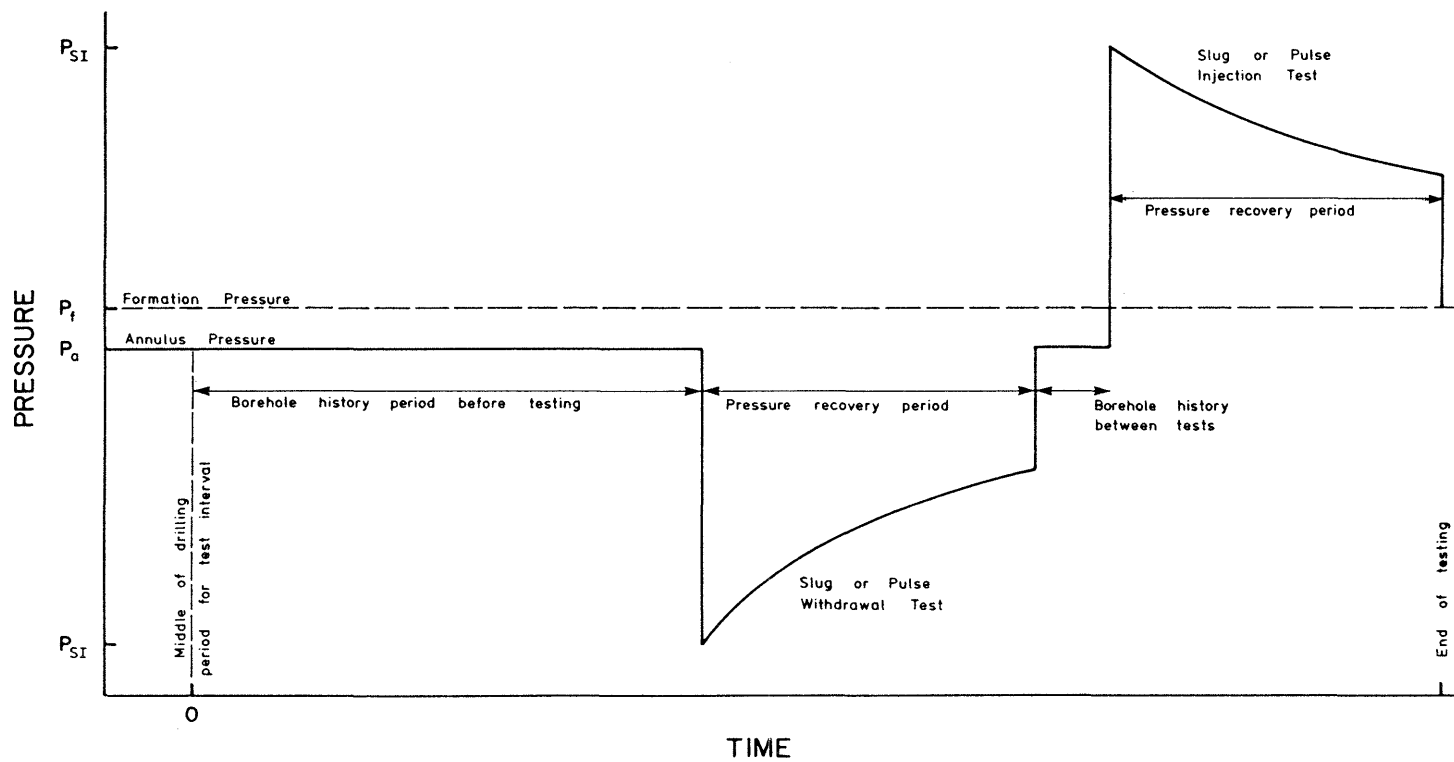


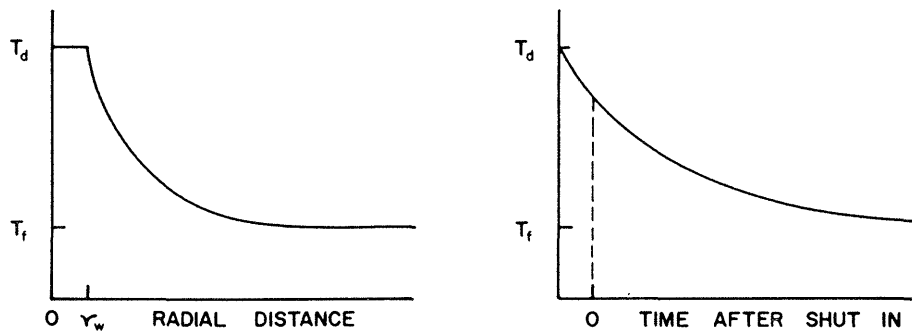
Figure 3.3-4 Schematic illustration of the borehole pressure history that develops during a testing sequence

Temperature profiles for cases with the drill fluid temperature greater than the formation temperature and also less than the formation temperature are shown schematically in Figures 3.4-1a and 3.4-1b, respectively. The net effect of the development of these temperature profiles in the formation is a variation in the borehole fluid temperature during the hydraulic testing period. These temperature variations result in significant pressure changes during pulse testing (i.e., under shut-in conditions), especially in low permeability formations, as a consequence of the thermal expansion (or contraction) of the fluid.

If a significant temperature change (i.e., 1 or 2°C) occurs over the testing period in response to a temperature differential between the rock and the borehole, the pressure in the interval will change due to the variation in temperature. The thermal expansion coefficient of water varies significantly over the potential range of subsurface temperatures (see Figure 3.2-1c). Consequently, the observed pressure change depends importantly on the temperature. Figure 3.4-2 illustrates the change in pressure due to a temperature change in a closed system (i.e., hypothetical interval with zero permeability). The figures were produced using the thermal expansion coefficient of water at the temperatures 20, 40, 60 and 80 °C. This graph serves to illustrate the possible magnitudes of pressure change resulting from thermal expansion or contraction of the borehole fluid. For instance, at a temperature around 40 °C, a 2 °C increase in temperature in a zero permeability shut-in interval will result in a pressure increase (expressed as head) of about 180 metres. In an actual geologic test interval, the increase in pressure due to a temperature rise is moderated somewhat by the pressure dissipation into the formation. Figure 3.4-2 further illustrates that thermally-induced pressure changes per degree Celcius temperature change are much greater at higher temperatures (e.g., 3.2 times greater at 80°C as compared to 20°C). Therefore, thermally-induced pressure changes are potentially of greater significance at larger depths within a borehole as a result of the increased temperature.

The pressure response in a high permeability zone is relatively insensitive to temperature changes. The insensitivity is due to the relative ease with which a high permeability zone dissipates any pressure

(a) DRILL FLUID TEMPERATURE > FORMATION TEMPERATURE



(b) DRILL FLUID TEMPERATURE < FORMATION TEMPERATURE

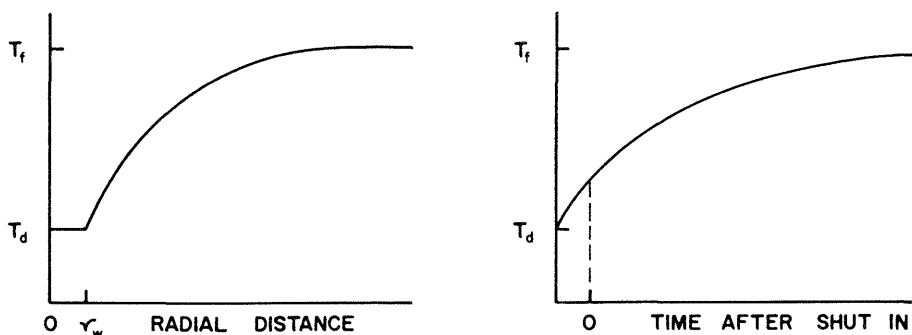


Figure 3.4-1

Schematic illustration of temperature profiles in the formation at the end of drilling and corresponding temperature variations in the borehole interval during testing for conditions of drill fluid temperature (a) greater than formation temperature and (b) less than formation temperature

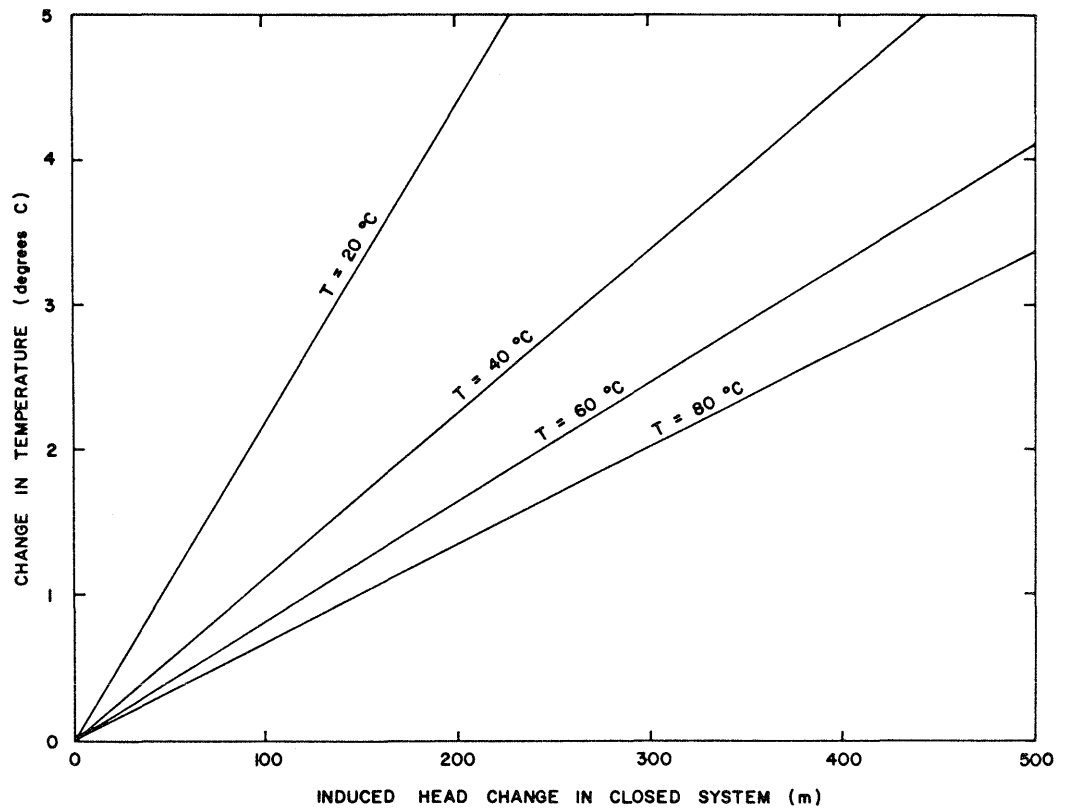


Figure 3.4-2 Induced head change resulting from a temperature change in the test interval at initial temperatures of 20, 40, 60 and 80 °C (assuming no fluid loss to the formation)

change, providing the zone has sufficient lateral extent to accommodate the pressure changes. It should be noted that testing of higher permeability zones would generally utilize slug tests which are not conducted under shut-in conditions, and therefore would involve thermally-induced pressure effects only to the extent that the water column variations are affected by thermal gradients and density differences. These effects would be much smaller; however, they could be significant, especially for cases involving large temperature changes with time and small-diameter tubing connected to the test interval.

For illustrative purposes, thermally-induced pressure effects on pulse tests are shown schematically in Figures 3.4-3 and 3.4-4 for the pressure conditions corresponding to formation pressure (P_f) greater than annulus pressure (P_a). It is important to note that the measured borehole pressure response under varying temperature conditions may "appear" in shape as a normal pressure response curve for tests of several hours to several days in length. However, analysis of such pressure response curves using standard analytical solution or type-curve analysis methods would yield incorrect permeability and formation pressure estimates, particularly in low permeability formations. The use of such analysis methods under varying-temperature conditions is incorrect since the basis of these methods ignores the important fluid pressure and temperature relationships that must be included.

Pulse injection or withdrawal tests are conducted on lower permeability zones since they allow the tests to be conducted more rapidly as compared to slug injection or withdrawal tests. Varying-temperature conditions existing in any zone requiring pulse tests will likely result in significant thermally-induced pressure responses. In situations where a section of borehole has been open to annulus conditions for a long period of time and inflows or outflows over that section are minimal, a quasi thermal equilibrium will likely be reached between the formation and the borehole fluid at any particular depth. Under these conditions, there may be cases where the temperatures remain relatively constant during subsequent hydraulic testing. An additional situation where thermal effects are not a problem is when the drill fluid and formation fluids are at equal temperatures. This situation is expected to exist over a limited region of the borehole length.

PRESSURE RESPONSE DURING PULSE INJECTION TEST
IN LOW PERMEABILITY FORMATION

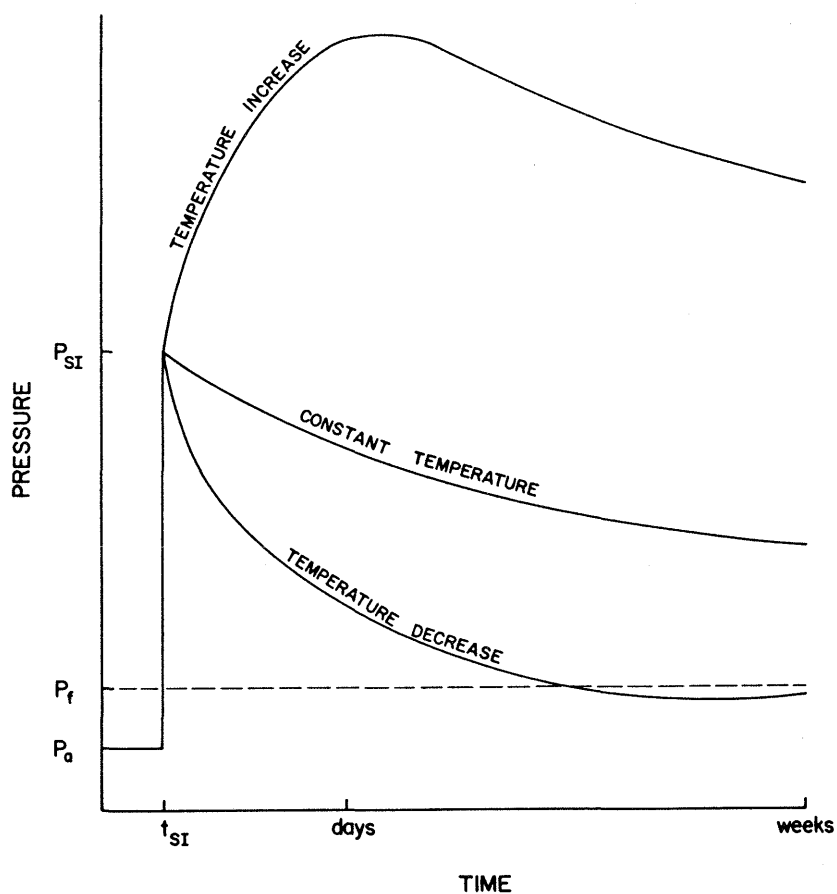


Figure 3.4-3

Schematic pressure responses during a pulse injection test in a low permeability formation for conditions corresponding to a temperature increase, a constant temperature and a temperature decrease

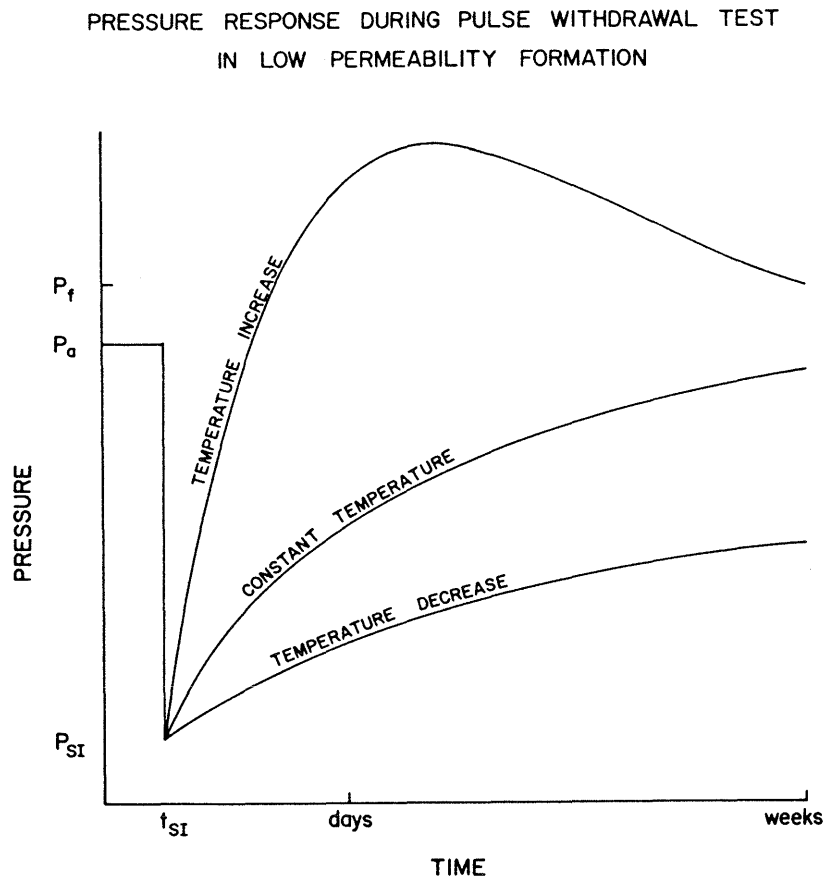


Figure 3.4-4

Schematic pressure responses during a pulse withdrawal test in a low permeability formation for conditions corresponding to a temperature increase, a constant temperature and a temperature decrease

3.5 Borehole/Formation Skin Effects

As a result of the drilling of the borehole, the permeability of the formation at and immediately surrounding the borehole wall may be altered. This borehole/formation skin may have a significant effect on the measured pressure response during hydraulic testing, resulting in incorrect estimates of both formation pressure and hydraulic conductivity. This permeability-altered skin zone may have either a higher or lower permeability than the surrounding formation. A higher permeability skin zone may occur in cases where the borehole wall and adjacent formation are eroded to some extent. This erosion may occur within both an intergranular porous media and fractures. In contrast, drilling-fluids such as mud may both invade the formation and build-up a filter cake at the borehole wall, thus causing a lower permeability skin zone. In some cases, plugging of the pore spaces and fractures may result from reactions between the drilling fluid and minerals in the formation (Lee, 1981). Even when drilling with water in rocks such as granites, the rock flour developed as a consequence of the drilling may clog the pore spaces and fractures near the borehole causing a permeability reduction.

For the case of using drill mud as the drilling fluid, the measured pressure response determined during hydraulic testing in intervals of intermediate to high hydraulic conductivity is likely affected by the influence of drill mud cake on the borehole wall and mud invasion into the formation. The purpose of drilling with mud is to prevent the loss of drilling fluid into the formation. The mud penetrates the formation immediately adjacent to the borehole wall causing the build-up of a mud cake. This mud cake acts as a low permeability layer to prevent further drill fluid migration. The magnitude of this effect is difficult to quantify. The penetration of the drilling mud into the formation and the corresponding mud cake build-up is dependent on various factors including:

- (1) properties of the drilling fluid (e.g., density, viscosity, size of particulates),
- (2) porosity of the formation, (3) pore size of the formation versus the size of particulates in the mud, (4) hydraulic conductivity of the formation, (5) hydraulic conductivity of the mud cake, (6) length of time the borehole is under open-hole mud-filled conditions, and (7) pressure differential between the mud-filled borehole and the formation.

In crystalline rocks as opposed to sedimentary rocks, skin effects are generally not considered to be as significant. The harder, denser crystalline rocks will resist erosion to some extent although it is still likely to occur. Dissolution of minerals in the borehole wall is also a less significant effect in crystalline rock. Because crystalline rocks are usually drilled with water rather than mud as the drilling fluid, clogging of the formation is much less of a problem.

The magnitude of skin effects are difficult to quantify but are related to the radius of influence of the hydraulic pressure response during testing, the thickness of the skin zone and the permeability contrast between the skin zone and the formation. A model sensitivity study conducted by Faust and Mercer (1984) has illustrated the difficulty in assessing the presence of skin effects. The modified pressure response caused by a lower permeability skin during a hydraulic test has the same characteristic shape and response as for a lower permeability formation. In this case, the formation hydraulic conductivity could be seriously underestimated. When the skin is of a higher permeability than the formation, the effect on the measured pressure response (and estimated hydraulic conductivity) is much less significant. In summary, the presence and characteristics (i.e., thickness and permeability) of a skin zone surrounding a borehole are very difficult to establish; however, their existence and effects must not be overlooked during interpretation of hydraulic tests.

3.6 Equipment Compliance Effects

With any downhole packer/transducer equipment configuration, there is a certain amount of non-rigidity or compliance in the equipment. The equipment compliance can be related to a number of things, including packer deformation or readjustment, entrapped air in the equipment located in a test interval, machined tolerances on the seating and positioning of various steel components and O-ring or other seals, etc.

Packer compliance (i.e., packer readjustment or deformation) during the progress of a hydraulic test is likely the most significant component of

equipment compliance effects. The significance of packer compliance during testing of low permeability geologic formations is poorly understood because of the very limited data base available in the literature. One example of compliance testing that has been conducted using a double packer system in a casing is presented by Thackston et al. (1984). They concluded that a small pressure build-up at a low rate after shut-in of a test interval in a low permeability formation will tend to have a relatively small compliance effect that will diminish within several hours whereas a large pressure build-up at a rapid rate could result in a pronounced effect on the measured pressure response. They reasoned that the late-time data from such a test would be more representative of the actual formation characteristics because compliance effects would diminish with time. Such a conclusion is difficult to substantiate without further compliance testing because the packer readjustment is a continuing process throughout a test in response to the head differential from zones above and below each of the packers as well as to the head differential from inside and outside of the packers.

Forster and Gale (1980, 1981) presented the results of a laboratory investigation of packer compliance in a 76 mm diameter simulated borehole. They compared the pressure responses in a borehole test cavity using various borehole seals (air or water filled inflatable packers) with a non-compliant steel plug and found packer compliance to result in an error in interpreted hydraulic conductivity by a factor of about 2.

The effects of equipment compliance were incorporated into the theoretical and field investigations by Hsieh et al. (1983) as part of the "pseudo compressibility term that represents the combined effect of water compressibility and equipment compliance". The storage factor for the water in the test interval was calculated as the volume of water multiplied by the specific weight of water multiplied by the pseudo compressibility factor. For ideally rigid equipment, the pseudo compressibility factor would be equal to the compressibility of water. For the more general and realistic case, the pseudo compressibility was determined from calibration using the equipment in a cased portion of a borehole. The pseudo compressibility was about 5 times the compressibility of water for their testing equipment and conditions.

Additional data on the significance of packer compliance is reported by Belanger et al. (1985) for flow and pressure buildup tests conducted in a borehole in a crystalline rock formation using an eight-packer system. The initial packer compliance effect from pressure release of a specific packer-isolated borehole interval was found to cause a rapid pressure response in an adjacent borehole interval.

For the case of a hydraulic test tool utilizing a single-packer equipment configuration with drill tubing connected to surface, the interval is shut-in by the closing of a downhole shut-in tool. The schematic diagram in Figure 3.6-1 can be used to illustrate some of the possible equipment related effects. The "shut-in" movement of the tool results in a "shut-in squeeze" which is a pressure increase in response to a small fluid injection into the test interval. The shut-in movement also results in a weight of one to several tons transferred to the tubing string which closes the shut-in valve. The added weight must, of course, be supported by the packer, which is inflated against the borehole wall. Since the packer and downhole system are not totally rigid, the increased weight tends to "compress" the isolated interval. In the case of single-packer and double-packer test configurations (see Figure 3.6-1 and 3.6-2), packer formation or readjustment may occur in response to the head differential imposed in the test zone at the start of a test and the changing head differential between zones during the progress of the test. Such packer compliance effects can lead to a modification of the measured pressure response within the borehole test interval.

Examples of the increased pressure which can result from weight transfer and consequently a reduction in the isolated interval length are presented in Figure 3.6-3 (assuming fluid properties at 40°C; i.e., fluid compressibility coefficient equal to $4.3 \times 10^{-10} \text{ pa}^{-1}$). It can be seen that if the length of a 10 metre test interval of a low permeability zone is reduced (or "squeezed") by 1 cm due to packer compliance, the resulting increase in head is more than 200 metres.

In order to develop a quantitative capability for analyzing pressure test data which includes compliance effects, the magnitude and shape of the compliance function must be known. This requirement can be met by observations of pressure responses within impermeable lengths of casing or "simulated boreholes" over a range of temperatures and applied loads on a single packer/hydrologic tool

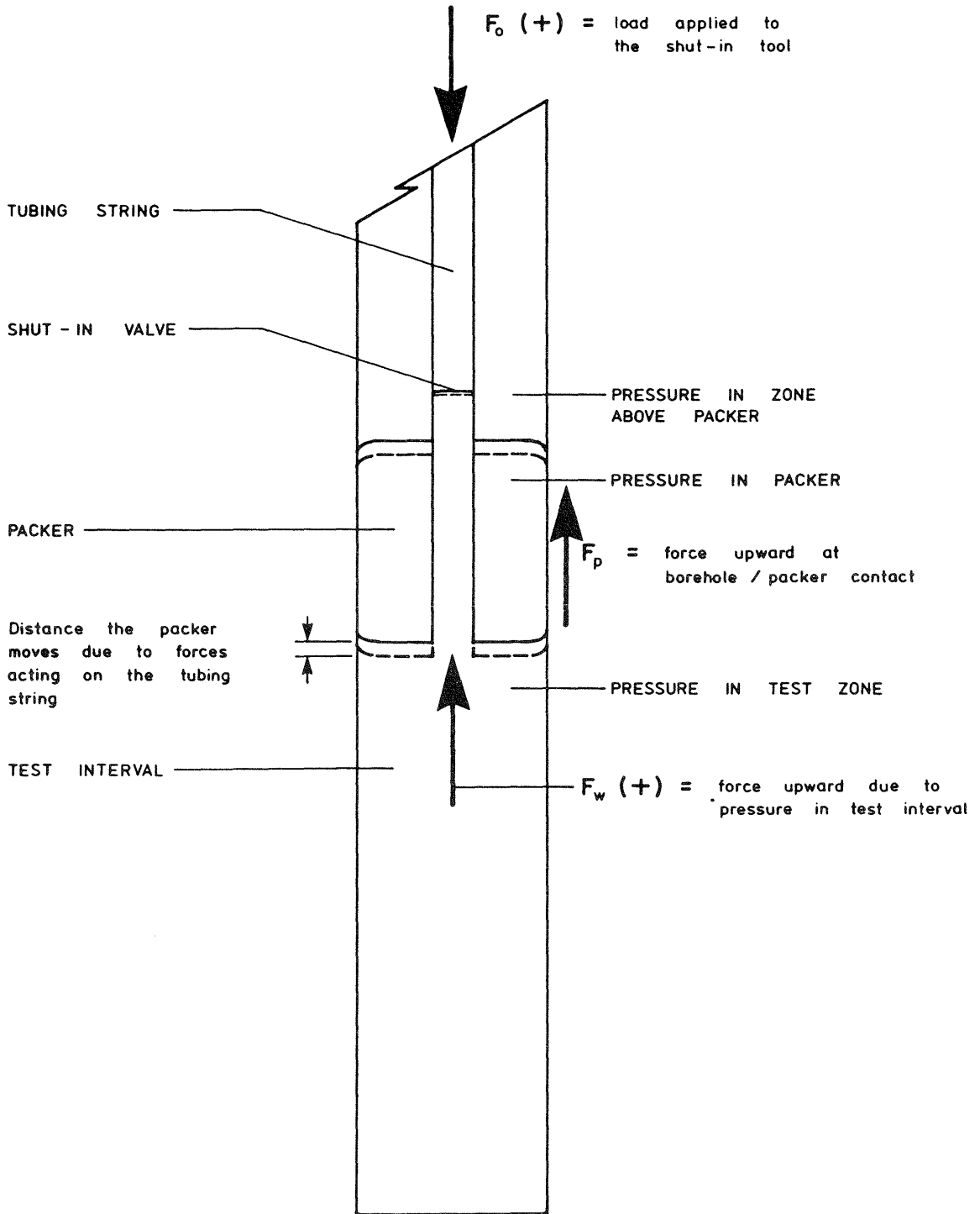


Figure 3.6-1

Schematic illustration of applied forces in a single-packer test configuration. Packer deformation may occur in response to the forces acting on the tubing string, the head differential imposed on the test zone at the start of a test and the changing head differential between zones

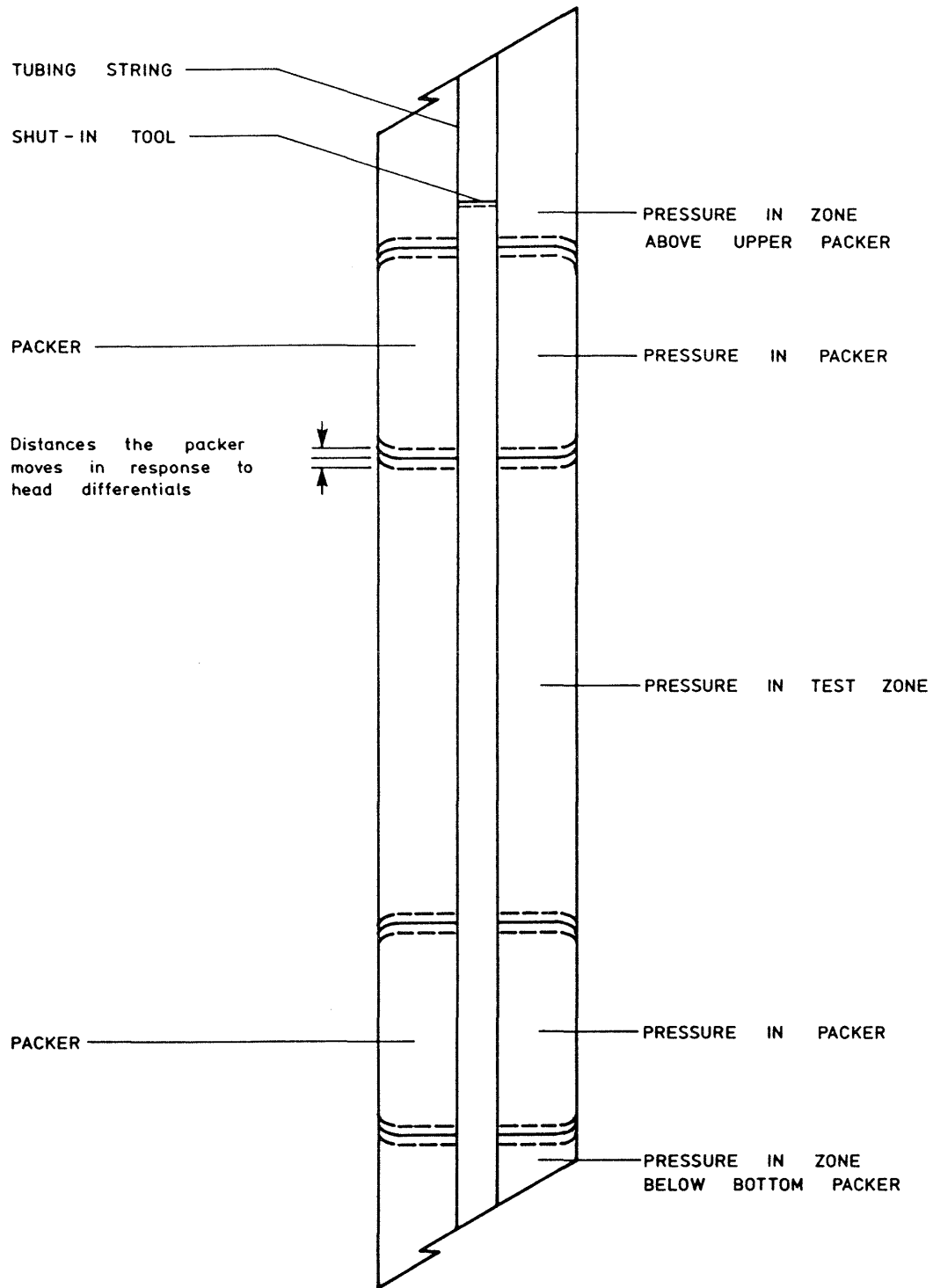


Figure 3.6-2

Schematic illustration of double-packer test configuration showing pressures in various zones. Packer deformation may occur in response to the head differential imposed in the test zone at the start of a test and the changing head differentials between zones during the progress of the test

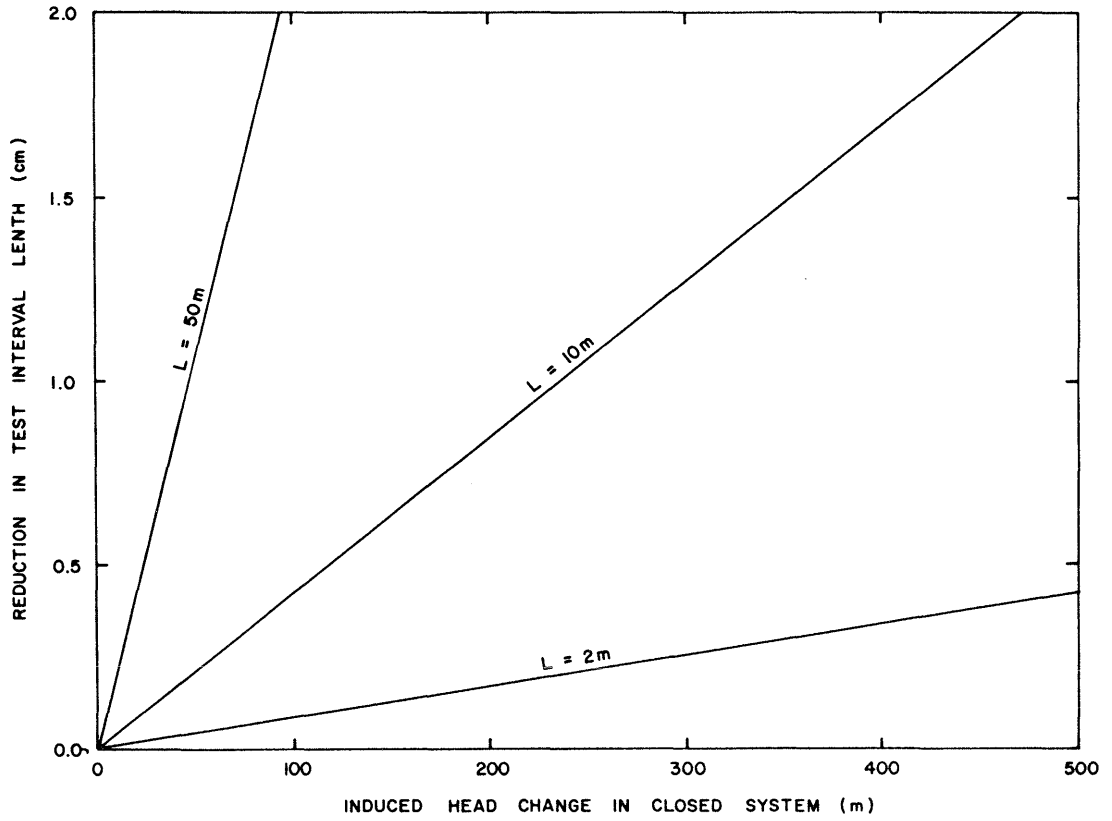


Figure 3.6-3 Induced head increase resulting from a reduction in test interval length for initial packed off intervals of 2, 10, and 50 m (assuming no fluid loss to the formation)

configuration. In the simplest case, the compliance can be treated as a step function, and its effect considered as part of the initial shut-in pressure. In more complicated cases the compliance is regarded as a time, pressure and load dependent mathematical function, with the shape and magnitude defined by several compliance related parameters. Examination of the pressure responses observed during the many single-packer tests conducted in the deep borehole in crystalline rock at Boettstein in northern Switzerland suggests that the bulk of the equipment compliance effects occur relatively rapidly. Presently it is considered reasonable to lump the associated pressure squeeze from packer compliance together with the shut-in squeeze to arrive at the initial starting pressure for a pulse test. Further testing of packer compliance effects under both laboratory and field conditions is necessary to substantiate the above assumption and to further quantify the significance of packer compliance on the measured pressure response during testing of low permeability formations.

3.7 Theory - Graph Theoretic Field Model (GTFM)

3.7.1 Data Analysis Requirements

The problem of borehole pressure history, thermally-induced pressure responses and borehole/formation skin effects in hydraulic tests was approached by development and application of a model to: (1) assist in developing an understanding of the relative importance of various parameters and conditions, and (2) provide an analytical capability for hydraulic test analysis which includes the above important phenomena.

As has been noted in previous subsections, the use of analytical solution and type-curve analysis methods based on the standard hydraulic testing procedures and equations is incorrect under certain conditions and will yield incorrect estimates for the formation parameters. It is essential in the analysis of the hydraulic testing data, to incorporate all important parameters and test conditions.

In order to simulate the system behaviour, it was first necessary to develop an appropriate mathematical model. There are two possible modeling approaches: analytical and numerical. An analytical model is one that solves exactly the governing equations which describe the system to be simulated, given specified initial conditions and boundary conditions. Although an exact solution is

obviously desirable, it can be extremely difficult, and in many cases impossible, to derive a solution for systems subject to complex boundary conditions and heterogenous properties. On the other hand, numerical models provide approximate solutions, but can be developed so that heterogeneities and complex boundary conditions may be incorporated into the model. The accuracy of the approximate solution may be maximized if the behaviour of the model in response to various numeric parameters is well understood. Since the task at hand is to simulate system response to special testing conditions which require they be modeled as mathematically complex boundary conditions, a numerical modeling approach was selected.

Prior to development of the numerical model it was necessary to specify the system which is to be modeled. For the borehole simulation model, the conceptualization of the actual physical system was simplified by the following assumptions:

- the formation interval being modeled is homogeneous (vertically), confined and of constant thickness;
- the major influence on the formation behaviour is the borehole (i.e., areal flow in the formation is negligible);
- no vertical component of flow exists in the formation interval being tested;
- the borehole fully penetrates the formation.

Given the above assumptions the physical system can be modeled as a one-dimensional radial flow system centred on the borehole. The numerical model was developed using a generalized Graph Theoretic Field Model (GTFM) approach as described below. The model was utilized to investigate the effects on the measured pressure during hydraulic testing as a result of borehole pressure history, thermally-induced pressure effect and borehole/formation skin effects. Applications of the model included a sensitivity study on the effects of variation of parameter values and testing conditions representative of typical field tests and analysis of hydraulic test data from the deep borehole in crystalline rock at Boettstein in northern Switzerland.

3.7.2 Theoretical Development

The Graph-Theoretic Field Model (GTFM) constitutes a generalized methodology for modeling the behaviour of field or continuum type problems. GTFM is based upon linear graph theory, continuum mechanics, and a spatial discretization procedure. Savage and Kesavan (1979) present generalized descriptions of the methodology.

GTFM differs fundamentally from other field modeling techniques (i.e., finite element method (FEM), and finite difference method (FDM)). Both FEM and FDM start with a continuous formulation, usually a partial differential equation, which is known to describe the field under study. A system of algebraic equations is derived through use of the appropriate technique and is then applied to a discretization representing the specific problem. With GTFM, the spatial discretization of the problem domain forms the basis for derivation of the model.

Discretization involves subdividing the problem domain into volumes (assuming that the domain is three-dimensional spatially), each represented by a node. The physical processes to be modeled are identified, and the existence of each discrete physical process recognized by incorporating a representation of the process into the discretization. The representation used is that of a directed graph edge between nodes in the discretization. When all physical processes are incorporated in this manner the resulting structure is known as the "field graph". Equations describing each physical process in the context of the field graph, written in terms of the "through" or "across" variables of the system under consideration, are known as terminal equations. "Through" and "across" are physical systems theory terms used to describe generic variable types. In the case of hydrogeologic modeling, the through variable is flow, while the across variable is hydraulic head. Combining the terminal equations with the mass balance relationships and the geometric information contained in the field graph results in a computer amenable system of algebraic equations which can be solved to approximate the behaviour of the field.

There are several GTFM formulations that can be used, depending upon whether the solution of the system is to result directly in nodal values for the through or across variables. As the purpose of this model is to analyze hydraulic testing results by comparison of model calculated results with data acquired during field hydraulic tests, model solution in terms of the across variable, hydraulic head, is most appropriate.

A rigorous application of the GTFM theory and methodology would require the definition of terms and procedures that are outside the scope of this report. A simplified technique will be presented here, with deviations from the rigorous techniques noted.

Spatial Discretization

The one-dimensional radial geometry of the system to be modeled allows discretization by subdividing the radial flow system into a series of concentric rings. The radial extent of each ring corresponds to a nodal point. A consistent node numbering scheme can be specified by having node numbers increase with radius from the centre of the borehole. The spacing of the concentric rings must reflect the physical attributes of the system being modeled. The main features of concern are the location of the physical boundaries, and the location of heterogeneities within the system.

Physical boundaries are:

- i) the borehole or well radius;
- ii) the exterior or outer boundary.

Incorporating the first boundary into the discretization is accomplished by placing a node at the borehole radius. Placement of the exterior boundary node is dependent on the particular boundary condition to be modeled. Zero flow boundaries at a specified radius dictate that a node be placed at the boundary radius. Practical considerations require that constant head boundaries at infinite radius be modeled by

specifying that the boundary node be located at a finite radius. Providing that the radius is sufficiently distant from the borehole radius, and that other numerical considerations are met, boundary effects on simulation results will be negligible.

The physical system described in earlier subsections has one heterogeneity of concern, the "skin zone". Modeling skin effects requires that one node be located at the interface between the skin zone and aquifer.

At this point the discretization consists of three nodes, one at each external boundary, and one at the interface between the skin zone and the aquifer. To adequately model the system behaviour, numerical considerations require that more nodes be placed in the discretization. Accordingly, a number of nodes are placed in the interval between the borehole node and the skin interface node, and between the skin interface node and the exterior boundary node. The spacing of these nodes is determined by practical and numerical considerations. In the skin zone and the area of the aquifer close to the borehole, where the most rapid head changes occur during hydraulic testing, the spacing between nodes should be relatively small. At radii further into the aquifer, node spacings may increase without deleterious effects on the model's results.

Figure 3.7-1 illustrates the final spatial discretization. Nodes in the skin zone are separated by a constant distance Δr_{skin} . Nodes in the aquifer are separated by a constant logarithmic increment Δa such that:

$$r_{i+1} = r_i e^{\Delta a} \quad (3.7-1)$$

where:

r_i radius of node i

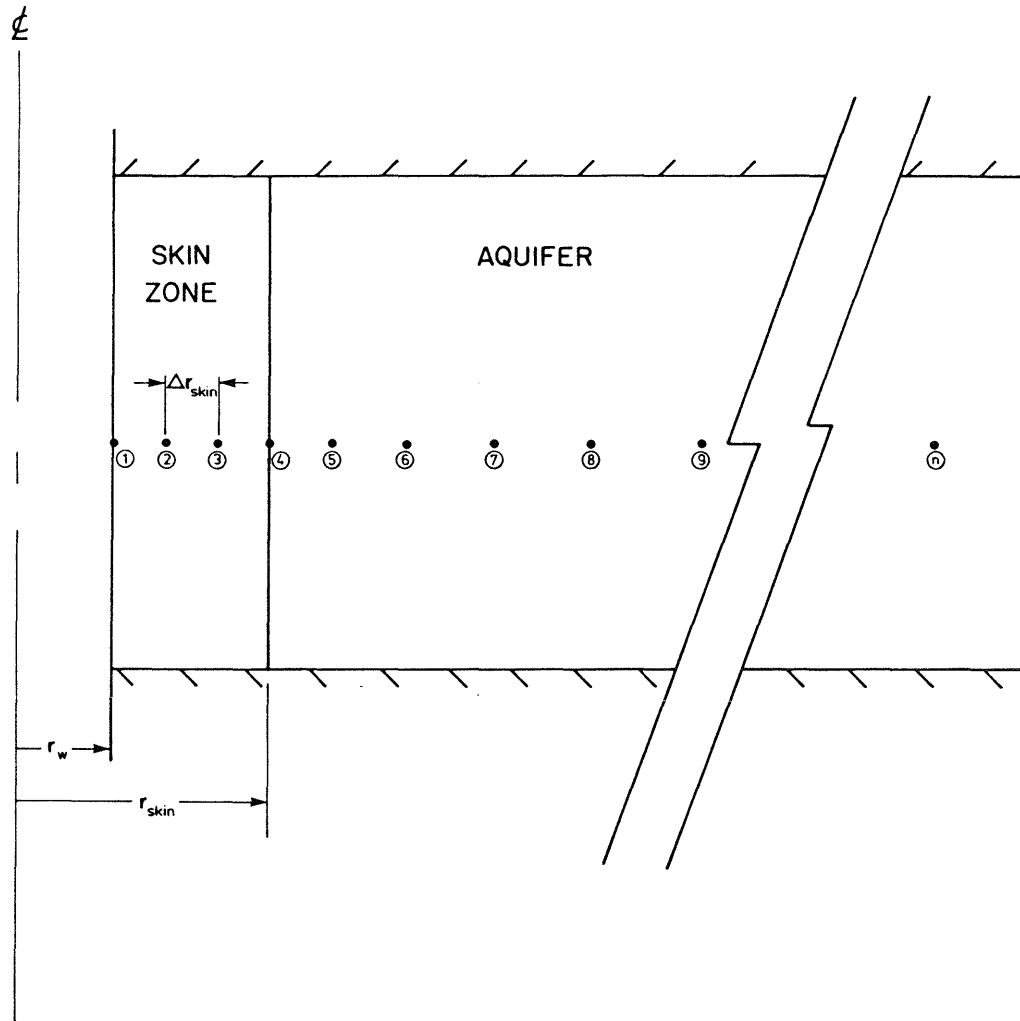


Figure 3.7-1 Schematic illustration of spatial discretization

Field Graph

The physical processes of concern are flow as per Darcy's Law, flow due to storage, and flow at boundary nodes.

Darcian flow is incorporated in the field graph by introduction of a directed graph edge between each adjacent node in the discretization. The direction of each edge is arbitrarily specified as towards the borehole node. This corresponds to an assumed direction of positive flow.

Flow due to storage is denoted by a graph edge directed into each node from an "auxillary node". This auxillary node is a "virtual node" in the sense that it does not actually exist. It is incorporated in the graph to alleviate the difficulty of representing temporal variation in a strictly spatial discretization. As flow due to storage is defined in terms of a time derivative, some mechanism for consideration of nonspatial properties is necessary. Again, the direction of the graph edge is arbitrarily specified, in this case towards the real node and away from the auxillary node.

Flow at boundary nodes is incorporated in the field graph as a separate graph edge at each of the two boundary nodes. The graph edge corresponds to flow into or out of the modeled system from or to the system environment. Flow at boundary nodes is between a datum node and the boundary node. The datum node is an auxillary node which provides a reference point for boundary through variables and nodal across variables in the modeled system.

Construction of the field graph is best illustrated by constructing graph fragments for each of the several classes of nodes in the system under consideration and subsequently combining the fragments to form a complete field graph. There are three node classes of concern:

- i) the borehole radius node;
- ii) non-boundary nodes;
- iii) exterior boundary node.

Figure 3.7-2a illustrates the field graph for the borehole radius node. The graph edge labelled d_1 refers to Darcian flow into the borehole radius node from the next adjacent node in the discretization. Edge $s2_1$ represents flow due to storage in the volume of the problem domain contributing to the boundary node. Edge w is flow from the modeled system into the wellbore.

The field graph fragment for a non-boundary node j is illustrated in Figure 3.7-2b. Nodes i , j , and k are in order of increasing radius. Edge d_i represents Darcian flow between nodes i and j . Similarly, edge d_j is Darcian flow between nodes j and k . Edge $s1_j$ is flow into node j due to storage in the volume of the problem domain between nodes i and j that contributes to node j . Edge $s2_j$ is flow into node j due to storage in the volume of the problem domain between nodes j and k that contributes to node j .

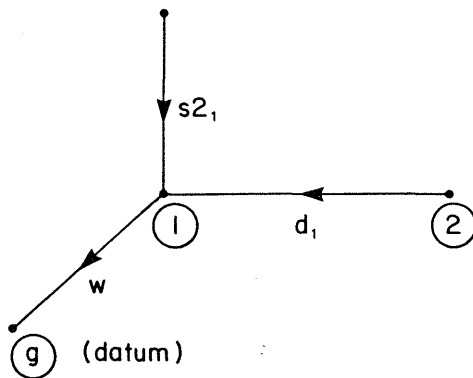
Figure 3.7-2c illustrates the field graph for the exterior boundary node labelled as node n . The graph edge labelled d_{n-1} refers to Darcian flow from the boundary node to the adjacent interior node. Edge $s1_n$ represents flow due to storage in the volume of the problem domain contributing to the boundary node. Edge b is flow from outside the problem domain into the modeled system.

Combining the graph fragments in Figures 3.7-2a through 3.7-2c with the spatial discretization from Figure 3.7-1 results in the field graph illustrated in Figure 3.7-3. The field graph in Figure 3.7-3 represents a moderate simplification of the GTFM procedure in that a second graph structure, used to delineate geometric information with respect to each node, is not included. The relative simplicity of the one-dimensional field being modeled allows the geometric information required to formulate the terminal equations to be readily extracted without resorting to the second graph structure.

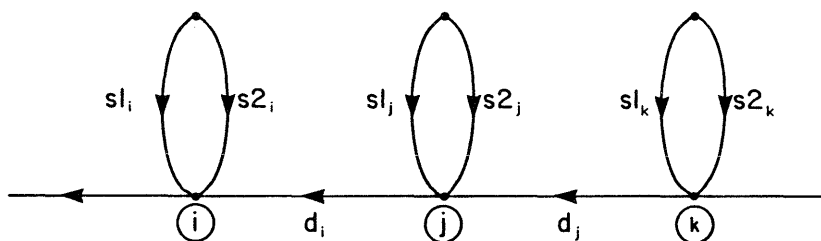
Terminal Equations

Terminal equations must be written for each edge in the field graph. The process can be simplified by writing generic equations for each type of graph edge, and substituting the appropriate node specific parameters when the matrix equations are formed.

a) Borehole radius node



b) Nonboundary node



c) Exterior node

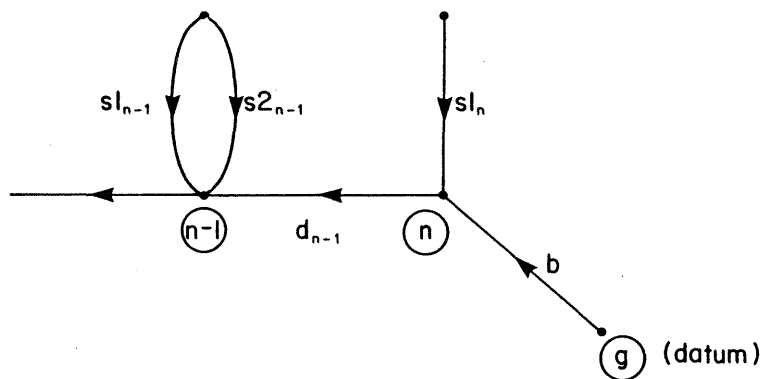


Figure 3.7-2 Field graph fragments for three classes of nodes

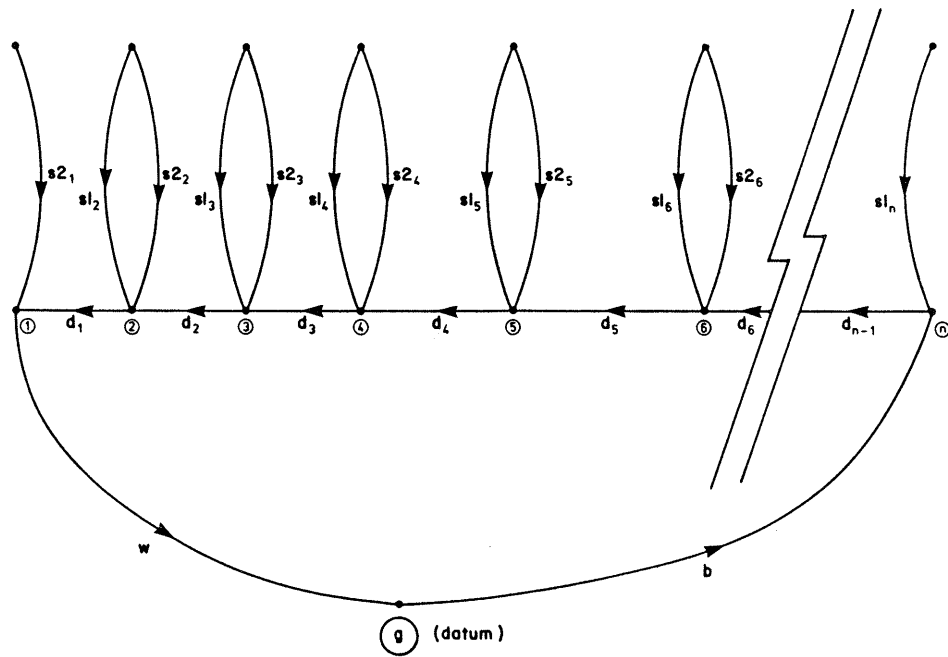


Figure 3.7-3 Field graph for problem discretization

Figure 3.7-4 is a representation of the field graph for three nodes i, j, and k, overlaying a diagram of the section of the aquifer being modeled. Terminal equations for the edges d_j , s_{1j} , and s_{2j} will be derived.

According to Darcy's Law:

$$q_d = - K A \frac{dh}{dl} \quad (3.7-2)$$

where:

q_d	flow, L^3t^{-1} ;
K	hydraulic conductivity, Lt^{-1} ;
A	cross sectional area, L^2 ;
dh/dl	differential of hydraulic head with respect to distance.

Edge d_j requires a matrix formulation relating the variables q_{d_j} , q_{d_k} , h_j and h_k where:

q_{d_j}	flow into node j due to edge d_j , L^3t^{-1} ;
q_{d_k}	flow out of node k due to edge d_j , L^3t^{-1} ;
h_j	hydraulic head at node j, L;
h_k	hydraulic head at node k, L.

Approximating the derivative term in equation 3.7-2 and applying Darcy's Law to graph edge d_j results in:

$$q_{d_j} = - K_j A_j \frac{(h_k - h_j)}{(r_k - r_j)} \quad (3.7-3)$$

$$q_{d_k} = K_j A_j \frac{(h_k - h_j)}{(r_k - r_j)} \quad (3.7-4)$$

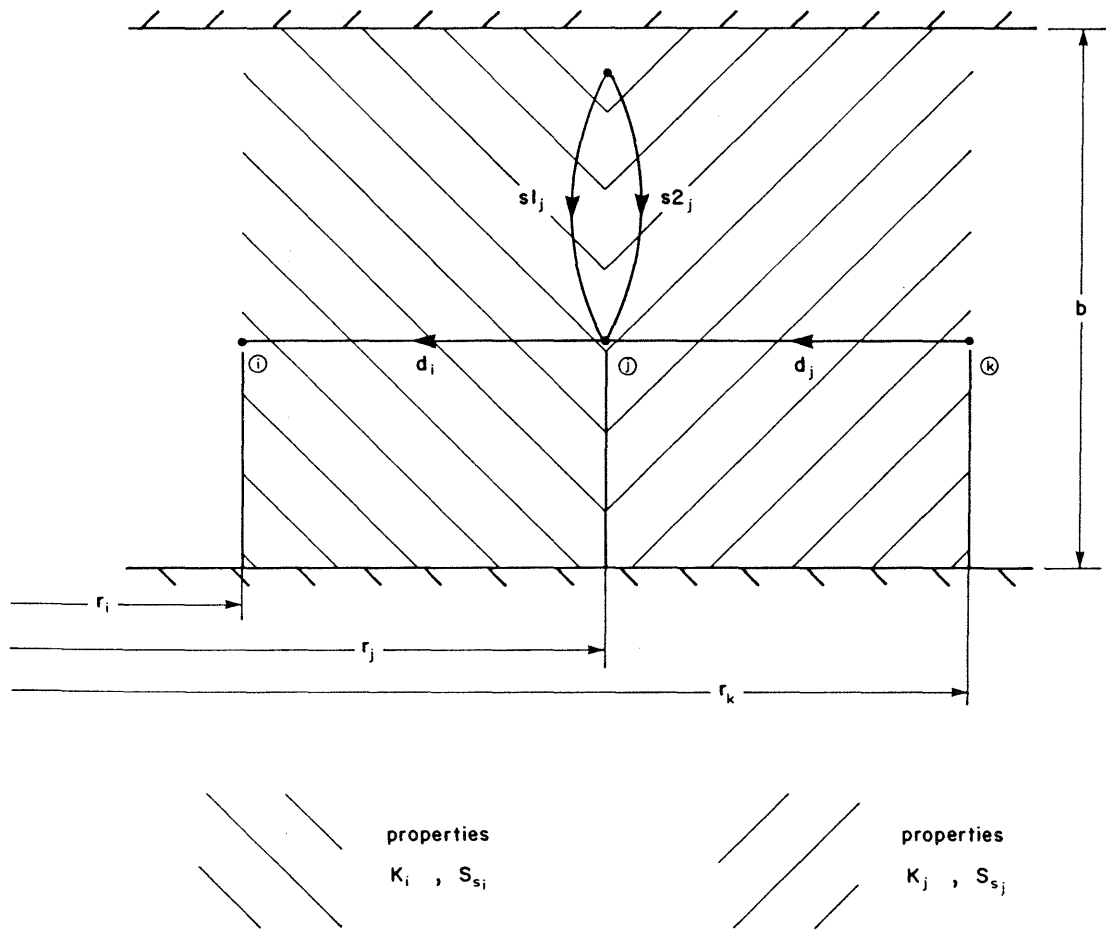


Figure 3.7-4 Field graph fragment illustrating geometric parameters and physical properties

where:

K_j hydraulic conductivity of the section of the problem domain bounded by nodes j and k , Lt^{-1} ;

A_j cross sectional area at a radius equal to the average of the radii of nodes j and k , L^2 .

In matrix form:

$$\begin{bmatrix} q_{d,j} \\ q_{d,k} \end{bmatrix} = D_j \begin{bmatrix} -1 & 1 \\ 1 & -1 \end{bmatrix} \begin{bmatrix} h_j \\ h_k \end{bmatrix} \quad (3.7-5)$$

where:

$$D_j = \frac{K_j A_j}{(r_k - r_j)} \quad (3.7-6)$$

The storativity equation is written:

$$q_s = S_s V \frac{dh}{dt} \quad (3.7-7)$$

where:

q_s flow, L^3t^{-1} ;

S_s specific storage, L^{-1} ;

V volume contributing to flow, L^3 ;

dh/dt derivative of hydraulic head with respect to time, Lt^{-1} .

The terminal equations for graph edges $s1_j$ and $s2_j$ relates the variables q_{s1_j} and q_{s2_j} to the time differential of h_j where:

q_{s1_j} flow into node j due to edge $s1_j$, L^3t^{-1} ;

q_{s2_j} flow into node j due to edge $s2_j$, L^3t^{-1} .

Applying the storativity equation to edge sl_j results in:

$$q_{sl_j} = S_{s_i} V_{l_j} \frac{dh_j}{dt} \quad (3.7-8)$$

where:

S_{s_i} specific storage of the section of the problem domain between nodes i and j , L^{-1} ;

V_{l_j} volume of the problem domain bounded by nodes i and j which contributes to node j , L^3 .

Simplifying equation 3.7-8 results in:

$$q_{sl_j} = E_j \frac{dh}{dt} \quad (3.7-9)$$

where:

$$E_j = S_{s_i} V_{l_j}$$

The terminal equation for s_{2j} is written:

$$q_{s_{2j}} = F_j \frac{dh}{dt} \quad (3.7-10)$$

where:

$$F_j = S_{s_j} V_{2j}$$

The terminal equation for the boundary condition at the wellbore varies according to the specific type of hydraulic test being modeled.

For isothermal pulse tests the terminal equation is:

$$q_w = V_w \rho C_w g \frac{dh_1}{dt} \quad (3.7-11)$$

where:

V_w volume of pressurized section of wellbore, L^3 ;

C_w compressibility of fluid in wellbore, $M^{-1}Lt^2$;

- 74 -

ρ density of fluid in wellbore,
ML⁻³;

g acceleration due to gravity, Lt⁻².

For nonisothermal pulse tests, a term describing the expansion or contraction of fluid in the borehole due to thermal effects is added to equation 3.7-11:

$$q_w = V_w \rho C_w g \frac{dh_1}{dt} - V_w C_t \frac{dT}{dt} \quad (3.7-12)$$

where:

C_t coefficient of thermal expansion
for fluid in the borehole,
T⁻¹;

dT/dt derivative of borehole fluid
temperature with respect to time,
Tt⁻¹.

The terminal equation for q_w for slug tests is described as:

$$q_w = \pi r_c^2 \frac{dh_1}{dt} \quad (3.7-13)$$

where:

r_c radius of the well casing or
standpipe, L.

Derivation of the terminal equation for a fixed head condition at the wellbore (i.e., borehole history cases) is not necessary as the model solution technique described subsequently incorporates the boundary condition directly.

Constant head boundary conditions at the exterior boundary of the discretization are modeled similarly to fixed head in the borehole. Zero flow exterior boundary conditions require specification of the terminal equation for edge b in Figure 3.7-2c. This is written as:

$$q_b = 0 \quad (3.7-14)$$

Formulation of the matrix equations follows.

Matrix Equations

Matrix equations can be formulated by applying the "vertex postulate" to each node in the discretization. The vertex postulate states that "the oriented sum of the through variable measurements implied by the edges incident on a given node is zero at any instant in time" (Savage and Kesavan, 1979). For example, applying the vertex postulate to the single node illustrated in Figure 3.7-5 results in:

$$-q_a + q_b + q_c = 0 \quad (3.7-15)$$

Applying the vertex postulate to the field graph illustrated in Figure 3.7-3 results in the following system of equations.

$$q_{d_1} + q_{s2_1} - q_w = 0 \quad (3.7-16)$$

$$q_{d_i} + q_{s1_i} + q_{s2_i} - q_{d_{i-1}} = 0 \quad (3.7-17)$$

$$i = 2..n-1$$

$$q_{s1_n} + q_b - q_{d_{n-1}} = 0 \quad (3.7-18)$$

Substitution of the terminal equations into equations 3.7-16, 3.7-17 and 3.7-18 is straightforward. For example, the matrix equations for a nonisothermal pulse test, using the terminal equation for q_w given in equation 3.7-12, and applying a fixed head exterior boundary condition results in:

$$\begin{bmatrix} A_{ii} \end{bmatrix} \begin{bmatrix} h_i \end{bmatrix} + \begin{bmatrix} B_{ii} \end{bmatrix} \left[\frac{dh_i}{dt} \right] + \begin{bmatrix} C_i \end{bmatrix} = \begin{bmatrix} 0 \end{bmatrix} \quad (3.7-19)$$

$$i = 1..n$$

where:

$$\left. \begin{aligned} A_{1,1} &= -D_1 \\ A_{1,2} &= D_1 \\ A_{i,i-1} &= D_{i-1} \\ A_{i,i} &= -D_{i-1} - D_i \\ A_{i,i+1} &= D_i \end{aligned} \right\} i = 2..n-1$$

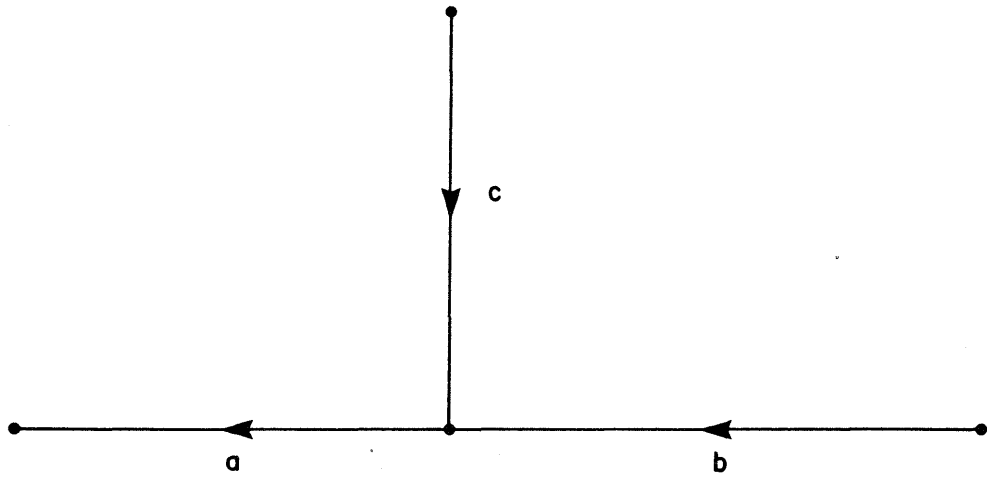


Figure 3.7-5 Example graph segment for illustrating vertex postulate

$$\begin{aligned}
 A_{n,n-1} &= D_{n-1} \\
 A_{n,n} &= -D_{n-1} \\
 B_{1,1} &= F_1 - V_w \rho C_w g \\
 B_{i,i} &= E_i + F_i & i = 2..n-1 \\
 B_{n,n} &= E_n
 \end{aligned}$$

$$C_1 = V_w C_t \frac{dT}{dt}$$

$$C_i = 0 \quad i = 2..n-1$$

$$C_n = q_b$$

Incorporating different boundary conditions will result in changes to matrix and vector entries $B_{1,1}$, C_1 , and C_n .

For isothermal pulse tests:

$$B_{1,1} = F_1 - V_w \rho C_w g$$

$$C_1 = 0$$

For slug tests:

$$B_{1,1} = F_1 - \pi r_c^2$$

$$C_1 = 0$$

For fixed head at the borehole:

$$B_{1,1} = F_1$$

$$C_1 = -q_w$$

For zero flow exterior boundaries:

$$C_n = 0$$

Converting the matrix equations given in equation 3.7-19 to a computer amenable form involves developing an approximation of time derivative terms and partitioning the resulting equations to account for fixed head boundaries.

Computer Implementation

Time derivatives are approximated with the fully implicit technique:

$$\frac{dh_i}{dt} = \frac{h_{i_t} - h_{i_{t-\Delta t}}}{\Delta t} \quad (3.7-20)$$

where:

h_{i_t} value of h at node i at time t, L;
 Δt time step size, t.

The time derivative of the thermal term in equation 3.7-12 is similarly approximated.

Substituting equation 3.7-20 into equation 3.7-19, and partitioning the resulting matrix equation to reflect any fixed head boundary conditions results in a system of m equations and m unknowns, where m equals the number of nodes in the field graph minus the number of fixed head boundary conditions. The equation can readily be solved using any standard matrix solution technique provided that initial conditions (i.e., h_i at $t = 0$ for $i = 1..n$) are available.

The modeling technique as described above simulates only single-well or single-borehole test types which, for the most part, can be readily solved with standard analytic procedures. However, most hydraulic tests performed under field conditions involve a sequence of tests, each of which can affect the results of subsequent tests. Analytic solutions, or type curves for hydraulic test analysis, are generally not capable of solving such complex cases. Analytic solutions can be implemented for application to field problems involving a test sequence; however, the computer implementation of these solutions is generally limited to sequences involving the same test type and is not amenable to problems involving a test sequence with various test types (e.g., pulse, slug, drill stem and flow tests). The model presented here (denoted GTFM) can be used to simulate multiple tests (i.e., test sequences) by using the head values at each node at the end of a test as the initial conditions for the subsequent test. Therefore GTFM is a very powerful general-purpose tool for the analysis of borehole tests under both isothermal and nonisothermal testing conditions.

3.7.3 Model Verification

The accuracy and ability of GTFM to simulate the borehole pressure from a variety of test types was verified by comparison to analytical solutions (see Chapter 2 for appropriate test types and corresponding analytical solutions) and, for cases involving borehole/formation skin effects, borehole pressure history and thermal effects, by comparison to results from the three-dimensional flow and heat transport finite-difference model SWIFT (Simulator for Waste Injection Flow and Transport). The verification examples and their corresponding figure numbers are summarized below:

Test Type	Figures	Analytical Solution or Numerical Model
Slug	3.7-6	Bredehoeft and Papadopulos (1980)
Pulse	3.7-7	Cooper et al. (1967)
Constant drawdown	3.7-8	Lohman (1972)
Pulse test (single fracture) - infinite radius	3.7-9a	Wang et al. (1978)
- finite radius - zero flow boundary	3.7-9b	Wang et al. (1978)
- pressure boundary	3.7-9c	Wang et al. (1978)
Slug test with borehole/ formation skin	3.7-10	SWIFT (results from Faust and Mercer), 1984
Pulse test with borehole pressure history and thermal effects	3.7-13	SWIFT

Hydraulic Tests (Isothermal Conditions)

The input parameters utilized in the simulations for isothermal test conditions (excepting the skin effects case which utilized the parameters from the Faust and Mercer (1984) paper) are summarized in Table 3.7-1. The test conditions, pressures and fluid properties were chosen as representative of testing that would be conducted at a depth of approximately 1000 metres. The value of hydraulic conductivity was varied in the range of 1×10^{-11} to 1×10^{-6} m/s for slug tests, 1×10^{-13} to 1×10^{-10} m/s for pulse tests and 1×10^{-12} to 1×10^{-8} m/s for constant drawdown tests.

For practical purposes, the comparison between GTFM and analytical solution results, for the isothermal cases (see Figures 3.7-6 to 3.7-9) are very good for all cases. The example for borehole/formation skin effects (see Figure 3.7-10) also compares well with the SWIFT model results. These examples illustrate that GTFM is an accurate and versatile data analysis tool for a variety of hydraulic test methodologies with various assumed boundary conditions.

Nonisothermal Pulse Test

To present a model verification of GTFM's ability to accurately simulate a hydraulic test with a significant thermally-induced pressure response, GTFM was compared to the SWIFT computer code. This simulator is a three-dimensional transient model which is capable of solving the coupled equations for fluid flow, solute and heat transport and brine migration in geologic media. The SWIFT model has been validated during numerous applications in the past decade. Full details on the governing equations, finite-difference formulation and solution techniques of the model are presented in other reference sources (e.g., Dillon et al., 1978, Reeves and Cranwell, 1981).

The SWIFT code incorporates directly all thermally-induced pressure changes in both the borehole and the rock and allows calculation of the appropriate pressure and thermal profiles radially into the formation. This comparison between GTFM and SWIFT is necessary because the GTFM model is based on the assumption that nonisothermal conditions have a pronounced effect on pressures in the borehole and an insignificant effect on pressures in the formation. The SWIFT model

Parameter	Value
Fluid compressibility, Pa^{-1}	4.3×10^{-10}
Fluid viscosity, $\text{kg m}^{-1}\text{s}^{-1}$	5.7×10^{-4}
Fluid density, kg m^{-3} ,	993
Fluid thermal expansion coefficient, $^{\circ}\text{C}^{-1}$	4.4×10^{-4}
Formation porosity	0.005
Formation compressibility, Pa^{-1}	2.3×10^{-11}
Test interval length, m	10.0
Borehole radius, m	0.0795
Tubing string (casing) radius, m	0.031
Storage coefficient	2.4×10^{-6}
Hydraulic conductivity, m s^{-1}	varied

Table 3.7-1 Summary of Parameter Values Utilized in Verification Cases Comparing GTFM to Analytical Solution Results

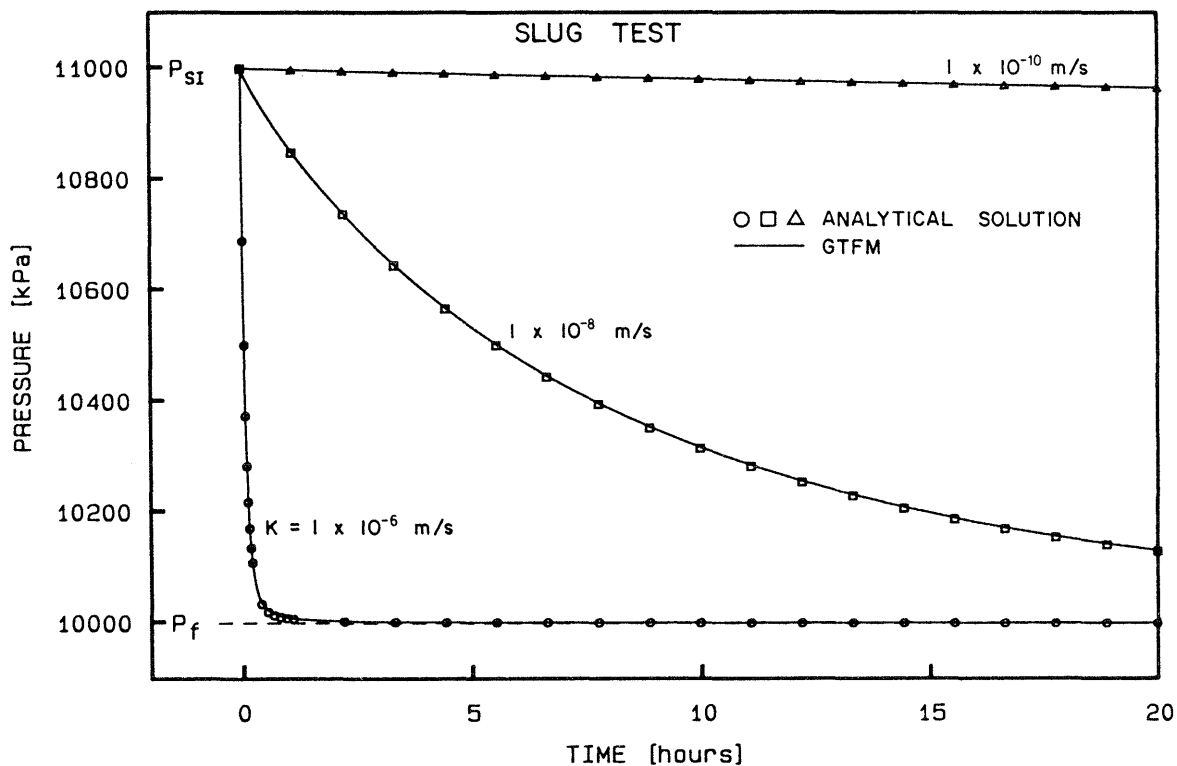


Figure 3.7-6 Comparison between GTFM and Cooper et al., (1967) analytical solution results

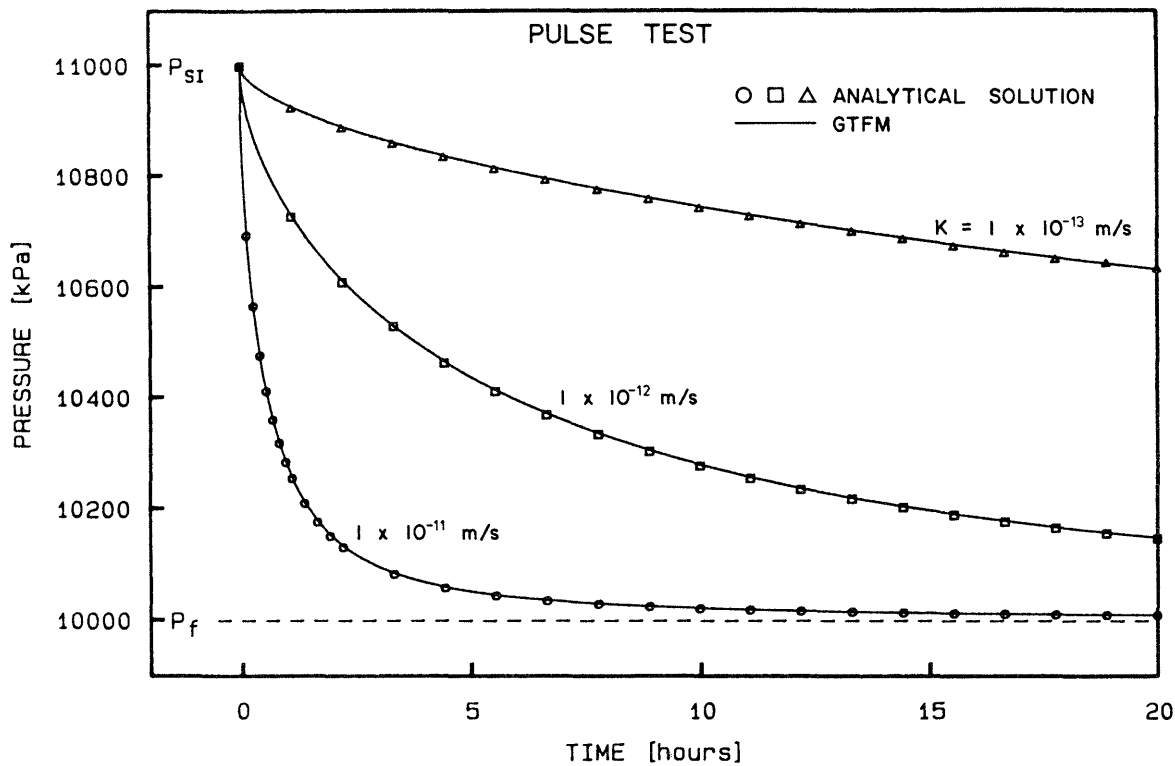


Figure 3.7-7 Comparison between GTFM and Bredehoeft and Papadopoulos (1980) analytical solution results

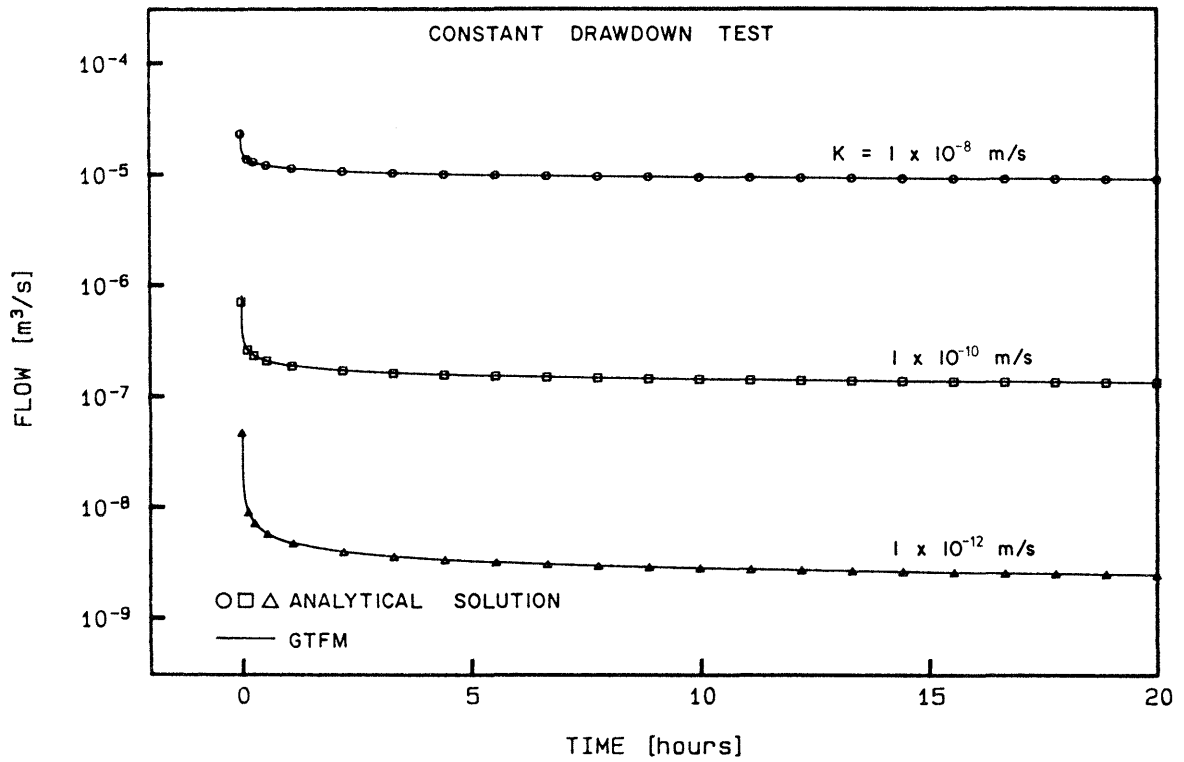


Figure 3.7-8 Comparison between GTFM and Lohman (1972) analytical solution results

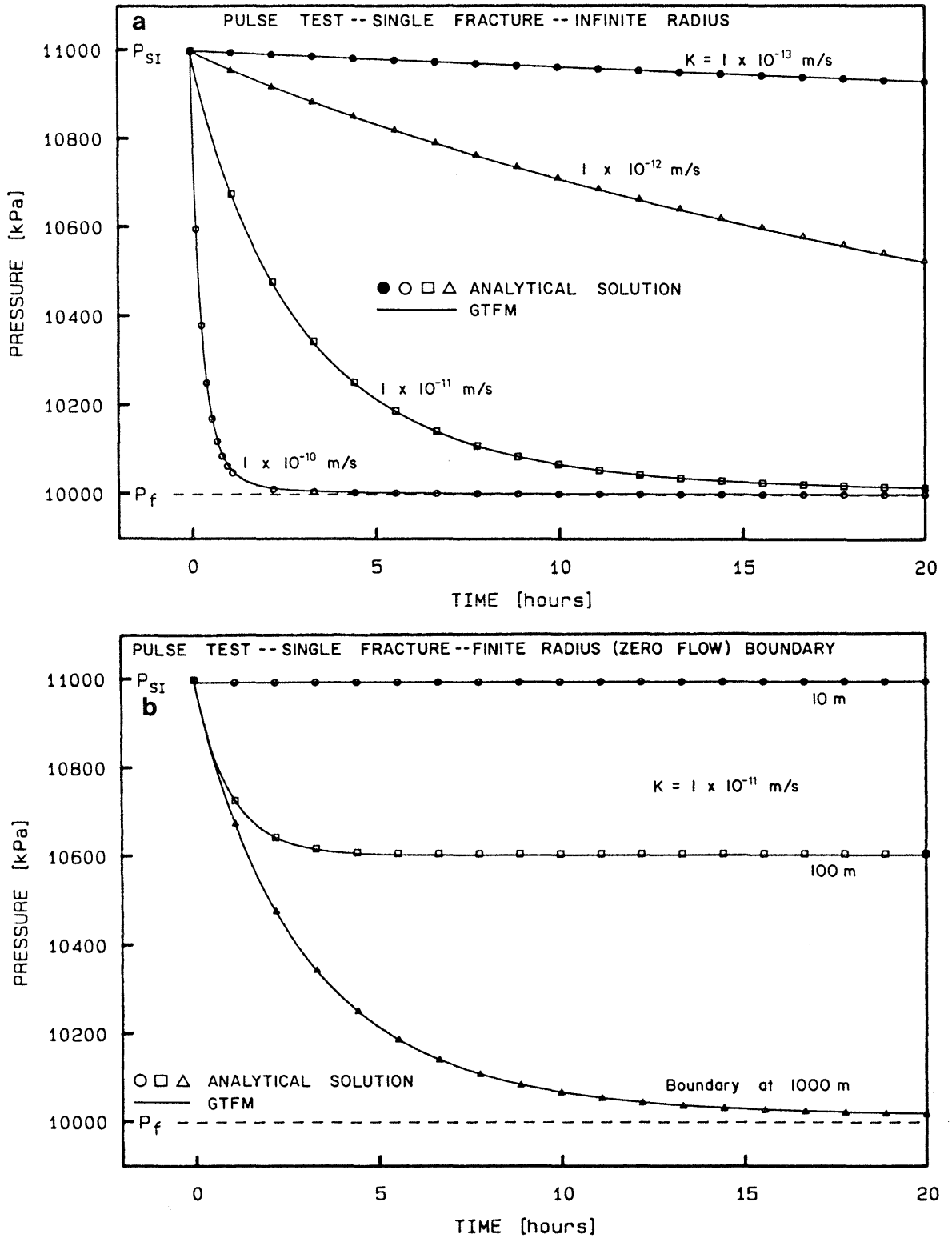


Figure 3.7-9 Comparison between GTFM and Wang et al. (1978) analytical solution results for (a) infinite radius and (b) finite radius with zero flow boundary

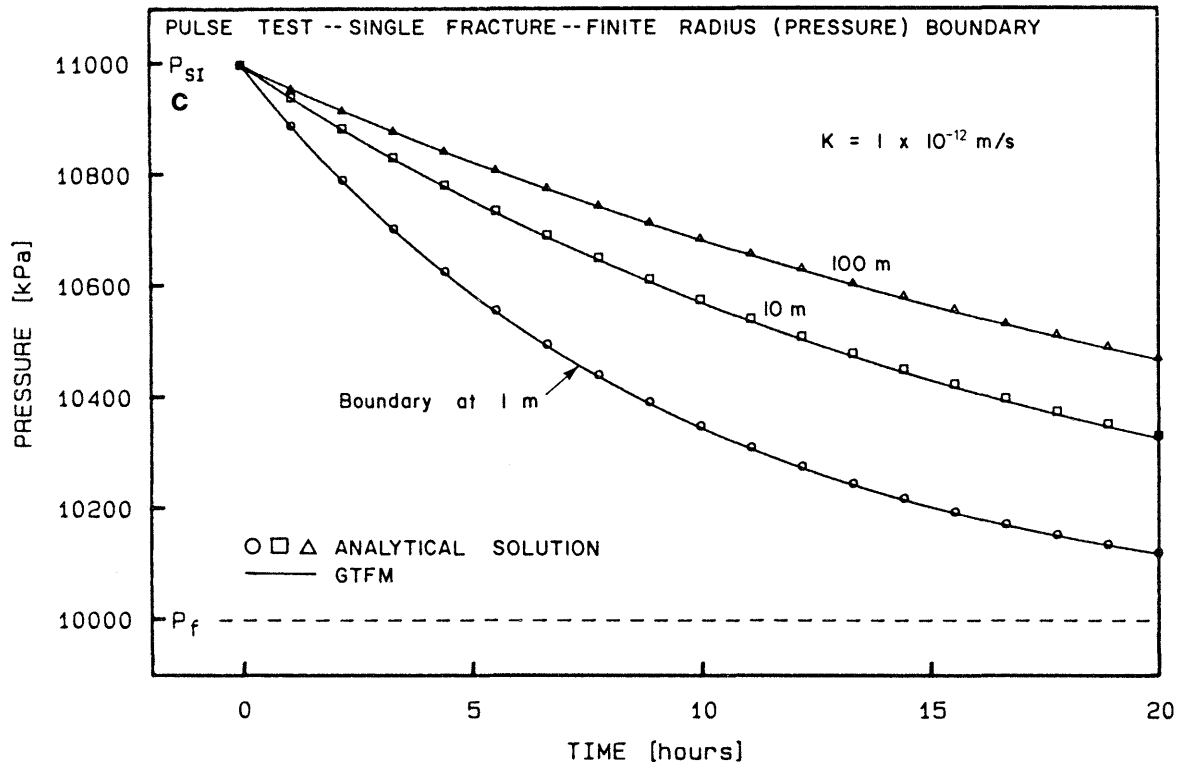


Figure 3.7-9 Comparison between GTFM and Wang et al. (1978) analytical solution results for (c) finite radius with constant pressure boundary

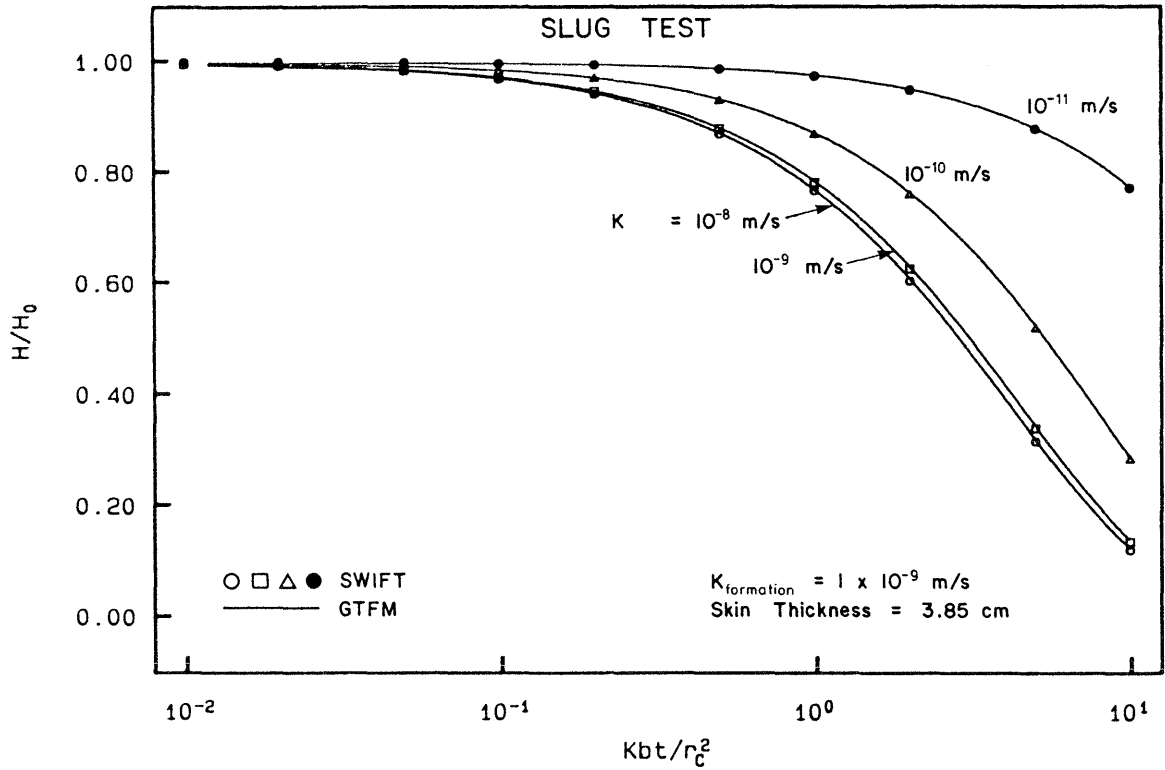


Figure 3.7-10 Comparison between GTFM and SWIFT (from Faust and Mercer, 1984) results for a borehole/formation skin

includes all of the important parameters required for simulating flow and heat transport in both the borehole and the formation including: fluid density, fluid compressibility, fluid thermal expansion coefficient, fluid viscosity, fluid heat capacity, formation hydraulic conductivity, formation thermal conductivity, formation heat capacity, formation rock density and formation porosity. The temperature and pressure dependence of fluid density and the temperature dependence of viscosity are also included.

The input parameter values utilized in the GTFM and SWIFT model simulations are summarized in Table 3.7-2. The test conditions for the SWIFT simulator illustrating the time periods with specified temperature and pressure (i.e., Dirichlet boundary conditions) in the borehole and the time periods with calculated responses are shown in Figure 3.7-11. These conditions and required times were chosen as typical for a field test sequence involving drilling a borehole interval, removing the drill string, running in the test tool and starting a pulse injection test. During the drilling period, a lower temperature skin is developed in the formation surrounding the borehole interval (see schematic illustration in Figures 3.3-1 and 3.4-1). The temperature of the borehole fluid rises during the post-drilling phases in response to the higher formation temperature.

The calculated temperature response in the borehole interval from the SWIFT simulation (see Figure 3.7-12) was utilized as input to the GTFM model. A comparison between the calculated pressure responses in the borehole interval from SWIFT and GTFM is shown in Figure 3.7-13.

Because of the low hydraulic conductivity (5×10^{-14} m/s) and the dramatically increasing increasing temperature, the pressure pulse does not decay towards the formation pressure or the annulus pressure but instead increases in magnitude due to a thermally induced pressure response. Both the GTFM and SWIFT models are able to simulate this phenomena. The difference in the results of the two models are considered mainly attributable to differences in their approach to handle nonisothermal borehole conditions. The pressure responses from the two models compare closely demonstrating the ability of the GTFM approach for analysis of nonisothermal borehole hydraulic tests.

Parameter	SWIFT	GTFM
Fluid compressibility, Pa ⁻¹	4.3 x 10 ⁻¹⁰	4.3 x 10 ⁻¹⁰
Fluid viscosity, kg m ⁻¹ s ⁻¹ , at 40 °C	7.0 x 10 ⁻⁴ (function of temp.)	not applicable (include in K)
Fluid density, kg m ⁻³ , at 40 °C and 7600 kPa	995.1 (function of temp. and pressure)	995.1 (constant)
Fluid thermal expansion coefficient, °C ⁻¹	3.8 x 10 ⁻⁴	3.8 x 10 ⁻⁴
Fluid heat capacity, J kg ⁻¹ °C ⁻¹	4.18 x 10 ³	not applicable
Formation hydraulic conductivity, m s ⁻¹	5.0 x 10 ⁻¹⁴	5.0 x 10 ⁻¹⁴
Formation porosity	0.005	0.005
Formation thermal conductivity, J m ⁻¹ s ⁻¹ °C ⁻¹	3.0	not applicable
Formation heat capacity, J m ⁻³ °C ⁻¹	2.4 x 10 ⁶	not applicable
Formation rock density, kg m ⁻³	2.67 x 10 ³	not applicable
Test interval length, m	10.0	10.0
Borehole radius, m	0.0795	0.0795
Storage coefficient	2.2 x 10 ⁻⁷	2.2 x 10 ⁻⁷
Formation pressure, kPa	7400	7400
Annulus pressure, kPa	7233	7233
Pressure at start of pulse injection test, kPa	7599	7599
Drill fluid temperature, °C	35.4	not applicable
Initial formation temperature °C	40.6	not applicable

Table 3.7-2 Summary of Parameter Values Utilized in
SWIFT - GTFM Model Comparison Case

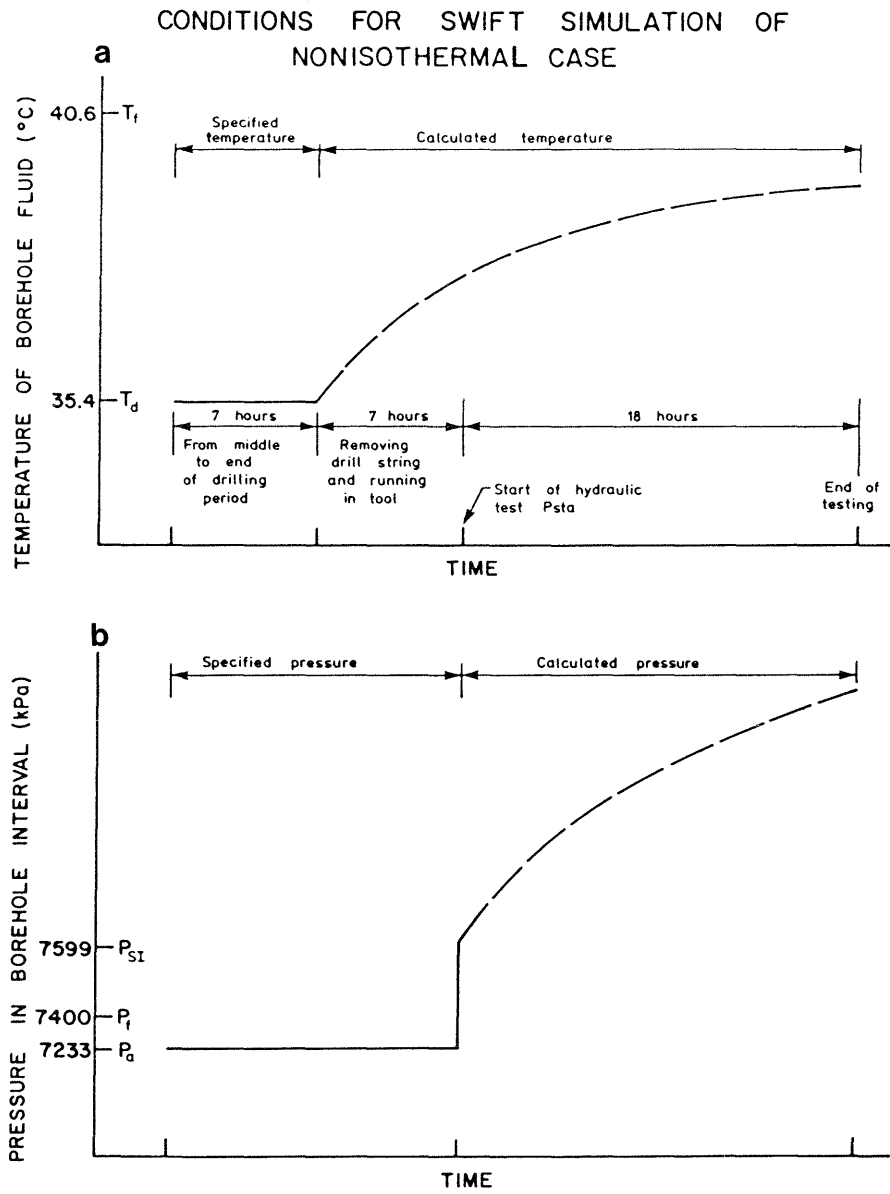


Figure 3.7-11 Conditions for SWIFT simulation of nonisothermal case: (a) borehole temperature response and (b) borehole pressure response

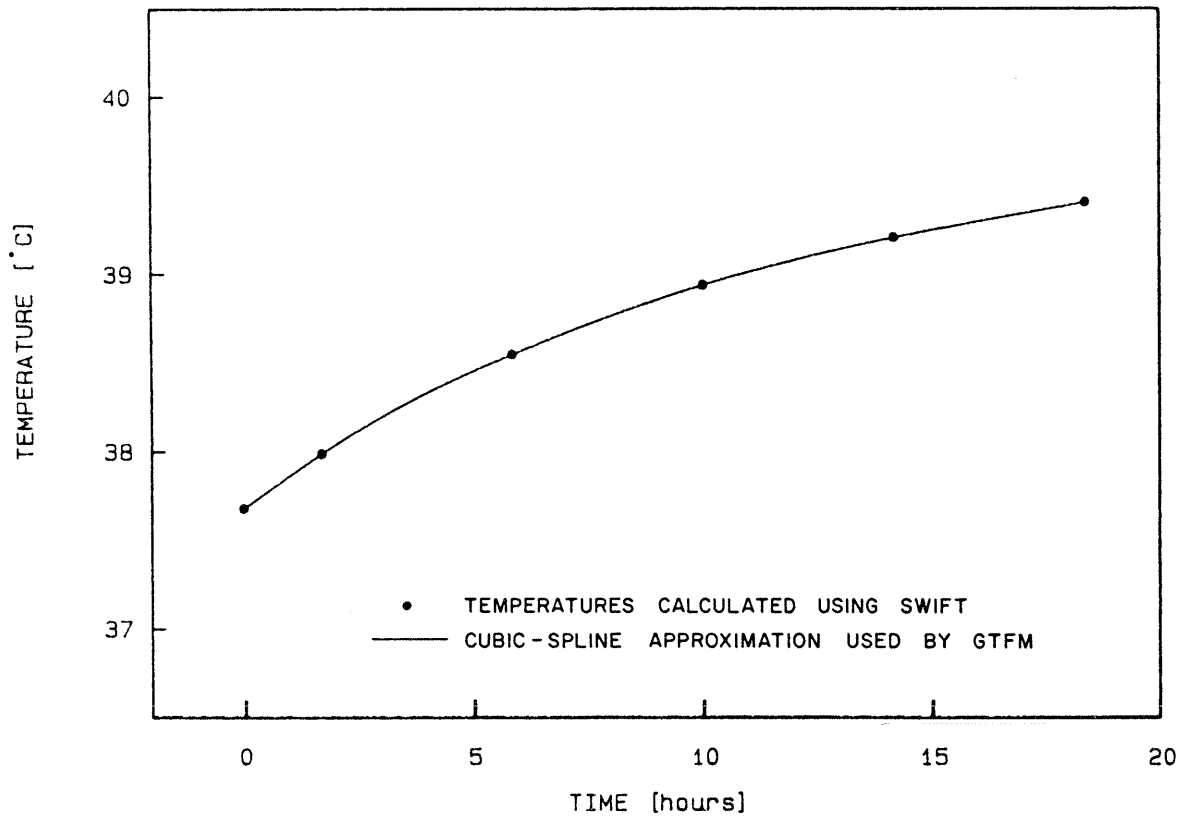


Figure 3.7-12 SWIFT calculated temperature response and cubic-spline approximation utilized in GTFM

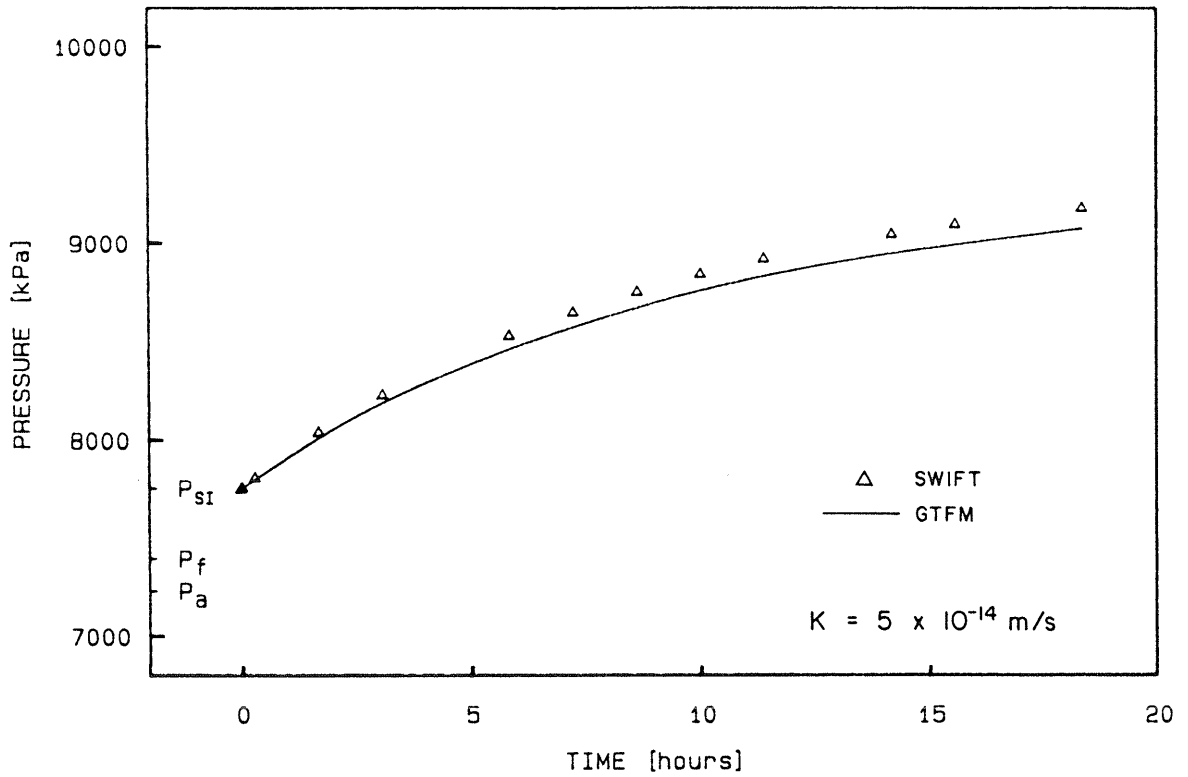


Figure 3.7-13 Comparison between GTFM and SWIFT calculated pressure responses

Although slight differences exist between the calculated model results, GTFM is considered an adequate and versatile method for analyzing nonisothermal borehole hydraulic tests. Because it is a much simpler model than SWIFT, it offers some advantages as a tool for routine hydraulic test analysis. For some cases such as those requiring a detailed understanding of the thermal regime within the formation, the SWIFT model would be the appropriate choice.

3.8 Parameter Sensitivity Analyses

A parameter sensitivity analysis was conducted using GTFM to investigate the effects of borehole pressure history, thermally-induced pressure effects and borehole/formation skin effects. Using the fluid and formation properties summarized in Table 3.7-1 and a range of formation hydraulic conductivities, GTFM simulations were conducted for a range of test conditions involving various borehole open periods, various borehole fluid temperature response curves and various borehole/formation skin hydraulic conductivities.

3.8.1 Borehole Pressure History

GTFM simulations were conducted to quantitatively investigate the effect of pretest borehole pressure history (see detailed discussion in section 3.3) on the pressure response during a subsequent pulse or slug injection or withdrawal test, for a range of borehole open periods and hydraulic conductivities. This effect is important with regards to the accuracy of the interpreted formation pressure and hydraulic conductivity from the measured pressure response from a field test. The simulation results presented in this subsection are for test conditions where the borehole fluid and the formation are at constant and equal temperature (i.e., isothermal conditions). The relative magnitudes of formation pressure (P_f), annulus pressure (P_a) corresponding to borehole overflow conditions and pressure at shut-in (P_{SI}) at the start of the tests are shown in Figure 3.8-1. The chosen simulation cases assume that the formation pressure is 300 kPa above the annulus pressure. Borehole open periods of 1, 30 and 365 days were chosen as

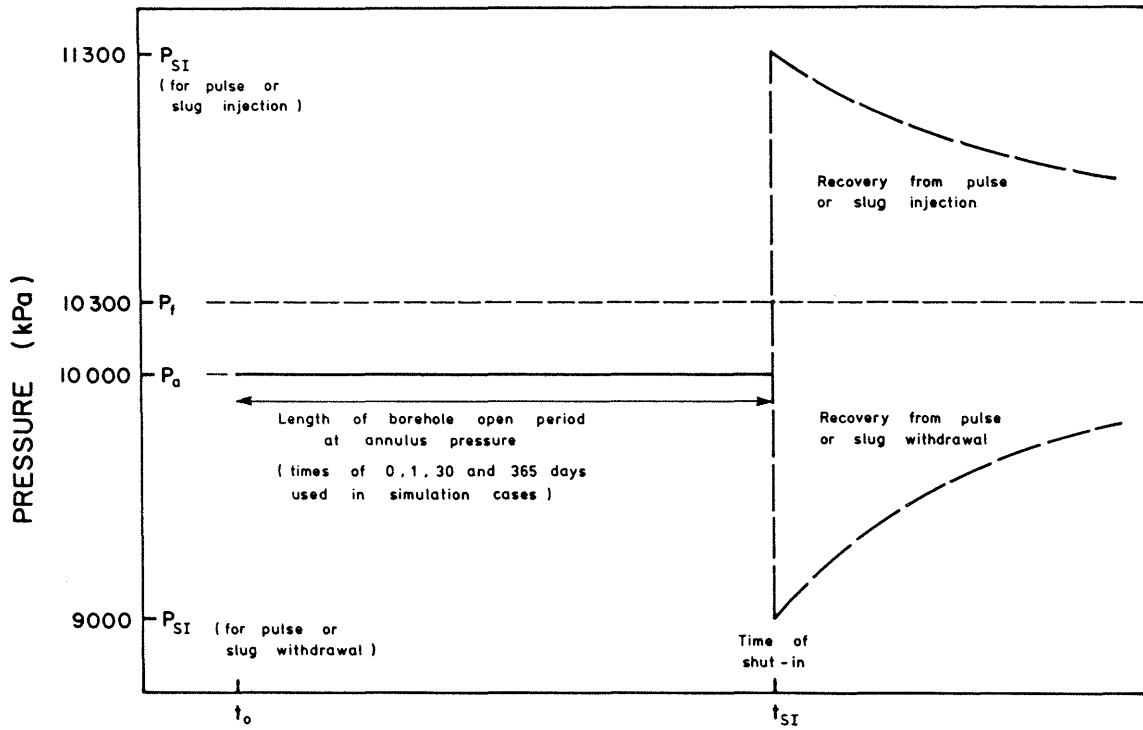


Figure 3.8-1 Illustration of the pretest conditions for the borehole pressure history simulation cases

representative of the length of open period corresponding to testing (1) immediately after drilling a short borehole interval, (2) during sequential testing of borehole segments after drilling a larger length of borehole (sometimes referred to as hydrogeologic reconnaissance logging), and (3) after a long open period during which geophysical logging and geochemical sampling may have been conducted. The case of zero borehole open period corresponding to the ideal conditions upon which analytical solution methods are based was also simulated and included for comparison purposes.

The GTFM calculated pressure responses are shown in Figures 3.8-2a to 3.8-2d for pulse injection tests and 3.8-3a to 3.8-3d for pulse withdrawal tests for hydraulic conductivities of 1×10^{-6} , 1×10^{-11} , 1×10^{-12} and 1×10^{-13} m/s. As expected, the length of time that the borehole is open to the annulus pressure has a strong effect on the pressure response during the progress of the pulse tests. The hydraulic conductivities interpreted from the illustrated pressure responses would be overestimated for the pulse injection tests and underestimated for the pulse withdrawal tests if the test data analysis did not include the effects of borehole pressure history. Of course the magnitude of the error in an analysis which did not include the borehole pressure history would be dependent on the relative magnitudes of formation pressure, annulus pressure and pressure at shut-in. As discussed in section 3.3, borehole hydraulic tests should be designed and conducted to minimize the effects of borehole pressure history.

The radial pressure profiles in the formation at the start of the pulse withdrawal tests are shown in Figures 3.8-4a to 3.8-4c for borehole open periods of 1, 30 and 365 days, respectively. The radial extent of the lower pressure skin as a consequence of the borehole open to the annulus pressure condition is strongly dependent on the magnitude of the formation hydraulic conductivity.

The GTFM calculated pressure responses for the slug withdrawal tests are shown in Figure 3.8-5a and 3.8-5b for hydraulic conductivities of 1×10^{-6} and 1×10^{-8} m/s, respectively. Similar to the effect on the pulse tests, the effect of a longer borehole open period is to result in a greater modification of the pressure response during the testing period.

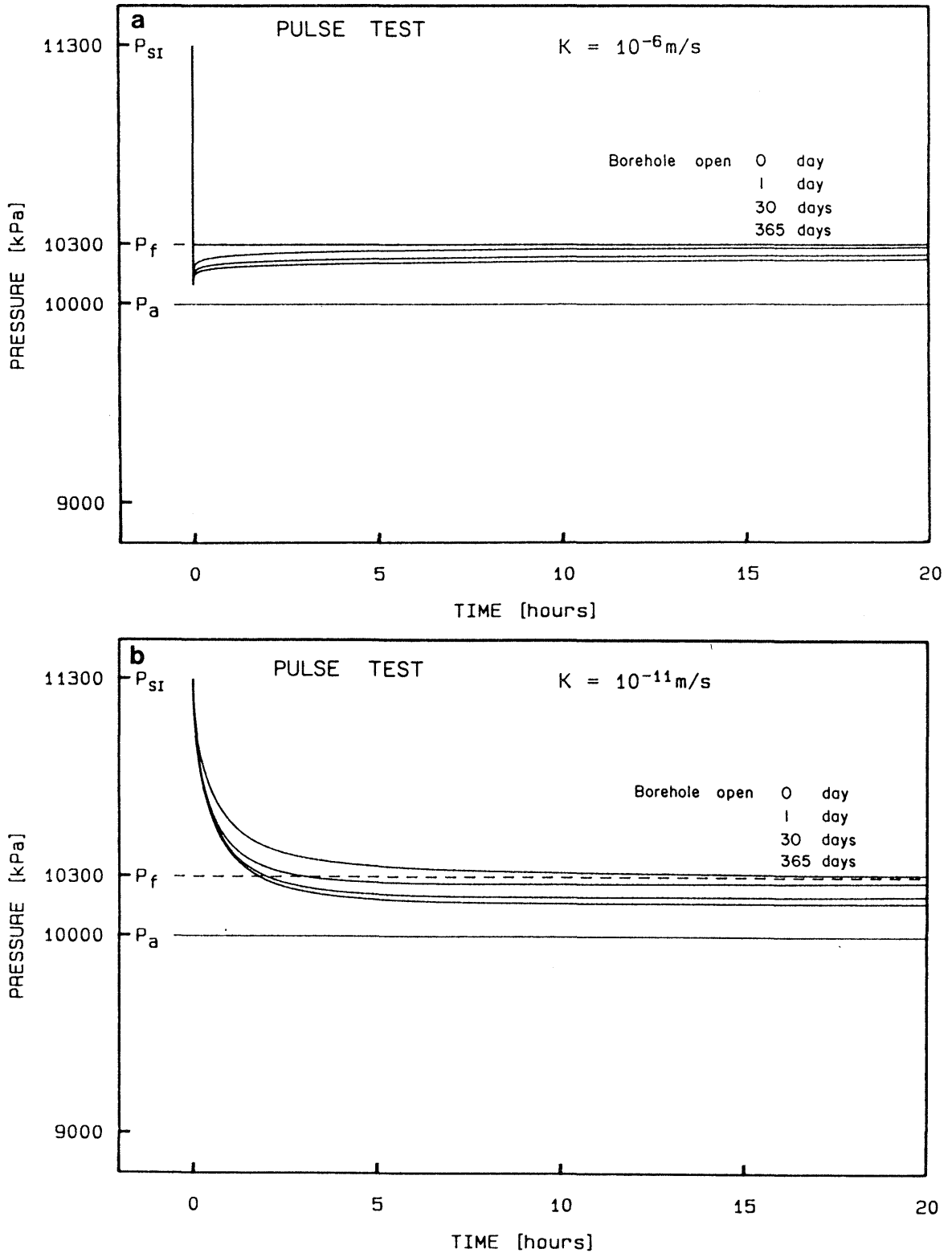


Figure 3.8-2 GTFM calculated borehole pressure response for borehole pressure history cases for a pulse injection test with formation hydraulic conductivities of (a) $1 \times 10^{-6} \text{ m/s}$ and (b) $1 \times 10^{-11} \text{ m/s}$

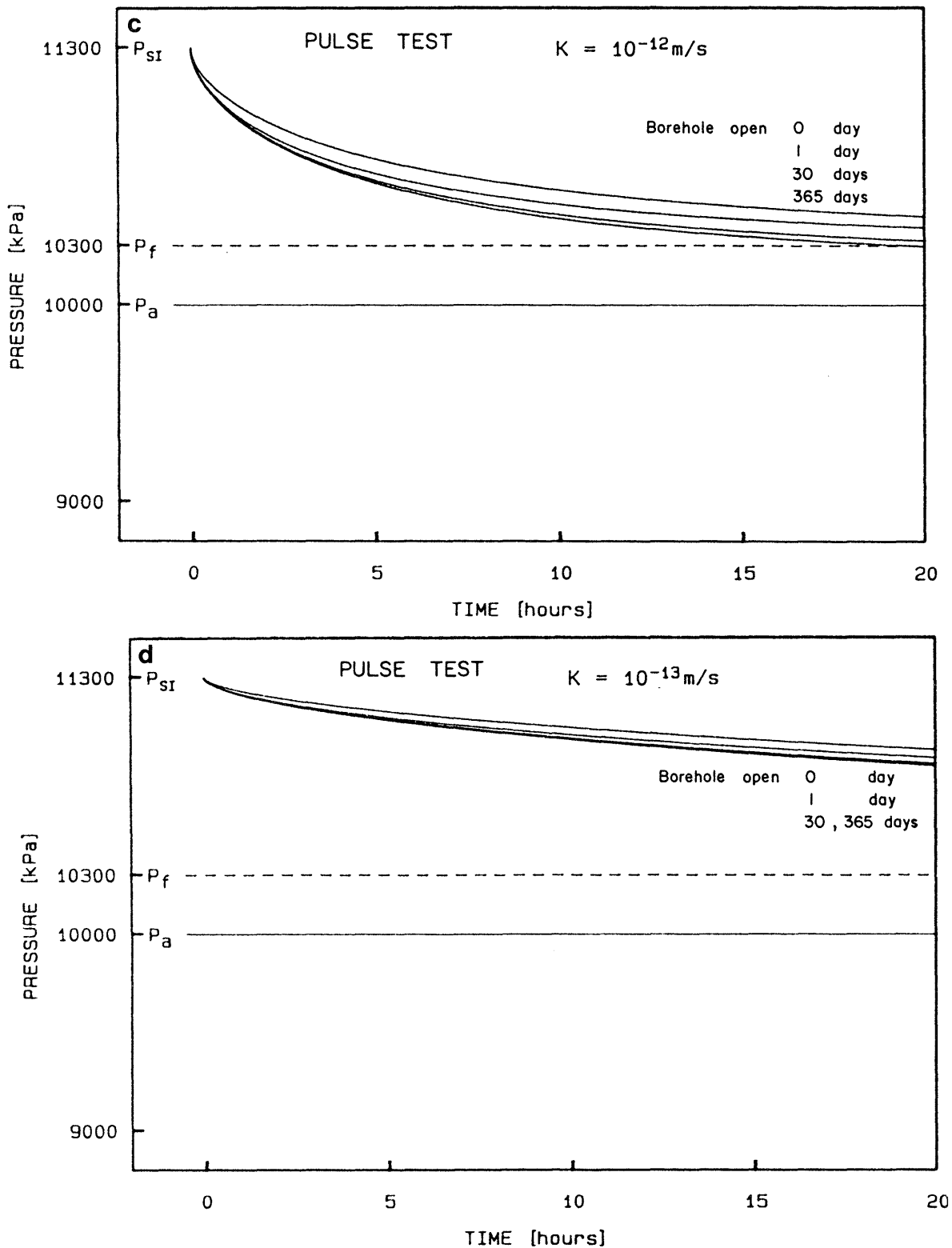


Figure 3.8-2 GTFM calculated borehole pressure response for borehole pressure history cases for a pulse injection test with formation hydraulic conductivities of (c) $1 \times 10^{-12} \text{ m/s}$ and (d) $1 \times 10^{-13} \text{ m/s}$

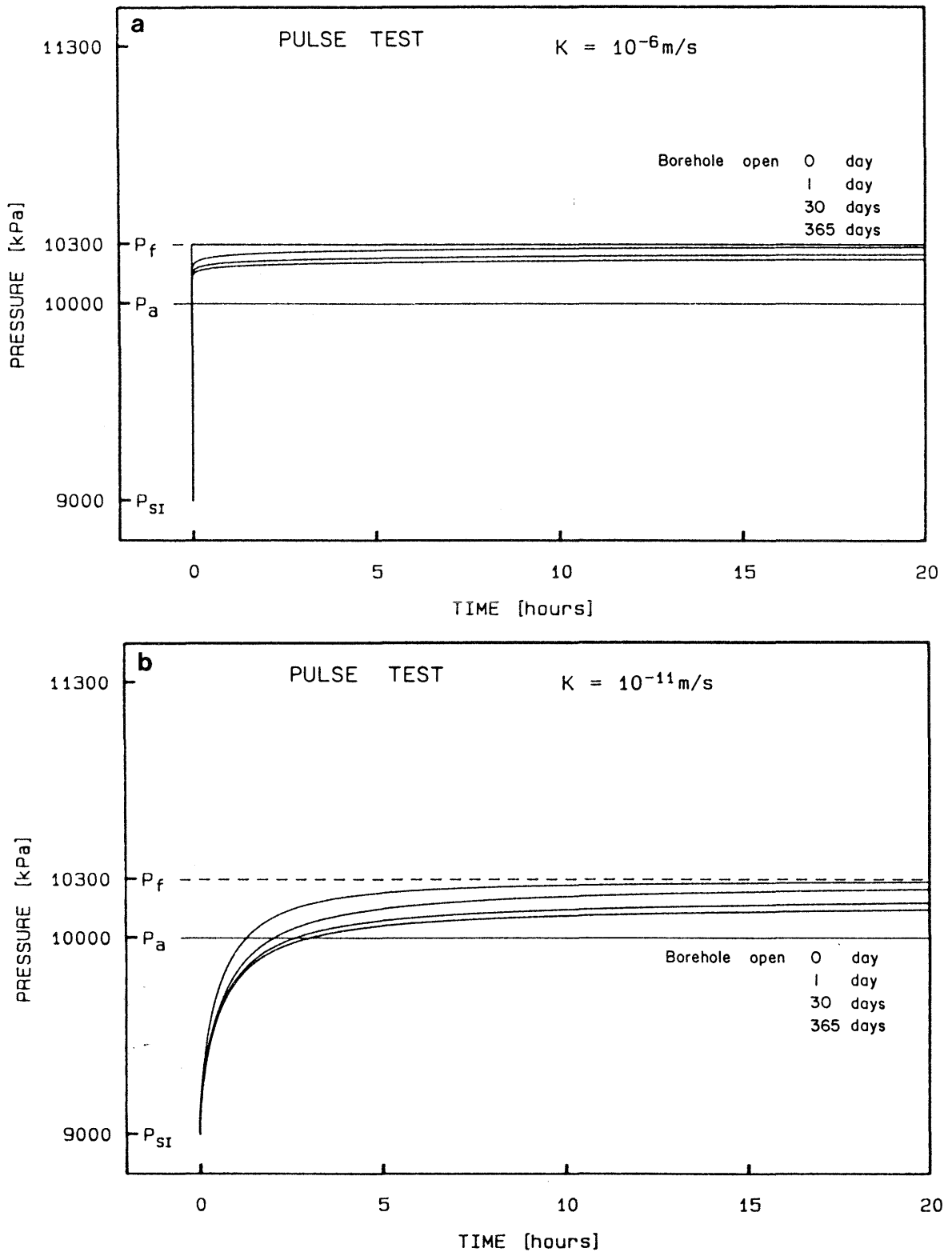


Figure 3.8-3 GTFM calculated borehole pressure response for borehole pressure history cases for a pulse withdrawal test with formation hydraulic conductivities of (a) $1 \times 10^{-6} \text{ m/s}$ and (b) $1 \times 10^{-11} \text{ m/s}$

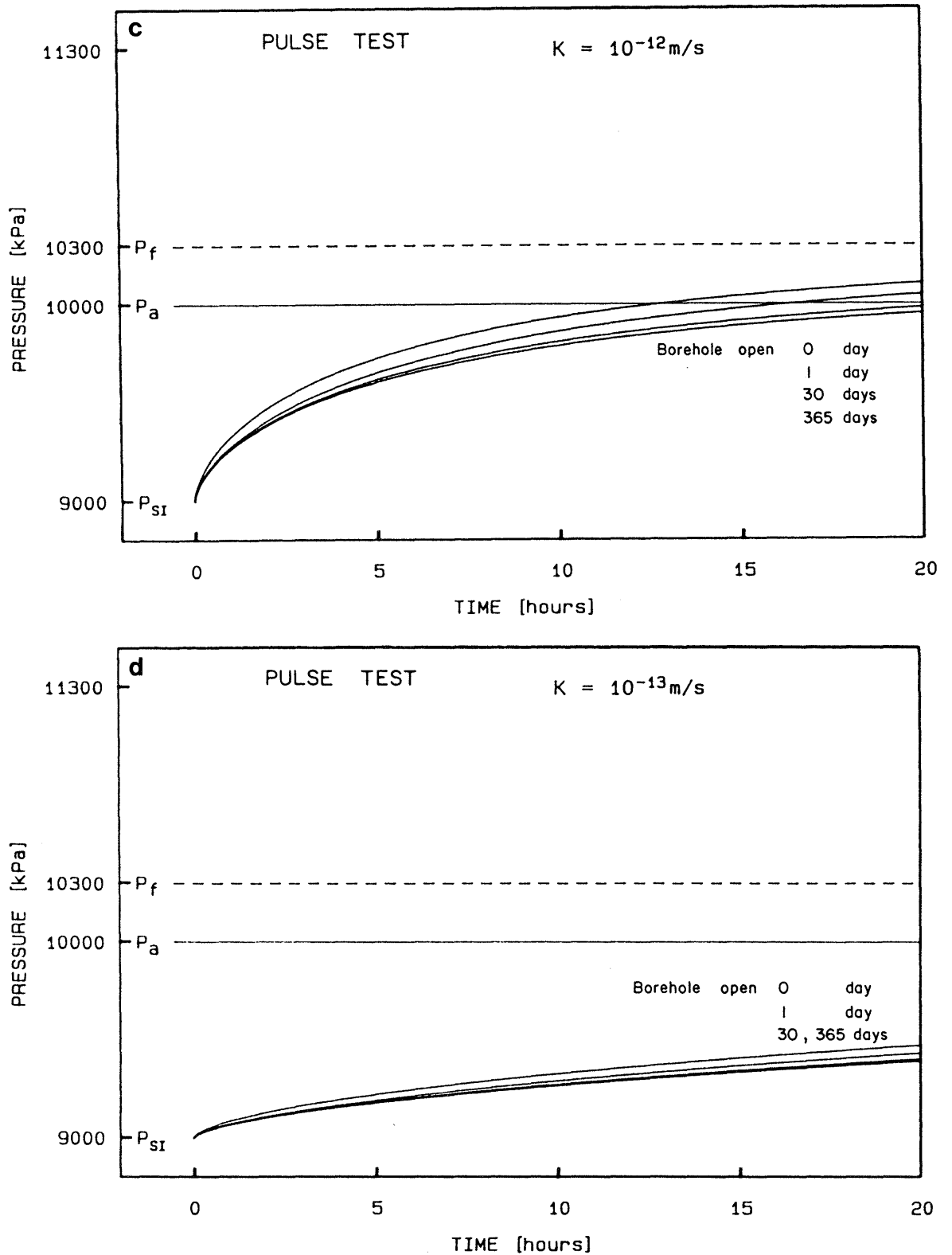


Figure 3.8-3 GTFM calculated borehole pressure response for borehole pressure history cases for a pulse withdrawal test with formation hydraulic conductivities of (c) $1 \times 10^{-12} \text{ m/s}$ and (d) $1 \times 10^{-13} \text{ m/s}$

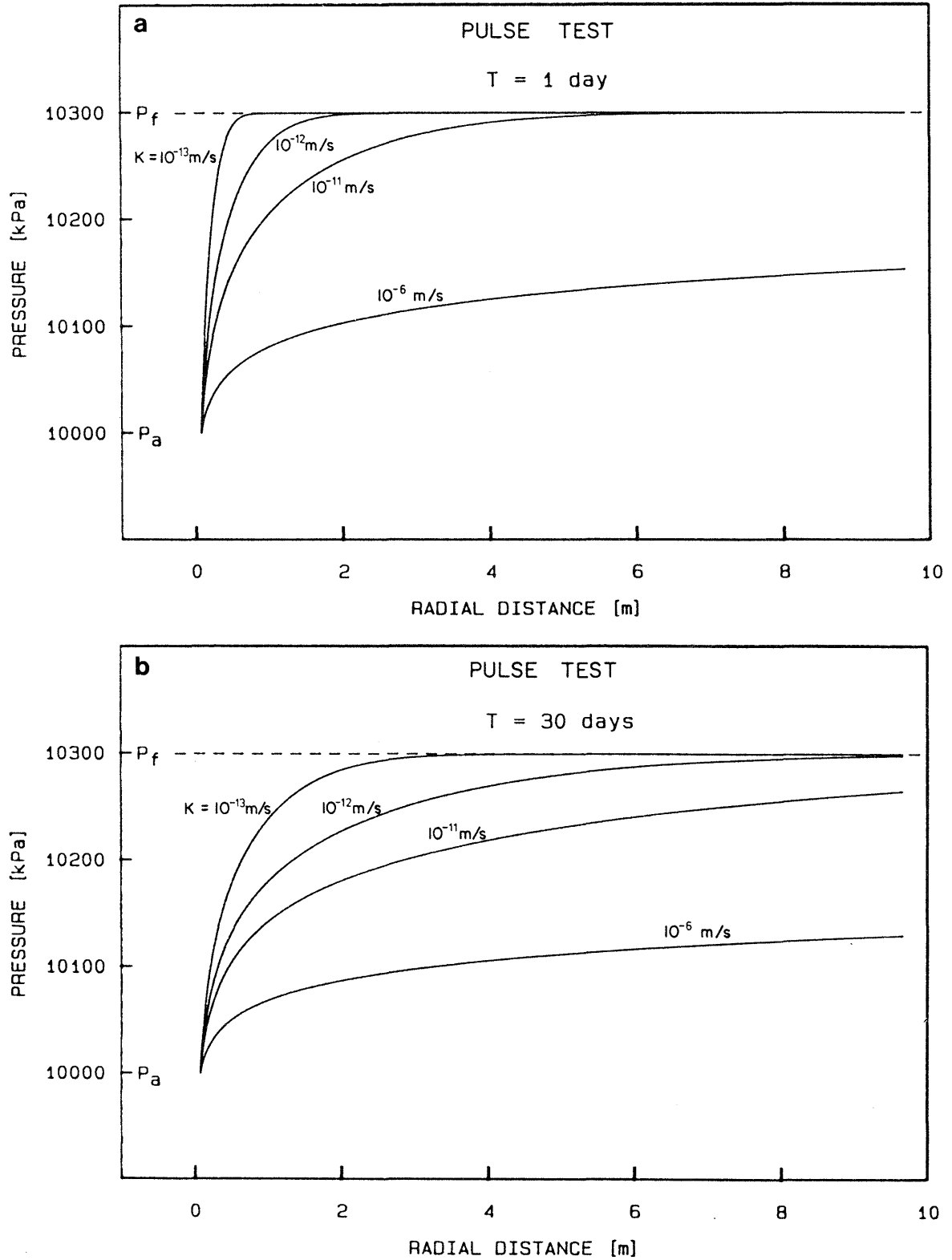


Figure 3.8-4

GTFM calculated radial pressure profiles in the formation at the start of the pulse withdrawal test of the borehole pressure history cases for borehole open periods of (a) 1 day and (b) 30 days

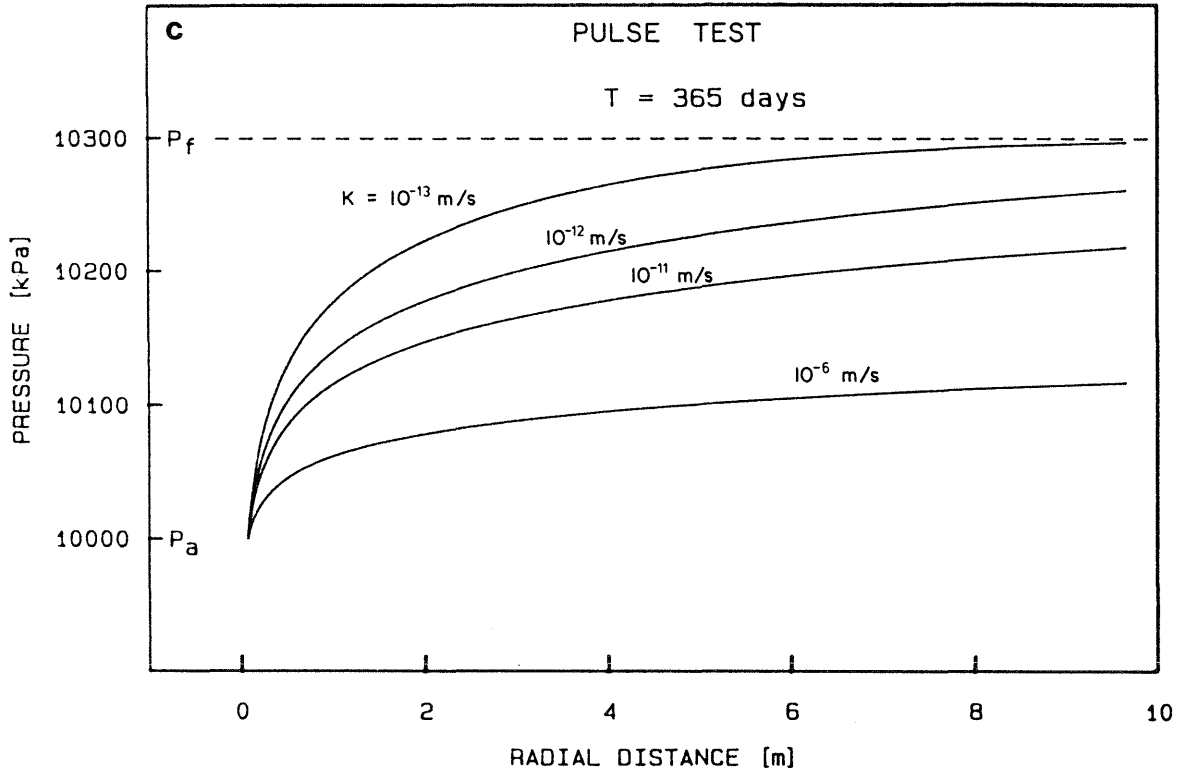


Figure 3.8-4 GTFM calculated radial pressure profiles in the formation at the start of the pulse withdrawal test of the borehole pressure history cases for borehole open periods of (c) 365 days

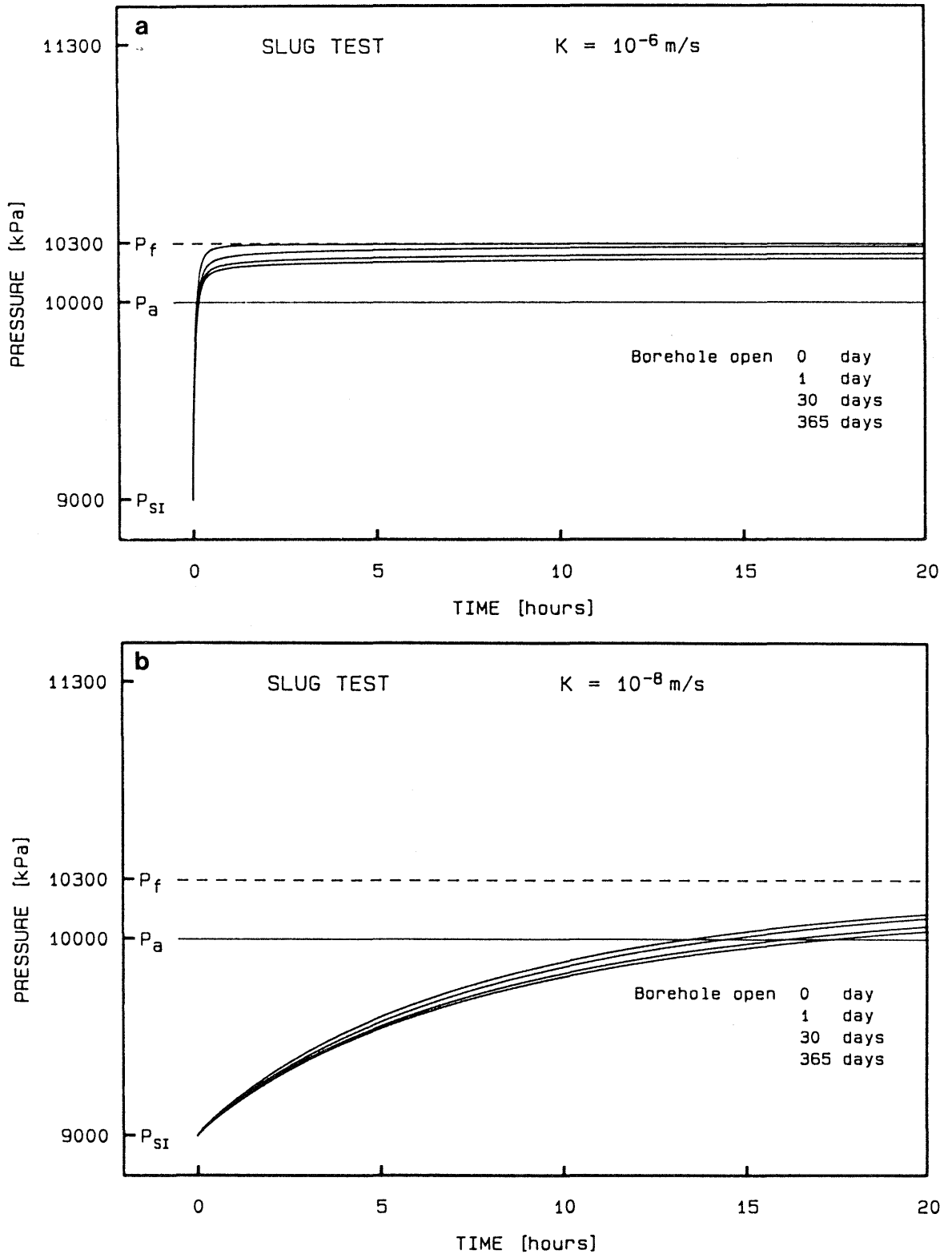


Figure 3.8-5 GTFM calculated borehole pressure response for borehole pressure history cases for a slug withdrawal test with formation hydraulic conductivities of (a) $1 \times 10^{-6} \text{ m/s}$ and (b) $1 \times 10^{-8} \text{ m/s}$

Borehole pressure history can result in uncertainty in the interpreted formation pressure if the monitoring period is not of sufficient length. As shown in Figures 3.8-2a and 3.8-3a for a hydraulic conductivity of 1×10^{-6} m/s, the initial pressure recovery during early time in the pulse tests was very rapid. Because of the lower pressure skin surrounding the borehole as a result of the borehole open period, the recovery to formation pressure is very slow after the initial rapid pressure recovery period. It can be seen that if a test was terminated after say 5 hours (see Figures 3.8-2a and 3.8-3a) because the pressure change per unit time was low and consequently interpreted as being approximately equal to formation pressure, then this interpreted pressure could significantly underestimate the true formation pressure.

3.8.2 Thermally-Induced Borehole Pressure Response

GTFM simulations were conducted to quantitatively investigate the effect of varying borehole fluid temperatures during pulse injection or withdrawal tests (see detailed discussion of causes and consequences of thermal effects in section 3.4). For simplicity, the formation pressure and annulus pressure were assumed equal to 10000 kPa and the pressure at shut-in equal to 11000 kPa for the pulse injection tests and 9000 kPa for the pulse withdrawal tests. The chosen temperature curves are illustrated in Figure 3.8-6 with temperature curves I, II and III indicative of isothermal conditions, moderate thermal effects and strong thermal effects, respectively. These temperature response curves are typical of those measured during hydraulic testing of the crystalline rock portion of the Boettstein borehole in northern Switzerland.

The GTFM calculated pressure responses are shown in Figure 3.8-7a and 3.8-7b for pulse injection and withdrawal tests, respectively, for a hydraulic conductivity of 1×10^{-12} m/s and the three temperature curves. It can be seen that thermally-induced pressure effects can dominate the pressure response during these hydraulic test conducted under shut-in conditions (i.e., pulse tests). Any analysis of the tests illustrated in Figure 3.8-7 for varying-temperature conditions that did not include thermal effects would yield very inaccurate and, for temperature curve III, misleading estimates of formation pressure and hydraulic conductivity.

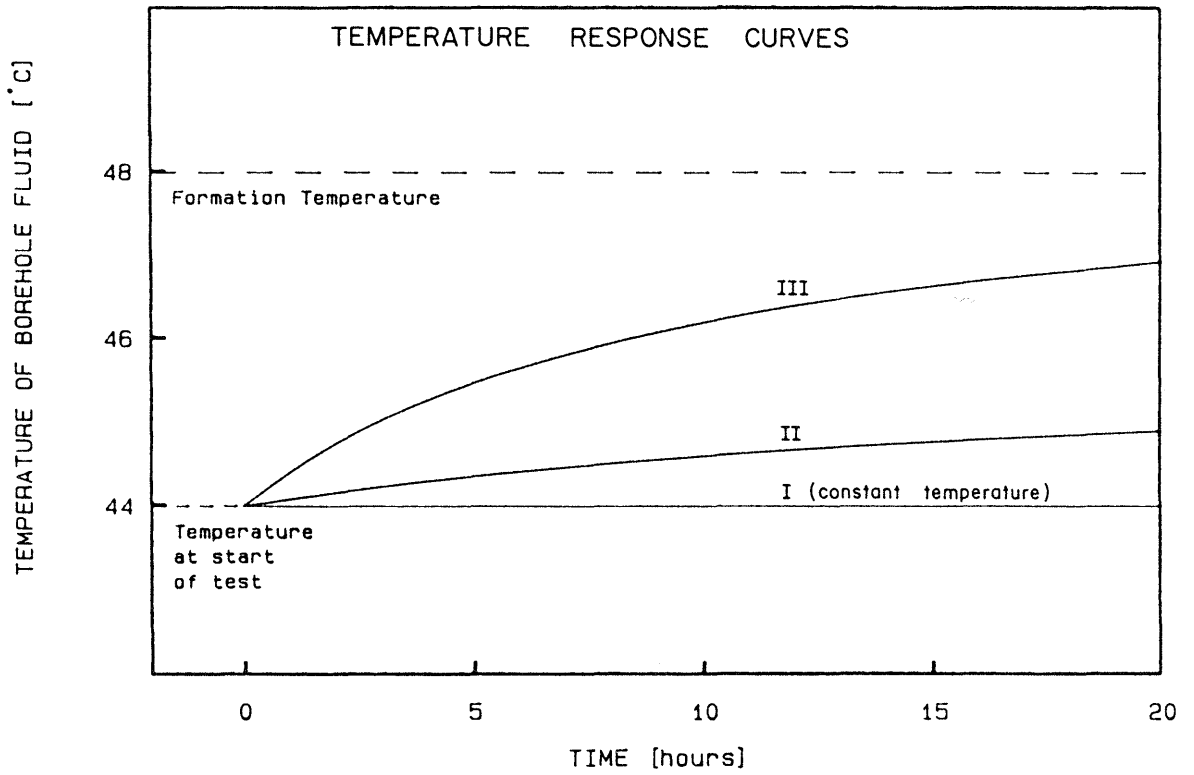


Figure 3.8-6 Temperature response curves utilized in GTFM calculated borehole pressure responses for the pulse test cases involving thermal effects

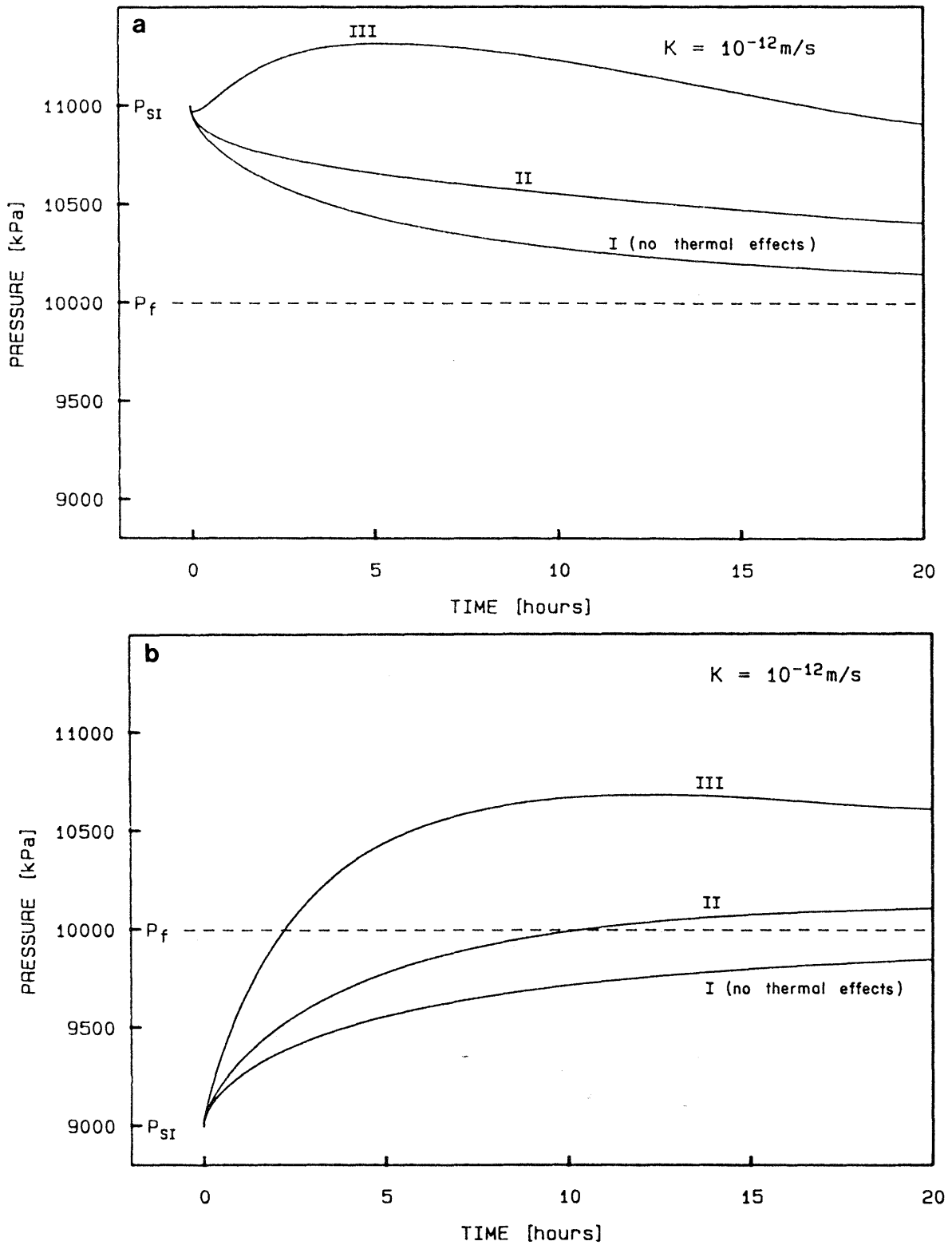


Figure 3.8-7 GTFM calculated borehole pressure responses for various temperature response curves for (a) pulse injection test and (b) pulse withdrawal test

The effect of varying temperature conditions is further illustrated in Figure 3.8-8 for temperature curve III with hydraulic conductivities of 1×10^{-13} , 1×10^{-12} , 1×10^{-11} and 1×10^{-10} m/s. For this chosen temperature curve, it can be seen that thermal effects are very significant at low hydraulic conductivities (i.e., below 1×10^{-11} m/s). Although not illustrated on Figure 3.8-8, thermal effects were minimal for hydraulic conductivities above 1×10^{-9} m/s. These figures serve to illustrate the potential importance of thermal effects on the measured pressure response during borehole hydraulic testing. Accurate downhole temperature measurements representative of the borehole fluid in the test interval are essential to (1) assess whether thermal effects are required in the data analysis and (2) provide the required input for the analysis. Otherwise, much of the uncertainty associated with formation pressures and hydraulic conductivities interpreted from low permeability formations could be attributed to the uncertainty in the temperature conditions in the borehole test interval.

3.8.3 Borehole/Formation Skin Effects

GTFM simulations were conducted to illustrate the effects that a lower or higher permeability zone of 1 cm thickness surrounding the borehole has on the borehole pressure response. The cases simulated are for slug and pulse tests with formation and annulus pressure equal to 10000 kPa and pressure at shut-in equal to 11000 kPa. The formation hydraulic conductivities were 1×10^{-8} m/s and 1×10^{-11} m/s for the slug and pulse tests, respectively. The hydraulic conductivity was varied several orders of magnitude higher and lower than the respective formation hydraulic conductivity.

The model-calculated results are illustrated in Figures 3.8-9 and 3.8-10 for the slug and pulse test cases, respectively. It can be seen that a higher permeability skin has an insignificant effect on the borehole pressure response. In contrast, a lower permeability skin can have a pronounced effect. The shape of the borehole pressure response curve for a case with a lower permeability skin is characteristic of the pressure response from a lower permeability formation. This illustrates a potential and important source of error in the estimation of formation hydraulic conductivity from borehole testing in cases where a borehole/formation skin may exist.

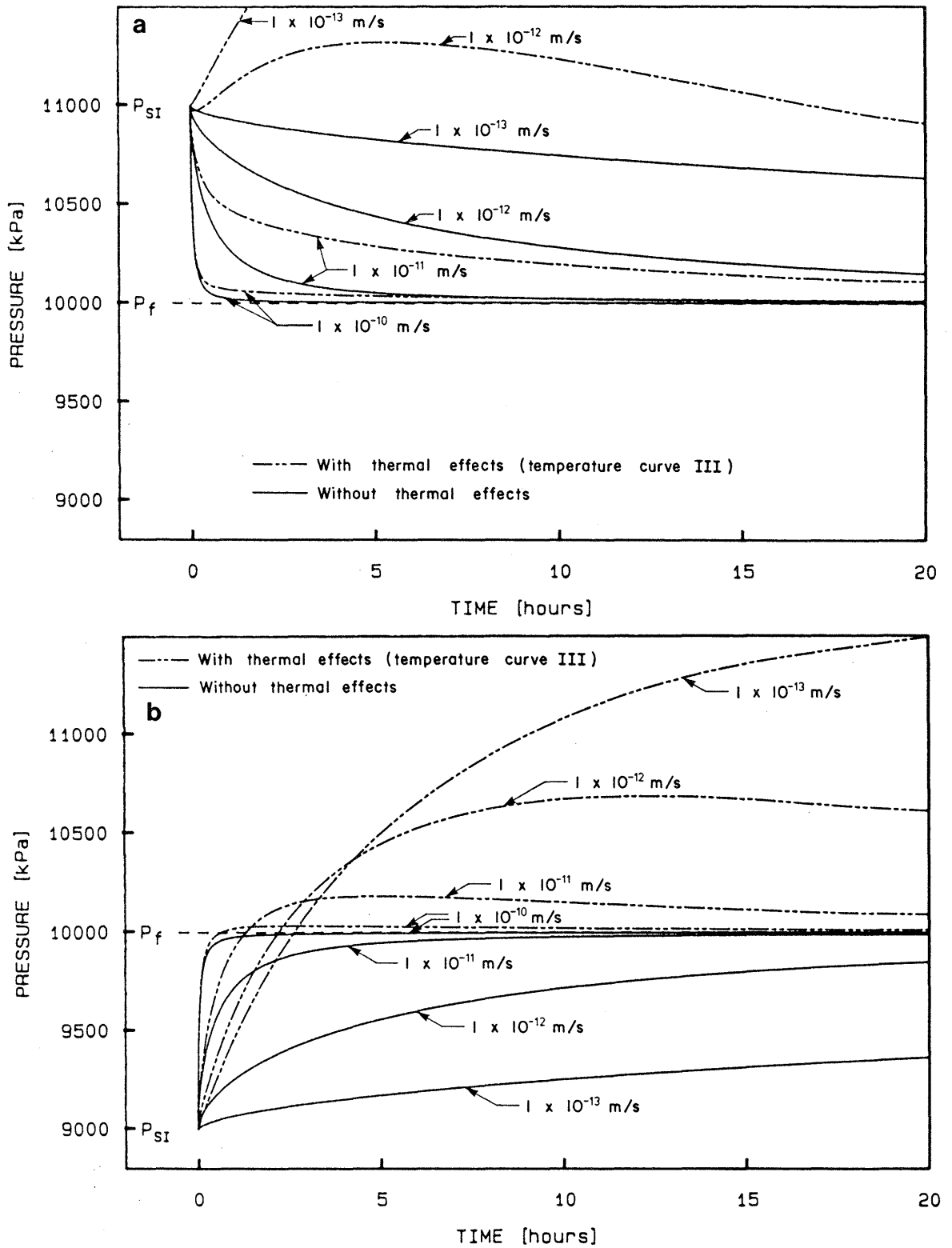


Figure 3.8-8 GTFM calculated borehole pressure responses for temperature response curve III and various hydraulic conductivities: (a) pulse injection test and (b) pulse withdrawal test

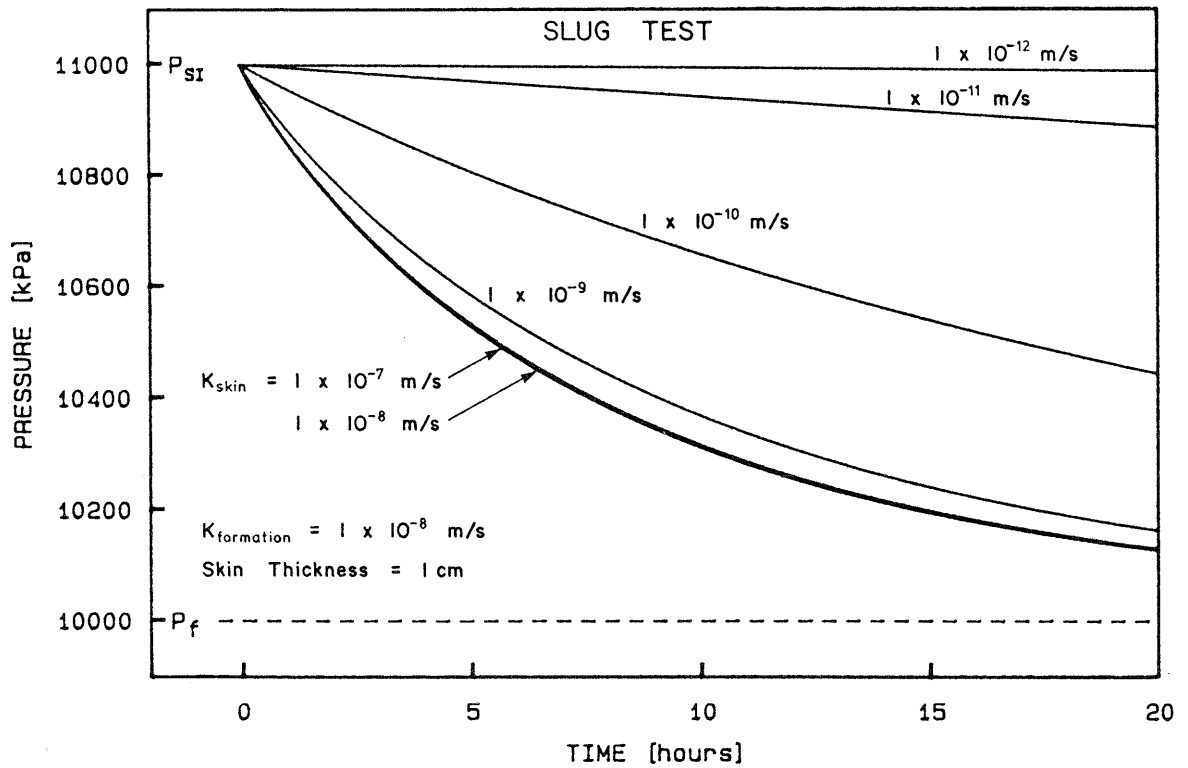


Figure 3.8-9 GTFM calculated borehole pressure responses for a slug test for cases involving a borehole/formation skin

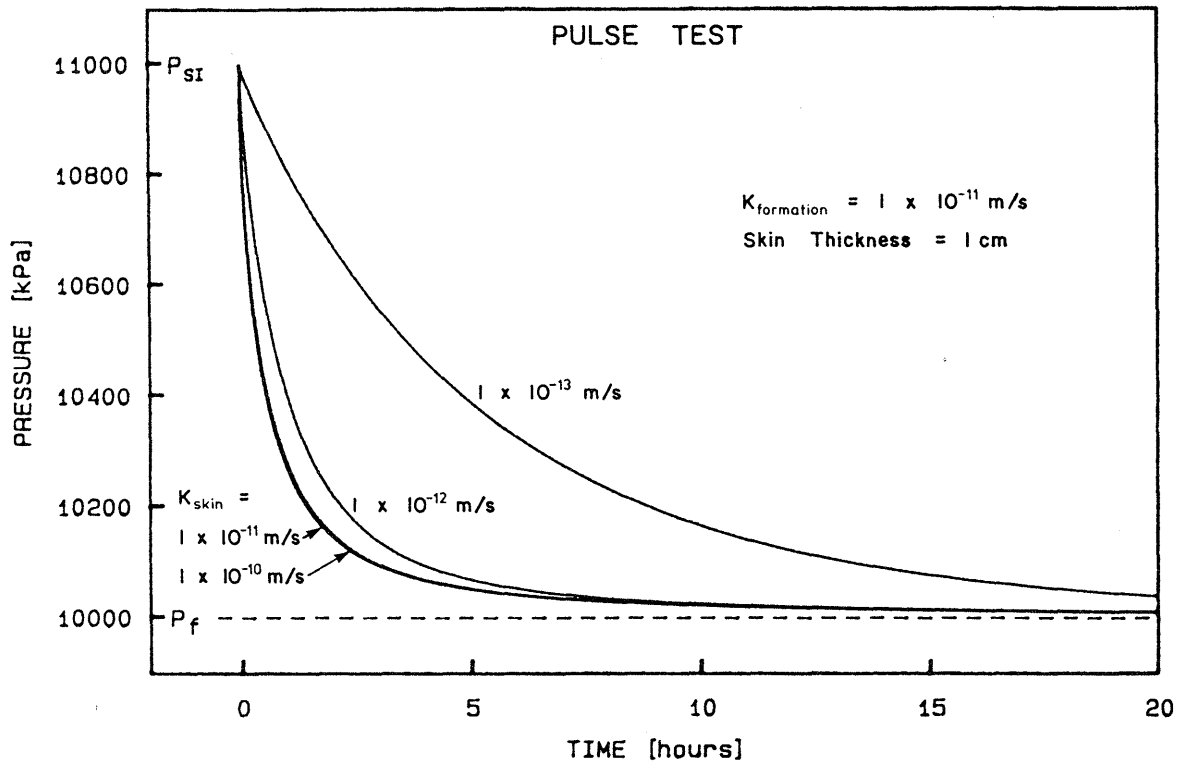


Figure 3.8-10 GTFM calculated borehole pressure responses for a pulse test for cases involving a borehole/formation skin

3.9 Applications

As examples of the application and capability of the GTFM simulation model, three field tests from the NAGRA crystalline rock drilling program in northern Switzerland will be presented. The examples are all taken from the hydraulic testing program in the Boettstein borehole and have been chosen to illustrate specific features of the model and to present field cases where the inclusion of borehole history, temperature and compliance effects are necessary in the analysis. The first example, Boettstein test 1326.2D, illustrates how the formation pressure and hydraulic conductivity can be estimated under isothermal conditions from a hydraulic test where the borehole has been open to annulus pressure conditions for 95 days. The second example, Boettstein test 735.8S, illustrates the use of GTFM for a nonisothermal case where the borehole has been open to annulus pressure for 14 hours (i.e., borehole history effects are less significant and thermal effects dominate the measured pressure response). The third example, Boettstein test 1497.8S, provides an illustration of a nonisothermal case with a moderate borehole history effect (i.e., the borehole is open to annulus conditions for 3.75 days) and a compliance effect (i.e., packer squeeze) caused by the addition of 3 tons of weight applied to the tubing string.

3.9.1 Boettstein Test 1326.2D

At this interval, long-term geochemical sampling was conducted for 42 days using Lynes equipment in a double packer configuration. The downhole transducer sensor package monitors pressures below the bottom packer, between the packers, and above the top packer using pressure transducers denoted P1, P2 and P3, respectively. Three temperature transducers are also located together in the sensor package and are denoted T1, T2 and T3. The 42 day pressure response monitored below the bottom packer was evaluated to determine the formation pressure or hydraulic head for the lower portion of the borehole.

The borehole interval length being monitored for this test case is 168.69 metres. When monitoring borehole intervals for formation pressure and hydraulic conductivity estimates, much shorter

lengths are recommended. Boettstein test 1326.2D was chosen to illustrate the use of the GTFM model in a case where borehole history effects are important and thermal effects can be neglected. However, the formation pressure estimated from this test is consistent with the formation pressure estimated at a corresponding depth from the subsequent long-term pressure recovery data using a Lynes eight-packer monitoring tool (Belanger et al., 1985).

The physical description of the test conditions is given in Table 3.9-1. Temperature at the transducers remained constant at about 59.5°C during testing. Because the borehole had been open for about 95 days, borehole history effects were significant and therefore, the pressure response was analyzed using the GTFM simulation model. The model parameters used in the data analysis are given in Table 3.9-2.

Borehole pretest pressure history used in the simulations consists of 95 days of open-hole conditions at an annulus pressure of 12950 kPa (see Figure 3.9-1). This time length represents an estimated time from the middle of the drilling period for the 168.69 metre borehole interval to the start of the testing.

A sensitivity study on estimated formation pressures and hydraulic conductivities was conducted with the GTFM model in order to calibrate a calculated pressure response to the field-measured pressure response. Assumed formation pressures starting at 13500 kPa and increasing in 50 kPa increments to 13700 kPa were used in five separate simulations. For this test, the pressure response was very sensitive to formation pressure as shown in Figures 3.9-2, 3.9-3A and 3.9-3B. The best-fit of the measured pressure response to the simulated pressure response occurs for a formation pressure of 13650 kPa at transducer depth and a hydraulic conductivity of 3×10^{-13} m/s (see Figure 3.9-2). The equivalent formation pressure at the centre of the test interval at 1416.95 m depth is 14659 kPa. A plot showing the tool and test interval configuration with the estimated transducer and test interval pressures is shown Figure 3.9-4.

Table 3.9-2 Model parameters for test data analysis
for Boettstein test 1326.2D

Parameter	Value
Formation	
Compressibility	$2 \times 10^{-11} \text{ Pa}^{-1}$
Porosity	0.005
Storage Coefficient*	3.6×10^{-5}
Fluid	
Compressibility	$4.34 \times 10^{-10} \text{ Pa}^{-1}$
Density	$9.88 \times 10^2 \text{ kg m}^{-3}$
Coefficient of thermal expansion	$5.10 \times 10^{-4} \text{ }^\circ\text{C}^{-1}$
Test Interval	
Length	168.69 m
Diameter (caliper)	0.165 m
Estimated formation pressure (at P1 elevation)	Variable: 13600, 13650 and 13700 kPa
Best-fit formation pressure	13650 kPa

* Storage coefficient is calculated from the formation/fluid properties and test interval length

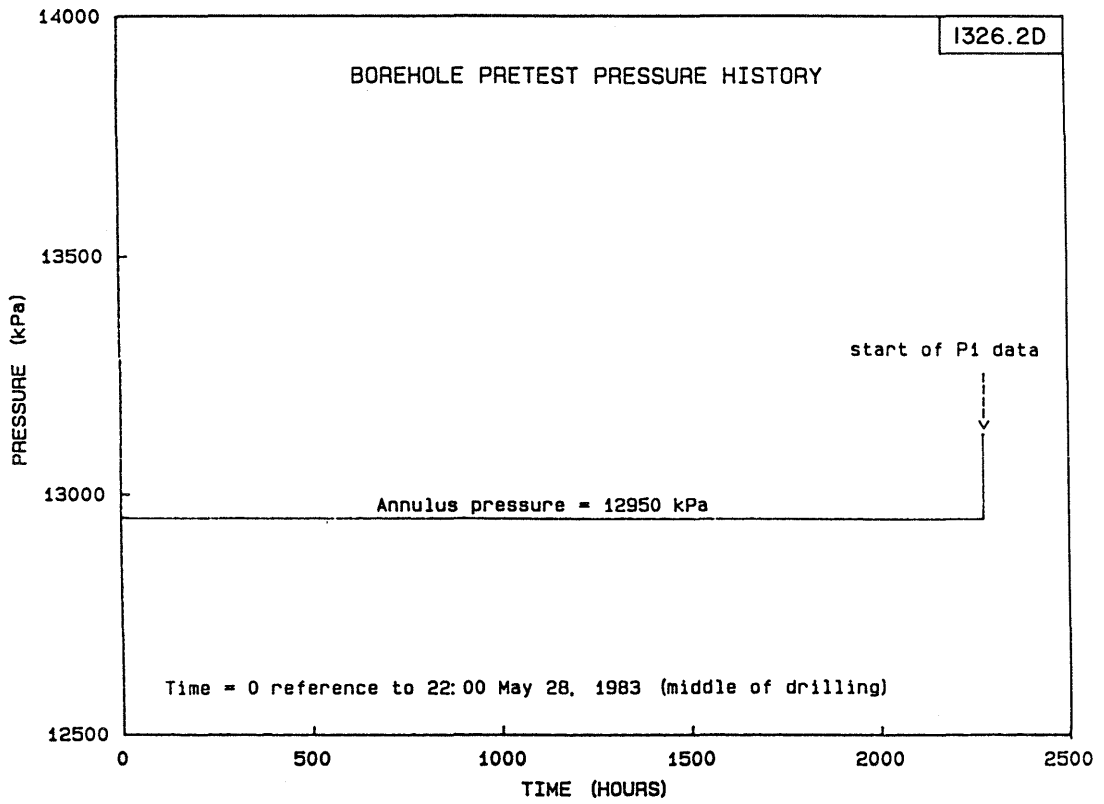


Figure 3.9-1 Assumed borehole pretest pressure history for Boettstein test 1326.2D

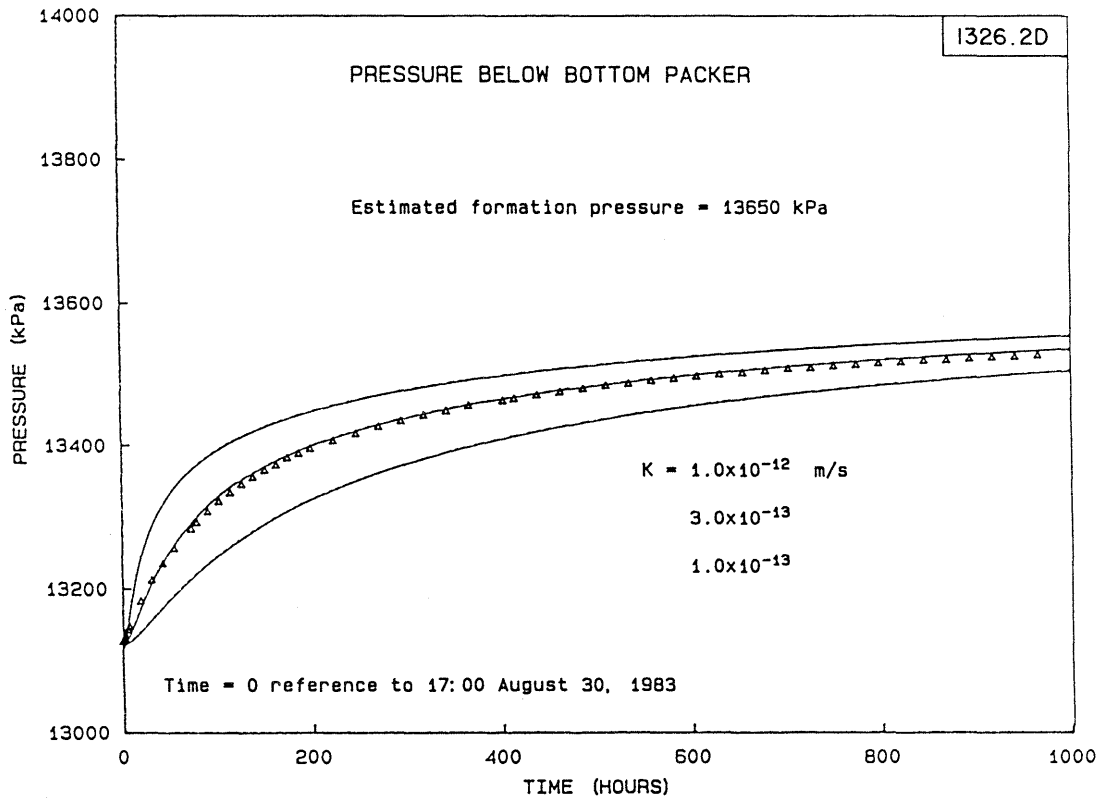


Figure 3.9-2 Measured (Δ) and best-fit simulated pressure response for Boettstein test 1326.2D using estimated formation pressures of 13650 kPa

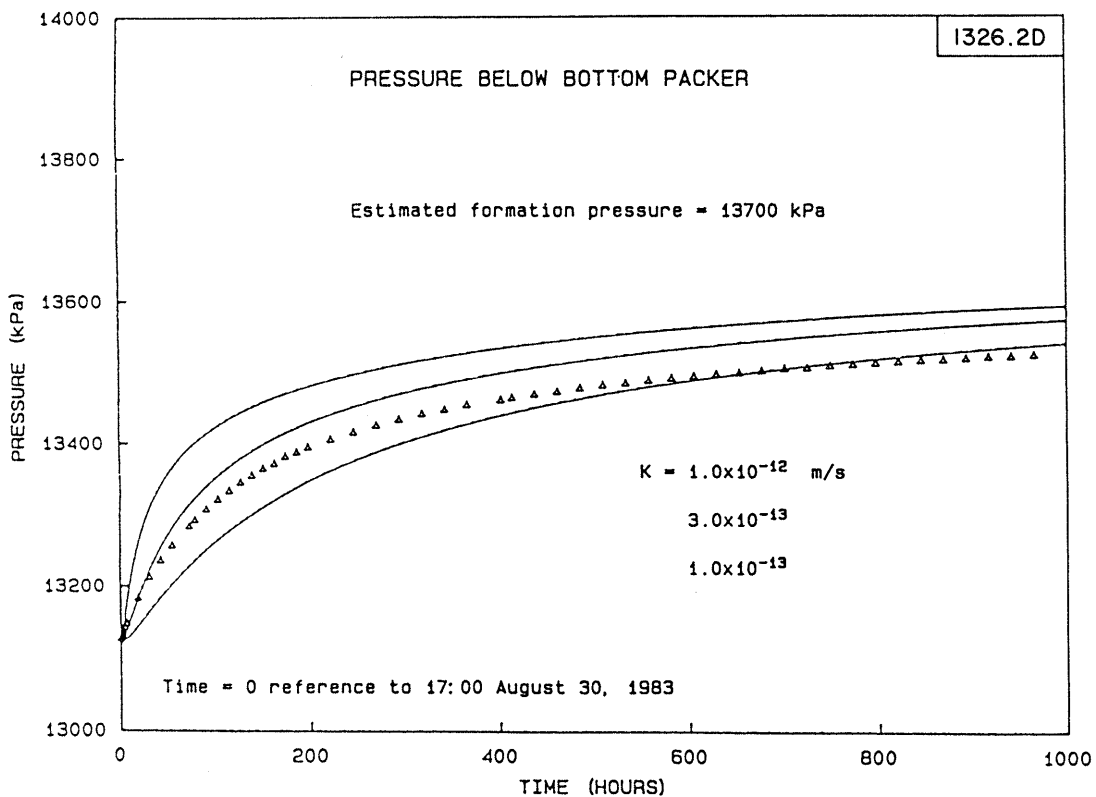
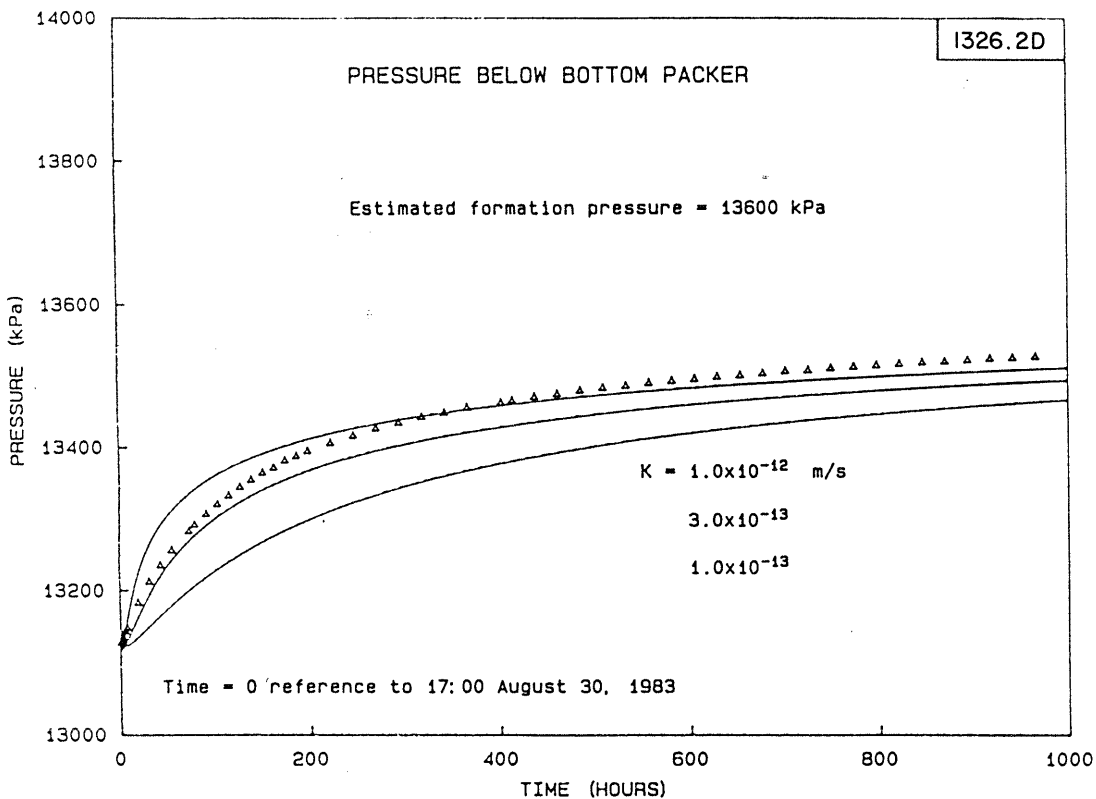


Figure 3.9-3 Measured (Δ) and simulated pressure response for Boettstein test 1326.2D using estimated formation pressure of (A) 13600 kPa and (B) 13700 kPa

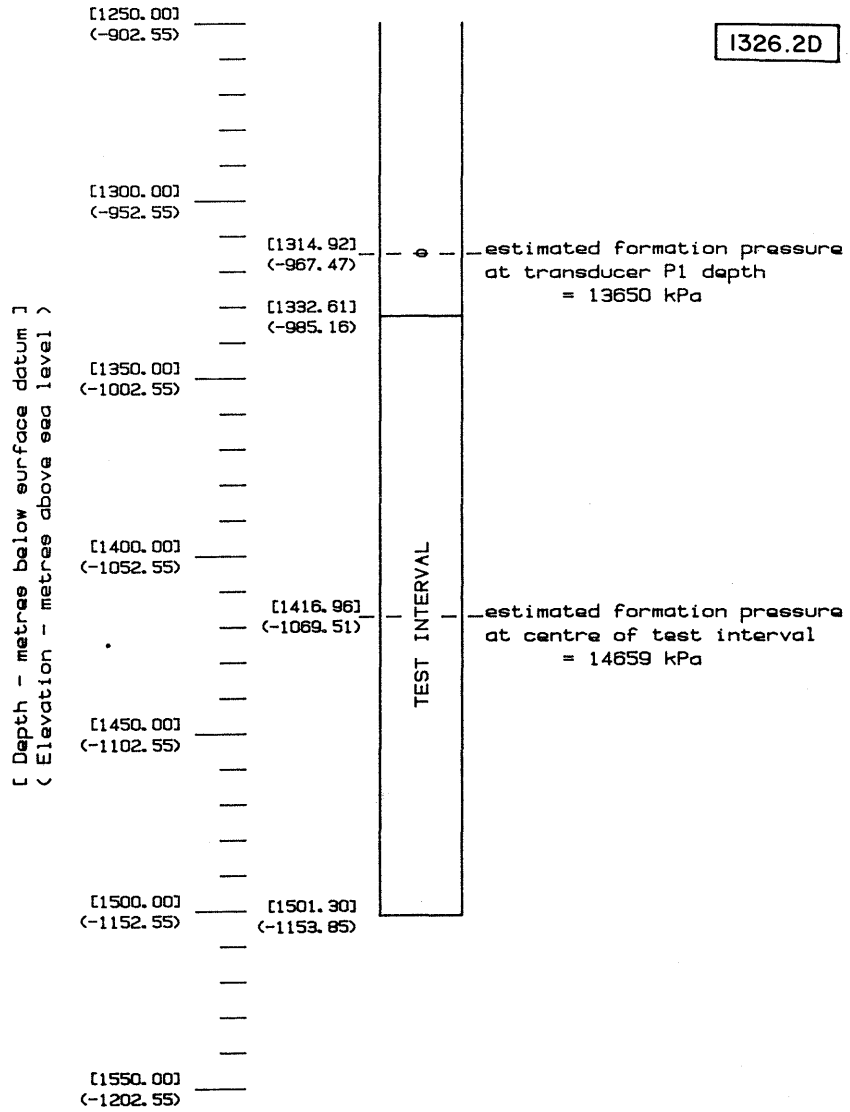


Figure 3.9-4 Schematic diagram showing equipment configuration and estimated formation pressure for Boettstein test 1326.2D

This example illustrates the usefulness of the GTFM model in estimating the formation pressures and hydraulic conductivity in an interval where there is a significant borehole history effect. Because of the long duration (42 days) of this test the annulus pressure is not the appropriate reference pressure for analysis purposes. If the annulus pressure had been used as the reference pressure then the predicted hydraulic conductivity would have been much higher and the formation pressure would have been underestimated by a considerable extent. By incorporating borehole history effects into the analysis, the determined hydraulic parameters more accurately represent the formation conditions.

3.9.2 Boettstein Test 735.8S

Boettstein test 735.8S was conducted shortly after drilling its corresponding test interval and utilized a single packer configuration. The physical description of the test conditions is given in Table 3.9-3. The hydraulic tests on the interval consisted of two pulse injection tests (designated Psta and Pw02) of 20.0 and 9.9 hours duration (see Figure 3.9-5). The measured temperature and pressure response data suggested that the test interval was of very low permeability and that the pressure response was dominated by thermal effects. Thus a model such as GTFM that incorporates temperature effects was necessary in the analysis of these pulse tests. Model parameters used in the analysis are given in Table 3.9-4.

The estimated formation head was assumed equal to 370 metres above mean sea level which corresponds to heads estimated at more permeable test intervals at about 400 and 620 metres depth. This head is equivalent to a formation pressure of 7413 kPa at the transducer probe depth. The effect of the borehole pretest pressure history (annulus pressure of 7225 kPa) for the 14 hours prior to the first pulse injection test (Psta) was included in the simulation (see Figure 3.9-6A).

The measured temperature response for temperature transducer T2 is shown in Figure 3.9-6B. The temperature responses for the other two temperature transducers showed significant temperature oscillations (considered to be an equipment-related problem) and, therefore, they were not included as representative of actual temperature conditions at the transducer probe. The cubic spline temperature curve for simulation purposes was approximated from

Table 3.9-3 Physical description of test conditions
for Boettstein test 735.8S

Test type: Single packer test
Geology of test interval: granite
Borehole fluid: water
Borehole diameter in test interval:
 - Drilled: 6.25 inch (0.159 m)
 - Calipered: 6.50 inch (0.165 m)
Depth to centre of test interval: 735.83 m
Test interval length: 7.65 m
Depth to top of test interval: 732.00 m
Depth to bottom of test interval: 739.65 m
Height of P2 transducer above centre of interval: 9.83 m
Depth to pressure transducer P2: 725.99 m
Datum elevation at ground surface: 347.45 m A.S.L.
Barometric pressure: 101 kPa
Tool specifications: 3.5 inch Lynes hydrological tool
Annulus pressure (P3): 7225 kPa
Drilling period of test interval: 05:42 - 19:42 February 10, 1983
Testing period (time and date): 00:42 - 06:40 February 11, 1983
Designations and sequence of tests: Psta, Pw02
Start of tests: Psta - 00:48 February 11
 Pw02 - 20:49 February 11
Temperature at probe:
 - Start of first test: 37.0 °C
 - End of testing: 39.5 °C

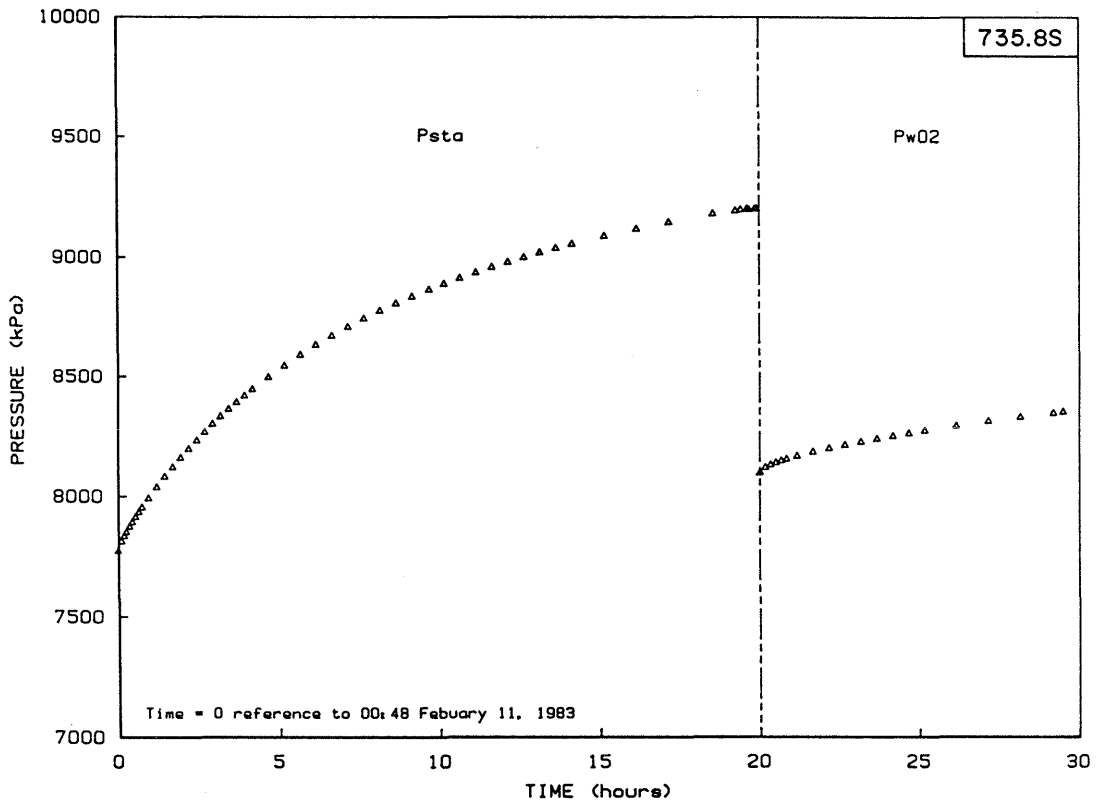


Figure 3.9-5 Measured (Δ) pressure data for test interval in Boettstein test 735.8S showing two pulse withdrawal tests, Psta and Pw02

Table 3.9-4 Model parameters for test data analysis
for Boettstein test 735.8S

Parameter	Value
Formation	
Compressibility	$2 \times 10^{-11} \text{ Pa}^{-1}$
Porosity	0.005
Storage Coefficient*	1.7×10^{-6}
Fluid	
Compressibility	$4.33 \times 10^{-10} \text{ Pa}^{-1}$
Density	$9.96 \times 10^2 \text{ kg m}^{-3}$
Coefficient of thermal expansion	$3.60 \times 10^{-4} \text{ }^\circ\text{C}^{-1}$
Test Interval	
Length	7.65 m
Diameter (caliper)	0.165 m
Estimated static formation pressure (at P2 elevation)	7413 kPa

* Storage coefficient is calculated from the formation/fluid properties and test interval length

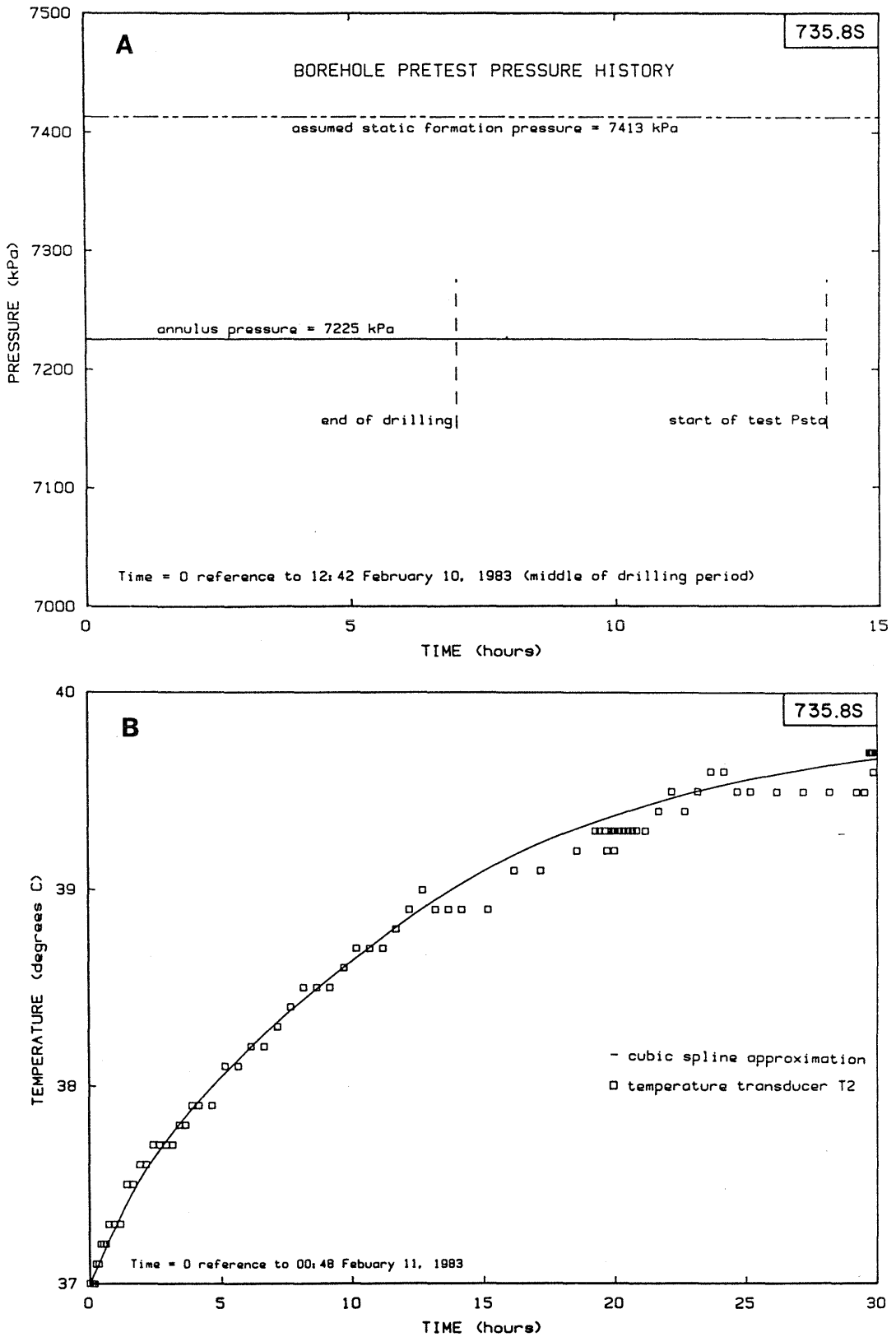


Figure 3.9-6 Boettstein test 735.8S: (A) Assumed borehole pretest pressure history, and (B) Temperature history data and cubic spline temperature curve used in simulations

the transducer T2 data as shown in Figure 3.9-6B. A total temperature change of 2.5 °C was measured during the two pulse tests. Some variations in the measured temperature trend were particularly noticeable following tool movements. This test illustrates the difficulty in obtaining temperature data representative of borehole conditions at the test interval depth. Equipment-related problems and fluid transfers during tool movements can have significant effects on the measured temperature response.

The measured and simulated pressure responses for tests Psta and Pw02 for a range of hydraulic conductivities are shown for comparison in Figure 3.9-7. The simulated pressure profile in the formation at the end of test Psta is utilized as the initial condition for simulating the pressure response during test Pw02. A hydraulic conductivity of 1×10^{-13} m/s provides a simulated pressure response that is in good agreement with the measured pressure data for both tests Psta and Pw02. Considering that there is some uncertainty in the actual temperature of the borehole fluid during the testing, the agreement between simulated and measured pressure responses suggests that the thermally-induced pressure effects have been incorporated successfully in the GTFM simulation to yield a reasonable estimate of the hydraulic conductivity. Without including thermal effects, analysis of this test sequence to obtain representative formation parameters (i.e., hydraulic conductivity) would not have been possible.

3.9.3 Boettstein Test 1497.8S

A long-term bottom-hole test, Boettstein test 1497.8S, was conducted with the objectives of investigating equipment compliance and obtaining an estimate of the formation pressure. Table 3.9-5 gives the physical description of the test conditions. The initial pressure after closing the shut-in tool with a one ton load was 15235 kPa (at probe depth) or 605 kPa above the annulus pressure of 14630 kPa. The interval pressure increased to 15679 kPa during the following 2.93 days (see Figure 3.9-8 for measured pressure response during testing)

At the time of the 2.93 days, the load on the shut-in tool was increased to 3 tons resulting in a rapid pressure increase to 15734 kPa. This 55 kPa pressure increase is the result of equipment compliance; that is, the increased load on the tool and packer assembly has caused a "squeeze" on the

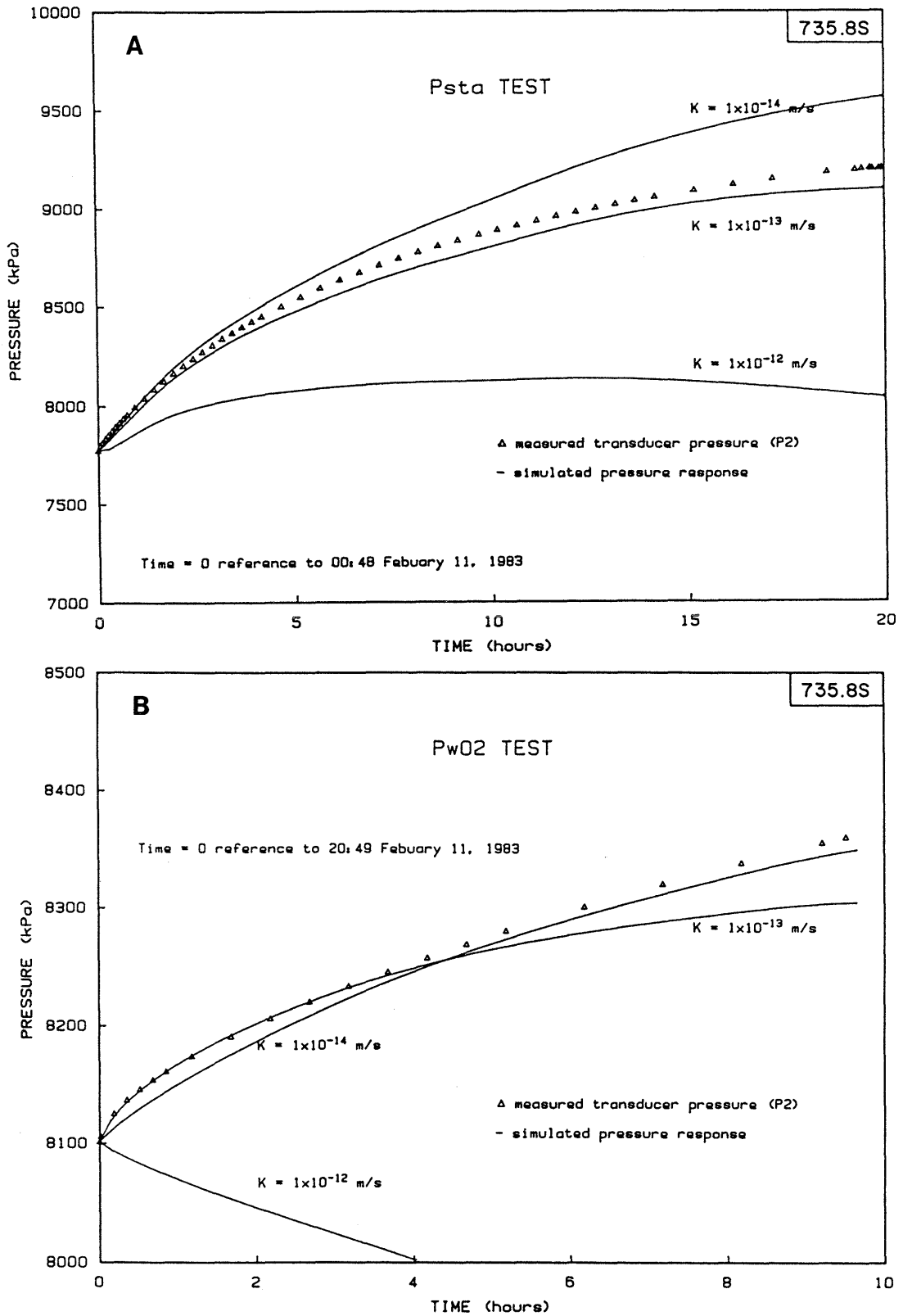


Figure 3.9-7 Measured (Δ) and simulated pressure response for Boettstein test 735.8S: (A) Test Psta showing best-fit hydraulic conductivity of 1×10^{-13} m/s, and (B) Test Pw02 showing best-fit hydraulic conductivity of 1×10^{-13} m/s

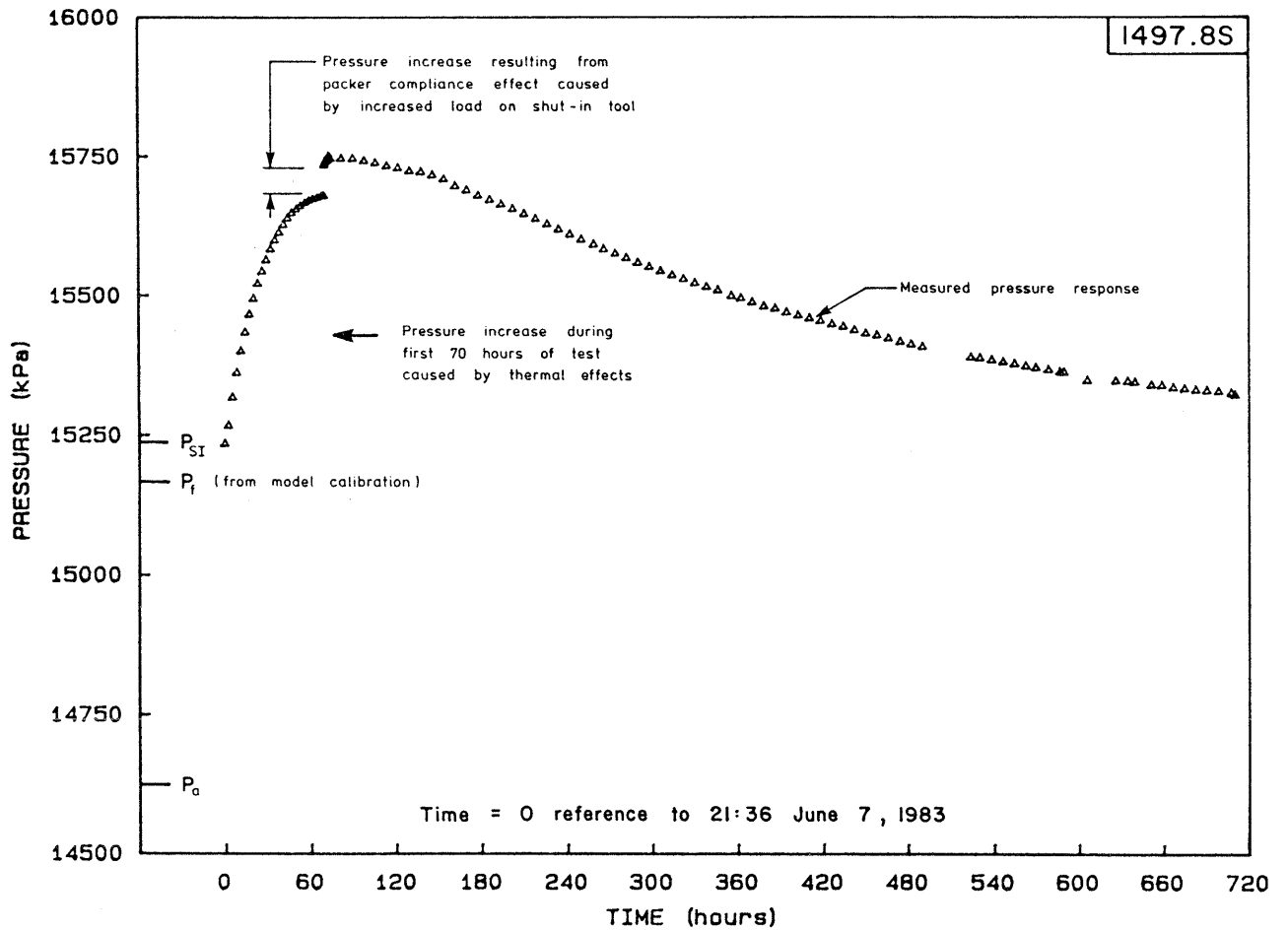


Figure 3.9-8

Measured interval pressure response for Boettstein test 1497.8S showing the initial pressure increase due to thermal effects, the 55 kPa pulse caused by packer "squeeze" and the subsequent pressure recovery

fluid in the test interval. Inspection of the test data suggests that the bulk of the pressure response (due to the increased load) is essentially instantaneous with a small time and/or pressure-dependent portion occurring during the following several hours. The pressure increase of 55 kPa corresponds to a calculated shortening of the test interval length (i.e., downward movement of the packer) by 0.2 mm, thus illustrating the dramatic effect that equipment compliance can have on the measured pressure in a borehole test interval. After increasing the load on the shut-in tool, the test interval monitoring was continued for a total testing time of about 31 days.

Examination of the measured temperature and pressure response data indicates that the test interval is of low permeability and that the pressure response is dominated by thermal expansion of the borehole fluid. The measured temperature responses for temperature transducers T1 and T2 exhibited an oscillatory behaviour. Therefore, the cubic spline temperature curve for simulation purposes using GTFM was approximated from the transducer T3 data (see Figure 3.9-9A). A temperature change of 1.0 °C was measured during the first 2.93 days and a total temperature change of 2.1 °C was observed during the 31 day testing period.

The calibration methodology chosen for analysis of the measured pressure response was:

- (1) estimate a formation pressure;
- (2) simulate the pressure profile in the formation resulting from borehole pretest pressure history (using an annulus pressure of 14630 kPa for 3.75 days as shown in Figure 3.9-9B);
- (3) vary the hydraulic conductivity until a close fit is obtained between the simulated and measured pressure responses during the first 2.93 day test period;
- (4) apply the 55 kPa pressure increase (from equipment compliance) as a pulse;
- (5) simulate the pressure response for the remainder of the 31 day test period using the hydraulic conductivity estimated from step 3 and compare with the measured pressure response;

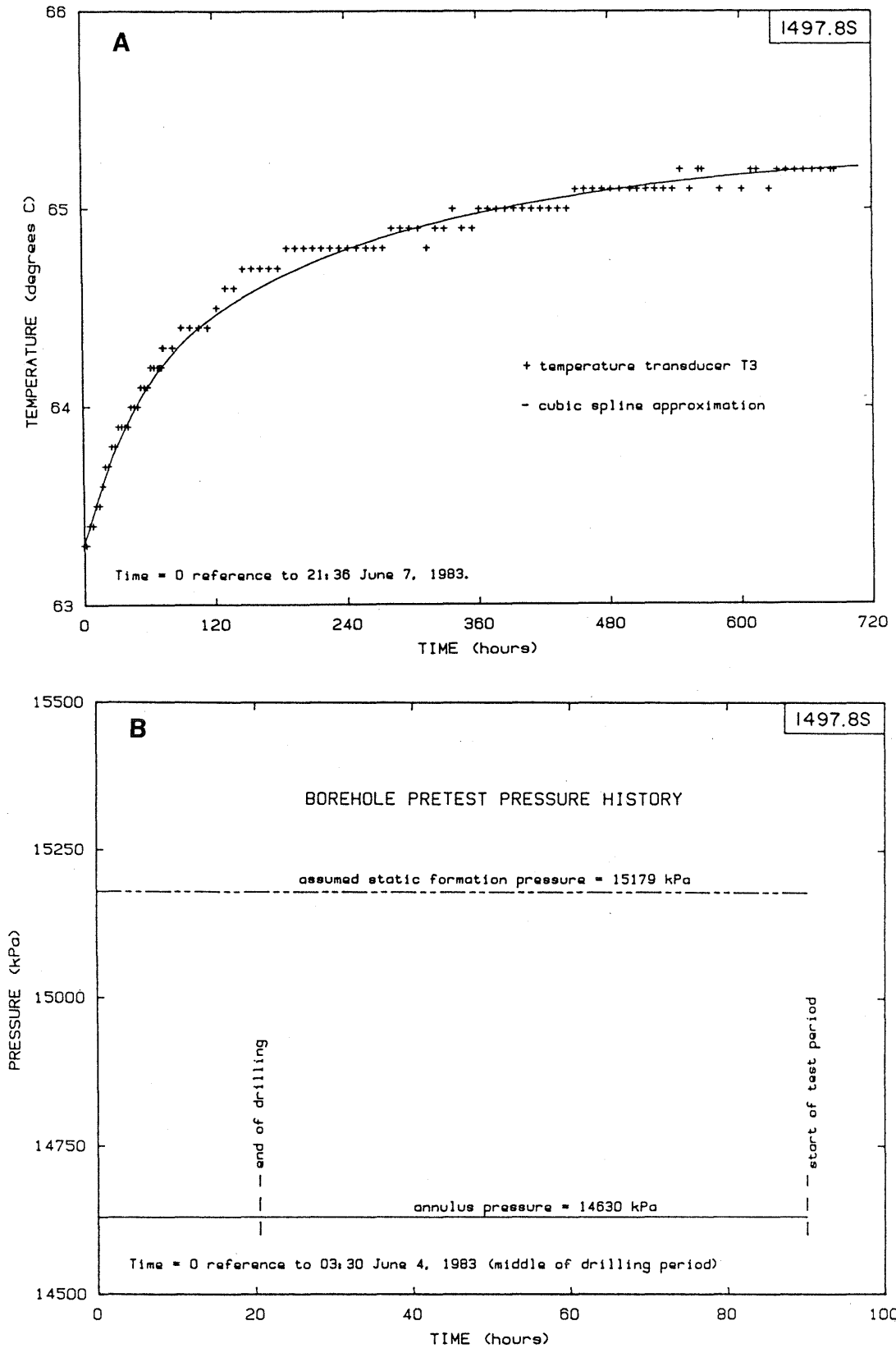


Figure 3.9-9 Boettstein test 1497.8S: (A) Temperature history data during testing and cubic spline temperature curve used in GTFM simulations, and (B) Assumed borehole pretest pressure history

and (6) repeat steps 1 to 5 using improved estimates of formation pressure based on the comparison in step 5.

Simulations using the GTFM model were conducted for estimated formation pressures in the following sequence: 14630, 15014, 15208, 15179 and 15344 kPa. The model parameters used in the data analysis are given in Table 3.9-6. Varying the estimated formation pressure resulted in changes in the best-fit hydraulic conductivity by only a factor of 2 during the first 2.93 days of the simulation period. However, the choice of formation pressure was very significant in obtaining a good fit between measured and simulated pressure responses for the remainder of the 31 day test period. A close agreement between measured and simulated pressure responses was obtained for a hydraulic conductivity of 9.5×10^{-14} m/s and a formation pressure of 15179 kPa at transducer probe depth (see Figure 3.9-10).

A parameter sensitivity study using GTFM was conducted to quantitatively investigate the effect of the magnitude of hydraulic conductivity and formation pressure in simulating the measured pressure response for Boettstein test 1497.8S. Figure 3.9-10 illustrates a comparison between measured and simulated pressure responses for: (i) hydraulic conductivities of 5×10^{-14} , 9.5×10^{-14} and 2×10^{-13} m/s with the best-fit formation pressure of 15179 kPa, and (ii) formation pressures of 15014, 15179 and 15344 kPa with a hydraulic conductivity of 9.5×10^{-14} m/s. The model-simulated pressure response curves indicate that the choice of formation pressure is very important in obtaining a good fit to the measured pressure response.

The equivalent formation pressure at the center of the test interval at 1497.7 m depth is 15272 kPa. A plot showing the tool and test interval configuration with the estimated transducer and test interval pressures is shown in Figure 3.9-11.

The results of this example show the versatility of the GTFM model in routine applications in borehole hydraulic testing programs. The ability of this simulation technique to model complex systems that include borehole history, temperature and compliance effects makes it a powerful analysis tool for borehole hydraulic tests. Accurate and routine analyses of tests such as Boettstein test 1497.8S

Table 3.9-6 Model parameters for test data analysis
for Boettstein test 1497.8S

Parameter	Value
Formation	
Compressibility	$2 \times 10^{-11} \text{ Pa}^{-1}$
Porosity	0.005
Storage Coefficient*	1.5×10^{-6}
Fluid	
Compressibility	$4.33 \times 10^{-10} \text{ Pa}^{-1}$
Density	$9.87 \times 10^2 \text{ kg m}^{-3}$
Coefficient of thermal expansion	$5.41 \times 10^{-4} \text{ }^\circ\text{C}^{-1}$
Test Interval	
Length	7.1 m
Diameter	0.159 m
Estimated static formation pressure (at P2 elevation)	15179 kPa

* Storage coefficient is calculated from the formation/fluid properties and test interval length

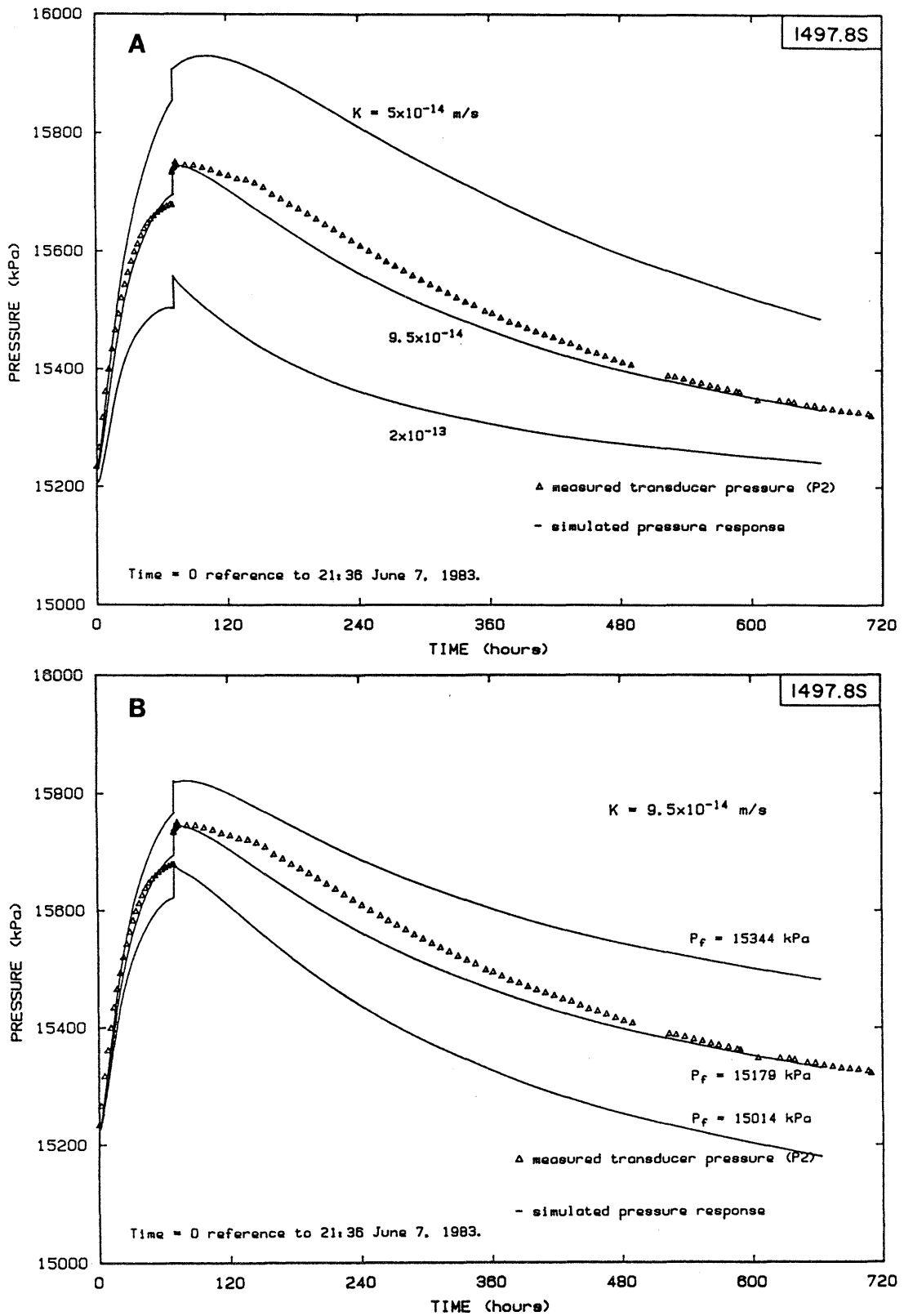


Figure 3.9-10 Boettstein test 1497.8S: (A) Sensitivity of simulated response to changes in hydraulic conductivity with best-fit hydraulic conductivity of $9.5 \times 10^{-14} \text{ m/s}$, and (B) Sensitivity of simulated response to changes in formation pressure with best-fit formation pressure of 15179 kPa

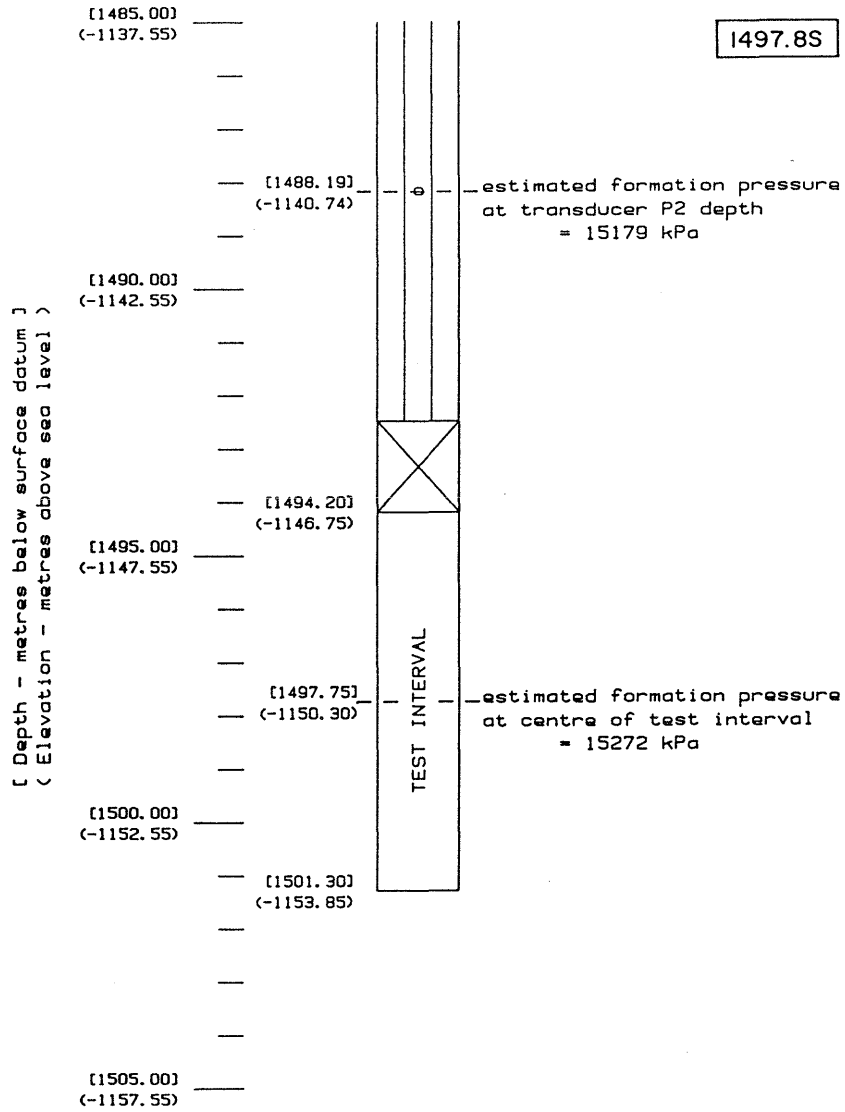


Figure 3.9-11 Schematic diagram showing equipment configuration and estimated formation pressure for Boettstein test 1497.8S.

would be impossible without models such as GTFM and, therefore, with the use of such simulation models optimal use of hydraulic testing data can be attained and accurate formation parameters can be determined.

4. PRACTICAL CONSIDERATIONS IN EVALUATING BOREHOLE HYDRAULIC TESTING RESULTS

4.1 Introduction

The purpose of this section is to evaluate, from a practical hydraulic testing point of view, all factors which may have an effect on the measured pressure response or the determination of formation pressure and hydraulic conductivity during a hydraulic testing program. In a hydraulic testing program where single or double packer equipment configurations are used to conduct slug, pulse or drill stem tests, a number of aspects contribute to the accuracy and uncertainty of the interpreted results. In order to increase the accuracy and reduce the uncertainty in the results it is necessary to have a thorough understanding of the theoretical basis of the tests and how factors such as pre-testing conditions, borehole/formation considerations, and fluid and equipment related effects contribute to the measured pressure response during hydraulic testing. In this section each of these factors are considered from a practical point of view and, where possible, the effect of these factors or considerations have been quantified to provide estimates of the resultant variation in the interpreted magnitude of hydraulic conductivity.

The context of the discussion is one in which pressure or permeability measurements are made in open boreholes using commercially available packer testing equipment (e.g., Lynes Inc. Hydrologic Tool and Packers). The practical considerations contained in this section have been developed as part of the NAGRA deep borehole testing program in crystalline rock in northern Switzerland. The chosen test conditions for illustrative purposes relate to the Boettstein borehole.

This hydraulic testing program in crystalline rock has utilized three types of testing procedures. The choice of test for a particular test interval is dependent on the relative magnitude of the hydraulic conductivity of the interval. This relationship may

be generalized as follows:

Test Type	Magnitude of Hydraulic Conductivity
Pulse test	Low ($< 10^{-10} \text{ ms}^{-1}$)
Slug test	Intermediate to high ($> 10^{-10} \text{ ms}^{-1}$)
Drill stem test	Intermediate to high ($> 10^{-10} \text{ ms}^{-1}$)

The important considerations when conducting or interpreting these types of hydraulic tests are discussed in the following subsections. The emphasis of the discussions in this report is on the interpretation of the hydraulic conductivities.

4.2 Theoretical Aspects

4.2.1 Conceptualization and Assumptions Regarding the Flow Regime

For conceptualization purposes, the flow regime during hydraulic testing in rock is generally assumed as analogous to a confined porous media aquifer. In the analogy the packers which isolate the test interval are considered coincident with the confining units of the aquifer. The test interval represents the aquifer in which ground water flow to or from the interval occurs radially (see Figure 4.2-1).

Using this conceptualization, the following simplifying assumptions are adopted:

- (1) The aquifer (test interval) is confined, infinite in areal extent and constant in thickness;
- (2) The aquifer is homogeneous;
- (3) Areal flow in the aquifer is negligible;
- (4) Initially, constant head exists across the aquifer;

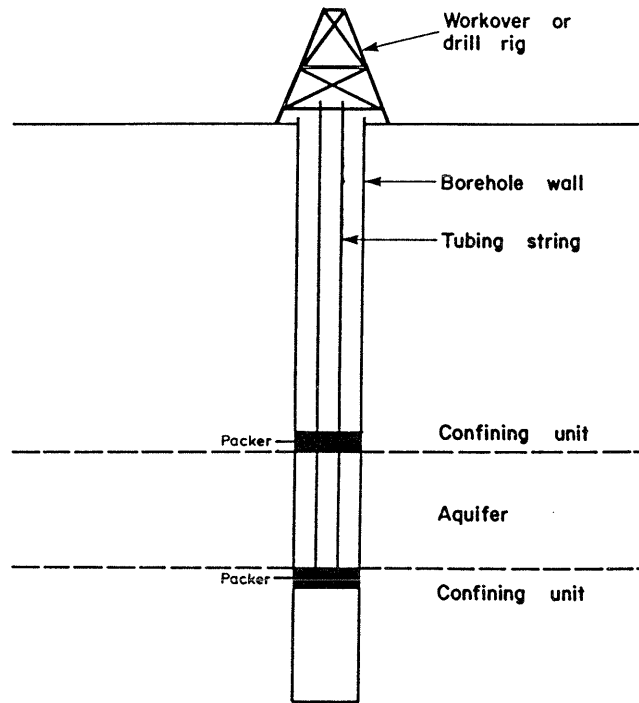


Figure 4.2-1 Idealized conceptualization of hydraulic testing in a packer-isolated interval

- (5) No vertical component of flow exists in the aquifer.

These assumptions have been universally applied in ground water problems in porous media to simplify the flow regime in a manner that is conducive to analysis. However, in terms of the conceptualization of the flow regime each assumption and its validity is worthy of further discussion.

Assumption number 1 in which the aquifer is confined, of infinite area extent and constant thickness, provides a number of difficulties with regards to the proposed conceptualization. The packers, although they isolate the interval do not confine flow in the formation nor do they limit flow in the formation to a specific thickness. The resulting effect during pressure dissipation or flow to or from the interval is that at each end of the interval, in the region of the packers, the flow regime is sub-horizontal as opposed to horizontal as in the centre of the interval. Thus, the tested zone affected by the flow is larger than that assumed with a constant thickness equal to the test interval length. The effect on a hydraulic conductivity determination is to yield a value that is larger than would be obtained in a totally confined system. However, this effect is likely to be dependent on the length of the test interval in comparison to the borehole diameter and volume of rock being influenced by the test (i.e., radius of influence). With a short interval (e.g., 1 metre) the end effects in relationship to the entire length would be significant while for a long interval (i.e., several metres to 10's of metres) the end effect would be negligible.

The assumption of infinite areal extent in terms of the conceptualization is generally acceptable because the zone of influence in the formation during testing is usually small in comparison to the total extent of the formation. Boundaries may be present within the radius of influence of a hydraulic test. Identification of such boundaries is a difficult task; however, their incorporation into the test data interpretation is recommended when their presence is established.

The homogeneous aquifer assumption (number 2) is one that is commonly used in ground water problems but is rarely achieved in reality. Heterogeneity in crystalline rock is difficult to quantify and unless the nature of the heterogeneity can be defined the

homogeneous assumption along the test interval length provides the simplest and possibly the most practical description of the variation of hydraulic conductivity with position in the formation (i.e., for the purpose of hydraulic conductivity profiling).

Assumption number 3, which states that areal flow in the formation is negligible, is an assumption that is justifiable when one considers the low flow rate in the formation under natural conditions (i.e., under low gradients) as compared to the high gradients and flows that are induced in the formation interval due to the hydraulic testing procedures (i.e., pulse, slug or pump tests).

Constant hydraulic head across the aquifer is an assumption (number 4) that is justifiable outside of the zone influenced by the drilling and pretest borehole pressure history. The hydraulic head in the immediate area of the borehole is likely to be affected by borehole history and result in the formation exhibiting dramatic differences in hydraulic head with short distances from the borehole. Borehole history can be compensated for by using models such as those described in Section 3. The effects of borehole pressure history are discussed in greater detail in section 4.3.

Assumption number 5, no vertical component of flow existing in the aquifer, can be addressed similar to assumption number 1. Although some vertical flow in the aquifer may occur as a result of sub-horizontal flow near the packers its effect in terms of the entire length of the test interval is likely to be small. Vertical flow which may occur naturally in the formation is likely to be of a small magnitude as compared to the horizontal flow induced by the hydraulic testing. The effect of sub-vertical fractures or higher permeability zones on this assumption is discussed in more detail in Section 4.4.

The assumptions as documented above cause some uncertainty in the results but are necessary to put the field situation into a conceptualization that allows an analysis of the field measured pressure data to determine formation hydraulic parameters. Where test intervals on the order of several metres to 10's of metres are used, the assumptions are generally appropriate but the confidence in the results may decrease as the test interval becomes much shorter or much longer. The influences on the formation parameter determinations associated with measurement scale are discussed in section 4.4.

4.2.2 Reference Pressure

When the hydraulic test data analysis for determining hydraulic conductivity is conducted using type-curve analysis methods or methods based on computer implementation of analytical solutions of slug and pulse tests (e.g., Cooper et al., 1967; Bredehoeft and Papadopoulos, 1980) a unique reference pressure must be either chosen or be determined as part of the type-curve analysis procedure. Therefore, the chosen or determined reference pressure must be carefully evaluated and take into consideration the following:

- estimated formation pressure (either from the measured pressure response for the tested interval or estimated from the expected hydraulic head based on comparison with measured formation pressures from adjacent test intervals.
- annulus pressures;
- duration of and pressure fluctuations during the borehole pressure history period.

For testing conditions applicable to where the formation pressure is significantly different from the annulus pressure, for example, the choice of reference pressure at the two possible extremes (i.e., either equal to annulus or formation pressure) could yield a variation in interpreted hydraulic conductivity by up to about one order of magnitude for the conditions representative of the Boettstein borehole.

The use of hydraulic test data analysis methods which include the effect of borehole pressure history generally allows a more accurate representation of borehole and formation pressure responses during testing. These analysis methods, while usually more time consuming, are justified for cases with borehole open periods from hours to weeks between drilling and testing, or where significant pressure fluctuations are imposed on a test interval during a testing sequence. With a long borehole open period (i.e., several months) prior to the start of hydraulic testing, a reference pressure at or near annulus pressure (but at least between annulus and formation pressure) is reasonable for data analysis of a short-term test (i.e., on the

order of hours to a day) using type-curve or computer implementation of analytical solution methods. It is assumed in the preceding discussion that suitable testing procedures are utilized; that is, a strong head or pressure differential is induced as the initial condition for the hydraulic tests (see discussion in Section 3 and procedures graphs in Section 5).

4.2.3 Estimation of Storage Coefficient

The specific storage of a saturated geologic medium is defined as the volume of water that a unit volume of the medium releases from storage under a unit decline in hydraulic head. This volume of water released from storage is dependent upon the compressibility of the fluid and the medium. Specific storage S_s can be expressed

$$S_s = g\rho(C_R + \theta C_W) \quad (4.2-1)$$

where

ρ	fluid density, ML^{-3} ;
g	gravitational constant, Lt^{-2} ;
C_R	rock or medium compressibility, $M^{-1}Lt^2$;
θ	porosity, dimensionless;
C_W	fluid compressibility, $M^{-1}Lt^2$;

The mathematical representation of the specific storage is dependent on the definition of the fluid and medium compressibilities. A detailed review of the various conventions for defining the medium compressibility is given by Narasimhan and Kanehiro (1980). The expression for specific storage noted above is based on a medium compressibility definition utilizing a normalization with respect to the bulk volume of the sample being tested. The medium compressibility C_R is expressed

$$C_R = \frac{\Delta\varepsilon}{\Delta\sigma} = -\frac{1}{V_b} \frac{\Delta V_v}{\Delta\sigma} \quad (4.2-2)$$

where

V_b	bulk volume, L^3 ;
V_v	volume of voids, L^3 ;
$\Delta\varepsilon$	change in strain, dimensionless;
$\Delta\sigma$	change in effective stress, ML^{-2}

If drainage is allowed, then $\Delta\sigma = \Delta p$ where p is the fluid pressure. This definition for C_R is referred to as the coefficient of volume change in the soil mechanics literature. For uniaxial loading, the ratio of stress to strain is the

Young's modulus. For three-dimensional loading, it is necessary to consider the bulk modulus which accounts for the volumetric strain. For the special case of equal stress in all directions, the bulk modulus, B , is expressed:

$$B = \frac{\sigma}{\Delta V_b / V_b} = \frac{E}{3(1-2U)} \quad (4.2-3)$$

where E Young's modulus, $ML^{-1}t^{-2}$;
 U Poisson's ratio.

The medium compressibility is the reciprocal of the bulk modulus for three-dimensional cases:

$$C_R = \frac{3(1-2U)}{E} \quad (4.2-4)$$

The stress-strain relationships for rocks or porous media are usually measured under laboratory conditions using a variety of experimental techniques. The methodologies involve measurements of load and corresponding strain under uniaxial or triaxial conditions.

The storage coefficient is equal to the product of the specific storage and the formation thickness. During double packer hydraulic testing, the full test interval length is usually chosen as the formation thickness because the portion of the test interval length most actively contributing to the pressure recovery is unknown. Using a representative range of values for the rock formation and the fluid properties, the calculated specific storage should range in magnitude between about 1×10^{-7} to $1 \times 10^{-6} m^{-1}$ for crystalline rock. Packer spacings used are typically in the range of several metres to several ten's of metres and, therefore, the expected range of storage coefficient values is from about 3×10^{-7} to 3×10^{-5} .

Type-curve analysis methods can yield unrealistic storage coefficients because they are based on ideal test conditions (i.e., they do not include borehole pressure history or thermally-induced borehole pressure effects). A storage coefficient chosen from type-curve analysis should be carefully evaluated to ensure that it is within a reasonable range of values. If the best-fit type curve indicates an unreasonable storage coefficient, then

it may be more desirable to bias the choice of type curve to correspond to one that is more representative of a reasonable storage coefficient. This procedure is recommended to allow an evaluation of the effect of the storage coefficient on the interpreted hydraulic conductivity when using type-curve analysis methods.

Examination of numerous hydraulic conductivity test interpretations indicates that the hydraulic conductivity determined is relatively insensitive to the chosen value for storage coefficient. For example, variation in the storage coefficient by several orders of magnitude will yield a variation in interpreted hydraulic conductivity of less than an order of magnitude.

4.3 Effects of Pre-Test Conditions

4.3.1 Borehole Pressure History

The effect of the pressure variations within the tested interval prior to the start of a hydraulic test or between hydraulic tests in a test sequence has been addressed in detail in Sections 3.4 and 3.8. This effect will be discussed only briefly in this section with regards to practical considerations in hydraulic testing.

The pressure within the borehole after drilling a test interval (referred to as annulus pressure) will, in general, be different from the in-situ formation pressure. This pressure difference results in the development of a pressure skin surrounding the borehole that is different in magnitude from the formation pressure. The net effect of the "pressure skin" developed during the drilling and pretest period is the development of testing conditions that do not meet the assumptions involved in data analysis methods using type curves or computer implementation of analytical solutions. For instance, the pressure recovery in the interval will not be simply related to the recovery to in-situ formation pressure from an initial pressure at the start of the test. The pressure skin developed during drilling and prior to testing will strongly affect the pressure recovery curve. The analysis of packer tests using type-curve or analytical solution methods could therefore yield

incorrect hydraulic conductivity estimates under conditions where the annulus pressure and formation pressure are different. Analysis methods (e.g., GTFM) may be utilized, where necessary, to incorporate the borehole history effect and, therefore, yield more accurate hydraulic conductivity estimates from the test data analysis.

Testing procedures are recommended that take into account the magnitude of the annulus and formation pressure and consequently are designed to minimize the borehole history effect. Pulse and slug tests should be conducted with an initial strong pressure pulse or head differential in comparison to both the annulus or formation pressure or the difference between them. Also, a long period open to annulus pressure conditions can cause a sufficiently large pressure skin to develop such that, for the purposes of hydraulic conductivity determination, the annulus pressure can be assumed as the "reference" or pretest pressure. Designing and conducting hydraulic tests which minimize borehole history effects can reduce the uncertainty in the interpreted hydraulic conductivity.

4.3.2 Thermally-Induced Borehole Pressure Response

Borehole pressure changes during testing as a result of nonisothermal testing conditions has been addressed in sections 3.4 and 3.8 and will be presented only briefly here. During and subsequent to drilling a test interval, a temperature profile is developed into the formation in response to the differential temperatures between the borehole fluid and the rock. The net effect of the development of these temperature profiles in the formation is a variation in the borehole fluid temperature during the hydraulic testing period. These temperature variations result in significant pressure changes during pulse testing (i.e., under shut-in conditions), especially in low permeability formations as a consequence of the thermal expansion (or contraction) of the fluid.

Pulse injection or withdrawal tests are conducted on lower permeability zones since they allow the tests to be conducted more rapidly as compared to slug injection or withdrawal tests. Varying-temperature conditions existing in any zone requiring pulse

tests will likely result in significant thermally-induced pressure responses. In contrast, the pressure response in a high permeability zone is relatively insensitive to temperature changes. The insensitivity is due to the relative ease with which a high permeability zone dissipates any pressure changes, providing the zone has sufficient lateral extent to accommodate the pressure changes. It should be noted that testing of higher permeability zones would generally utilize slug tests, which are not conducted under shut-in conditions, and therefore are not affected by thermally-induced pressure changes.

Analysis methods have been developed and utilized, where necessary, to account for thermally-induced pressure effects to allow more accurate formation pressure and hydraulic conductivity estimates to be determined from the test data. However, the representativeness of the temperature response measured at the transducer probe depth of average temperature conditions within the test interval is an area of uncertainty. It should be noted that in most cases the temperature transducers are located above the packed-off interval (e.g., Lynes equipment) and that the transducers and the tool may not be in temperature equilibrium with the borehole fluid. While in most cases the temperature response above and within the test interval is believed to be similar, accurate temperatures representative of the test interval are necessary to provide confidence in the interpreted results. Much of the uncertainty associated with the formation pressure and hydraulic conductivity determinations in low permeability zones conducted during or immediately subsequent to the drilling phase is as a result of the uncertainty in the temperature response. Testing procedures are recommended that minimize the thermal problem. For example, a long borehole period under passive (i.e., nonpumping) conditions can result in a near equilibrium being reached between the borehole and the thermal skin in the formation surrounding the borehole.

4.4 Borehole/Formation Considerations

4.4.1 Borehole Diameter

The borehole diameter is a parameter in the data analysis that is subject to a variation from the original drilled diameter and, therefore, presents an additional source of uncertainty. The variation in the diameter of the borehole is due to erosion of the borehole wall during the drilling phase. Immediately after drilling a borehole interval, the borehole diameter is at or the same as the bit diameter for most depths in crystalline rock. As drilling continues the rotation of the drill rods within the borehole, the removal and insertion of drill equipment in the borehole and the circulation of borehole fluid all contribute to the erosion of the borehole wall. In areas of softer rock or poor rock quality, the erosion of the borehole wall can be significant.

To obtain an estimate of the borehole diameter during hydraulic testing the drilled diameter or the caliper logs can be used. If testing occurs shortly after the interval has been drilled then the drilled diameter is likely to be representative of the actual borehole diameter. If, however, the borehole has been open and drilling has progressed for a long period of time, the borehole may be significantly different from the drilled diameter. Caliper logs can be used to obtain an estimate of the average diameter for the interval, but the caliper logs are usually conducted at infrequent time intervals. The most recent caliper log may show a one or two month time lag with the testing phase and therefore the caliper log may not be representative of the borehole diameter during testing. The chosen borehole diameter from the caliper logs could underestimate the actual borehole diameter resulting in an error in the borehole radius and volume for data analysis purposes.

The borehole diameter, as is shown by caliper logs, is very irregular if borehole wall erosion has had a significant effect. In the analysis of the test data a depth-integrated average diameter may be utilized. This average diameter is a realistic estimate but the average diameter used in the analysis assumes a constant diameter for the entire test interval length when in fact the surface is

irregular. The effect of an irregular borehole diameter on the hydraulic conductivity results is difficult to quantify. The entire test interval may not be contributing equally to head or pressure dissipation during a hydraulic test but rather zones having lesser or greater borehole diameter within the test interval may be dominating. Because it is not possible to ascertain the portions of the test interval that are controlling the measured pressure responses, the utilization of an integrated average diameter over the borehole test interval length is considered the best estimate for data analysis purposes.

Calculations were conducted using a computer implementation of the Bredehoeft and Papadopoulos (1980) and Cooper et al. (1967) analytical solutions to quantify the effects of an error in the choice of borehole diameter when analyzing hydraulic pulse and slug test data respectively. Borehole diameters ranging from a drilled diameter of 0.159 m to an assumed maximum eroded borehole diameter of 0.3 m were investigated. The parameter values chosen are summarized below:

Fluid density	991 kg m ⁻³
Fluid compressibility	4.3 x 10 ⁻¹⁰ Pa ⁻¹
Rock compressibility	2.0 x 10 ⁻¹¹ Pa ⁻¹
Rock matrix porosity	0.005
Specific storage	2.15 x 10 ⁻⁷ m ⁻¹
Test interval length	10.0 m
Hydraulic conductivity	
- Pulse test	10 ⁻¹¹ ms ⁻¹
- Slug test	10 ⁻⁶ ms ⁻¹
Casing (tubing) string diameter	0.03 m
Borehole diameter	0.159, 0.2 and 0.3 m

The results of the sensitivity studies on borehole diameter are shown in Figure 4.4-1 for the pulse test and Figure 4.4-2 for the slug test. For the pulse test an actual diameter of 0.30 m and a $K = 1 \times 10^{-11}$ m/s can also be matched using the drilled diameter of 0.159 m and a lower hydraulic conductivity of 3×10^{-12} m/s. Similarly a diameter of 0.20 m and a $K = 1 \times 10^{-11}$ m/s can be matched with a drilled diameter of 0.159 m and a $K = 6 \times 10^{-12}$ m/s. The simulations for these examples cases illustrate the maximum error in not using the correct borehole diameter in analysing pulse tests was on the order of a factor of 3. For the slug test (Figure 4.4-2),

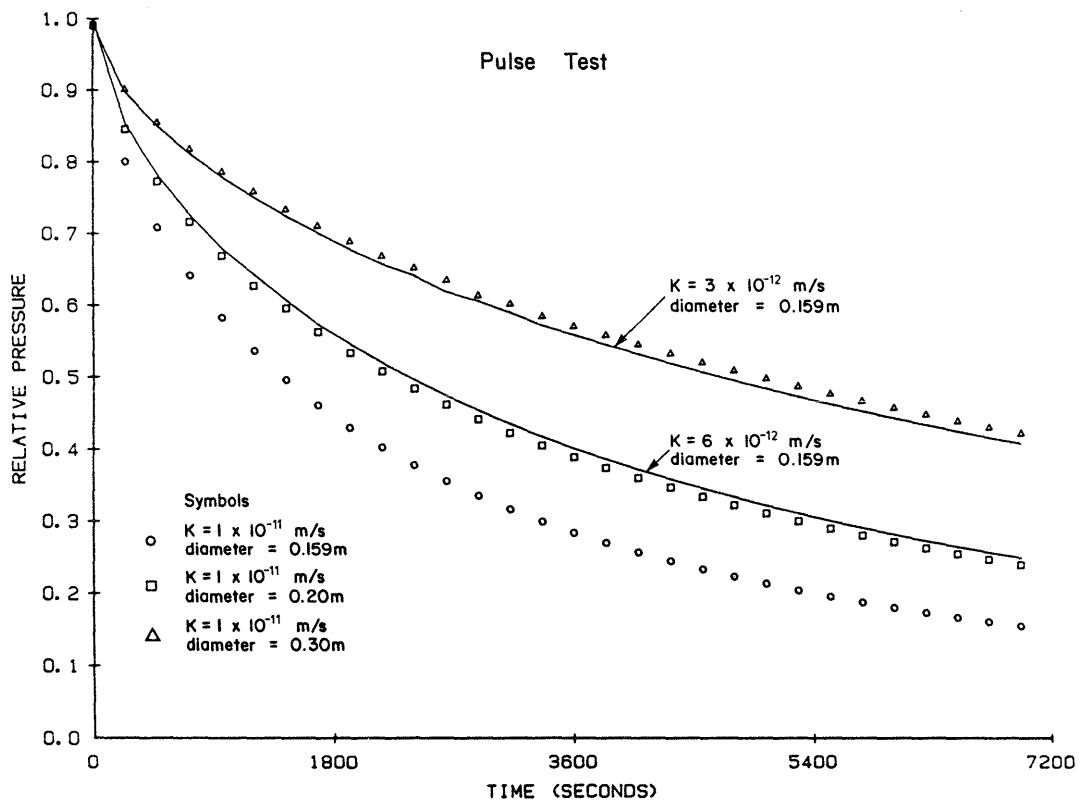


Figure 4.4-1 Calculation of the effect of borehole diameter on calculated pressure response for a pulse test using the Bredehoeft and Papadopoulos (1980) analytical solution

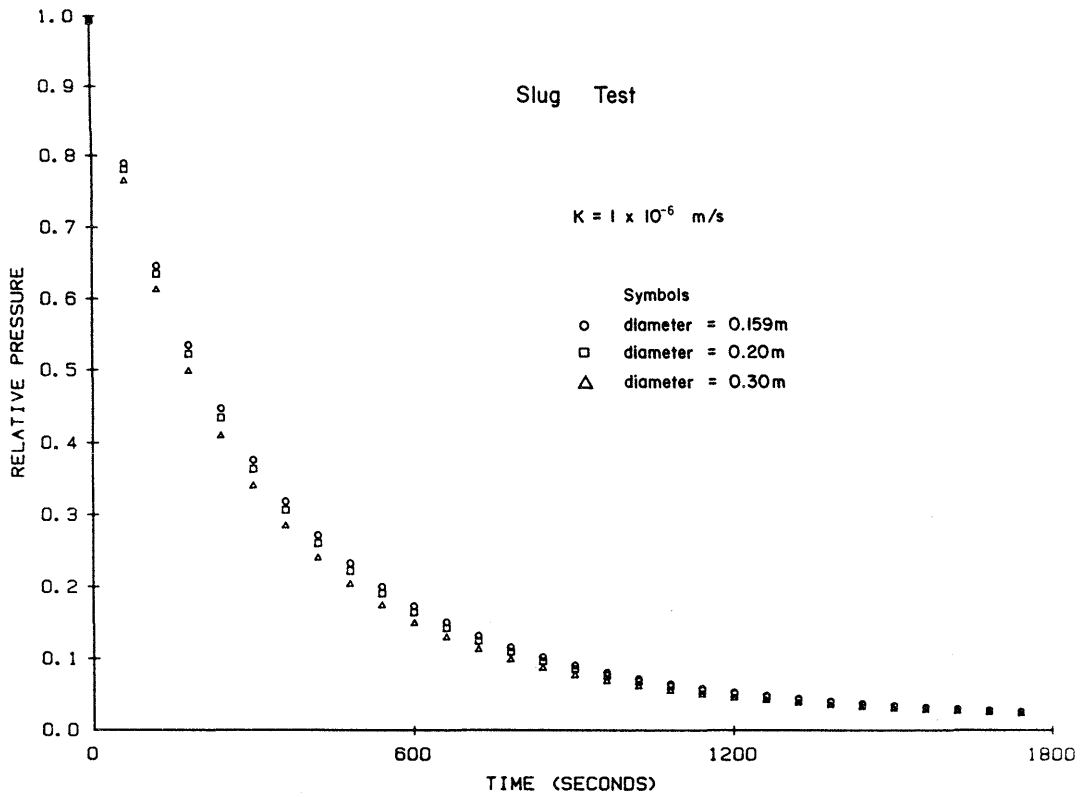


Figure 4.4-2

Calculation of the effect of borehole diameter on calculated pressure for a pulse test using the Cooper et al. (1967) analytical solution

the diameter has little effect on the simulated pressure response as each of the three diameters (0.159, 0.20 and 0.30 m) produce an almost identical pressure response at the same hydraulic conductivity (1×10^{-6} m/s).

4.4.2 Measurement Scale

It is usually assumed that the monitoring system is measuring a representative elementary volume (REV) of the hydrogeologic regime. A REV is the lower limit of a volume of porous or fractured medium for which the hydrogeologic parameters, processes or conceptualizations are valid. It then becomes necessary to ensure that the sampled volume is representative of the medium of interest. In porous media the REV could depend on the degree of interconnection between pore spaces, which depends on such properties as grain size, compaction, lithification or secondary mineralization. In a fractured media the REV could depend on the fracture frequency, fracture set orientation, fracture length or continuity. The size of the REV is then dependent on the media and is specific to the individual parameter.

In the case at hand, the measurement of hydraulic conductivity can be greatly influenced by the choice of measurement scale. Crystalline rock usually contains fractures at discrete intervals. It then becomes necessary to choose a measurement scale that is either representative of the rock mass including the fractures or a scale that is specific to individual fractures and blocks of intact rock. For example, a long test interval may include one or several fractures separated by intact rock. Hydraulic tests on this interval may be representative of the rock mass as a whole even though shorter specific intervals containing fractures may have hydraulic conductivities that are dramatically different.

The measurement scale also has a significant effect on the appropriate analytical technique that is required for analysis of the hydraulic tests. If large blocks of crystalline rock are tested such

that spatially defined values of hydraulic conductivity, porosity and compressibility can be defined, porous media approximations can be used in the analyses. If smaller intervals are tested than the flow in individual fractures will dominate and the appropriate method of analysis may, in some cases, be a fracture flow model.

For test intervals indicating low to intermediate hydraulic conductivity, additional testing could be conducted using a variety of packer spacings and testing depths to attempt to derive a more detailed evaluation of the nature of the hydraulic conductivity (i.e., homogeneous zones, discrete fractures, matrix flow only, etc.). However, it must be emphasized that the implementation of such a detailed testing program to provide this information could increase the efforts of the hydraulic testing program by an order of magnitude.

The length of the test interval in comparison to the portion or portions of the test interval that are dominating the head or pressure dissipation during a hydraulic test is an important consideration. Ideally from a flow conceptualization and analysis point of view, the full test interval should be contributing. However, it is generally not possible to ascertain the most important portions of the test interval and their relative permeability and, therefore, the full test interval length is usually chosen when estimating the storage coefficient and interpreting the hydraulic conductivity. The transmissivity of the tested interval is determined from the data analysis procedures. The hydraulic conductivity is calculated as the transmissivity divided by the formation thickness (i.e., portion of test interval contributing to most significant proportion of the pressure dissipation during the test) within the test interval (see Figure 4.4-3). The formation thickness is usually assumed as the test interval length. In cases where the formation zone is, for example, a factor of 10 smaller than the test interval length, the interpreted hydraulic conductivity would also be in error by a factor of 10. The net effect of averaging over the full test interval length is to overestimate and underestimate the hydraulic conductivity in the lower and higher hydraulic conductivity portions, respectively, of the tested interval.

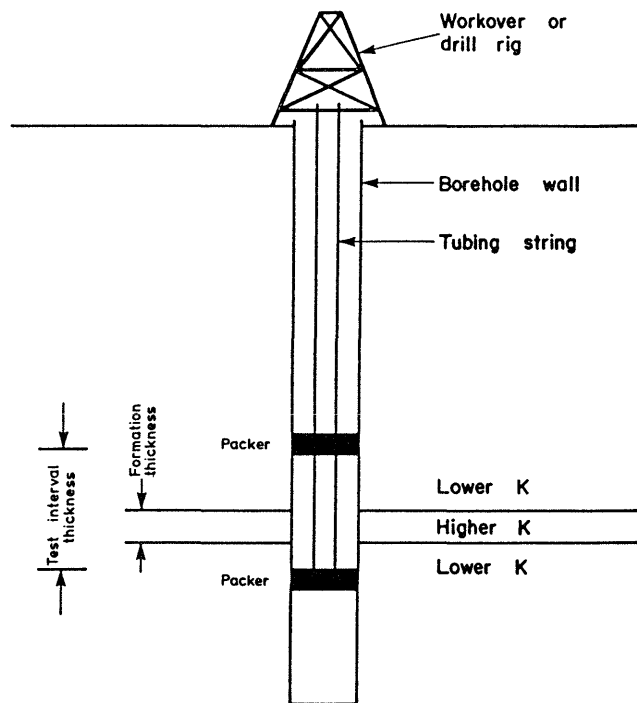


Figure 4.4-3 Conceptualization of the importance of measurement scale illustrating a case with the packer-isolated interval being much larger than the formation thickness

4.4.3 Radius of Influence

The radius of influence or the extent into the formation that is being hydraulically tested is an important consideration when evaluating the representativeness of the interpreted hydraulic conductivity to the actual rock formation. As with conducting physical measurements on any natural system, uncertainty will always exist as to the representativeness or transferability of the measurement scale to larger scales of interest.

Pulse Tests

Simulations were conducted using the GTFM simulation model to investigate the radial zone of tested rock during pulse testing utilizing the following parameter values:

Fluid density	991 kg m ⁻³
Fluid compressibility	4.3 x 10 ⁻¹⁰ Pa ⁻¹
Rock compressibility	2.0 x 10 ⁻¹¹ Pa ⁻¹
Rock matrix porosity	0.005
Specific storage	2.15 x 10 ⁻⁷ m ⁻¹
Test interval length	10.0 m
Borehole radius	0.0795 m
Hydraulic conductivity	10 ⁻¹¹ , 10 ⁻¹² and 10 ⁻¹³ ms ⁻¹

For discussion purposes, it is assumed that the radius of tested rock corresponds to the radius to which the change in pressure is 10 percent of the borehole pressure pulse. The radial pressure profiles produced at 6 and 12 hours from simulations are illustrated in Figures 4.4-4, 4.4-5, and 4.4-6 for hydraulic conductivities of 1 x 10⁻¹¹, 1 x 10⁻¹² and 1 x 10⁻¹³ m/s, respectively. The simulation results are presented in terms of relative pressure versus radial distance. The "relative pressure" corresponds to the proportion of the initial pressure pulse imposed for the hydraulic test. A radial distance of 7.95 centimetres corresponds to the position of the borehole wall. The radial distance of tested rock is determined as the distance between the borehole wall and the radial extent to which the change in pressure is

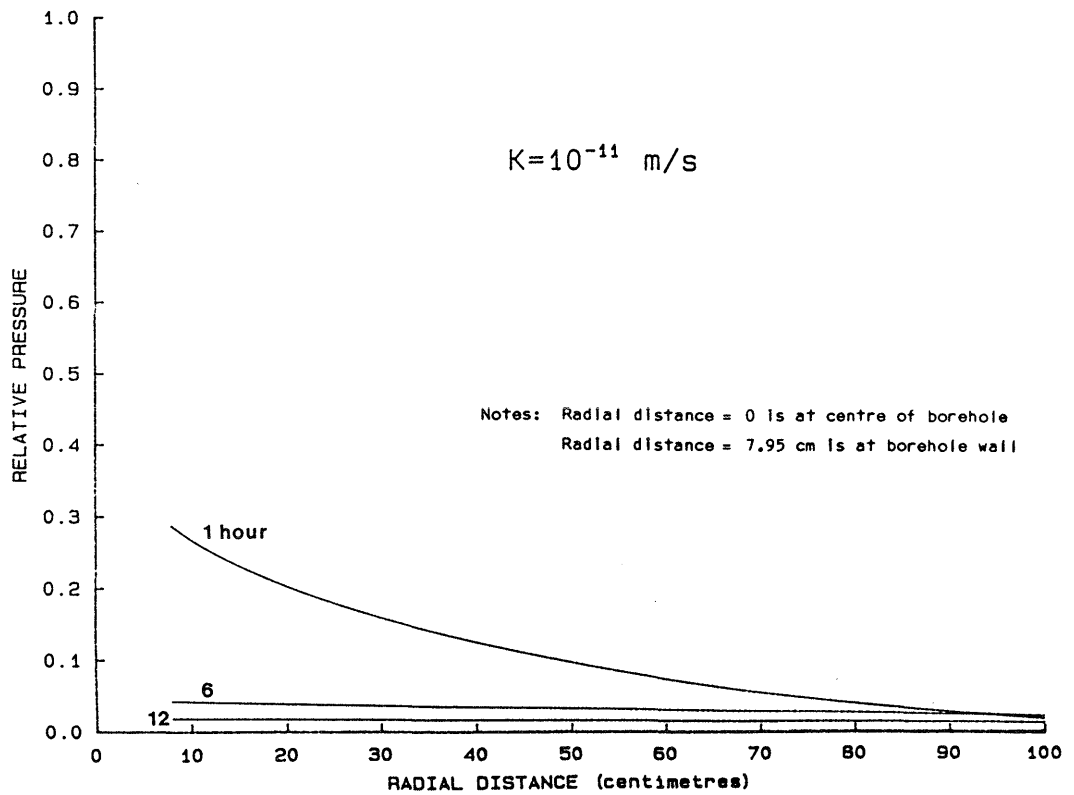


Figure 4.4-4 Radial pressure profiles into the rock formation for various times during a pulse test for a formation hydraulic conductivity of 1×10^{-11} m/s

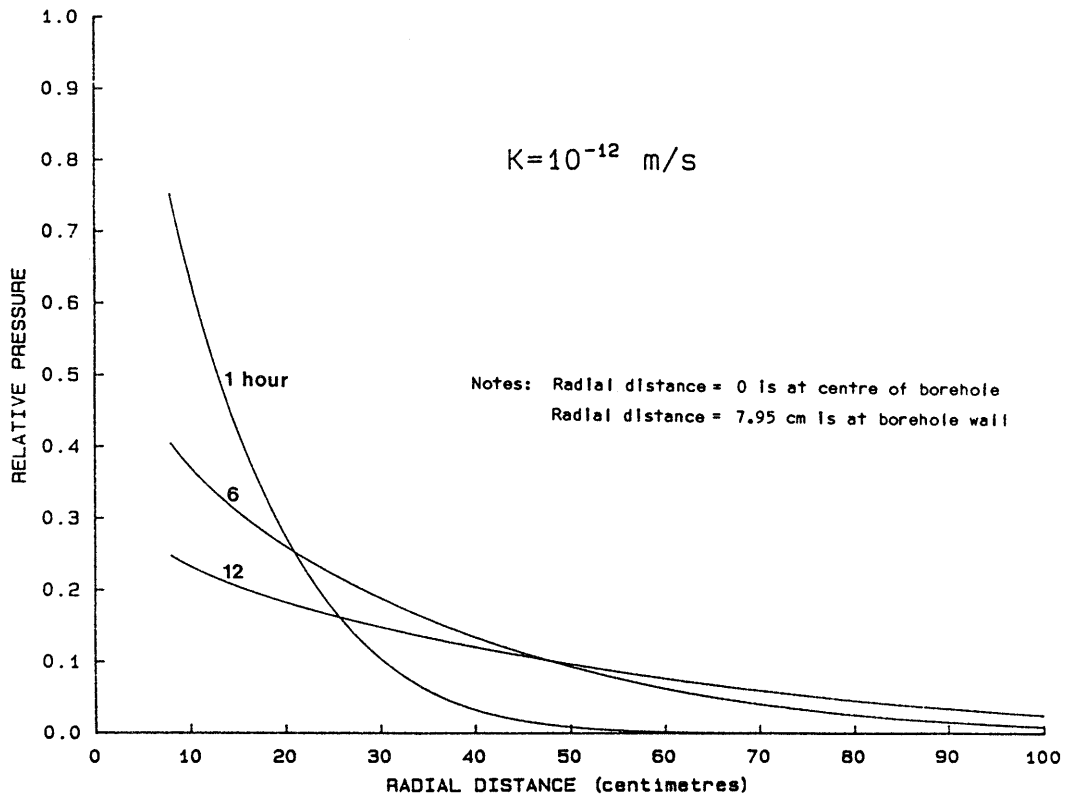


Figure 4.4-5

Radial pressure profiles into the rock formation for various times during a pulse test for a formation hydraulic conductivity of 1×10^{-12} m/s

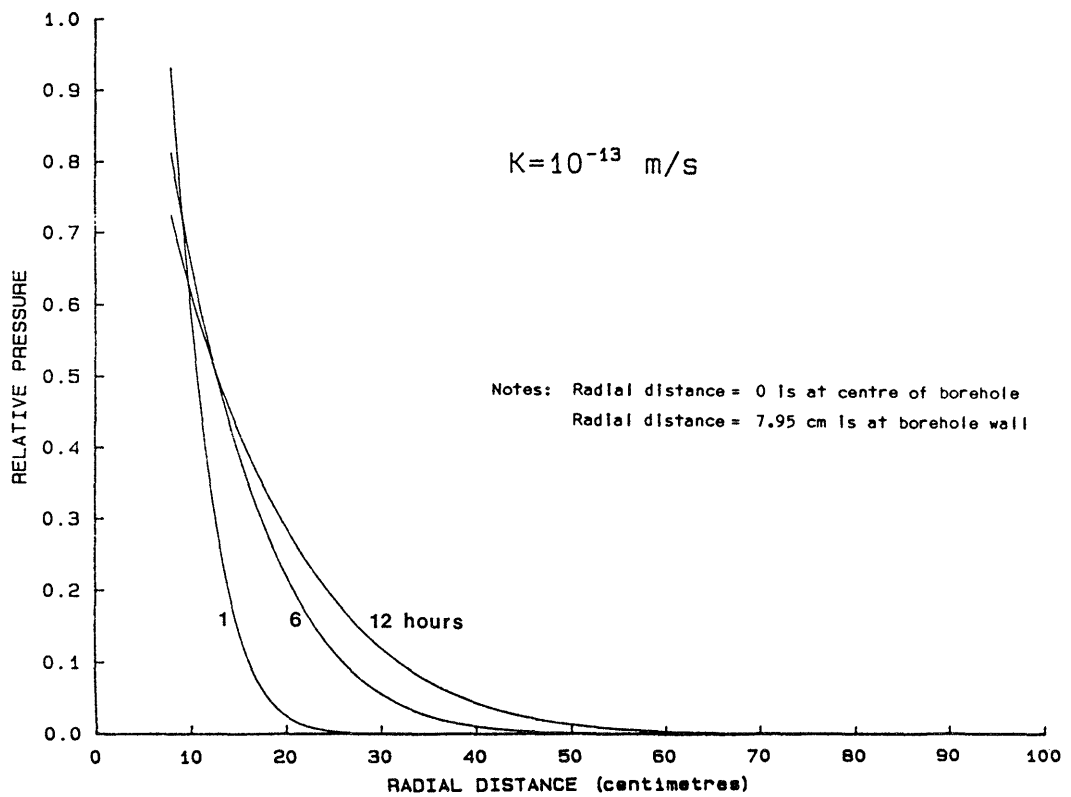


Figure 4.4-6 Radial pressure profiles into the rock formation for various times during a pulse test for a formation hydraulic conductivity of 1×10^{-13} m/s

10 percent of the borehole pressure pulse. The GTFM results are summarized below:

Hydraulic Conductivity (ms^{-1})	Radial Distance of Tested Rock (centimetres)	
	6 hour test	12 hour test
1×10^{-11}	43	43
1×10^{-12}	41	42
1×10^{-13}	18	25

The radial distance of tested rock for hydraulic conductivities less than 1×10^{-11} m/s is in the range of 18 to 43 centimetres for the hydraulic testing parameters given above. (Note: the maximum radial distance is shown in the table but this distance may not necessarily correspond to the end of the test. In fact, for the higher hydraulic conductivity case, the maximum radial distance is obtained after a very short period of time).

The radial distances of tested rock noted above are considerably larger than any zone expected to be associated with the borehole wall or skin disturbed by drilling. Therefore, the hydraulic conductivity values determined from hydraulic testing are not considered to have been affected significantly by the conditions of the borehole wall but rather they are indicative of the rock outside of any borehole wall region affected by drilling disturbances.

Slug Tests

The radius of influence of tested rock was also evaluated for slug tests using the GTFM simulation model. The chosen parameter values were the same as

for the pulse test simulations discussed above with the change or addition of the following:

Hydraulic conductivity 10^{-6} , 10^{-8} and 10^{-10} ms^{-1}
 Tubing (casing radius) 0.03 m

Similar to the criterion used for the pulse tests, it was assumed that the radius of tested rock corresponds to the radius to which the change in pressure is 10 percent of the initial borehole head differential. The radial pressure profiles for simulation times up to 6 hours are shown in Figures 4.4-7, 4.4-8 and 4.4-9 for the hydraulic conductivities of 1×10^{-6} , 1×10^{-8} and 1×10^{-10} m/s, respectively. The radius of influence determinations are summarized below:

Hydraulic Conductivity (ms^{-1})	Radial Distance of Tested Rock (metres)
10^{-6}	18
10^{-8}	20
10^{-10}	4

The radial distance of tested rock during slug tests is on the order of 4 to 20 metres for the hydraulic testing parameters given above. (Note: As in the pulse tests the maximum radial distance is reported in the table which may or may not correspond to the end of the test.) Slug tests, because of the large radial distances of tested rock, provide hydraulic conductivity values that are typical of the rock far outside of any zones affected by drilling or skin effects.

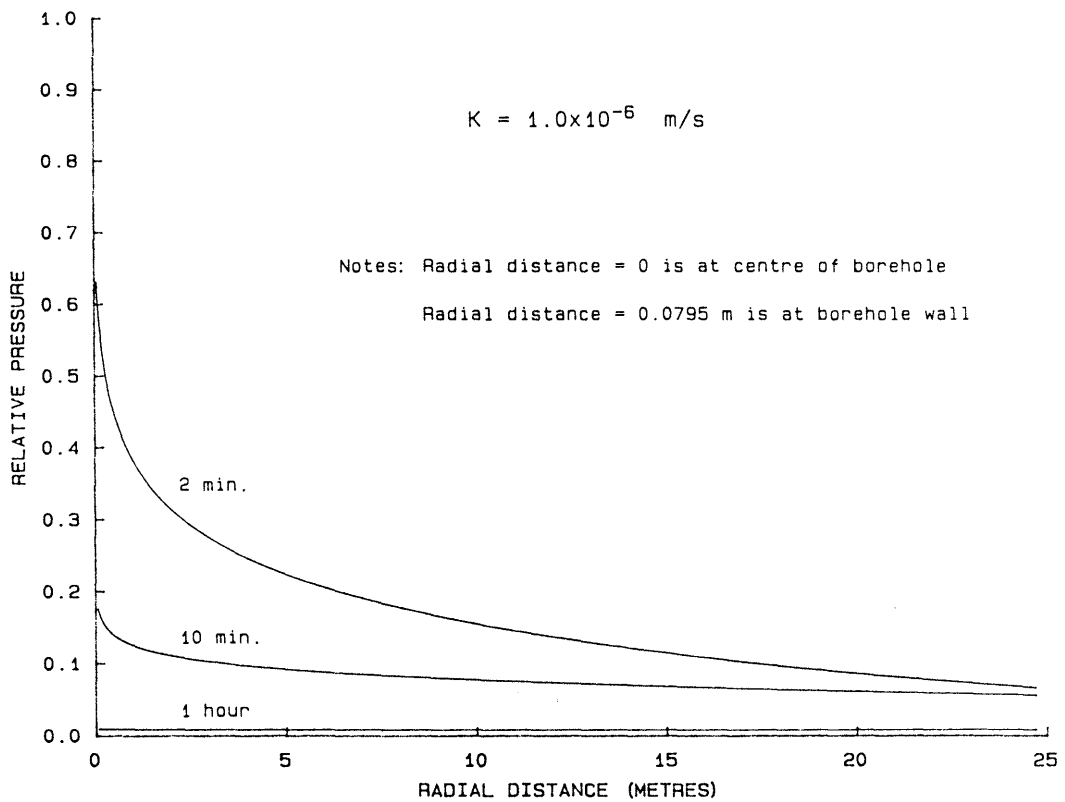


Figure 4.4-7 Radial pressure profiles into the rock formation for various times during a slug test for a formation hydraulic conductivity of 10^{-6} m/s

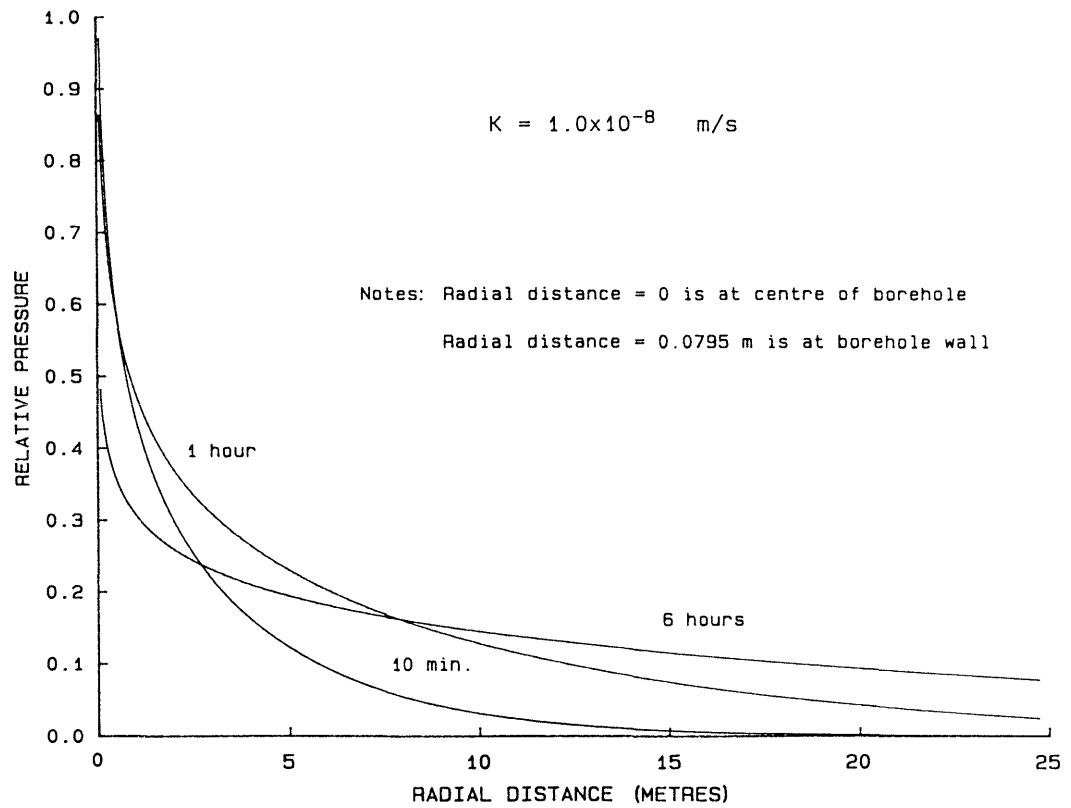


Figure 4.4-8 Radial pressure profiles into the rock formation for various times during a slug test for a formation hydraulic conductivity of $1 \times 10^{-8} \text{ m/s}$

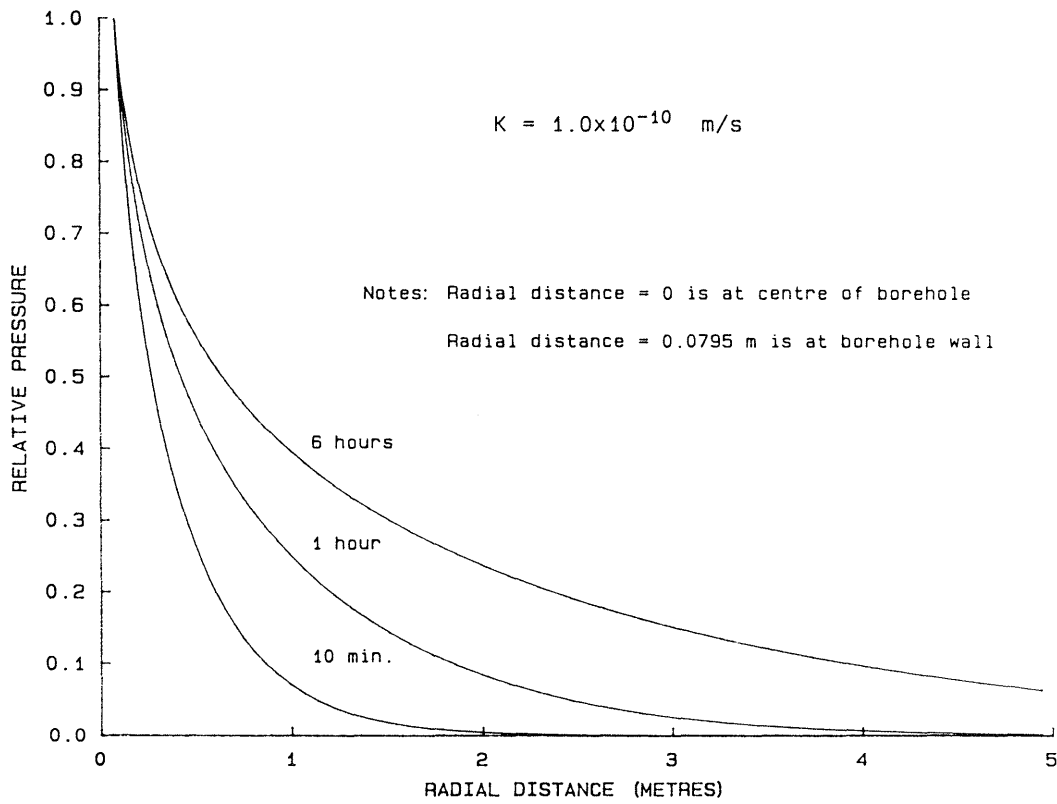


Figure 4.4-9

Radial pressure profiles into the rock formation for various times during a slug test for a formation hydraulic conductivity of $1 \times 10^{-10} \text{ m/s}$

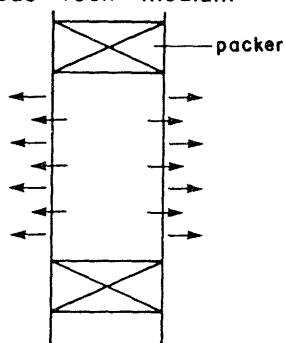
4.4.4 Porous Media Versus Fracture Flow Analyses

The use of fracture flow models such as the solutions published by Wang et al. (1978) are somewhat restrictive in that the theory is based on very idealized assumptions regarding physical conditions, such as the existence of either a single fracture or a known number of identical contributing fractures (from a hydraulic perspective) within the test interval. Such an understanding of the most important fractures within a test interval is rarely, if ever, attained. Therefore, the porous-media based analysis methods are considered adequate, if not preferable, to the fracture flow analysis methods for many cases. Some fracture flow models do allow interaction between the fracture fluid and the rock matrix blocks (i.e., Barker and Black, 1983). The three flow models, porous media flow, single fracture flow and fractured/matrix flow are shown schematically in Figure 4.4-10.

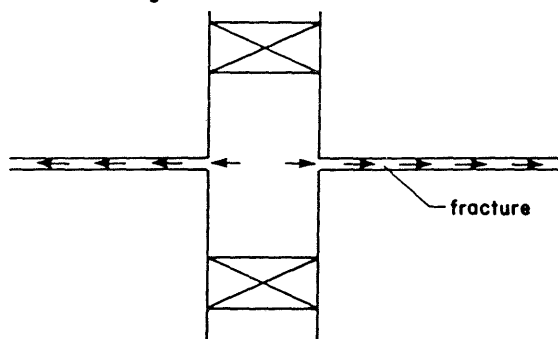
To provide insight into and a comparison of results between fracture flow and porous media analysis methods, simulations were conducted using a computer implementation of the Wang et al. (1978) and Bredehoeft and Papadopoulos (1980) analytical solutions respectively. Simulations were conducted using the following parameters:

	Wang et al. (1978)	Bredehoeft and Papadopoulos (1980)
Fluid density (kg m^{-3})	991	991
Fluid viscosity ($\text{kg m}^{-1}\text{s}^{-1}$)	5×10^{-4}	not applicable
Fluid compressibility (Pa^{-1})	4.3×10^{-10}	4.3×10^{-10}
Rock matrix porosity	not applicable	0.005
Rock compressibility (Pa^{-1})	not applicable	2.0×10^{-11}
Specific storage (m^{-1})	not applicable	2.15×10^{-7}
Borehole radius (m)	0.0795	0.0795
Test interval length (m)	10.0	10.0
Hydraulic conductivity (ms^{-1})	see Figure	see Figure
Fracture aperture (m)	see below	not applicable

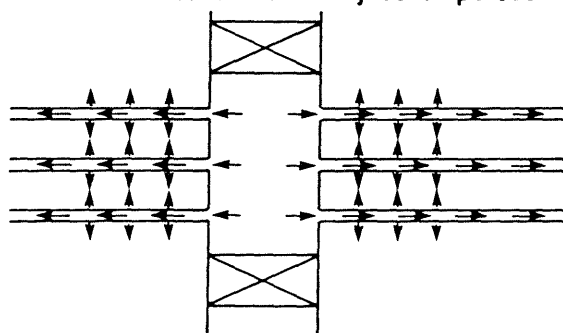
(a) Flow in porous rock medium



(b) Flow in single discrete fracture



(c) Flow in fractures and adjacent porous rock matrix

Figure 4.4-10

Schematic illustration of three different types of flow models (a) porous media flow model (e.g., Bredehoeft and Papadopoulos, 1980) where flow occurs throughout the homogeneous media, (b) single fracture flow model (e.g., Wang et al., 1978) where flow occurs in the fractures only and (c) fracture/matrix flow model (e.g., Barker and Black, 1983) where flow occurs in fractures and between fractures in the rock matrix.

The fracture apertures utilized in the Wang et al. (1978) simulation are 2.6, 3.9, 5.6, 8.4 and 12.2 μm corresponding to hydraulic conductivities of 3×10^{-12} , 1×10^{-11} , 3×10^{-11} , 1×10^{-10} , and 3×10^{-10} m/s respectively. The simulation results are shown plotted in Figure 4.4-11. The calculated pressure responses for the two analytical solutions have notably different shapes. The difference in pressure responses are a consequence of the assumptions involved in the two conceptualizations. The Wang et al. (1978) solution is based on the assumption of flow or pressure dissipation from the packer-isolated borehole interval into a single fracture surrounded by essentially impermeable rock. In the fracture flow conceptualization, the driving force for flow (resulting in pressure changes) from the wellbore into the fracture is the result of the compressibility of the water only whereas for the porous media case compressibility effects are accounted for in both the water and the rock. For the parameter values chosen, comparable pressure responses are obtained with the hydraulic conductivity for the fracture model being a factor of about 3 to 5 higher than for the porous media model. The factor of 3 to 5 difference is likely to be a maximum at low hydraulic conductivities (less than $K = 1 \times 10^{-11}$ m/s or fracture aperture = 3.9 μm) and will be less at higher permeabilities.

In comparison, Barker and Black (1983) state that in reference to fracture/matrix flow models versus porous media models the porous media model has a "derived aquifer transmissivity (that) will always be over estimated, but by a factor which is unlikely to exceed three". The conclusions from these results are that a single fracture flow model will overestimate the hydraulic conductivity as compared to a porous media model and the porous media flow model will overestimate the hydraulic conductivity as compared to a fracture/matrix flow model (see schematic illustration of flow regimes in Figure 4.4-10). Thus, if a fracture flow model is used in the analysis when the system is actually a fracture and matrix flow system then the hydraulic conductivity could be overestimated by about an order of magnitude.

4.4.5 Orientation of Fractures or Higher Permeability Zones

Fractures or higher permeability zones intersecting the borehole at a right angle will produce a

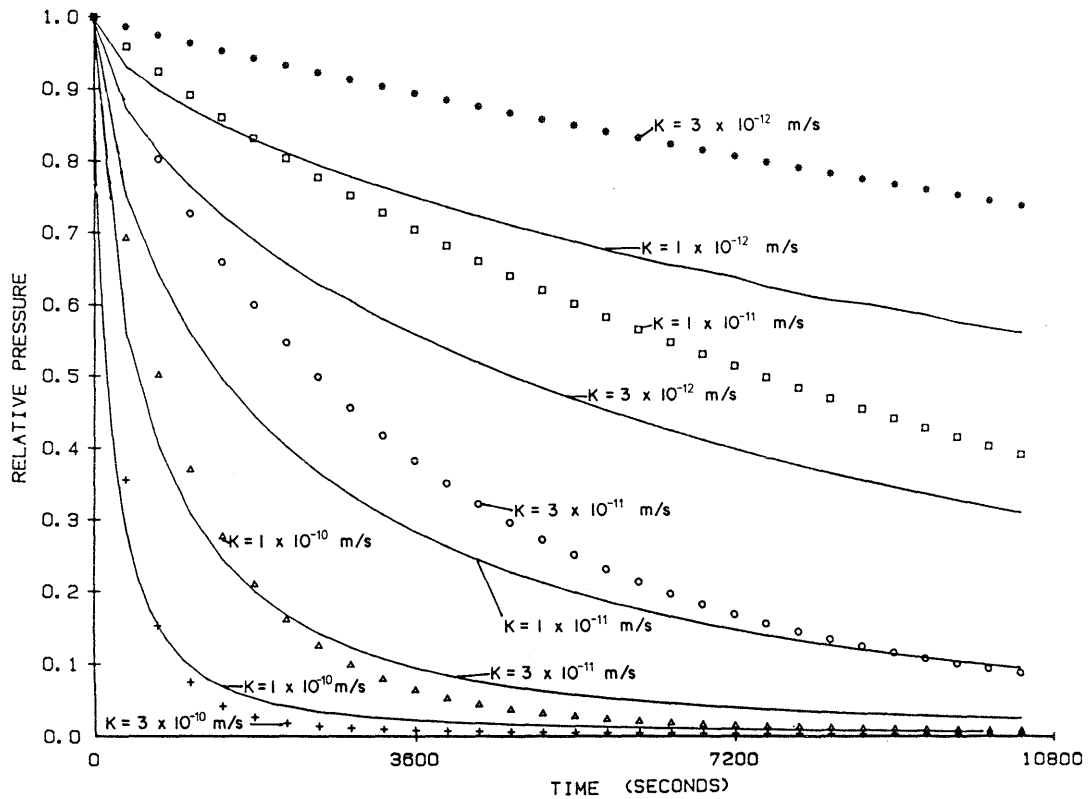


Figure 4.4-11 Comparison between fracture flow simulation results (symbols) using Wang et al. (1978) solution and porous media simulation results (lines) using Bredehoeft and Papadopoulos (1980) for various hydraulic conductivities

pressure response that is different from a fracture or higher permeability zone of similar aperture or thickness that intersect the borehole at an angle less than 90°. For a subhorizontal fracture the wellbore - fracture contact is an ellipse rather than a circle and therefore has a larger contact area. Because the contact area is larger the pressure recovery will be faster producing an overestimation of hydraulic conductivity than that which would have been obtained for a similar horizontal fracture. Therefore, without knowing the orientation of a fracture which is contributing to the hydraulic conductivity of an interval, the hydraulic conductivity may be uncertain. The magnitude of this uncertainty will increase for larger angles from the horizontal. For example, from theoretical results presented in Wang et al. (1978), it can be estimated that the aperture would be overestimated by a factor of 1.2 for a subhorizontal fracture at 66° or equivalently to an overestimate of hydraulic conductivity by a factor of 1.7.

4.4.6 Higher or Lower Permeability Skin Surrounding the Borehole

Skin effects on the borehole wall or immediately surrounding the borehole have been discussed in Section 3.5 and are worthy of examination from a practical hydraulic testing point of view. A higher permeability skin could develop on the borehole wall due to erosion caused by drilling or dissolution of minerals caused by circulated drilling fluids. Lower permeability skin effects may be caused by drilling fluid or rock flour (present in the borehole due to drilling) clogging or blocking fractures, cracks or pores in the formation or even by the precipitation of infilling materials in fractures or pores.

In crystalline rocks as opposed to sedimentary rocks, skin effects are not considered to be as significant. The harder, denser crystalline rocks will resist erosion to some extent although it is still likely to occur. Dissolution of minerals in the borehole wall is also a less significant effect in crystalline rock. Because crystalline rocks are not drilled using drill mud, clogging of the formation will be minimized.

The influence or magnitude of skin effects are difficult to quantify but are likely related to the radius of influence described above. If the radius of influence is large then skin effects may be less significant and the hydraulic conductivity determined from the interval will be representative of the formation rather than the borehole skin. On the other hand, if the radius of influence is small or the skin affected zone is thick then the hydraulic conductivity is likely to be that of the borehole skin.

4.5 Fluid Considerations

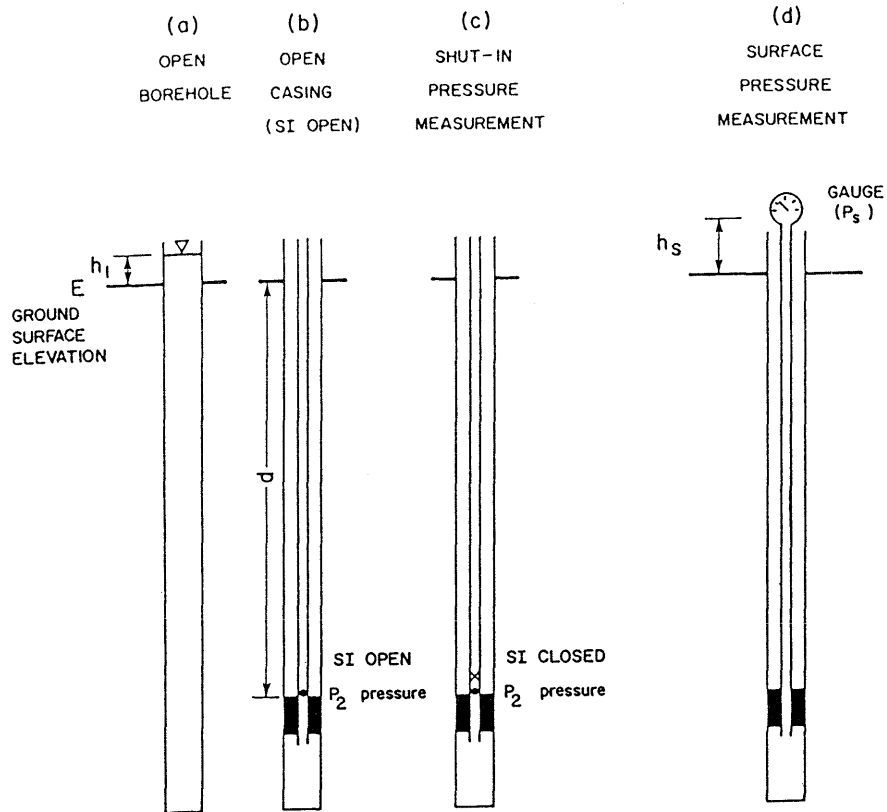
Calculations involving hydraulic heads and formation pressures require estimates of the borehole and formation fluid densities. All formation pressures and hydraulic heads must be evaluated in a consistent manner to allow a comparison of the calculated hydraulic heads corresponding to the different test intervals or formations. Examples of the various field conditions under which formation pressures or water levels may be measured within deep drilling programs are shown schematically in Figure 4.5-1 and include:

- (a) water levels measured in an open borehole or a partially cased borehole with an open interval at the bottom;
- (b) downhole pressure measurement with the test interval open to the tubing string above the hydrologic or drill stem test tools;
- (c) downhole pressure measurement with a gauge connected to tubing extending to an isolated borehole interval.

The variation in fluid density along the length of the borehole and between various formation depths is an important factor affecting the interpretation of representative formation pressures.

The factors influencing fluid density are:

- pressure;
- temperature;
- salinity (dissolved constituents).



PARAMETERS

- E = GROUND SURFACE ELEVATION
- h_1 = WATER LEVEL HEIGHT ABOVE DATUM
- P_2 = TRANSDUCER PRESSURE MEASUREMENT
- B = BAROMETRIC PRESSURE
- d = DEPTH OF MEASURING POINT BELOW DATUM
- h_s = HEIGHT OF GAUGE ABOVE DATUM
- P_s = SURFACE PRESSURE GAUGE MEASUREMENT
- G = GRAVITATIONAL ACCELERATION
- $\rho(z)$ = FLUID DENSITY WITH DEPTH (FUNCTION OF TEMPERATURE, PRESSURE AND SALINITY)

(NOTE: SI REFERS TO SHUT-IN TOOL)

Figure 4.5-1 Various field conditions under which formation pressures or water levels are measured

For analysis of hydraulic test data for the determination of hydraulic conductivity, the density, viscosity, compressibility and thermal expansion coefficient (for some cases) of the in-situ fluids are required. It is usually assumed that the borehole and formation fluids have the same properties. Measurement of the fluid specific gravity at surface conditions and temperature and pressure at in-situ conditions allow the determination of relatively accurate estimates for density and viscosity for use in hydraulic conductivity analyses. The following table shows the variations in the fluid properties considering temperature and pressure effects only for two depths in a crystalline rock formation representative of conditions at the Boettstein borehole site in northern Switzerland.

Depth (m)	Density (kg m ⁻³)	Viscosity (kg m ⁻¹ s ⁻¹)	Compressibility (Pa ⁻¹)	Thermal Expansion Coefficient (°C ⁻¹)
315	998	9.0 x 10 ⁻⁴	4.4 x 10 ⁻¹⁰	2.5 x 10 ⁻⁴
1500	988	4.4 x 10 ⁻⁴	4.3 x 10 ⁻¹⁰	5.5 x 10 ⁻⁴

Fluid viscosity and thermal expansion coefficient exhibit the greatest variation with depth because of their strong temperature dependence. Choice of representative fluid property values during test analyses is necessary to achieve as accurate as possible, estimates of hydraulic conductivity.

4.6 Equipment Consideration

4.6.1 Accuracy of Equipment Readings and Depth Measurements

Equipment considerations may be important with regards to uncertainties in the hydraulic testing results. These considerations include uncertainties in the temperature transducer response and in the

accuracy of the pressure transducer probe. For example Lynes, Inc. (1984) report the accuracy for their triple transducer pressure-temperature probe as follows:

Operating Range	Absolute Accuracy	Resolution
0 - 125°C	$\pm 1^\circ\text{C}$	0.1°C
0 - 6000 PSIA (0-41370 kPa)	$\pm 0.05\%$ Full scale	0.005% Full Scale

The reported accuracy of the pressure transducer is about 20 kPa or about 2 metres of water. Similar magnitudes of uncertainty should be considered in all pressure measurements and pressure responses used in formation pressure and hydraulic conductivity determinations.

Another uncertainty which may be included in this category is the accuracy of the borehole and test interval depth measurements. It should be recognized that the depth measurements of test intervals may be recorded in centimetres but it is unlikely that the accuracy, especially at depth, is greater than tens of centimetres and is most likely only accurate to the nearest metre.

Borehole depth measurements can also depend on the borehole deviation from vertical. The difference between true vertical depth and measured depth could have a dramatic effect on depth measurements and hydraulic head determination and, therefore, should be addressed in any calculations involving hydraulic head.

Errors in depth measurements may also be a serious problem when an attempt is made to return to retest a previously tested interval. Differences in interpreted hydraulic conductivity could result from small variations in the actual borehole interval being tested.

4.6.2 Equipment Compliance

Equipment compliance has been discussed in Section 3.6 but it is worthwhile to consider the practical aspects of equipment compliance when conducting hydraulic tests. Compliance effects occur as a result of non-rigidity in the equipment.

Rubber packers and O-rings and entrapped air in the system will tend to compress when a pressure pulse is applied during testing. If, for example, the pressure in the interval is increased as in a pulse injection test then the packers will also be compressed causing a slight increase in the test section volume. As the pressure in the interval decreases the packers will slowly return to their original shape. In addition, the packers may be responding to pressure changes in the zones both above and below the test interval. Because the test interval volume is changing due to the compliance effect, the hydraulic response due solely to the formation is difficult to determine.

Another compliance effect which was described in section 3.6 is the packer squeeze effect which is caused by extreme weight being applied to the packers during a tool movement. Both compliance effects can significantly affect the accuracy of the results during hydraulic testing. In order to minimize the effects of compliance, a number of suggestions have been developed which include:

- Packer compliance tests should be conducted under both laboratory and field conditions to determine the system compliance. Packer compliance should be compared to a non-compliant packer (i.e., steel plug) in a laboratory test cell prior to field testing. Field compliance effects should be measured using the entire equipment system in a blank section of casing.
- The weight applied during tool movements when using single and double packer configurations connected with drill tubing to surface should be constant during the test and kept to the minimum required to reduce packer squeeze.
- Inflation pressures above annulus pressure should be at least an order of magnitude greater than the maximum pressure differential applied during testing.
- For formations of lower hydraulic conductivity, the significance of compliance effects increases. Therefore at low permeabilities less compliant systems are desirable.

Equipment compliance have been shown to cause at least a factor of 2 variation in hydraulic conductivity (Forster and Gale, 1980) and it is therefore necessary to quantify compliance effects

during hydraulic testing. Only through detailed laboratory and field compliance testing can these effects be evaluated. By the utilization of careful testing procedures compliance effects can be minimized.

4.6.3 Testing Procedures and Equipment Difficulties

Testing procedures should be utilized which will provide suitable hydraulic test data for hydraulic conductivity determination. Examples of problems which may develop include:

- poor initial conditions (insufficient pressure differential) for pulse and slug tests;
- shut-in squeeze during closing the shut-in tool for the pressure build-up period of a drill-stem test;
- equipment difficulties or malfunctions (e.g., leaking shut-in tool; packers slipping on borehole wall; packer deflation or rupture);
- streaming of fluid down the bore of the tubing string during a flow period;
- insufficient overlap of adjacent test intervals during the H-logging activities.

The hydraulic tests should be designed and monitored to minimize the above types of problems. Careful examination of the measured pressure responses during testing is necessary in order to identify testing problems and take appropriate action (e.g., equipment replacement; repeating the previous tool movement in order to obtain the correct initial conditions for a test). Where a testing problem is identified after the test has been completed, it may be necessary to re-test the corresponding borehole interval. During the analysis of all hydraulic tests, the possibility of the above-noted testing problems should be assessed as part of the data interpretation/evaluation phases before recommendations are made with regard to the interpreted formation parameters.

4.7 Summary

The various factors that should be considered when interpreting the measured pressure responses during hydraulic testing and thus the determinations of the formation hydraulic parameters (i.e., formation pressure and hydraulic conductivity) have been presented in the previous sections. The uncertainty in hydraulic conductivity can be minimized by the careful examination of testing conditions (e.g., isothermal versus nonisothermal conditions) and testing procedures (i.e., identification and correction for poor test initial conditions or equipment difficulties/malfunctions), choice of assumed parameter values (e.g., rock and fluid properties, reference pressure, storage coefficient), choice of appropriate data analysis methods (e.g., porous media versus fracture flow models; inclusion of borehole history and thermal effects), examination of borehole physical conditions (e.g., borehole erosion and possible skin effects) and examination of the appropriateness of the selected measurement scale (i.e., packer spacing).

Four approaches can be utilized to provide some quantification of the uncertainty associated with the hydraulic conductivities interpreted from hydraulic testing:

- (1) Examination of the repeatability of the interpreted hydraulic conductivity for a particular test interval depth using a series of tests in a testing sequence. Examination of results from repeat testing at a later time at or approximately at the same test interval depth may also be conducted;
- (2) Sensitivity analysis on the parameters involved for simulation of each borehole hydraulic test;
- (3) Sensitivity analysis on the hydraulic conductivity distribution utilized in local or regional scale ground water flow model simulations;
- (4) Formal uncertainty analysis using equivalent stochastic models for parameter estimation.

The repeatability of the interpreted hydraulic conductivity from various tests in a test sequence (approach 1) should be routinely evaluated in the data analysis phase. Examination of test intervals that had either a sequence of pulse tests or a sequence of slug tests should indicate a close comparison (within a factor of 2) in interpreted hydraulic conductivity. Comparison of results from different test types, such as pulse and slug or pulse and drill-stem tests, should also show a relatively close comparison.

At present, sensitivity analyses (approach 2) can be implemented routinely using computer-based data analysis models such as GTFM as described in Section 3.7. Additional sensitivity results have been presented above in this report. By consideration of the various factors addressed in this report during the data analysis phase, the uncertainty in the magnitude of the hydraulic conductivities can be reduced during the determination of hydraulic conductivity values.

Sensitivity and uncertainty analyses utilizing approaches (3) and (4) with ground water flow and equivalent stochastic models, respectively, could be beneficial in future assessments of the hydraulic conductivity data base if they are warranted.

Field testing procedures should be modified during a borehole hydraulic testing program in order to optimize the program both with regards to testing time and improvements in the hydraulic test data base. The identification and quantification of the importance of factors such as borehole pressure history and thermally-induced pressure effects should lead to the adoption of test procedures (see Section 5) to minimize the significance of these factors and the development and application of sophisticated data analysis techniques (see Section 3) to allow a more accurate determination of hydraulic conductivities from hydraulic tests. These modifications in the testing and analysis methods will serve to reduce the uncertainty in the interpreted formation hydraulic parameters.

5. GUIDELINES FOR FORMATION PRESSURE MEASUREMENT AND BOREHOLE HYDRAULIC TESTING USING LYNES HYDROLOGIC TOOL

5.1 Introduction

This section addresses the detailed procedures recommended for accurate hydraulic testing at depth. They have been developed during the NAGRA deep drilling program and apply to equipment systems involving hydrologic test tools with downhole sensor instrumentation and single and double packer equipment configurations connected with drill tubing to surface (e.g., LYNES Inc. hydrologic test tools). The purpose of these recommendations is to provide guidance to field personnel responsible for making decisions during a field testing program. The specific guidelines presented deal with the difficult case of pressure measurement at depth in low permeability formations where the formation temperature is most likely higher than the circulating drill fluid temperature. Under these circumstances the effects of borehole thermal and pressure histories, as well as equipment compliance, are most pronounced. Although the guidelines are specifically for pressure measurement the borehole thermal history and pressure history are similarly significant in tests to determine hydraulic conductivity.

A Procedures Chart and Schematic Pressure Response Curves have been produced that incorporate detailed effects of borehole interval pressure and temperature variances from in-situ formation pressure and temperature; however, equipment compliance effects are not directly included in the chart and response curves, due to the uncertainty in the nature and magnitude of the compliance function (see Section 3.6). Depending on the compliance function specific to individual packer and tool configurations, equipment compliance could increase or decrease the rate of pressure change during any given testing sequence. If the equipment compliance function is completely elastic in nature, "casing tests" (pressure response tests in blank casing with no effective permeability) can provide adequate information to include equipment compliance in the analysis. In the case of a totally elastic compliance response, compliance can be extracted directly from the test interval storativity. However, elastic behavior is a special case of the

more general case of compliance presented in section 3.6. There does not exist adequate data on equipment compliance to quantitatively assess either the significance or relative magnitude of the effects of compliance. A detailed laboratory and field-verified testing program will be necessary to quantitatively incorporate equipment compliance into the guidelines for field hydraulic test interpretation. The guidelines presented in this section attempt to minimize compliance related to packer inflation by allowing sufficient time for packer "square-off". The limited laboratory test data available for the Lynes packers suggest that virtually all compliance related to packer inflation is complete within 1 hour of inflation.

The guidelines are based on several premises which include the fact that most field testing programs are subject to time (i.e., financial) constraints, in particular with respect to interruption of drilling for the purpose of pressure measurement. For this reason, the primary decision points in the guidelines are time-related, in effect all relating to a theoretical " t_{max} " which is the maximum allowable or affordable time period over which a pressure measurements on a selected borehole test interval can be made. If there is sufficient quantitative information (i.e., pressure/temperature relationships) early in a test to indicate that it is not possible to achieve a representative pressure measurement within t_{max} the test is halted and drilling is resumed.

It is also necessary to estimate the in-situ formation pressure with respect to annulus overflow pressure in order to use the guidelines (this is usually necessary to conduct a permeability analysis as well). The requirement is essentially an estimate of whether the undisturbed formation pressure is above or below annulus overflow pressure. It is usually possible to provide the formation pressure estimate based on more easily conducted measurements in high permeability zones within the same borehole. It is necessary to make these estimates because many alternate decisions are based on whether the estimated formation pressure is above or below annulus pressure.

Once the maximum allowable time for measurement (t_{max}) has been determined and the formation pressure estimated, it is then a matter of running in the testing tool and conducting the test

utilizing the maximum possible information from pre-test measurements. This information includes drilling history, annulus overflow elevation, drill fluid temperature, estimated formation temperature (from temperature logs and gradient extrapolations), drilling mud density, drill logs, fracture logs, etc. The guidelines are designed to assist the field hydrogeologist in decision making and application of hydraulic testing principles. Application of these principles in the context of single packer tests for formation pressure measurements and double packer tests for hydraulic conductivity profiling are discussed below. For illustrative purposes, the guidelines are designed with specifications related to the hydrologic test tools manufactured by LYNES Inc.

5.2 Single Packer Testing for Estimation of Formation Pressure

5.2.1 Objectives

A single packer test refers to the use of a single packer to isolate a recently drilled interval for the purpose of formation pressure measurement. The interval is isolated between the packer and the bottom of the hole immediately after drilling due to the time constraints on how long the borehole can remain open and still provide accurate formation pressure measurements within a reasonable monitoring period. These constraints are discussed in Section 3. Other information is also obtained during a test, such as estimates of hydraulic parameters and information regarding the potential of the interval for geochemical sampling; however, these are considered, within the context of the guidelines, to be complementary and secondary to the primary objective of measurement of the formation pressure representative of conditions prior to the drilling and testing disturbances.

5.2.2 Procedures

In a single packer test the drill string is removed from the borehole and the hydrologic test tool (with a single packer) is lowered on tubing to the selected depth. The packer is inflated, allowed to "square-off" (i.e., complete inflation and rubber

expansion/readjustment) after which testing procedures begin. The procedures and tool movements required to achieve isolation result in an "applied-load" or weight which the packer should bear of between 0.5 and 1 ton. This weight is sufficient to keep the shut-in valve closed but not so large as to over-compress the interval and cause excessive pressures to occur by "squeezing" the interval. A practical example of the effect of various applied loads is presented in section 3.9.3.

The procedures chart and schematic pressure response curves form the basis of the guidelines. The chart and curves are cross-referenced using the times (t_1 , t_2 , etc.) and each box in the chart is subscripted by the possible response curves which could have led to that point in the chart. The times (t_1 , t_2 , t_3 , t_4 , t_{max}) during testing are directly related to:

- the maximum allowed testing period;
- thermally induced pressure effects: dependent on the temperature differential between the drilling fluid and the rock and the length of time the interval has been subjected to drill fluid temperature;
- borehole pressure history effects: dependent on the pressure differential between the drilling annulus overflow and the in-situ formation pressure and the length of time the interval has been subjected to annulus pressure.

With the above conditions defined, a minimum permeability can be derived which will allow correct formation pressure measurement within the allowable time t_{max} , and the times t_1 , t_2 , t_3 , and t_4 can be assigned. However, some estimation and technical judgement is required. In most instances, there are some relatively permeable zones which can provide accurate and reproducible pressure measurements. These pressure measurements provide the basis for estimating the formation pressure ($P_{form\ est}$) in subsequent intervals. Other observations are also employed to estimate the pressure, such as drill fluid monitoring (i.e., changes in rate of inflow or loss from the borehole and drill water tracer concentration data). However, even if the actual formation pressure is exceptionally high or

low compared to the estimated formation pressure, there is allowance in the procedures to ensure that these pressures are obtained and that the test is not aborted due to temperature or compliance related effects, provided results can be obtained within t_{max} . The times (t_1, t_2, t_3, t_4) have been developed based on analysis and interpretation of field data and conditions observed from numerous hydraulic tests in the NAGRA deep boreholes, in conjunction with numerous theoretical calculations over the range of hydraulic conductivities, pressures, and temperatures likely to be encountered. These analysis and theoretical calculations are presented in Section 3. Section 3 addresses fluid properties and pressure/temperature relationships as well as equipment compliance and related effects. Also presented are calculations related to borehole history and length of time an interval has been open to flowing annulus or drilling fluid overflow pressure.

The recommended times, based on the above analyses and calculations and a maximum test period (starting at t_0) of 20 hours, for illustrative purposes, are:

- t_1 1 hour
- t_2 2 hours
- t_3 6 hours
- t_4 16 hours
- t_{max} 20 hours

An optional confirmatory pulse or slug injection or withdrawal test is performed at the completion of every pressure measurement. The injection or withdrawal test is designed to approach the previously measured formation pressure from the opposite direction of the shut-in pulse, thereby reducing uncertainty in the pressure measurement. The withdrawal or injection tests should be completed within t_{max} . Continuation of the test beyond t_{max} would be done on direction of the field co-ordinator or the management. Otherwise all test procedures should be completed with times $t_2 < t < t_{max}$, or between 2 and 20 hours in the context of the above example.

The general procedures, commencing and ending with transducer calibration checks, to be followed in conducting either a single or double packer downhole test are provided in the following flow chart (Figure 5.2-1). There is no allowance for equipment malfunction or downtime. Should equipment malfunction occur at any point above "STOP TEST" in the flow chart, an estimate of the time required to correct the problem should be made and the field co-ordinator or the management consulted for a decision on whether to resume drilling or effect repairs and resume testing.

The procedures chart (see Figure 5.2-2) for in-situ pressure measurement addresses the interrelationships between pressure, temperature and borehole history as they relate to the possible observed pressure responses following interval isolation and an initial "shut-in squeeze pressure". The procedures are somewhat different depending on whether the estimated pressure in the formation is above or below the annulus pressure (i.e., separate schematic response curves are provided for each instance as shown in Figures 5.2-3 and 5.2-4). The annulus pressure refers to the downhole pressure corresponding to the elevation of the overflow of drilling fluid at the wellhead.

The procedures chart is self-explanatory except for definition of the terms and abbreviations. The following describes the terminology and defines the abbreviations utilized in the procedures chart.

- $t_{1,2,3,4}$ times corresponding to the schematic response curves.
- t_{max} maximum allowable time period over which a pressure measurement can be made or a hydraulic test conducted.
- $P_{formation\ est}$ the estimated formation pressure in the interval (prior to the drilling/testing disturbances) based on previous tests, drill fluid monitoring (outflow/inflow quantity, tracer concentration) and core observations.
- $P_{formation}$ new estimate of formation pressure determined from the test.

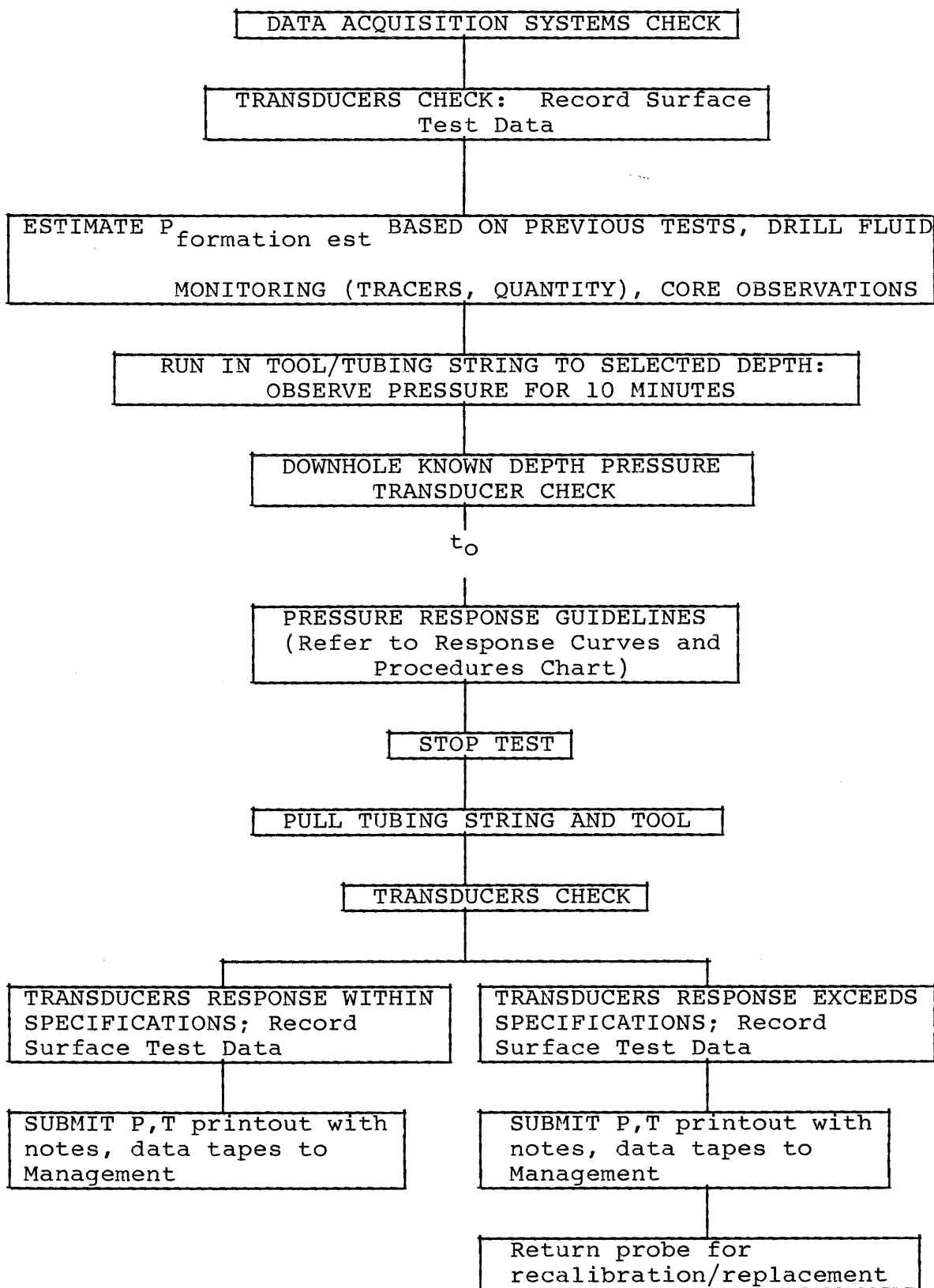
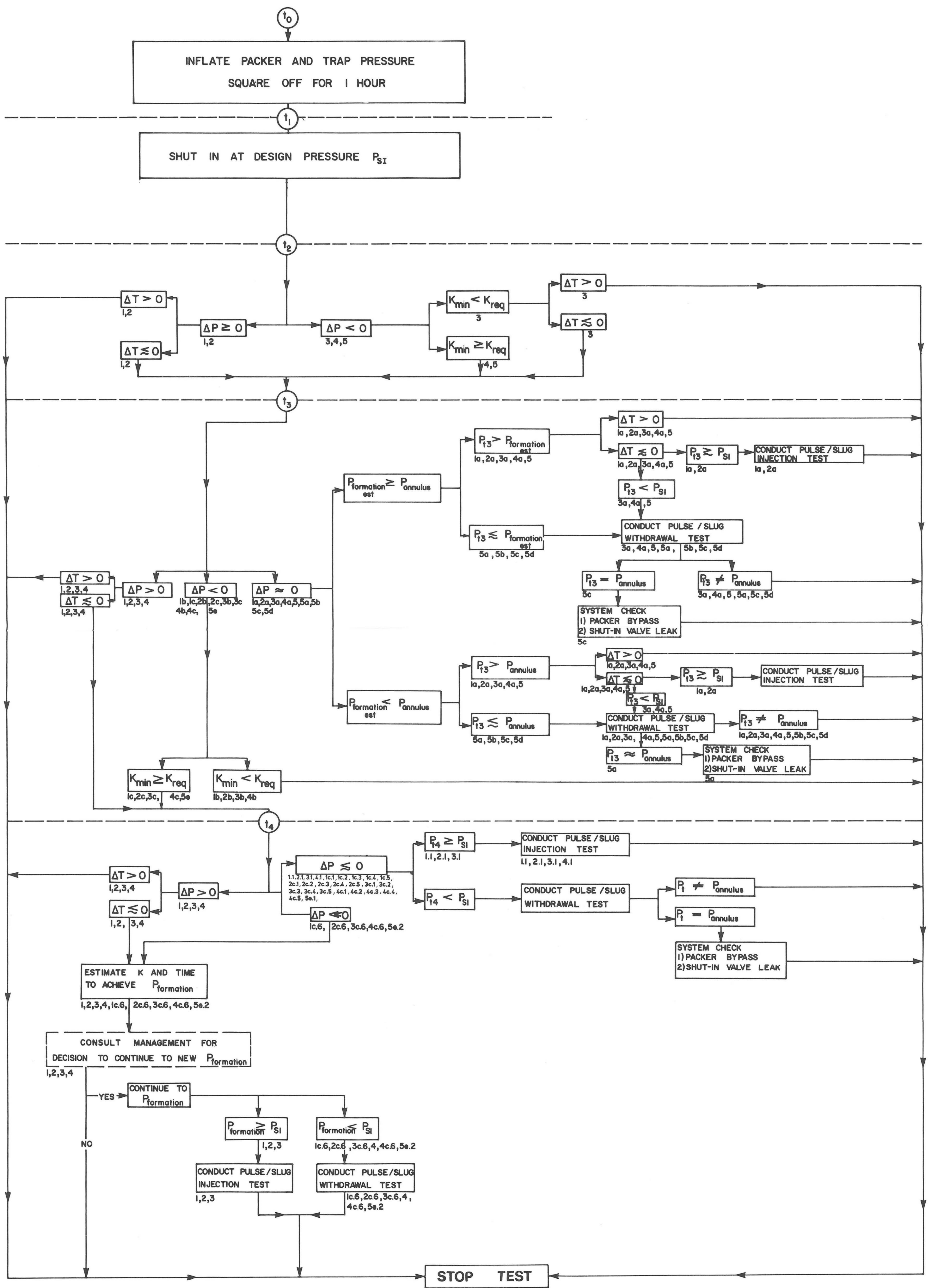


Figure 5.2-1 Flow chart for formation pressure measurement with LYNES hydrologic test tool

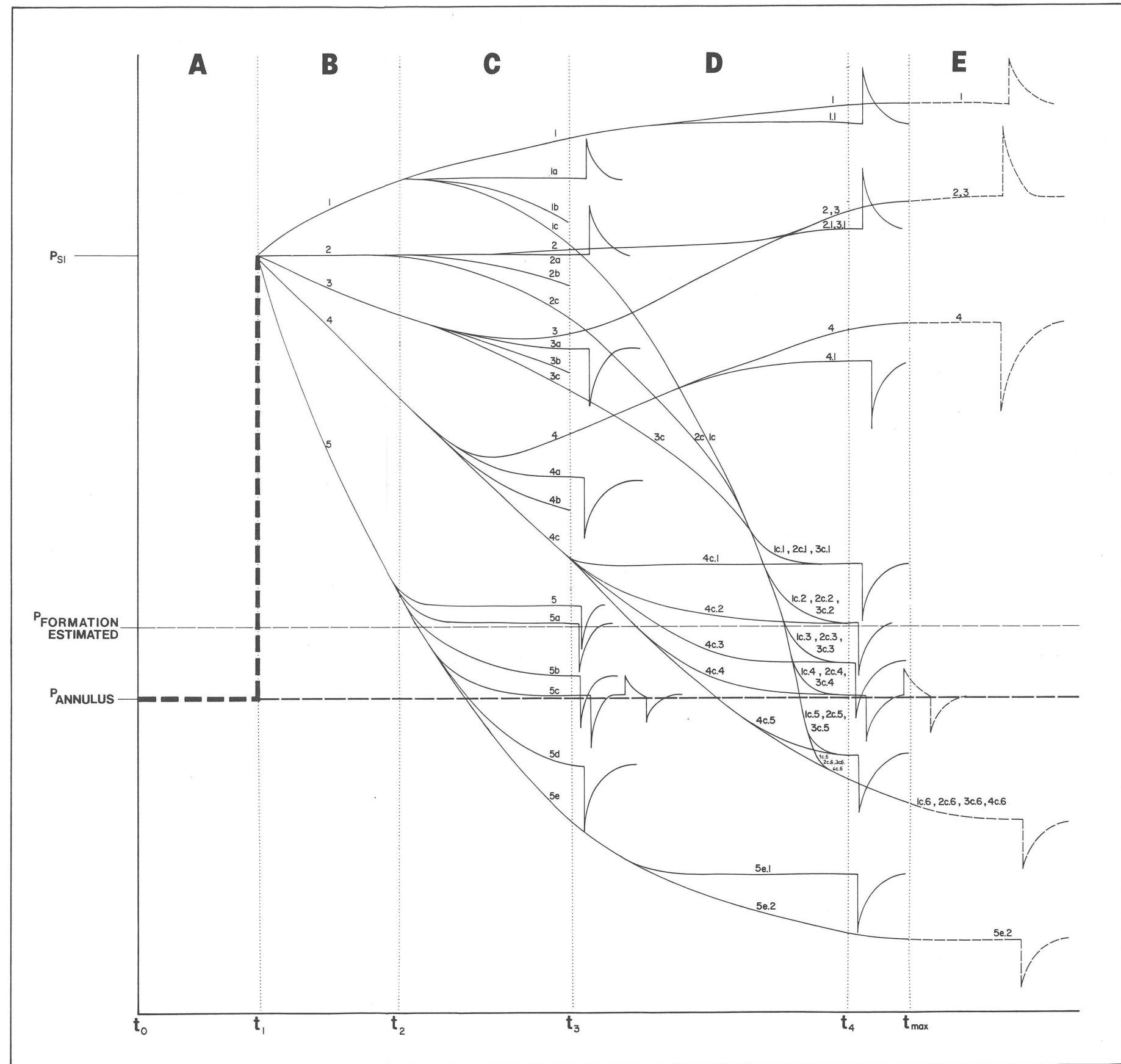
PROCEDURES CHART



LEGEND

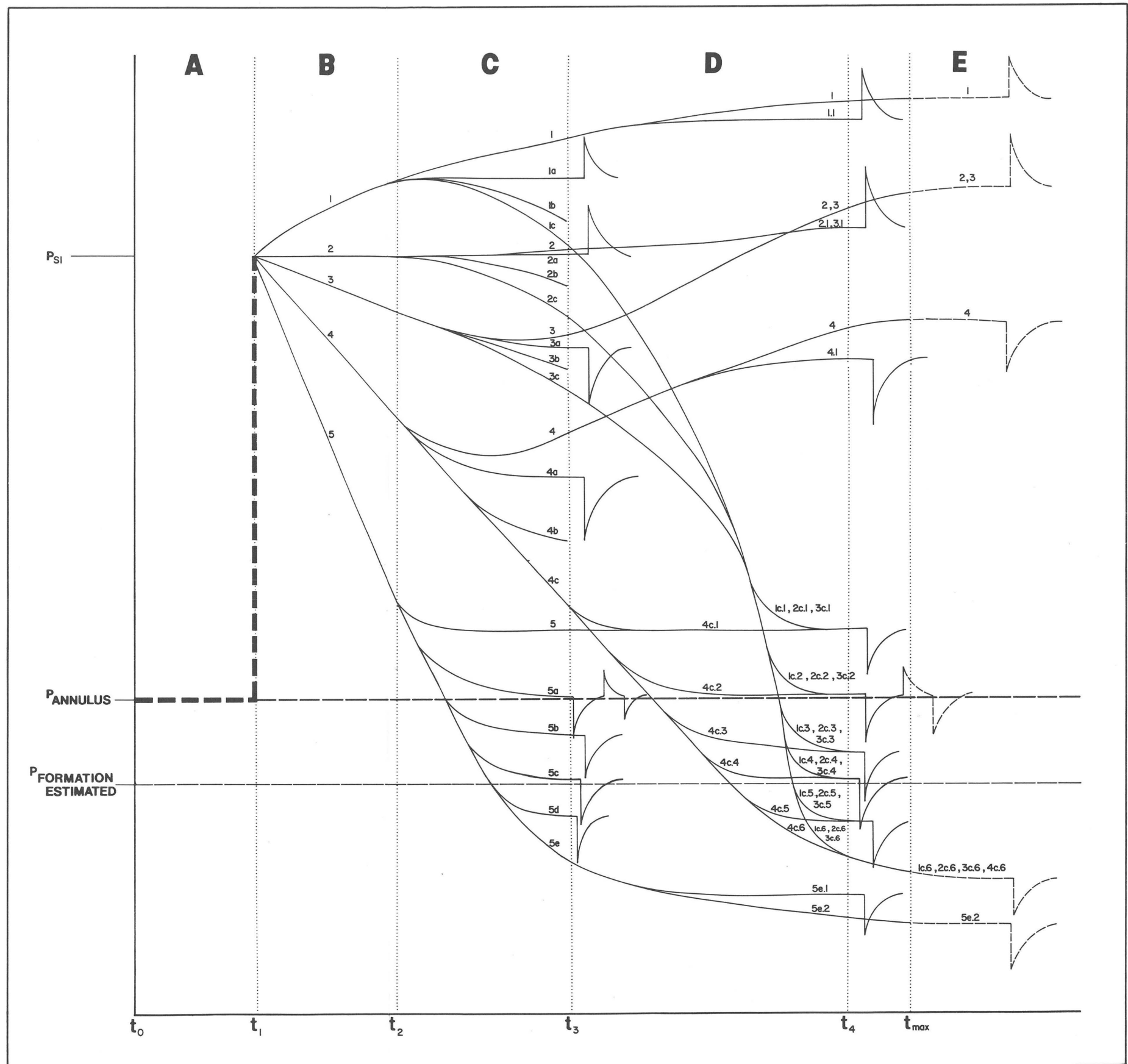
- $t_{1,2,3,4}$ times corresponding to the schematic response curves.
- $P_{formation\ est}$ the estimated formation pressure in the interval (prior to the drilling/testing disturbances) based on previous tests, drill fluid monitoring (outflow/inflow quantity, tracer concentration) and core observations.
- $P_{formation}$ new estimate of formation pressure determined from the test.
- $P_{annulus}$ the downhole pressure corresponding to the elevation of the overflow of drilling fluid at the wellhead.
- P_{SI} the pressure in the test interval at time of shut-in, resulting from all influences, including pressure prior to shut-in, "shut-in squeeze", applied load, compliance, etc. This pressure is chosen before the start of the test based on the annulus pressure, an estimate of the anticipated formation pressure and the "designed" pressure pulse differential required for the pulse test. This pressure is also the starting pressure for any subsequent test analysis.
- ΔP the change in pressure at the preceding time designation, above the illustrated box. For example, procedures and ΔP 's between t_2 and t_3 on the procedures chart relate to the time t_2 . ΔP does not refer to the change in pressure between t_2 and t_3 but rather refers to the slope and magnitude of the pressure change at t_2 .
 $\Delta P > 0$, indicates an increase in pressure
 $\Delta P < 0$, indicates a decrease in pressure
 $\Delta P \approx 0$, indicates approximately no change in pressure.
- ΔT the change in temperature at the preceding time designation, above the illustrated box. For example, procedures and ΔT 's between t_2 and t_3 on the procedures chart relate to the time t_2 . ΔT does not refer to the change in temperature between t_2 and t_3 but rather refers to the slope and magnitude of the pressure change at t_2 .
 $\Delta T > 0$, indicates an increase in temperature
 $\Delta T < 0$, indicates a decrease in temperature
 $\Delta T \approx 0$, indicates approximately no change in temperature
- K_{req} the hydraulic conductivity required to obtain 85% recovery from P_{SI} within t_{max} . K_{req} is approximated using the estimated $P_{formation\ est}$ and the length of time the interval has been open to annulus pressure (see section 3.8.1 for details). For a t_{max} of 20 hours and a borehole open period up to 48 hours, K_{req} is about 10^{-10} m/s.
- K_{min} the hydraulic conductivity required to obtain 85% recovery from P_{SI} within t_{max} . K_{min} is used for direct comparison to K_{req} . K_{min} is estimated from the pressure response data obtained between t_1 and t_2 and between t_2 and t_3 , under the conditions where $\Delta P < 0$. The estimate is made using standard type curve (hydraulic response) analysis on the pressure data. If temperature effects are significant with $\Delta T > 0$, K_{min} will be less than K_{req} , resulting in "STOP TEST".
- PULSE/SLUG WITHDRAWAL/INJECTION TEST an instantaneous decrease or increase in the pressure or water level in the test interval, with subsequent monitoring of pressure response of water level recovery monitoring of pressure response or water level (see sections 2.3 and 2.4).

Figure 5.2-2 Procedures for in-situ pressure measurement



PRESSURE RESPONSE CURVES $P_{\text{FORMATION EST}} > P_{\text{ANNULUS}}$

Figure 5.2-3 Pressure response curves:
 $P_{\text{formations est}} > P_{\text{annulus}}$



PRESSURE RESPONSE CURVES $P_{\text{FORMATION EST}} < P_{\text{ANNULUS}}$

Figure 5.2-4 Pressure response curves:
 $P_{\text{formations est}} > P_{\text{annulus}}$

- $P_{annulus}$ the downhole pressure corresponding to the elevation of the overflow of drilling fluid at the wellhead.
- P_{SI} the pressure in the test interval at time of shut-in, resulting from all influences, including pressure prior to shut-in, "shut-in squeeze", applied load, compliance, etc. This pressure is chosen before the start of the test based on the annulus pressure, an estimate of the anticipated formation pressure and the "designed" pressure pulse differential required for the pulse test. This pressure is also the starting pressure for any subsequent test analysis.
- ΔP the change in pressure at the preceding time designation, above the illustrated box. For example, procedures and ΔP 's between t_2 and t_3 on the procedures chart relate to the time t_2 . ΔP does not refer to the change in pressure between t_2 and t_3 but rather refers to the slope and magnitude of the pressure change at t_2 .
 $\Delta P > 0$, indicates an increase in pressure
 $\Delta P < 0$, indicates a decrease in pressure
 $\Delta P \approx 0$, indicates approximately no change in pressure.
- ΔT the change in temperature at the preceding time designation, above the illustrated box. For example, procedures and ΔT 's between t_2 and t_3 on the procedures chart relate to the time t_2 . ΔT does not refer to the change in temperature between t_2 and t_3 but rather refers to the slope and magnitude of the pressure change at t_2 .

- 185 -

$\Delta T > 0$, indicates an increase in temperature

$\Delta T < 0$, indicates a decrease in temperature

$\Delta T \approx 0$, indicates approximately no change in temperature

- K_{req} the hydraulic conductivity required to obtain 85% recovery from P_{SI} within t_{max} . K_{req} is approximated using the estimated $P_{formation\ est}$ and the length of time the interval has been open to annulus pressure (see section 3.8.1 for details). For a t_{max} of 20 hours and a borehole open period up to 48 hours, K_{req} is about 10^{-10} m/s.
- K_{min} the hydraulic conductivity required to obtain 85% recovery from P_{SI} within t_{max} . K_{min} is used for direct comparison to K_{req} . K_{min} is estimated from the pressure response data obtained between t_1 and t_2 and between t_2 and t_3 , under the conditions where $\Delta P < 0$. The estimate is made using standard type curve (hydraulic response) analysis on the pressure data. If temperature effects are significant with $\Delta T > 0$, K_{min} will be less than K_{req} , resulting in "STOP TEST".
- PULSE/SLUG WITHDRAWAL/INJECTION TEST an instantaneous decrease or increase in the pressure or water level in the test interval, with subsequent monitoring of pressure response or water level recovery (see Sections 2.3 and 2.4).

5.2.3 Pressure Response Curves

Two schematic response curve diagrams are provided (see Figures 5.2-3 and 5.2-4): one with

Pformation est above Pannulus and one with Pformation est below Pannulus. The primary difference between the two are concerned with the decisions and systems checks related to packer bypass (i.e., inadequate packer seats) or shut-in valve leaks. The differences between the decision and systems checks are illustrated on the Procedures Chart between t_3 and t_4 .

For discussion purposes, the response curves of Pformation est > Pannulus will be used. There are 5 "master curves" illustrated which can possibly develop in response to the shut-in squeeze pressure. The pressure P_{SI} is important because it provides a common point of departure and, since it is always above Pformation est and Pannulus, it serves to limit the number of possible responses. The Master Curves and their subsets are briefly explained below. (Segment A on the response curve is common to all the Master Curves).

Master Curve 1

Segment B

1 could be responding to high formation pressure in high or low K interval; pressure increase could be due to rising temperatures in a low K interval

Segment C

1 responding to high in-situ pressure

1a new in-situ pressure

1b temperature response has peaked, however K_{min} is not sufficiently high to achieve Pformation est in the allowed time

1c temperature response has peaked and K_{min} is high enough to continue the test

Segment D

1 responding to high in-situ pressure

1.1, 1c.1 new in-situ pressure
1c.3, 1c.5

1c.2 measured pressure = Pformation est

- 187 -

1c.4 measured pressure = P_{annulus} ;
requires system check

1c.6 formation pressure appears very low;
requires more time for pressure
measurement

Segment E

1, 1c.6 new formation pressure

Master Curve 2

Segment B

2 could be correct formation pressure,
or pressure remains elevated due to
temperature effects, or permeability
is very low

Segment C

2 new formation pressure is greater
than P_{SI} or temperature is
increasing

2a new formation pressure

2b temperature effects have peaked, or
were not present, however K_{min}
is not sufficiently high to continue

2c temperature effects have peaked, or
were not present, and K_{min} is
high enough to continue

Segment D

2 responding to high in-situ pressure

2.1, 2c.1 new in-situ pressure
2c.3, 2c.5

2c.2 measured pressure = $P_{\text{formation est}}$

2c.4 measured pressure = P_{annulus} ;
requires system check

2c.6 formation pressure appears very low;
requires more time for pressure
measurement

Segment E

2, 2c.6 new formation pressure

Master Curve 3

Segment B

3 pressure dropping slowly, could be low K and/or increasing temperature effects

Segment C

3 pressure could be rising due to temperature increasing, or possible borehole "skin" effect (pressure around borehole during drilling is lower than formation pressure, therefore a low pressure "skin" has developed, resulting in the earlier portions of the response being more rapid)

3a new in-situ pressure

3b possible continued temperature effects, however K_{min} is not sufficiently high to continue

3c possible continued temperature effects, however K_{min} is high enough to continue

Segment D

3 responding to high formation pressure

3.1, 3c.1 new in-situ pressure
3c.3, 3c.5

3c.2 measured pressure = $P_{formation}$ est

3c.4 measured pressure = $P_{annulus}$;
requires systems check

3c.6 formation pressure appears very low;
requires more time for pressure measurement

Segment E

3, 3c.6 new in-situ pressure

Master Curve 4

Segment B

4 pressure dropping relatively rapidly;
could be either intermediate K or relatively high K with temperature effects

Segment C

- 4 pressure could be rising due to temperature or possible borehole "skin" effect (pressure around borehole during drilling is lower than formation pressure, therefore a low pressure "skin" has developed resulting in the earlier portions of the response being more rapid)
- 4a new formation pressure
- 4b possible temperature or "skin" effects reduce rate of pressure drop; K_{min} is not sufficiently high to continue
- 4c possible continued temperature effects, however K_{min} is high enough to continue

Segment D

- 4 responding to high formation pressure
- 4.1, 4c.1 new in-situ pressure
4c.3, 4c.5
- 4c.2 measured pressure = $P_{formation}$ est
- 4c.4 measured pressure = $P_{annulus}$;
requires system check
- 4c.6 formation pressure appears very low;
requires more time for pressure measurement

Segment E

- 4, 4c.6 new formation pressure

Master Curve 5

Segment B

- 5 indicates very high K, temperature effects are minimal

Segment C

- 5, 5b, 5d new formation pressure
- 5a measured pressure = $P_{formation}$ est
- 5c measured pressure = $P_{annulus}$;
requires system check

5e formation pressure appears very low; requires more time for pressure measurement

Segment D

5e.1 new formation pressure

5e.2 pressure appears very low; requires more time for pressure measurement

Segment E

5e.2 new in-situ pressure

The schematic pressure response curves for the case of $P_{\text{formation}} \text{ est} < P_{\text{annulus}}$ (Figure 5.2-3) are developed from the same starting point and the same set of 5 Master Curves.

5.3 Hydrogeologic Reconnaissance Logging for Hydraulic Conductivity Profiling

5.3.1 Objective

Reconnaissance logging refers to double packer tests conducted under open borehole conditions for the purpose of obtaining a hydraulic conductivity profile of the entire borehole. The reconnaissance log is usually done with a constant packer spacing (between 5 and 25 meters) and a small overlap to ensure the entire open borehole has been tested.

5.3.2 Procedures

The interval to be tested is isolated between the packers after inflation. A pulse or slug injection or withdrawal test is then conducted and the pressure response is analyzed for hydraulic conductivity. Borehole pressure history and thermal effects will be minimal during the reconnaissance logging provided the borehole has been open for a long period under passive conditions (i.e., not pumping or flushing) before the logging is performed. As a consequence of the long borehole open period a quasi-equilibrium of pressure and temperature will likely have been established between the borehole fluid column and the formation in the immediate vicinity of the borehole. Under these circumstances P_{annulus} rather than $P_{\text{formation}}$ is the preferred reference pressure.

During the short period of testing the pressure pulse (P_{SI}) will attempt to return to Pannulus. The quasi-equilibrium conditions result in relatively predictable borehole pressure and temperature conditions, at least over the time period of any individual hydraulic conductivity test on an interval. Should the response developed during the test show significant deviations from the predicted response, the most likely source of difficulty will be packer seats (i.e., packer bypass) or equipment malfunctions such as leaking shut-in valve or malfunctioning transducers.

Under the circumstances when the reconnaissance log commences immediately after drilling, the same principles discussed in section 5.2 and detailed in the Procedures Chart (Figure 5.2-2) and Response Curves (Figures 5.2-3 and 5.2-4) can be used as the basis for decision making in the field.

5.3.3 Pressure Response Curves

Schematic pressure response curves have not been developed for reconnaissance logging due to the less complicated testing results which should derive from the quasi-equilibrium of borehole/formation pressure and temperature that should have developed prior to testing. There are, however, special circumstances which arise that can result in pressure responses more complicated than would normally be expected. The theoretical basis of these difficulties is discussed in Section 4 with practical examples provided as appropriate.

6. REFERENCES

- Barker, J.A. and J.H. Black, 1983. Slug tests in fissured aquifers. *Water Resources Research*, Vol. 19, No. 6, pp. 1558-1564.
- Belanger, D.W., J.F. Pickens and G.J. Saulnier, 1984. Analysis of Pressure and Flow Data from the Long-Term Monitoring Tool in Boettstein Borehole. NAGRA Technischer Bericht 85-39.
- Black, J.H. and K.L. Kipp, Jr., 1981. Determination of hydrogeological parameters using sinusoidal pressure tests: A theoretical appraisal. *Water Resources Research*, Vol. 17, No. 3, pp. 686-692.
- Bredehoeft, J.D. and S.S. Papadopoulos, 1980. A method for determining the hydraulic properties of tight formations. *Water Resources Research*, Vol. 16, No. 1, pp. 233-238.
- Cooper, H.H. Jr., and C.E. Jacob, 1946. A generalized graphical method for evaluating formation constants and summarizing well-field history. *American Geophysical Union Transaction*, Vol. 27, No. 4, pp. 526-534.
- Cooper, H.H. Jr., J.D. Bredehoeft and S.S. Papadopoulos, 1967. Response of a finite-diameter well to an instantaneous charge of water. *Water Resources Research*, Vol. 3, No. 1, pp. 263-269.
- Dillon, R.T., R.B. Lantz and S.B. Pahwa, 1978. Risk Methodology for Geologic Disposal of Radioactive Waste: The Sandia Waste Isolation Flow and Transport (SWIFT) Model. Prepared for the U.S. Nuclear Regulatory Commission, Sandia National Laboratories, Albuquerque, New Mexico.
- Earlougher, R.C., 1977. Pressure Buildup Testing. *Advances in Well Test Analysis*. Monograph Volume 5, Soc. of Petroleum Engineers of AIME, New York.
- Faust, C.R. and J.W. Mercer, 1984. Evaluation of slug tests in wells containing a finite-thickness skin. *Water Resources Research*, Vol. 20, No. 4, pp. 504-506.

- Forster, C.B. and J.E. Gale, 1981. Injection versus pressure pulse borehole tests in fractured crystalline rocks - Observations and recent experiences. Proceedings of Third Invitational Well Testing Symposium, pp. 74-83, University of California, Lawrence Berkeley Laboratory, Berkeley, California.
- Forster, C.B. and J.E. Gale, 1980. A Laboratory Assessment of the Use of Borehole Pressure Transients to Measure the Permeability of Fractured Rock Masses. Lawrence Berkeley Laboratory, Report No. 8674.
- Hsieh, P.A., S.P. Neuman and E.S. Simpson, 1983. Pressure Testing of Fractured Rocks -- A Methodology Employing Three-Dimensional Cross-Hole Tests. Prepared for U.S. Nuclear Regulatory Commission, NUREG/CR-2313.
- Hubbert, M.K., 1940. The theory of ground-water motion. Journal Geology, Vol. 48, pp. 785-819.
- Hvorslev, M.J., 1951. Time Lag and Soil Permeability in Ground Water Observations. U.S. Army Corps. Engineers Waterways Experimental Station Bulletin 36, Vicksburg, Miss.
- Jacob, C.E., 1940. On the flow of water in an elastic artesian aquifer. American Geophysical Union Transaction, Vol. 21, pp. 574-586.
- Jacob, C.E. and S.W. Lohman, 1952. Nonsteady flow to a well of constant drawdown in an extensive aquifer. American Geophysical Union, Transactions, Vol. 33, pp. 559-569.
- Johnson, C.R., R.A. Greenkorn and E.G. Woods, 1966. Pulse-Testing: A new method for describing reservoir flow properties between wells. Journal of Petroleum Tech., Trans. AIME, Vol. 237, pp. 1599-1604.
- Lee, J., 1982. Well Testing. SPE Textbook Series, Vol. 1, Soc. of Petroleum Engineers of AIME, New York.
- Lohman, S.W., 1972. Ground-Water Hydraulics. Geological Survey Professional Paper 708.
- Matthews, C.S. and D.G. Russell, 1967. Pressure Buildup Analysis. Pressure Buildup and Flow Tests in Wells. Monograph Volume 1, Soc. of Petroleum Engineers of AIME, New York.

- Narasimhan, T.N. and B.Y. Kanehiro, 1980. A note on the meaning of storage coefficient. Water Resources Research, Vol. 16, No. 2, pp. 423-429.
- Nelson, R.W. and P.L. Oberlander, 1984. Considerations of a Nonhomogeneous Fluid in the Deep Groundwater Flow System at Hanford. Prepared for Basalt Waste Isolation Program, Pacific Northwest Laboratory, Report No. 5285 (DRAFT).
- Papadopoulos, S.S., J.D. Bredehoeft and H.H. Cooper Jr, 1973. On the analysis of "slug test" data. Water Resources Research, Vol. 9, No. 4, pp. 1087-1089.
- Peterson, E., F. Burns, P. Lagus, K. Lie and E. Wu, 1983. Operation of a Guarded Straddle Packer System. Report No. 459, Office of Nuclear Waste Isolation, Columbus, Ohio.
- Reeves, M. and R.M. Cranwell, 1981. User's Manual for the Sandia Waste - Isolation Flow and Transport Model (SWIFT). Prepared for the U.S. Nuclear Regulatory Commission. Sandia National Laboratories, Albuquerque, New Mexico, Release 4.81.
- Savage, G.J. and H.K. Kesavan, 1979. The graph theoretic field model - I. Modelling and formulations. Journal of the Franklin Institute, Vol. 307, pp. 107-147.
- Thackston, J.W., L.M. Preslo, D.E. Hoexter and N. Donnelly, 1984. Results of Hydraulic Tests at Gibson Dome No. 1, Elk Ridge No. 2, and E.J. Kubat Boreholes, Paradox Basin, Utah. Report No. 491, Office of Nuclear Waste Isolation, Columbus, Ohio.
- Theis, C.V., 1935. The relation between the lowering of the piezometric surface and the rate and duration of discharge of a well using ground-water storage. American Geophysical Union Trans, Vol. 16, pp. 519-524.
- Wang, J.S.Y., T.N. Narisimhan, C.F. Tsang and P.A. Witherspoon, 1978. Transient Flow in Tight Fractures. Proceedings of Invitational Well Testing Symposium, pp. 103-116, University of California, Lawrence Berkeley Laboratory, Berkeley California.